Supplementary Information

Enabling high-turnover methanol-to-syngas reforming

Andreas Bonde[1,2*‡], Gabriel M. F. Batista[1,2*‡], Michal Gurský[3], and Troels Skrydstrup[1,2*]

[1]Carbon Dioxide Activation Center (CADIAC), Interdisciplinary Nanoscience Center (iNANO), Department of Chemistry, Aarhus University, 8000 Aarhus C, Denmark.

[2]Novo Nordisk Foundation CO_2 Research Center (CORC), Aarhus University, 8000 Aarhus, Denmark.

[3]Institute of Organic Chemistry, Catalysis and Petrochemistry, Slovak University of Technology, Bratislava, Slovak Republic.

‡These authors contributed equally.

*Corresponding authors. Email: bonde@inano.au.dk, gmfb@inano.au.dk, ts@chem.au.dk

Contents

General Considerations

All chemicals were purchased from Sigma-Aldrich, Doug Discovery, Tokyo Chemical Industry (TCI), or Strem, and were used as received without further purification. Unless otherwise stated, all non-aqueous reactions were performed in either oven-dried or flame-dried apparatus under an atmosphere of argon using dried solvents. Solvents used in the argon-filled glovebox were dried according to standard procedures and degassed with argon. Flash column chromatography (FCC) was carried out using silica gel (230-400 mesh particle size, 60 Å pore size) as stationary phase. Automated flash column chromatography (AFCC) was carried out with Interchim PuriFlash XS520Plus with 30 µm prepacked columns. All NMR spectra were recorded on a Bruker 400 MHz Ascend spectrometer. Chemical shifts in ^{1}H and ^{13}C NMR spectra are reported in ppm relative to the solvent residual peak stated. NMR spectra are reported as: chemical shift (peak multiplicity; *J*-coupling constant(s) in Hz; integration). Peak multiplicities are abbreviated as: s = singlet, bs = broad singlet, d = doublet, t = triplet, q = quartet, quin = quintet, sept = septet, and m = multiplet. GC of gaseous products were obtained with an SRI Multiple Gas Analyzer #5 equipped with both thermal conductivity detector (TCD) and flame ionisation detector (FID).

HRMS spectral analysis was measured with a Bruker Maxis Impact Spectrometer using electrospray ionisation (ESI).

Continuous Flow Setup

All reported continuous flow experiments were performed on the apparatus shown in Figure S3.1. An in-house manufactured gas-tight GL-45 lid fitted with a NBR70 O-ring having four ¼-28 flat-bottom ports is mounted on a 20 mL GL-45-necked bottle containing the catalyst solution. The first port connects to the HPLC pump using PTFE (1/8" OD x 1.59 mm ID) tubing equipped with a 2 µm stainless-steel filter to prevent particles from entering pump head. The filtered solution is then pumped through a stainless steel (1/16" OD x 1.00 mm ID) reaction loop (1.6 mL volume) embedded in an in-house made stainless steel heating block insulated with a vermiculite cap and aluminium foil. Following the reaction loop, the heated mixture of catalyst solution and gaseous products enter a cooling coil (1/16" OD vs 1.00 mm ID) set to 0 °C. A back-pressure regulator is inserted downstream from the cooling section to set the desired reaction pressure. After the back-pressure regulator, a PTFE (1/8" OD x 1.59 mm ID) tube connects to a Y-connector providing a constant stream of argon carrier gas set by an Alicat mass flow controller before the mixture re-enters the GL-45 bottle through the second port. The PTFE tube exits into the bottom of the GL-45 bottle to effectively function as a gas-liquid separator. A 1/8" PTFE (1/8" OD x 1.59 mm ID) tube placed in the headspace exits through the third port which is connected to a solvent trap (10 mL) cooled to -78 °C before being fed continuously into the SRI Multiple Gas Analyzer #5 apparatus for analysis. The fourth port is either capped or equipped with an inlet for the addition of solutions. Thus, the catalyst solution is continuously recirculated through the system (6.0 mL total volume) while generated gaseous products are analysed by the GC.

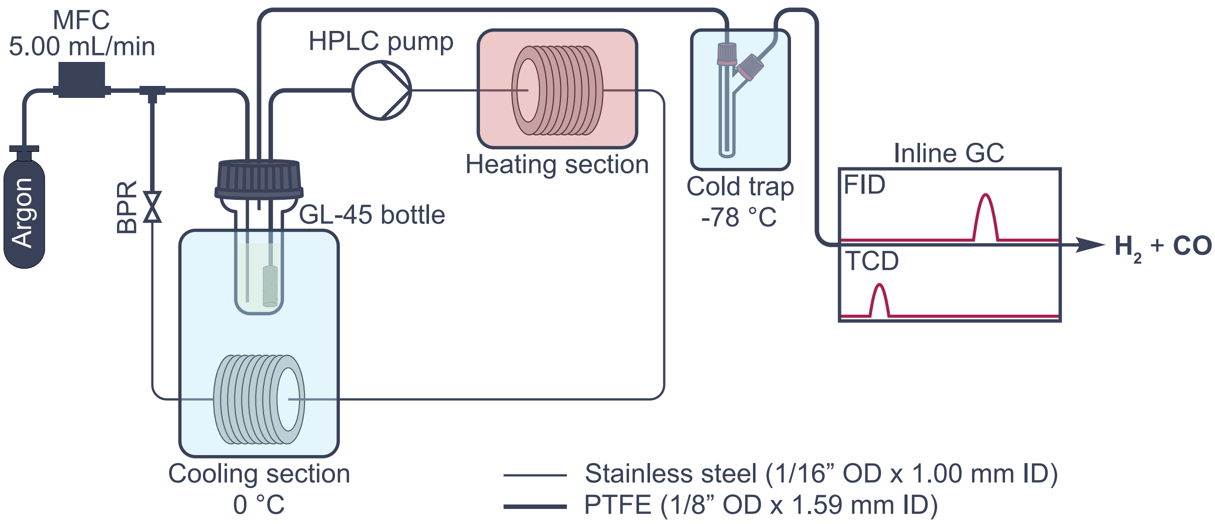

Figure S1. Schematic representation of the continuous flow setup.

Ligand and Complex Abbreviations

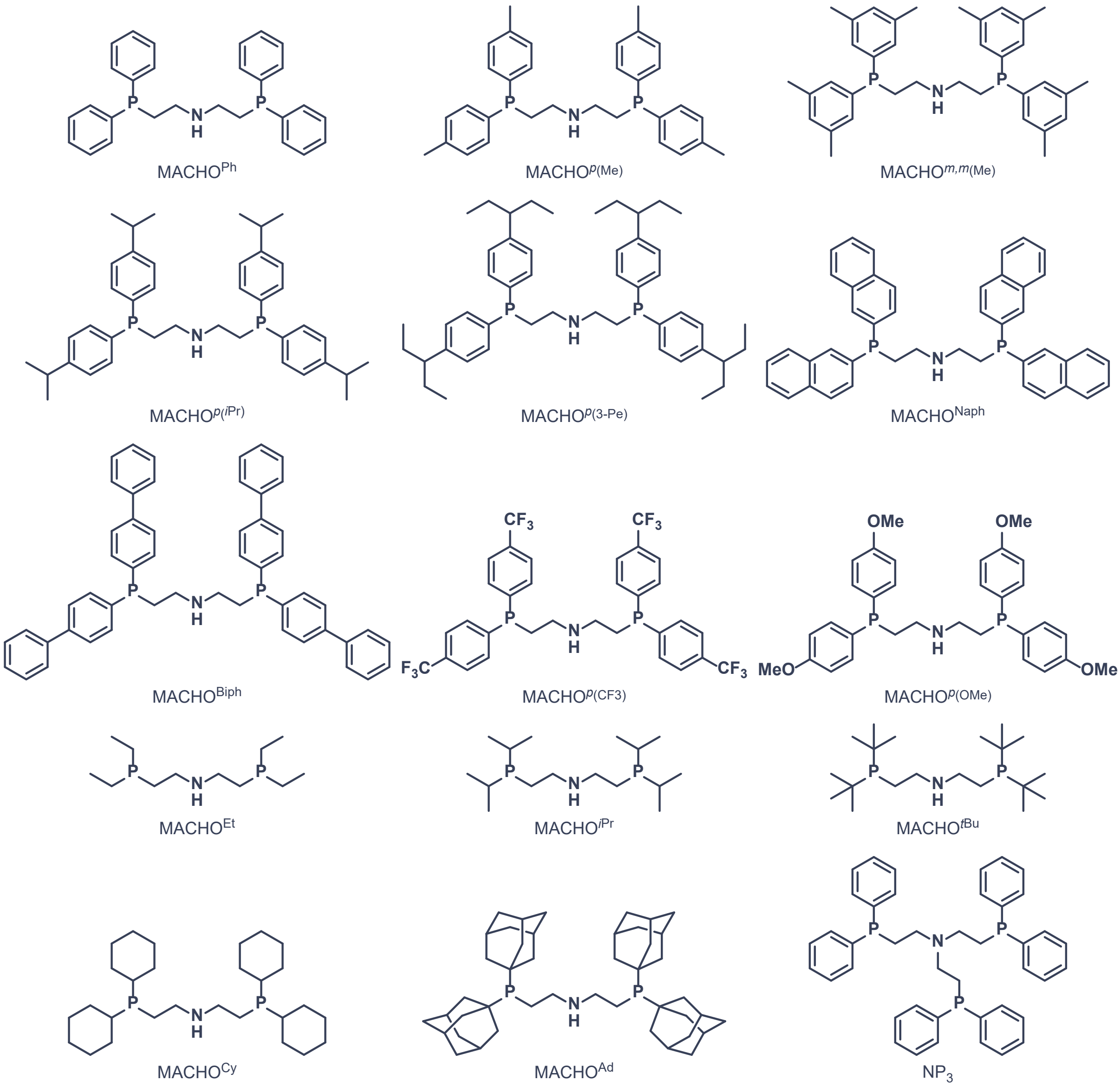

Figure S2. Overview of all MACHO^{R} and tridentate ligands.

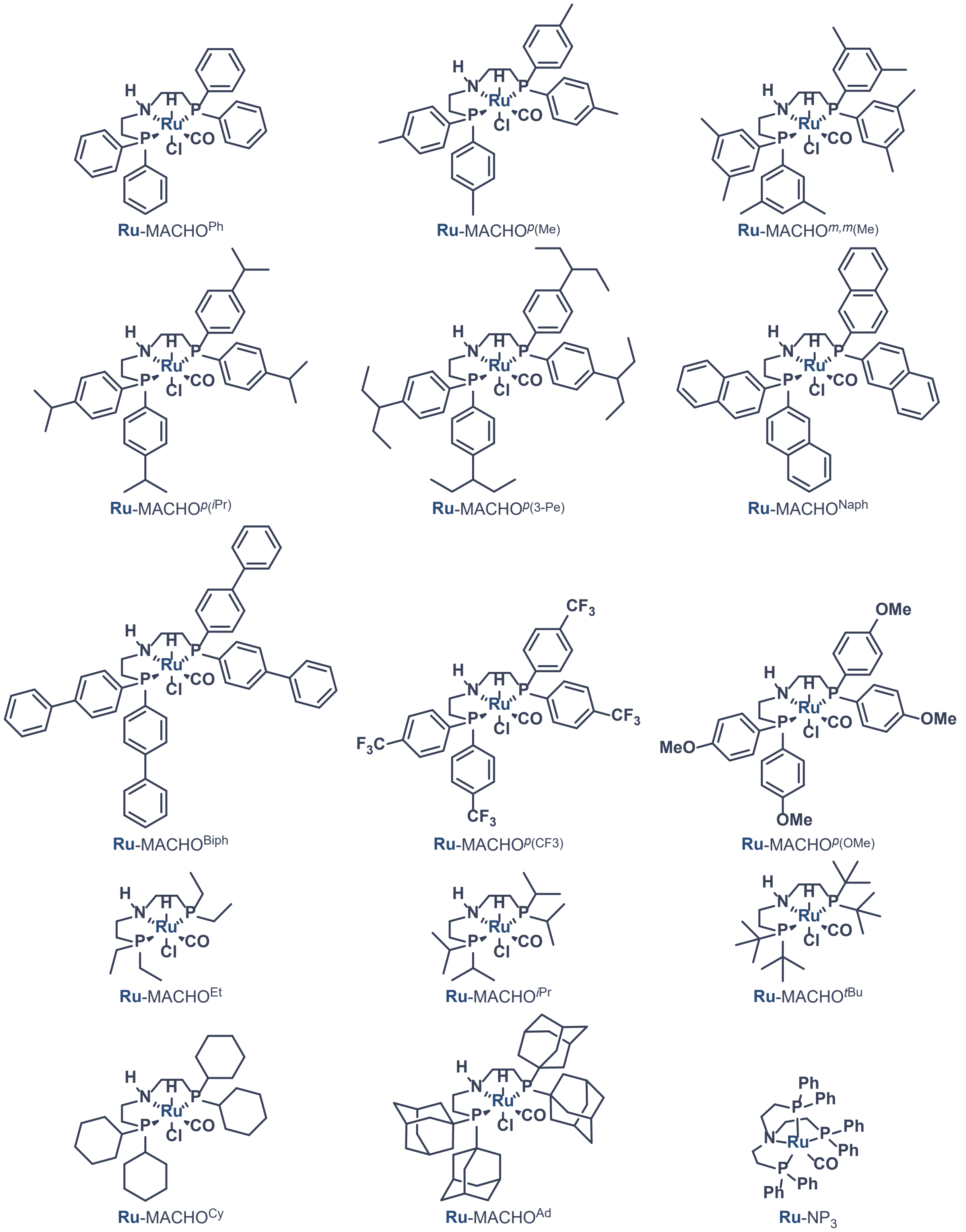

Figure S3. Overview of all Ru-MACHO^R and tridentate complexes.

Calibration of the Inline Gas Chromatography Instrument

Calibration of the inline GC instrument (SRI Multiple Gas Analyzer #5) was conducted using calibration gas cylinders for low concentrations and an in-house manufactured gas mixer for high concentrations. For low concentrations, the desired calibration gas cylinder was connected to the GC via a mass flow controller (5 mL/min). For high concentrations, pure gases from high-pressure cylinders were connected to the gas mixer via mass flow controllers (5 mL/min total), which were thoroughly mixed by stirring prior to entering the GC. For each calibration point, an average of 5 entries were performed with maximum 4% deviation between lowest and highest sample. Hydrogen was measured using TCD, while carbon monoxide was measured on both TCD and FID for high and low concentrations, respectively.

Table S1. TCD calibration data for high amounts of hydrogen (≥60,000 ppm).

#	H_2 [ppm]	Areas					Avg. area	SD	CV
1	$2.0 \cdot 10^4$	1874	1878	1880	1882	1881	1879	2.83	0.151
2	$6.0 \cdot 10^4$	5650	5636	5622	5615	5616	5628	13.39	0.238
3	$10 \cdot 10^4$	8744	8757	8755	8746	8762	8751	5.59	0.064
4	$15 \cdot 10^4$	12616	12738	12598	12577	12558	12617	63.35	0.502
5	$25 \cdot 10^4$	20646	20645	20631	20625	20615	20632	11.86	0.057
6	$35 \cdot 10^4$	27602	27602	27610	27608	27600	27604	3.88	0.014
7	$46 \cdot 10^4$	34732	34774	34770	34788	34808	34774	25.02	0.072
8	$60 \cdot 10^4$	43699	43730	43747	43746	43714	43727	18.56	0.042

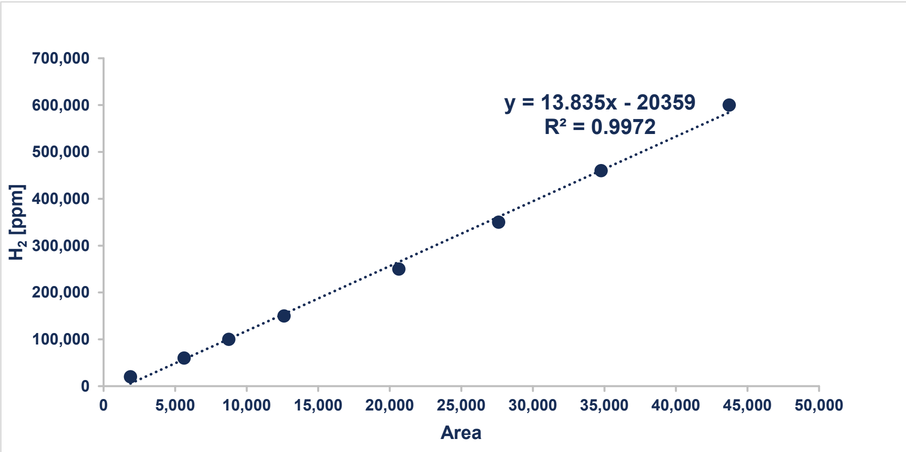

Table S2. TCD calibration data for low amounts of hydrogen (< 60,000 ppm).

#	H_2 [ppm]	Areas					Avg. area	SD	CV
1	50	3	3	4	3	4	3	0.49	14.409
2	100.1	8	8	8	8	8	8	0.00	0.000
3	1001	92	93	91	93	93	92	0.80	0.866
4	5006	477	477	479	467	469	474	4.83	1.020
5	$9.83 \cdot 10^3$	947	951	951	950	943	948	3.07	0.324
6	$2.0 \cdot 10^4$	1874	1878	1880	1882	1881	1879	2.83	0.151
7	$6.0 \cdot 10^4$	5650	5636	5622	5615	5616	5628	13.39	0.238

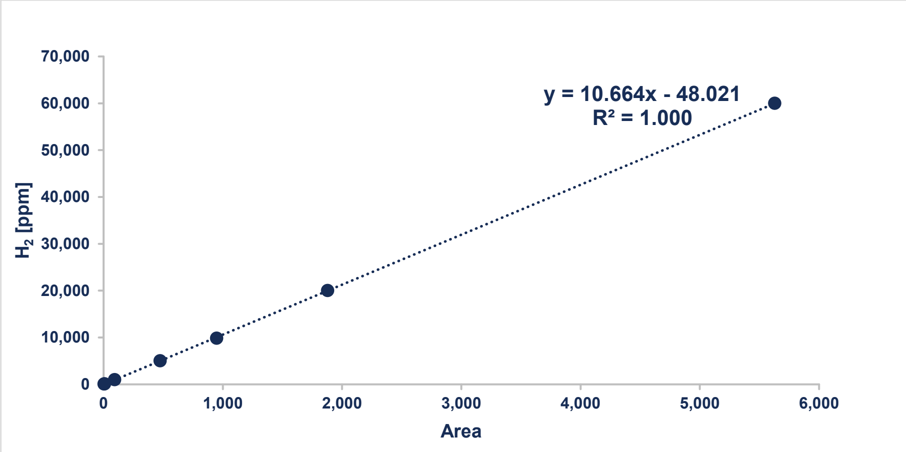

Table S3. TCD calibration data for high amounts of carbon monoxide (≥50,000 ppm).

#	CO [ppm]	Areas					Avg. area	SD	CV
1	$2.0 \cdot 10^4$	190	186	184	184	183	185	2.50	1.35
2	$6.0 \cdot 10^4$	557	560	560	562	564	561	2.33	0.42
3	$10 \cdot 10^4$	979	977	978	979	977	978	0.89	0.09
4	$17 \cdot 10^4$	1687	1691	1689	1690	1684	1688	2.48	0.15
5	$25 \cdot 10^4$	2402	2404	2407	2411	2407	2406	3.06	0.13
6	$35 \cdot 10^4$	3343	3351	3318	3333	3483	3366	59.72	1.77
7	$46 \cdot 10^4$	4406	4390	4407	4416	4399	4404	8.69	0.20
8	$64 \cdot 10^4$	6257	6277	6267	6276	6279	6271	8.21	0.13
9	$75 \cdot 10^4$	7363	7355	7362	7371	7372	7365	6.28	0.09

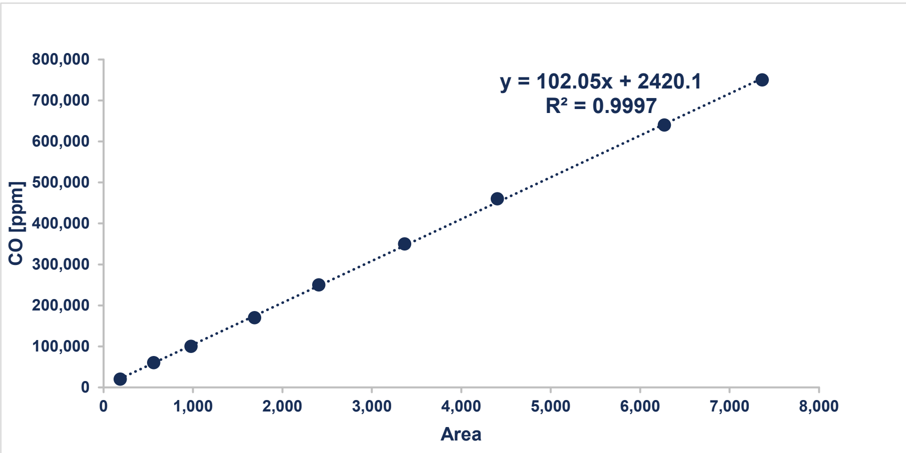

Table S4. FID calibration data for low amounts of carbon monoxide (< 50,000 ppm).

#	CO [ppm]	Areas					Avg. area	SD	CV
1	100.3	28	28	28	27	28	28	0.40	1.44
2	1007	300	289	292	291	290	292	3.93	1.34
3	5003	1457	1458	1455	1454	1464	1458	3.50	0.24
4	10020	2954	2966	2988	2987	2980	2975	13.11	0.44
5	$2.0 \cdot 10^4$	5386	5300	5268	5264	5248	5293	49.37	0.93

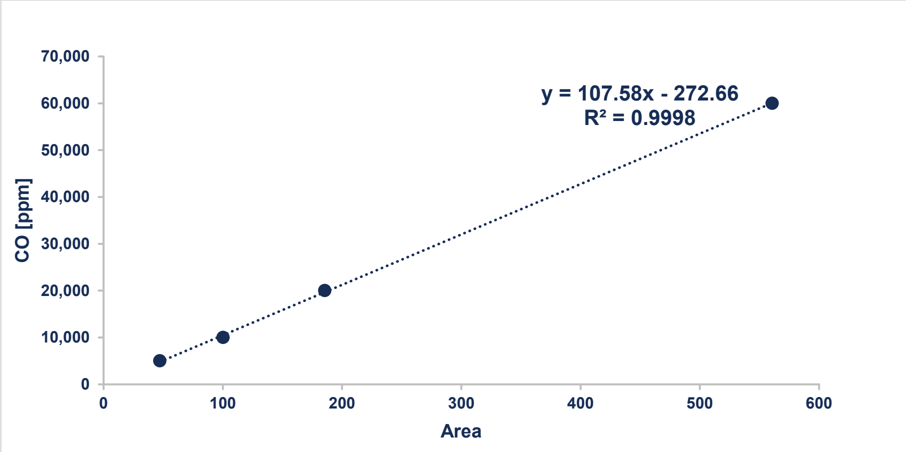

Calculation Example of Measured Inline GC Data

The concentration, C, of hydrogen and carbon monoxide is determined using the following calibration equations:

$$\text{For} \geq 60{,}000 \text{ ppm H}_2 \text{ (TCD)}: C_{\mathrm{H_2}} = 13.835 \cdot Area_{\mathrm{H_2}} - 20359$$

$$\text{For} < 60{,}000 \text{ ppm H}_2 \text{ (TCD)}: C_{\mathrm{H_2}} = 10.664 \cdot Area_{\mathrm{H_2}} - 48.021$$

$$\text{For} \geq 50{,}000 \text{ ppm CO (TCD)}: C_{\mathrm{CO}} = 102.05 \cdot Area_{\mathrm{CO}} + 2420.1$$

$$\text{For} < 50{,}000 \text{ ppm CO (FID)}: C_{\mathrm{CO}} = 3.7401 \cdot Area_{\mathrm{CO}} - 288.63$$

The total volumetric flow rate of gases into the inline GC, V_{tot}, is given by the sum of flow rates: the argon carrier gas, $\dot{V}_{\mathrm{Ar}}$, generated hydrogen, $\dot{V}_{\mathrm{H_2}}$, and generated carbon monoxide, $\dot{V}_{\mathrm{CO}}$, and is expressed as:

$$V_{tot} = \dot{V}_{\mathrm{Ar}} + \dot{V}_{\mathrm{H_2}} + \dot{V}_{\mathrm{CO}}$$

The volumetric contributions of generated hydrogen and carbon monoxide are defined as:

$$\dot{V}_{\mathrm{H_2}} = V_{tot} \cdot \frac{C_{\mathrm{H_2}}}{10^6}$$

$$\dot{V}_{\mathrm{CO}} = V_{tot} \cdot \frac{C_{\mathrm{CO}}}{10^6}$$

Substituting these expressions into the total flow equation yields:

$$V_{tot} = \dot{V}_{\mathrm{Ar}} + V_{tot} \cdot \frac{C_{\mathrm{H_2}}}{10^6} + V_{tot} \cdot \frac{C_{\mathrm{CO}}}{10^6}$$

And rearranging for V_{tot}:

$$V_{tot} = \frac{\dot{V}_{\mathrm{Ar}}}{1 - \frac{C_{\mathrm{H_2}}}{10^6} - \frac{C_{\mathrm{CO}}}{10^6}}$$

The molar quantities of hydrogen and carbon monoxide generated over a 20-minute interval are then calculated as:

$$n_{\mathrm{H_2}} = \frac{V_{tot} \cdot 20 \text{ min} \cdot \frac{C_{\mathrm{H_2}}}{10^6}}{V_m}$$

$$n_{CO} = \frac{V_{tot} \cdot 20\ \text{min} \cdot \frac{C_{CO}}{10^6}}{V_m}$$

Given that the molar volume, V_m, is determined using the ideal gas law:

$$V_m = \frac{R \cdot T}{P} = \frac{8.206 \cdot 10^{-2}\ \frac{\text{L} \cdot \text{atm}}{\text{K} \cdot \text{mol}} \cdot 293\ \text{K}}{1.00\ \text{atm}} = 24.04\ \frac{\text{L}}{\text{mol}}$$

These expressions enable the quantification of hydrogen and carbon monoxide production under the given experimental conditions.

Table S5. General data example. Using Ru-MACHO^{Ph} (20 µmol), *t*BuOK (200 µmol), methanol (20 mL), flow rate (2.50 mL/min), BPR (100 psi), and 150 °C for 3 hours.

Time [min]	Area		Concentration [ppm]		Total flow [mL/min]
	H_2	CO	H_2	CO	
0	47095	1580	631200	163659	24.37
20	39214	2489	522167	256423	22.58
40	37181	2427	494040	250095	19.54
60	35713	2379	473730	245197	17.79
80	34796	2235	461044	230502	16.21
100	33362	2165	441204	223358	14.91
120	33343	2056	440941	212235	14.42
140	31644	2007	417436	207234	13.32
160	31389	2001	413908	206622	13.18
180	29350	1877	385698	193968	11.90

Table S5. Continued.

Time [min]	*n* [mmol]		Ratio (H_2/CO)	TOF		Accumulated *n* [mmol]	
	H_2	CO		H_2	CO	H_2	CO
0	12.80	3.32	3.86	1920	498	12.80	3.32
20	9.81	4.82	2.04	1471	723	22.61	8.14
40	8.03	4.07	1.98	1205	610	30.64	12.20
60	7.01	3.63	1.93	1052	544	37.65	15.83
80	6.22	3.11	2.00	933	466	43.86	18.94
100	5.47	2.77	1.98	821	415	49.33	21.71
120	5.29	2.55	2.08	793	382	54.62	24.25
140	4.63	2.30	2.01	694	344	59.25	26.55
160	4.54	2.26	2.00	680	340	63.78	28.81
180	3.82	1.92	1.99	572	288	67.60	30.73

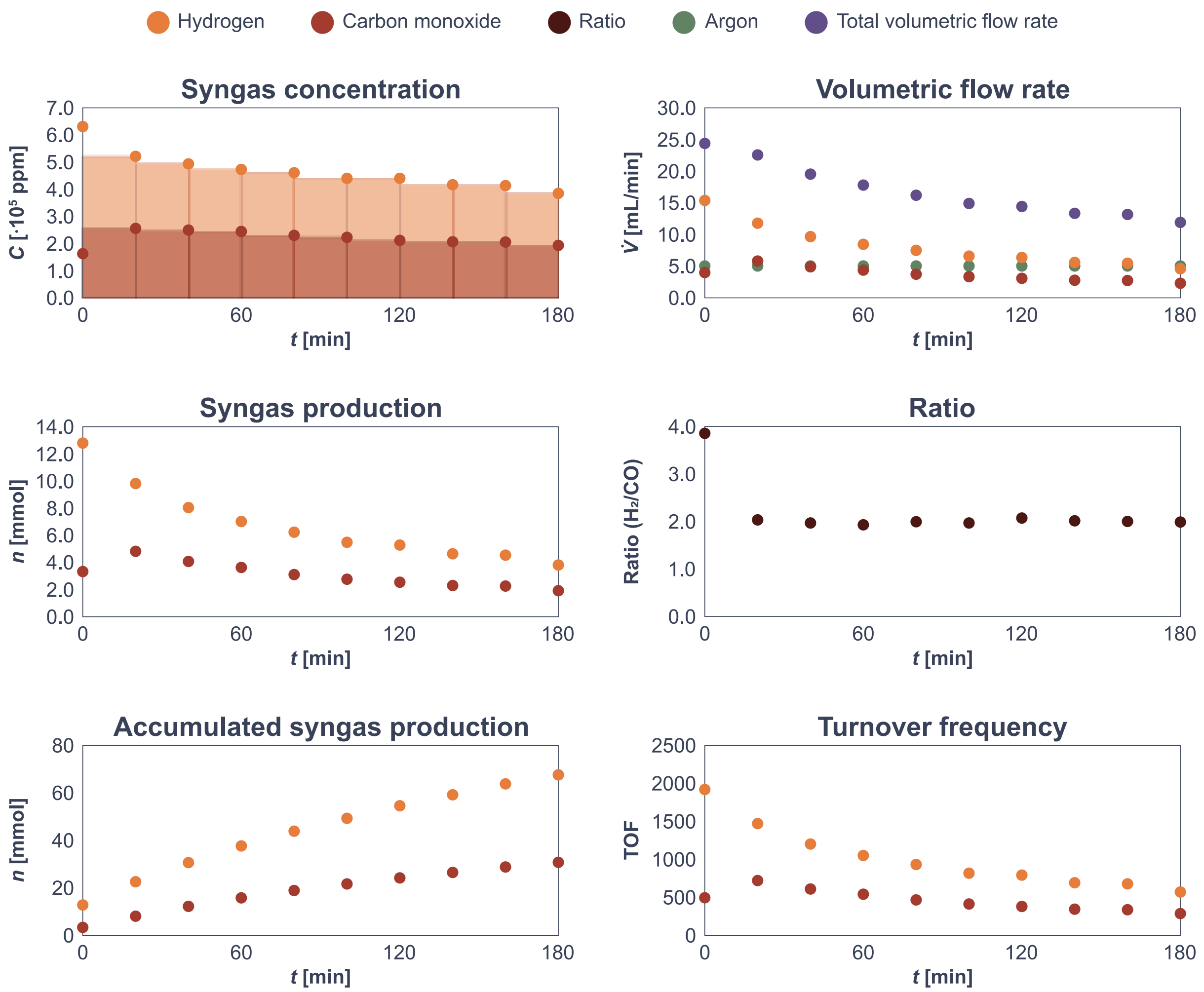

Figure S4. General data example. Using Ru-MACHO^{Ph} (20 µmol), *t*BuOK (200 µmol), methanol (20 mL), flow rate (2.50 mL/min), BPR (100 psi), and 150 °C for 3 hours.

Design of Experiments #1

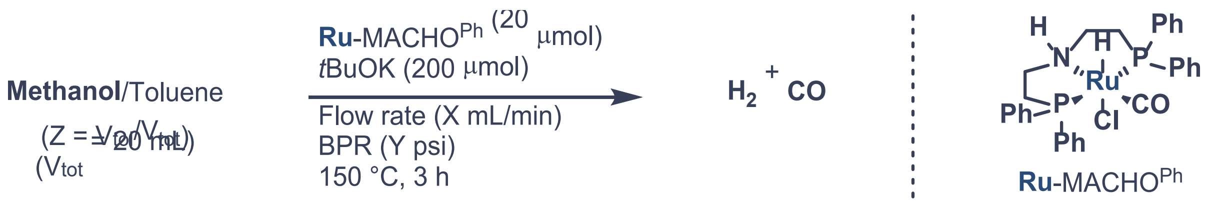

Inside a glovebox, a 20 mL GL-45 bottle (bottle A) was charged with Ru-MACHO^{Ph} (12.1 mg, 20 µmol), methanol and/or toluene (14 mL), and *t*BuOK (22.4 mg, 200 µmol). In addition, a 100 mL GL-45 bottle (bottle B) was charged with methanol (50 mL). Both bottles were capped and taken outside the glovebox.

Outside the glovebox, the back-pressure regulator was exchanged for the desired pressure (Y psi), and the flow system described above (Continuous Flow Setup) was flushed with methanol (100 mL) into a waste container under air. The gas-tight GL-45 lid was then transferred to bottle B, and the flow system was flushed again into a waste container by disconnecting the returning line at the Y-connection, while being extensively degassed using argon. After flushing methanol (40 mL), the returning line was reconnected to the Y-connection, restoring the closed-loop flow system. Once flushing was complete and the flow system filled with methanol (6 mL), the gas-tight GL-45 lid was transferred to bottle A, and the flow system was operated for 5 minutes at a flow rate of 10.00 mL/min. After 5 minutes, the flow rate

(X mL/min) was adjusted to the desired value, the mass flow controller changed to 5.00 mL/min, and the inline GC connected. Following an additional 5 minutes of operation under the desired conditions, the inline GC was started, and the composition of the produced syngas was measured at 20-minute intervals.

Table S6. Summary of results for the first DoE.

#	Flow rate [X mL/min]	BPR [Y psi]	Dilution [Z = V_{tol}/V_{tot}]	*n* [mmol] H_2	*n* [mmol] CO	Ratio (H_2/CO)
1	2.50	500	0.50	7.31	3.10	2.35
2	1.00	100	0.50	59.31	28.31	2.09
3	1.00	250	0.70	4.95	1.92	2.57
4	2.50	500	0.20	3.80	1.57	2.42
5	4.00	250	0.20	4.61	1.66	2.77
6	2.50	1000	0.20	3.27	1.18	2.77
7	2.50	100	0.00	54.80	27.41	2.00
8	1.00	1000	0.00	1.56	0.56	2.80
9	4.00	1000	0.70	8.21	2.34	3.52
10	1.00	500	0.20	2.45	0.94	2.62
11	0.50	250	0.00	1.18	0.32	3.63
12	2.50	500	0.50	5.76	1.86	3.10
13	4.00	1000	0.00	2.81	1.20	2.35
14	0.50	1000	0.50	2.08	0.51	4.06
15	1.00	1000	0.70	4.75	1.88	2.52
16	4.00	100	0.70	34.15	13.64	2.50

Design of Experiments #2

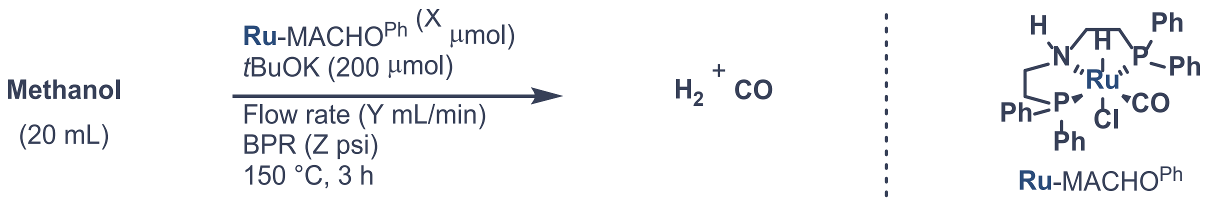

Inside a glovebox, a catalyst stock solution of Ru-MACHO^{Ph} in methanol (0.50 mL / 1.0 µmol catalyst) was prepared by stirring until a homogenous suspension was obtained. To a 20 mL GL-45 bottle (bottle A) charged with *t*BuOK (22.4 mg, 200 µmol), was added Ru-MACHO^{Ph} stock solution (X µmol) via syringe, followed by dilution with methanol to a total of volume of 14 mL. In addition, a 100 mL GL-45 bottle (bottle B) was charged with methanol (50 mL). Both bottles were capped and taken outside the glovebox.

Outside the glovebox, the back-pressure regulator was exchanged for the desired pressure (Z psi), the flow system described above (Continuous Flow Setup) was flushed with methanol (100 mL) into a waste container under air. The gas-tight GL-45 lid was then transferred to bottle B, and the flow system was flushed again into a waste container by disconnecting the returning line at the Y-connection, while being extensively degassed using argon. After flushing methanol (40 mL), the returning line was reconnected to the Y-connection, restoring the closed-loop flow system. Once flushing was complete and the flow system filled with methanol (6 mL), the gas-tight GL-45 lid was transferred to bottle A, and the flow system was operated for 5 minutes at a flow rate of 10.00 mL/min. After 5 minutes, the flow rate (Y mL/min) was adjusted to the desired value, the mass flow controller changed to 5.00 mL/min, and the inline GC connected. Following an additional 5 minutes of operation under the desired conditions, the inline GC was started, and the composition of the produced syngas was measured at 20-minute intervals.

Table S7. Summary of results for the second DoE.

#	Catalyst loading [X µmol]	Flow rate [Y mL/min]	BPR [Z psi]	*n* [mmol] H_2	*n* [mmol] CO	Ratio (H_2/CO)
1	2.0	1.00	100	29.94	14.82	2.02
2	2.0	4.00	100	30.24	15.02	2.01
3	2.0	2.50	75	32.44	16.14	2.01
4	20	2.50	100	67.29	34.52	1.95
5	2.0	2.50	40	11.94	5.96	2.00
6	0.20	2.50	75	8.93	4.30	2.08
7	2.0	4.00	75	29.76	14.63	2.03
8	0.20	1.00	100	7.58	3.65	2.08
9	0.20	4.00	100	8.66	4.02	2.15
10	0.20	4.00	40	2.69	1.44	1.87
11	20	1.00	40	11.73	6.35	1.85
12	0.20	2.50	100	8.86	4.33	2.05
13	20	4.00	40	16.26	8.23	1.98
14	2.0	1.00	75	27.04	13.60	1.99
15	2.0	2.50	40	9.98	4.97	2.01
16	0.20	1.00	40	2.94	1.47	2.00

General Procedure for Ru-MACHO^R Complex Scope

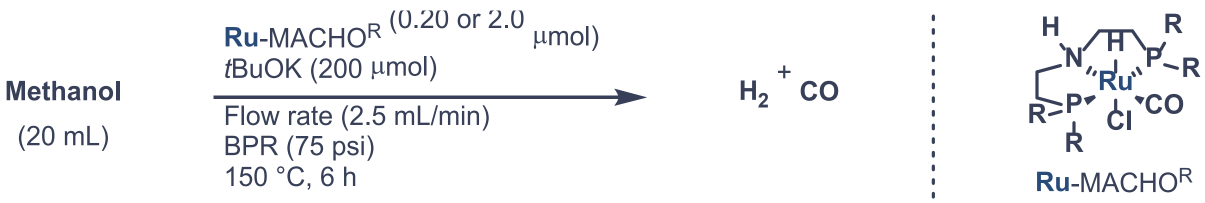

Inside a glovebox, a catalyst stock solution of Ru-MACHO-derivative in methanol (0.50 mL / 1.0 µmol catalyst) was prepared by stirring until a homogenous solution or suspension was obtained. To a 20 mL GL-45 bottle (bottle A) charged with *t*BuOK (22.4 mg, 200 µmol), was added Ru-MACHO-derivative stock solution (2.0 or 0.20 µmol) via syringe, followed by dilution with methanol to a total of volume of 14 mL. In addition, a 100 mL GL-45 bottle (bottle B) was charged with methanol (50 mL). Both bottles were capped and taken outside the glovebox.

Outside the glovebox, the flow system described above (Continuous Flow Setup) equipped with a back-pressure regulator (75 psi), was flushed with methanol (100 mL) into a waste container under air. The gas-tight GL-45 lid was then transferred to bottle B, and the flow system was flushed again into a waste container by disconnecting the returning line at the Y-connection, while being extensively degassed using argon. After flushing methanol (40 mL), the returning line was reconnected to the Y-connection, restoring the closed-loop flow system. Once flushing was complete and the flow system filled with methanol (6 mL), the gas-tight GL-45 lid was transferred to bottle A, and the flow system was operated for 5 minutes at a flow rate of 10.00 mL/min. After 5 minutes, the flow rate was adjusted to 2.50 mL/min, the mass flow controller changed to 5.00 mL/min, and the inline GC connected. Following an additional 5 minutes of operation under the desired conditions, the inline GC was started, and the composition of the produced syngas was measured at 20-minute intervals.

Table S8. Summary of results for Ru-MACHO^{R} (2.0 µmol). All entries are given as an average of two.

Time [min]	Ru-MACHO^{Ph} TOF [h^{-1}] H_2	Ru-MACHO^{Ph} TOF [h^{-1}] CO	Ru-MACHO^{Ph} Ratio (H_2/CO)	Ru-MACHO$^{p(Me)}$ TOF [h^{-1}] H_2	Ru-MACHO$^{p(Me)}$ TOF [h^{-1}] CO	Ru-MACHO$^{p(Me)}$ Ratio (H_2/CO)
0	9693	2698	3.60	6888	1749	3.93
20	9198	4490	2.06	6834	3195	2.14
40	7856	3953	1.99	6370	3140	2.03
60	6850	3462	1.98	5899	2912	2.03
80	6276	3181	1.97	5382	2669	2.02
100	5400	2726	1.98	5190	2592	2.00
120	4911	2507	1.96	4958	2464	2.01
140	4153	2088	1.99	4342	2147	2.02
160	3803	1925	1.98	4024	1992	2.02
180	3165	1582	2.00	3755	1860	2.02
200	2942	1493	1.97	3404	1688	2.02
220	2459	1237	1.99	3214	1594	2.02
240	2167	1087	1.99	3017	1494	2.02
260	1954	989	1.98	2710	1331	2.04
280	1694	861	1.97	2441	1196	2.04
300	1408	709	1.99	2265	1119	2.03
320	1254	636	1.97	2100	1046	2.01
340	1113	568	1.96	1952	965	2.02
360	1003	512	1.96	1753	867	2.02

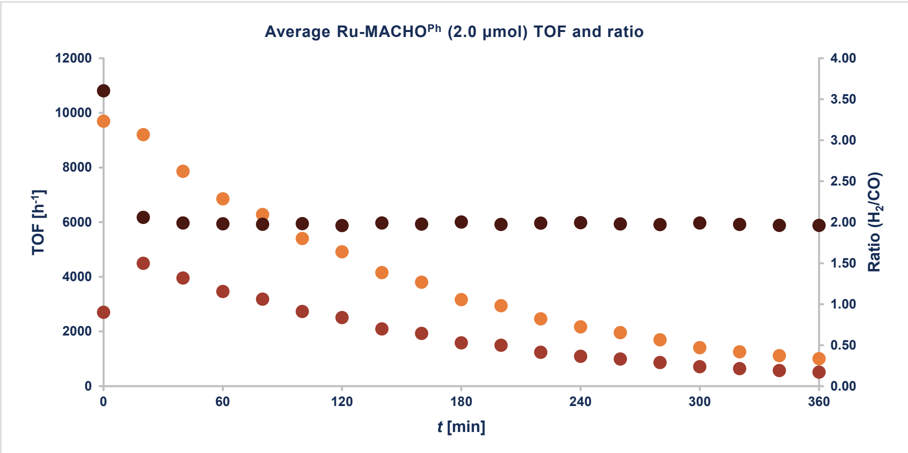

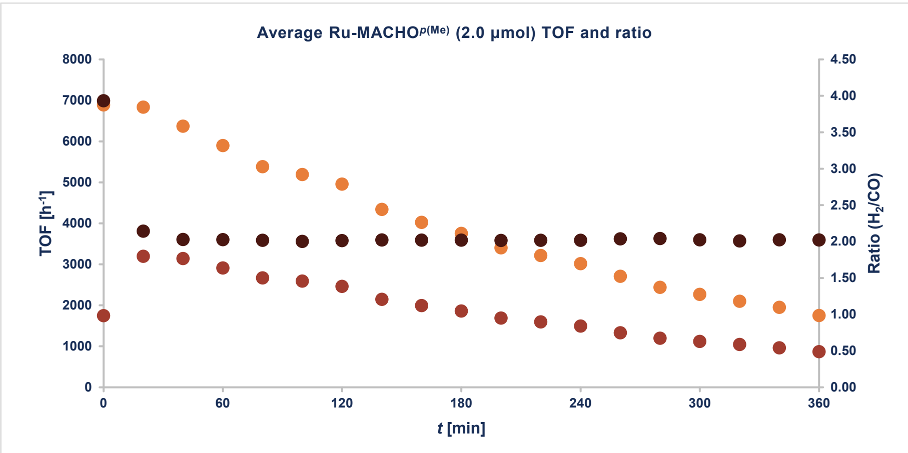

Table S8. Summary of results for Ru-MACHO^R (2.0 µmol). *Continued*.

Time [min]	Ru-MACHO$^{m,m(Me)}$ TOF [h^{-1}] H_2	CO	Ratio (H_2/CO)	Ru-MACHO$^{p(iPr)}$ TOF [h^{-1}] H_2	CO	Ratio (H_2/CO)
0	6570	1706	3.86	6587	1743	3.84
20	6067	2818	2.15	6841	3288	2.10
40	5938	2877	2.06	6177	3055	2.03
60	5622	2774	2.03	5519	2753	2.01
80	5286	2589	2.04	5018	2494	2.02
100	5065	2489	2.04	4395	2182	2.02
120	4776	2340	2.04	4280	2143	2.00
140	4350	2135	2.04	3580	1776	2.02
160	4099	2015	2.03	3191	1581	2.02
180	3864	1900	2.03	2933	1450	2.02
200	3626	1778	2.04	2698	1326	2.04
220	3499	1709	2.05	2417	1203	2.01
240	3223	1574	2.05	2226	1099	2.02
260	2985	1467	2.03	2019	1003	2.01
280	2741	1338	2.05	1795	884	2.03
300	2681	1317	2.04	1598	792	2.02
320	2509	1233	2.04	1509	757	1.99
340	2297	1124	2.04	1382	689	2.01
360	2154	1058	2.04	1235	618	2.00

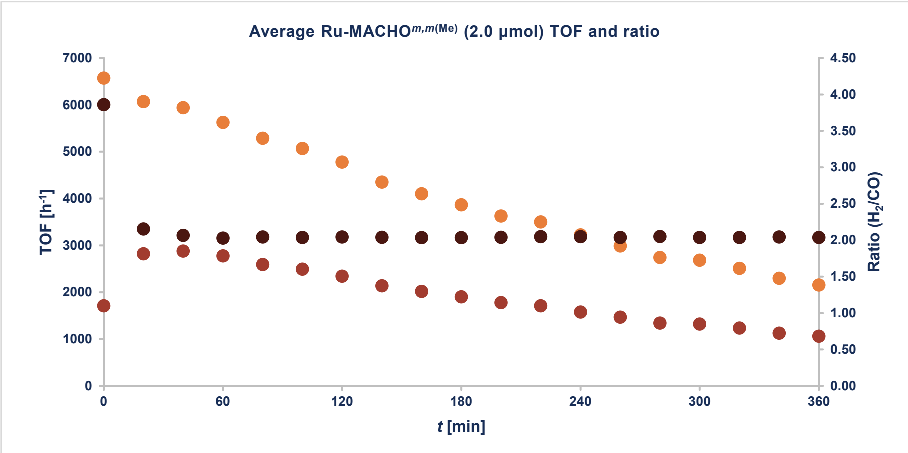

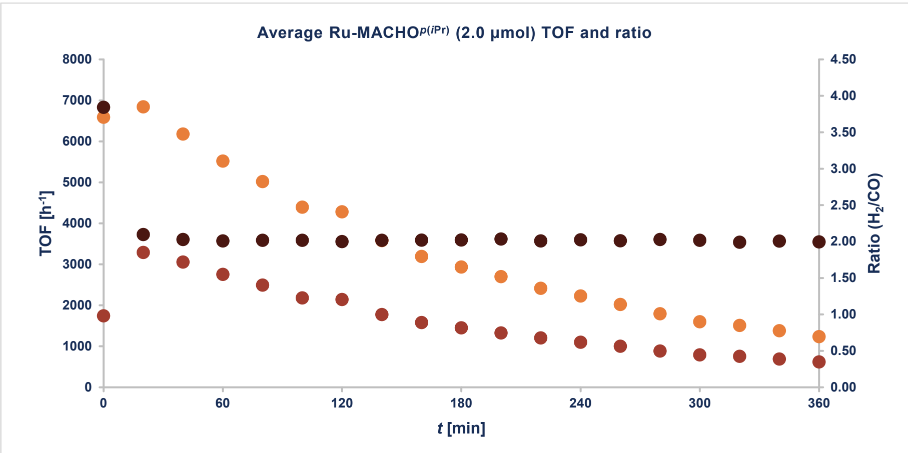

Table S8. Summary of results for Ru-MACHO^R (2.0 µmol). *Continued*.

Time [min]	Ru-MACHO$^{p(3\text{-Pe})}$ TOF [h^{-1}] H_2	CO	Ratio (H_2/CO)	Ru-MACHO^{Naph} TOF [h^{-1}] H_2	CO	Ratio (H_2/CO)
0	5858	790	7.47	3014	538	5.64
20	7435	2720	2.72	4599	2062	2.23
40	6252	2849	2.20	3531	1788	1.98
60	5156	2566	2.02	3006	1538	1.96
80	4548	2346	1.94	2541	1292	1.96
100	4650	2401	1.95	2233	1116	2.00
120	3810	1957	1.95	1966	994	1.98
140	3503	1811	1.94	1784	880	2.03
160	3386	1715	1.98	1617	825	1.96
180	3140	1590	1.98	1506	733	2.06
200	2833	1438	1.97	1390	679	2.05
220	2653	1370	1.93	1309	642	2.04
240	2544	1283	1.98	1243	593	2.10
260	2231	1143	1.95	1183	585	2.02
280	2030	1049	1.93	1137	554	2.05
300	1898	975	1.95	1078	545	1.98
320	1771	903	1.96	1024	504	2.03
340	1615	838	1.93	993	492	2.02
360	1491	771	1.93	944	473	2.00

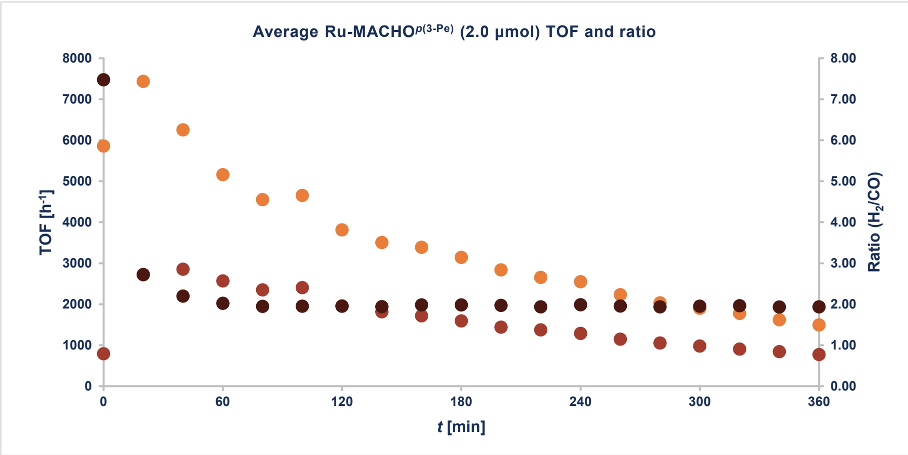

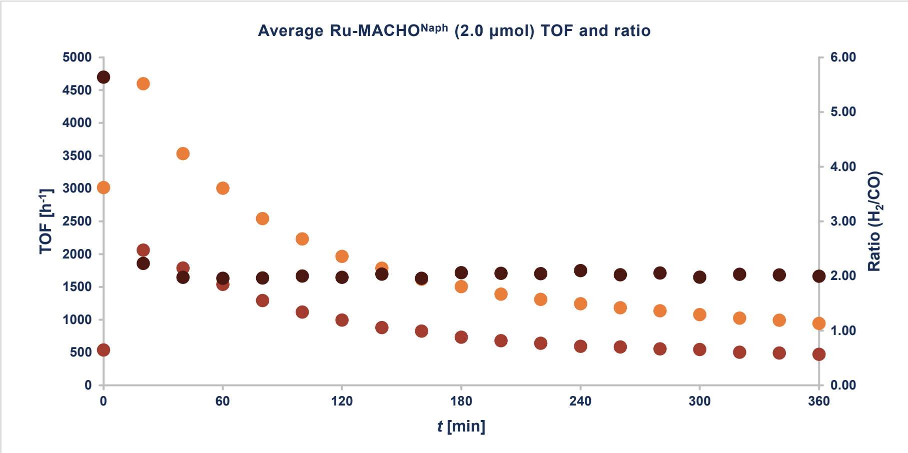

Table S8. Summary of results for Ru-MACHO[R] (2.0 μmol). *Continued*.

Time [min]	Ru-MACHO[Biph] TOF [h^{-1}] H_2	CO	Ratio (H_2/CO)	Ru-MACHO[p(CF3)] TOF [h^{-1}] H_2	CO	Ratio (H_2/CO)
0	3612	942	3.85	2470	599	4.12
20	5235	2409	2.17	3662	1624	2.25
40	3937	2016	1.95	3473	1641	2.12
60	3216	1643	1.96	3342	1617	2.07
80	2685	1374	1.95	3192	1555	2.05
100	2287	1164	1.97	3055	1452	2.10
120	1994	994	2.01	2906	1400	2.08
140	1763	888	1.98	2745	1322	2.08
160	1568	782	2.01	2585	1270	2.04
180	1409	716	1.97	2428	1186	2.05
200	1274	633	2.01	2236	1093	2.05
220	1161	586	1.98	2060	1019	2.02
240	1048	523	2.01	1887	929	2.03
260	969	492	1.97	1672	833	2.01
280	885	455	1.95	1488	753	1.98
300	811	415	1.96	1275	649	1.96
320	746	387	1.93	1055	545	1.93
340	680	362	1.88	870	470	1.85
360	624	326	1.91	682	376	1.81

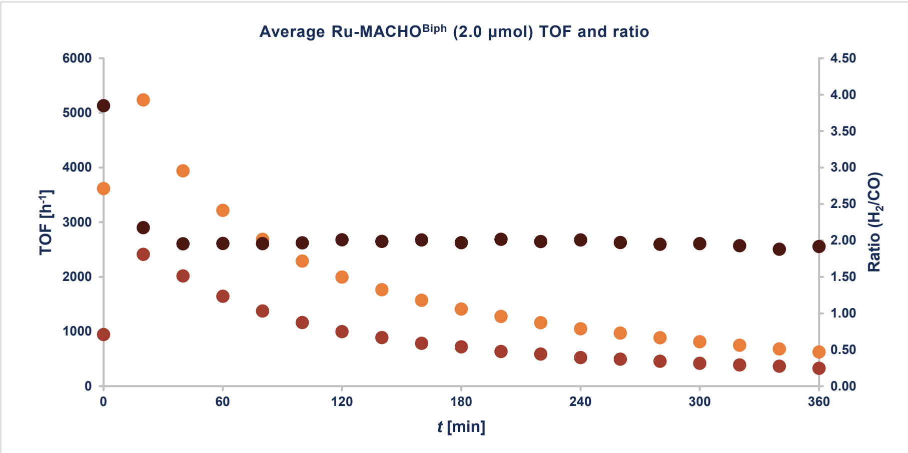

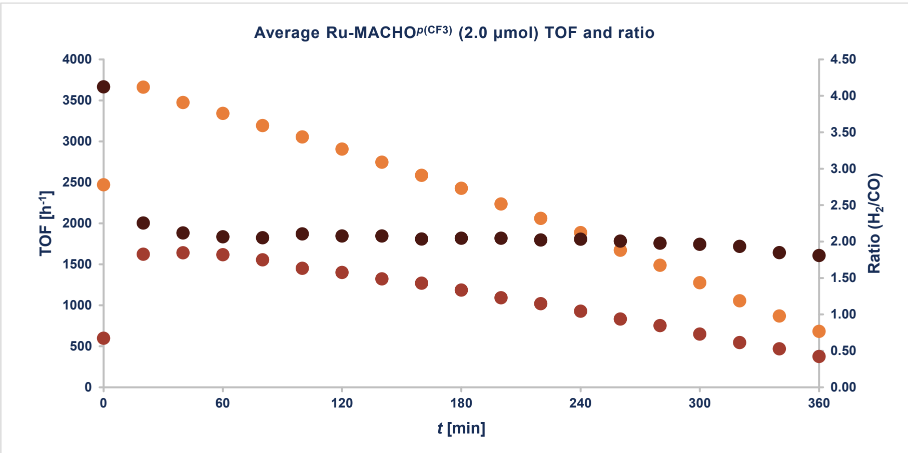

Table S8. Summary of results for Ru-MACHO^R (2.0 µmol). *Continued*.

Time [min]	Ru-MACHO$^{p(OMe)}$ TOF [h^{-1}] H$_2$	CO	Ratio (H$_2$/CO)	Ru-MACHO^{Et} TOF [h^{-1}] H$_2$	CO	Ratio (H$_2$/CO)
0	6134	1516	4.08	1568	168	9.83
20	5609	2553	2.20	2751	1073	2.57
40	5252	2549	2.06	2548	1156	2.21
60	4950	2465	2.01	2453	1130	2.17
80	4905	2434	2.02	2407	1112	2.17
100	4644	2281	2.04	2347	1069	2.20
120	4272	2096	2.04	2269	1044	2.18
140	3886	1911	2.03	2209	1022	2.16
160	3666	1804	2.03	2061	954	2.16
180	3531	1740	2.03	1953	913	2.14
200	3289	1614	2.04	2148	986	2.18
220	3037	1479	2.05	1951	896	2.18
240	2765	1352	2.04	1829	848	2.16
260	2608	1281	2.04	1837	837	2.20
280	2466	1217	2.03	1847	828	2.23
300	2364	1162	2.04	1808	824	2.19
320	2209	1081	2.04	1651	774	2.13
340	2118	1033	2.05	1567	735	2.13
360	1919	940	2.04	1579	751	2.10

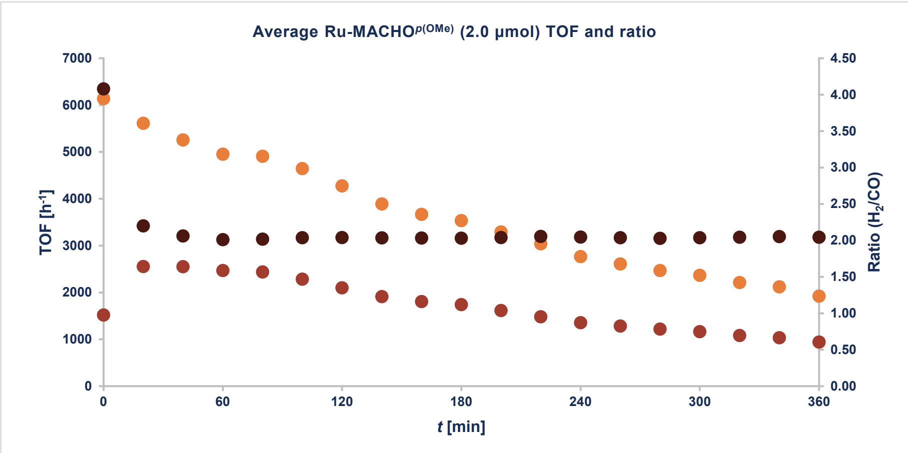

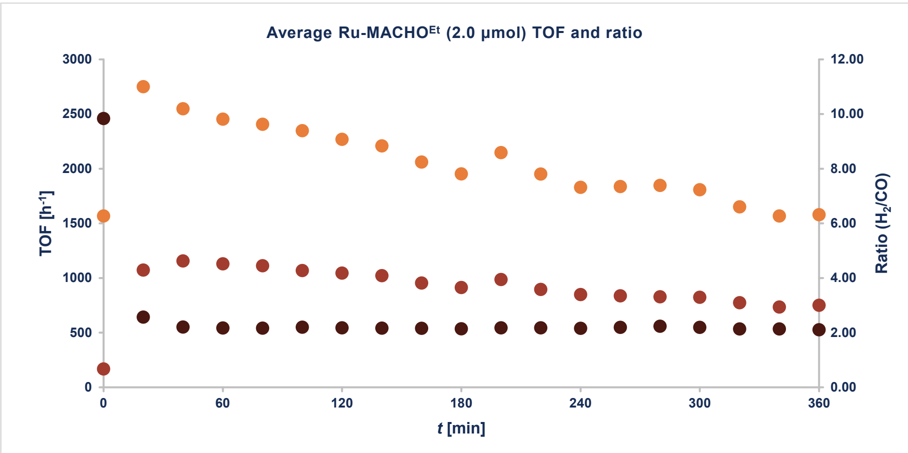

Table S8. Summary of results for Ru-MACHO^{R} (2.0 µmol). *Continued*.

Time [min]	Ru-MACHO^{iPr} TOF [h^{-1}] H_2	Ru-MACHO^{iPr} TOF [h^{-1}] CO	Ru-MACHO^{iPr} Ratio (H_2/CO)	Ru-MACHO^{iBu} TOF [h^{-1}] H_2	Ru-MACHO^{iBu} TOF [h^{-1}] CO	Ru-MACHO^{iBu} Ratio (H_2/CO)
0	4506	1713	3.19	765	119	6.41
20	6129	2924	2.09	820	256	3.19
40	5778	2792	2.07	319	144	2.22
60	5593	2722	2.05	276	114	2.41
80	5367	2639	2.03	239	101	2.38
100	5177	2543	2.03	218	93	2.34
120	4963	2415	2.05	202	87	2.33
140	4700	2307	2.04	192	82	2.35
160	4539	2221	2.04	180	78	2.30
180	4267	2084	2.05	170	74	2.33
200	4130	2027	2.04	165	71	2.32
220	3921	1909	2.05	155	68	2.29
240	3645	1774	2.05	146	64	2.28
260	3456	1694	2.04	140	60	2.36
280	3265	1611	2.03	130	57	2.32
300	3081	1510	2.04	128	55	2.37
320	2964	1438	2.06	118	51	2.33
340	2690	1325	2.03	115	49	2.38
360	2444	1218	2.00	107	47	2.34

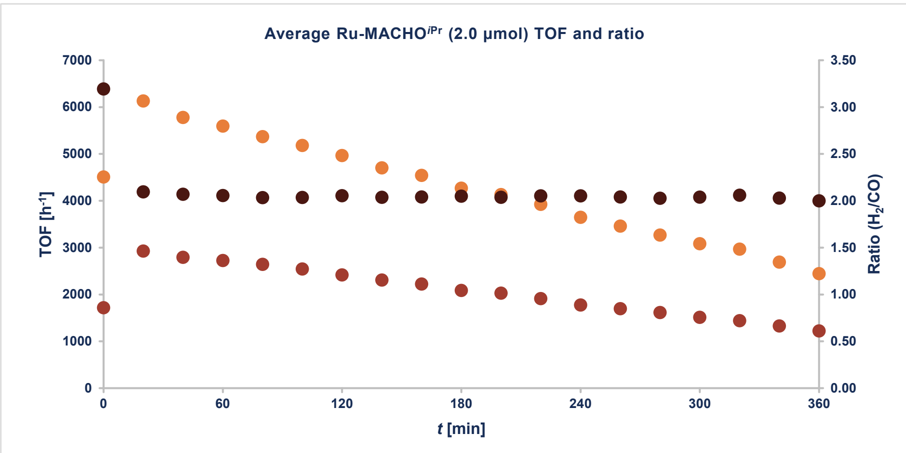

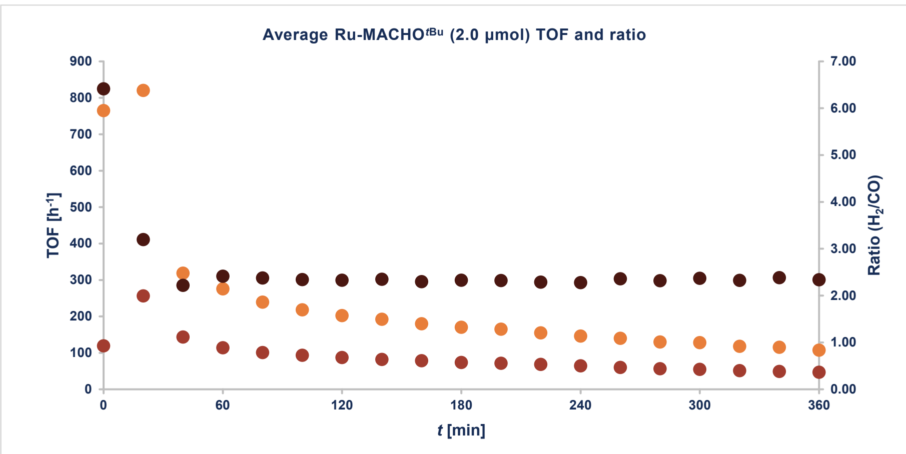

Table S8. Summary of results for Ru-MACHO^{R} (2.0 µmol). *Continued*.

Time [min]	Ru-MACHO^{Cy} TOF [h^{-1}] H_2	CO	Ratio (H_2/CO)	Ru-MACHO^{Ad} TOF [h^{-1}] H_2	CO	Ratio (H_2/CO)
0	2725	605	4.56	208	22	11.16
20	4634	2102	2.20	515	162	3.19
40	4947	2313	2.14	246	105	2.33
60	4418	2074	2.13	164	74	2.21
80	4520	2139	2.11	133	61	2.19
100	4706	2216	2.12	122	55	2.20
120	4489	2111	2.13	115	52	2.21
140	4211	1989	2.12	111	50	2.20
160	4456	2107	2.11	107	49	2.21
180	4290	2016	2.13	108	49	2.21
200	3828	1812	2.11	103	47	2.18
220	4053	1903	2.13	99	45	2.19
240	3771	1772	2.13	97	45	2.16
260	3623	1706	2.12	96	44	2.17
280	3828	1794	2.13	92	42	2.19
300	3435	1612	2.13	89	41	2.18
320	3301	1568	2.10	87	40	2.17
340	3404	1598	2.13	85	39	2.19
360	3046	1436	2.12	80	37	2.20

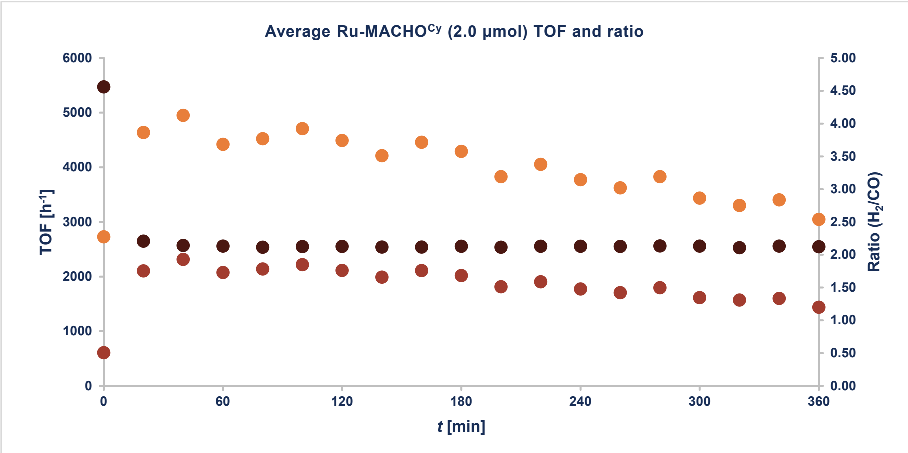

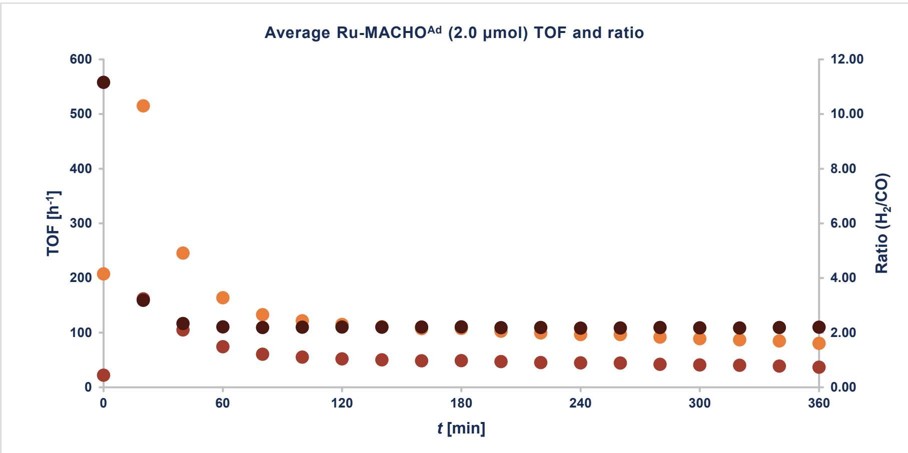

Table S9. Summary of results for Ru-MACHO[R] (0.20 µmol). All entries are given as an average of two.

Time [min]	Ru-MACHO[Ph] TOF [h⁻¹] H_2	Ru-MACHO[Ph] TOF [h⁻¹] CO	Ru-MACHO[Ph] Ratio (H_2/CO)	Ru-MACHO[p(Me)] TOF [h⁻¹] H_2	Ru-MACHO[p(Me)] TOF [h⁻¹] CO	Ru-MACHO[p(Me)] Ratio (H_2/CO)
0	6099	1012	5.93	8120	1342	6.06
20	21883	8787	2.51	19332	8212	2.36
40	19520	9355	2.09	17906	8436	2.12
60	17097	8423	2.03	17031	7922	2.15
80	14605	7283	2.01	15476	7236	2.14
100	12635	6392	1.98	13968	6638	2.10
120	10379	5342	1.94	12989	6385	2.03
140	8628	4555	1.89	12256	5998	2.04
160	7049	3698	1.90	11364	5341	2.13
180	5694	2897	1.94	9970	4801	2.08
200	4740	2452	1.91	8998	4571	1.97
220	3845	2056	1.86	8405	4114	2.05
240	3233	1747	1.85	7252	3324	2.18
260	2848	1532	1.87	6478	3074	2.11
280	2424	1296	1.88	5706	2816	2.03
300	2154	1148	1.89	5070	2594	1.95
320	1916	1012	1.91	4434	2352	1.88
340	1701	885	1.94	3911	2132	1.84
360	1549	796	1.96	3451	1920	1.80

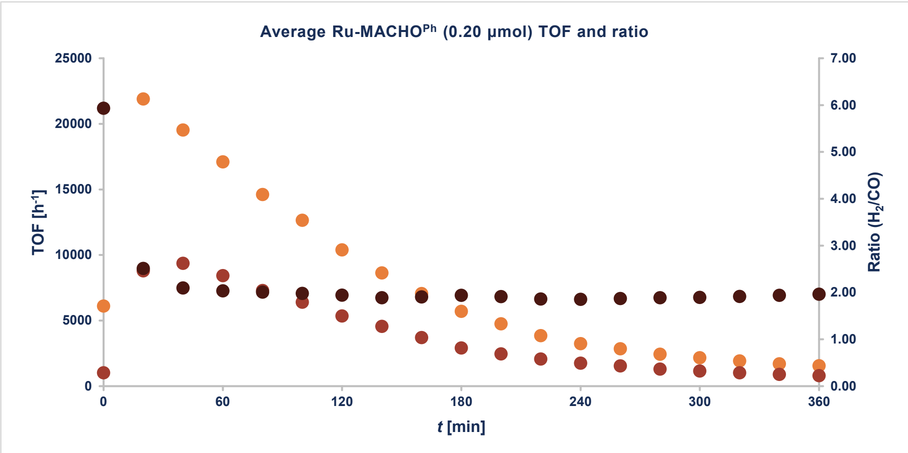

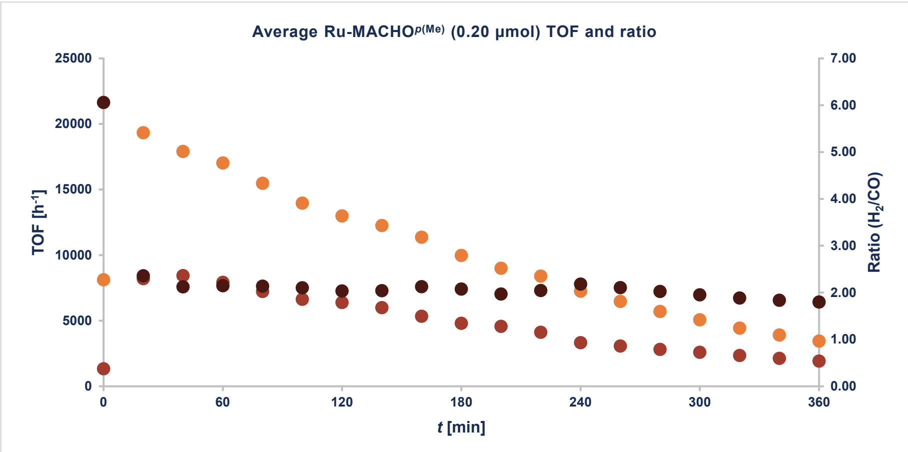

Table S9. Summary of results for Ru-MACHO^R (0.20 µmol). *Continued*.

Time [min]	Ru-MACHO$^{m,m(\mathrm{Me})}$ TOF [h^{-1}] H_2	CO	Ratio (H_2/CO)	Ru-MACHO$^{p(i\mathrm{Pr})}$ TOF [h^{-1}] H_2	CO	Ratio (H_2/CO)
0	5594	798	7.38	5547	856	6.55
20	14575	4974	2.94	19927	7822	2.56
40	13394	5961	2.25	18992	8870	2.15
60	12355	5867	2.11	17448	8401	2.08
80	11782	5692	2.07	16243	7888	2.06
100	10884	5328	2.04	14662	7210	2.03
120	10145	5016	2.02	13201	6508	2.03
140	9270	4656	1.99	11933	5953	2.00
160	8402	4260	1.97	10681	5395	1.98
180	7739	3735	2.09	9510	4838	1.96
200	7150	3257	2.19	8616	4444	1.94
220	6606	3076	2.15	7310	3663	2.00
240	5969	2856	2.09	6371	3086	2.06
260	5314	2646	2.01	5621	2821	1.98
280	4651	2418	1.92	5015	2562	1.95
300	4160	2195	1.90	4431	2301	1.92
320	3818	2013	1.90	3854	2047	1.88
340	3587	1903	1.88	3511	1866	1.88
360	3168	1684	1.88	3224	1710	1.89

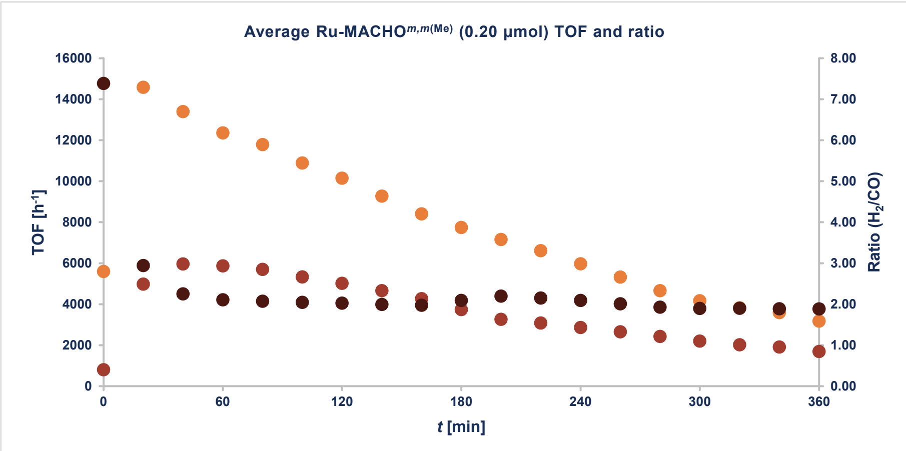

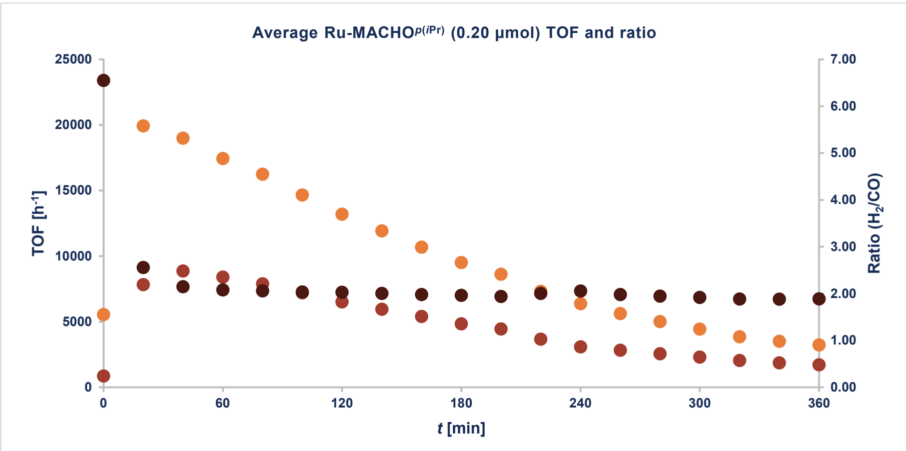

Table S9. Summary of results for Ru-MACHO^{R} (0.20 µmol). *Continued*.

Time [min]	Ru-MACHO$^{p(3\text{-Pe})}$ TOF [h^{-1}] H_2	CO	Ratio (H_2/CO)	Ru-MACHO^{Naph} TOF [h^{-1}] H_2	CO	Ratio (H_2/CO)
0	3182	331	9.67	1701	180	10.29
20	13229	4966	2.73	8837	2338	3.79
40	13005	5708	2.28	10397	4184	2.49
60	12153	5591	2.17	9769	4533	2.15
80	11391	5386	2.11	9008	4479	2.01
100	10806	5215	2.07	8172	4120	1.98
120	10449	4985	2.10	7549	3653	2.09
140	9642	4687	2.06	6856	3369	2.05
160	8979	4409	2.04	6412	2968	2.15
180	8623	4273	2.02	5981	2821	2.11
200	8022	3761	2.15	5391	2605	2.06
220	7247	3199	2.27	5061	2509	2.01
240	6789	3054	2.22	4803	2399	2.00
260	6323	2913	2.17	4404	2227	1.98
280	5945	2792	2.13	4060	2080	1.95
300	5384	2607	2.07	3784	1969	1.93
320	5024	2492	2.02	3523	1813	1.94
340	4546	2321	1.96	3333	1733	1.93
360	4233	2184	1.94	3099	1611	1.93

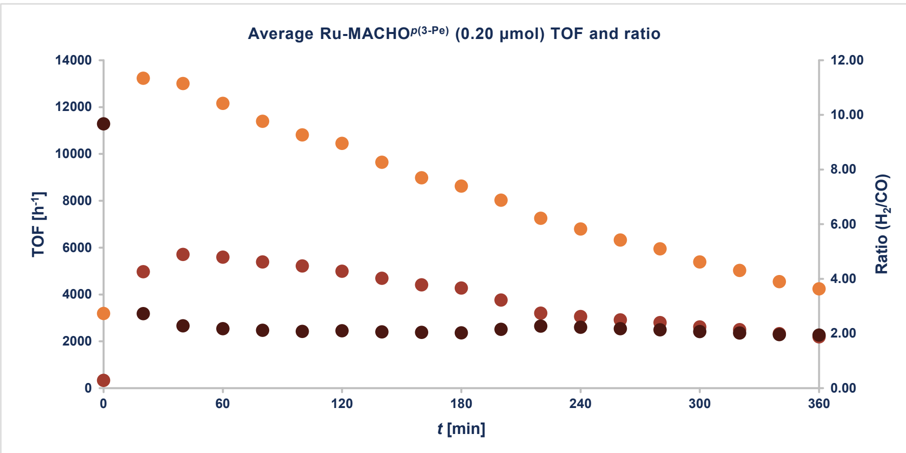

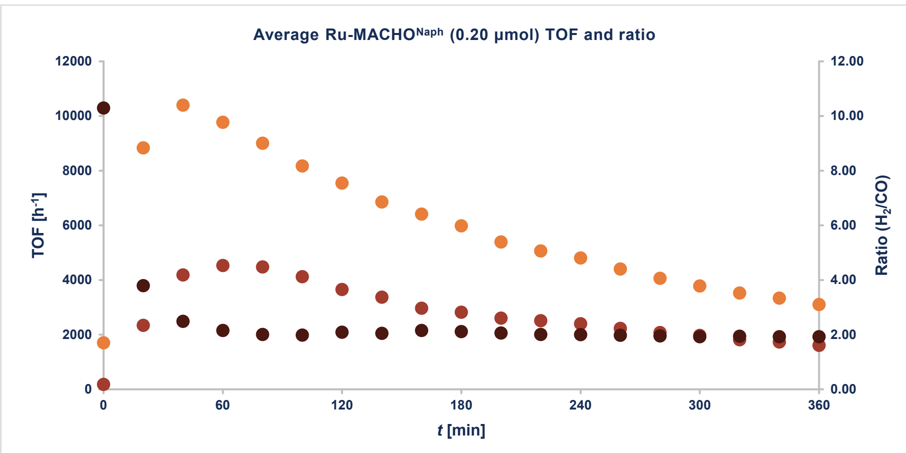

Table S9. Summary of results for Ru-MACHO^{R} (0.20 µmol). *Continued.*

Time [min]	Ru-MACHO^{Biph} TOF [h^{-1}] H_2	CO	Ratio (H_2/CO)	Ru-MACHO$^{p(CF3)}$ TOF [h^{-1}] H_2	CO	Ratio (H_2/CO)
0	3417	496	7.18	2747	366	7.52
20	10055	3023	3.35	7908	2562	3.08
40	9136	3873	2.37	6569	2762	2.37
60	7417	3516	2.12	5103	2504	2.03
80	6068	2656	2.31	4012	2137	1.87
100	4708	2416	1.94	3133	1722	1.82
120	3933	2121	1.86	2439	1379	1.76
140	3288	1788	1.84	1856	1043	1.78
160	2767	1504	1.84	1422	784	1.82
180	2315	1244	1.86	1155	628	1.84
200	1966	1061	1.86	966	508	1.90
220	1679	893	1.88	827	424	1.95
240	1447	757	1.91	730	364	2.00
260	1264	649	1.95	666	326	2.04
280	1129	576	1.96	617	296	2.08
300	1021	514	1.98	584	278	2.10
320	935	468	2.00	552	261	2.11
340	816	391	2.09	524	245	2.14
360	777	382	2.03	502	234	2.15

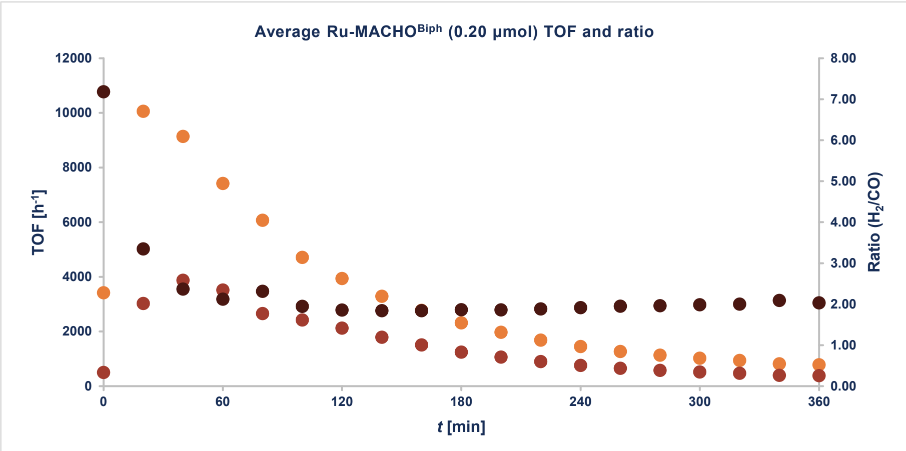

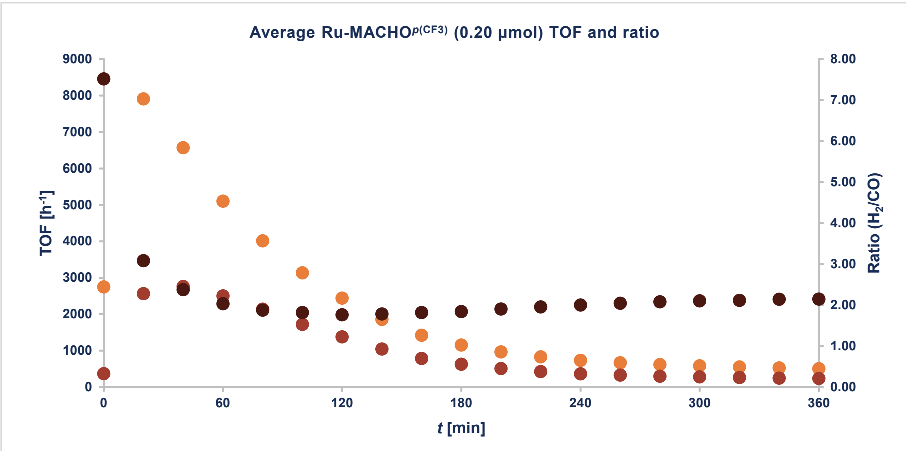

Table S9. Summary of results for Ru-MACHO[R] (0.20 µmol). *Continued*.

Time [min]	Ru-MACHO$^{p(OMe)}$ TOF [h^{-1}] H_2	Ru-MACHO$^{p(OMe)}$ TOF [h^{-1}] CO	Ru-MACHO$^{p(OMe)}$ Ratio (H_2/CO)	Ru-MACHO^{Et} TOF [h^{-1}] H_2	Ru-MACHO^{Et} TOF [h^{-1}] CO	Ru-MACHO^{Et} Ratio (H_2/CO)
0	4510	698	6.48	2166	206	11.03
20	13659	5037	2.71	9654	2179	4.43
40	12496	5666	2.21	7809	2362	3.30
60	12315	5905	2.09	7087	2369	2.99
80	11121	5441	2.04	6887	2385	2.89
100	10515	5212	2.02	6522	2327	2.80
120	9290	4707	1.97	6466	2355	2.74
140	8613	4339	1.99	5907	2235	2.64
160	7983	4074	1.96	5815	2208	2.63
180	7235	3509	2.08	5522	2132	2.58
200	6417	2952	2.17	5007	2023	2.47
220	5977	2834	2.11	4820	1966	2.45
240	5230	2582	2.03	4894	1988	2.46
260	4665	2391	1.95	4743	1967	2.41
280	4290	2248	1.91	4434	1860	2.38
300	4035	2090	1.93	4367	1854	2.36
320	3718	1936	1.92	4271	1835	2.33
340	3276	1715	1.91	4135	1799	2.30
360	2974	1560	1.91	4123	1803	2.28

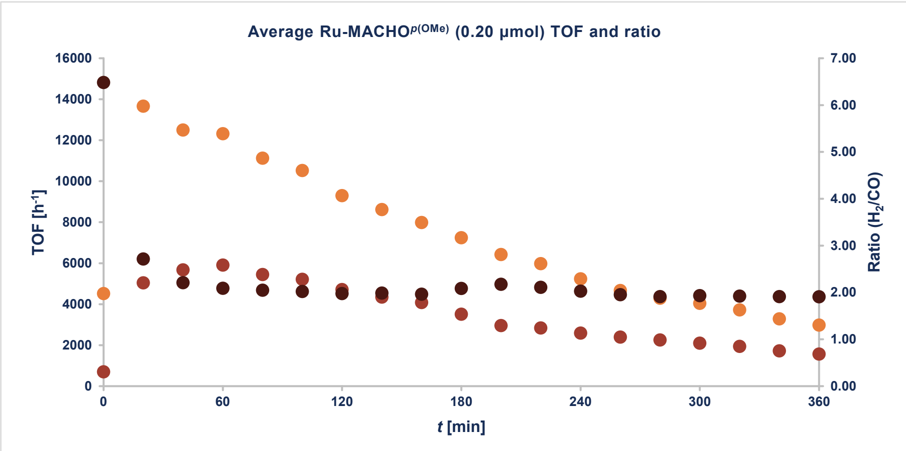

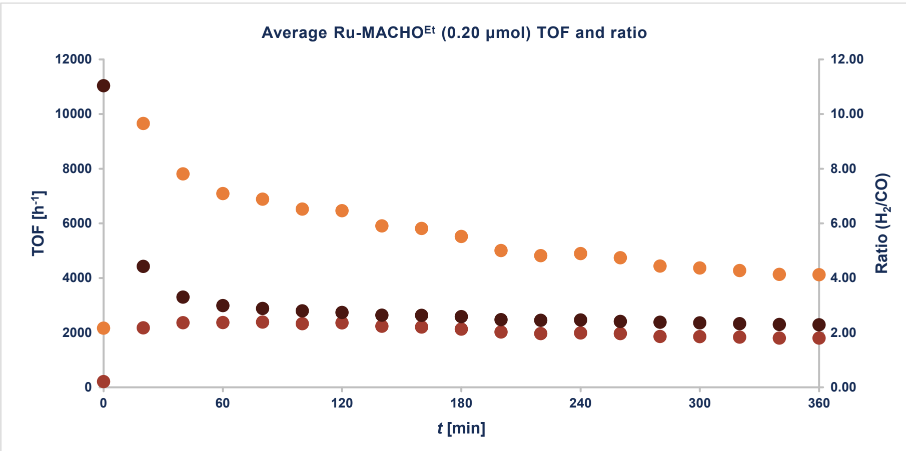

Table S9. Summary of results for Ru-MACHO^{R} (0.20 µmol). *Continued.*

Time [min]	Ru-MACHO^{iPr} TOF [h^{-1}] H_2	CO	Ratio (H_2/CO)	Ru-MACHO^{tBu} TOF [h^{-1}] H_2	CO	Ratio (H_2/CO)
0	721	87	8.46	850	67	12.69
20	8482	2185	3.88	1827	407	4.50
40	7709	2379	3.24	636	170	3.76
60	6671	2261	2.95	397	111	3.61
80	5938	2133	2.78	344	98	3.56
100	5109	1966	2.60	323	94	3.49
120	4250	1782	2.38	301	90	3.39
140	3675	1580	2.33	295	89	3.33
160	3288	1463	2.25	278	85	3.30
180	3066	1375	2.23	266	83	3.20
200	2634	1217	2.16	266	85	3.16
220	2475	1151	2.15	254	81	3.13
240	2314	1089	2.13	240	78	3.08
260	2162	1021	2.12	242	79	3.05
280	2068	977	2.12	231	77	3.00
300	1952	932	2.09	230	78	2.96
320	1891	898	2.11	228	76	3.00
340	1766	841	2.10	221	74	2.98
360	1688	811	2.08	216	74	2.92

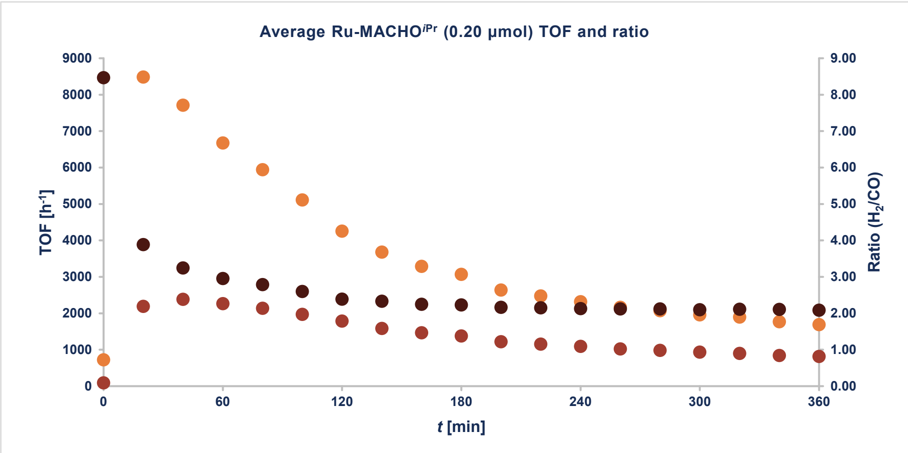

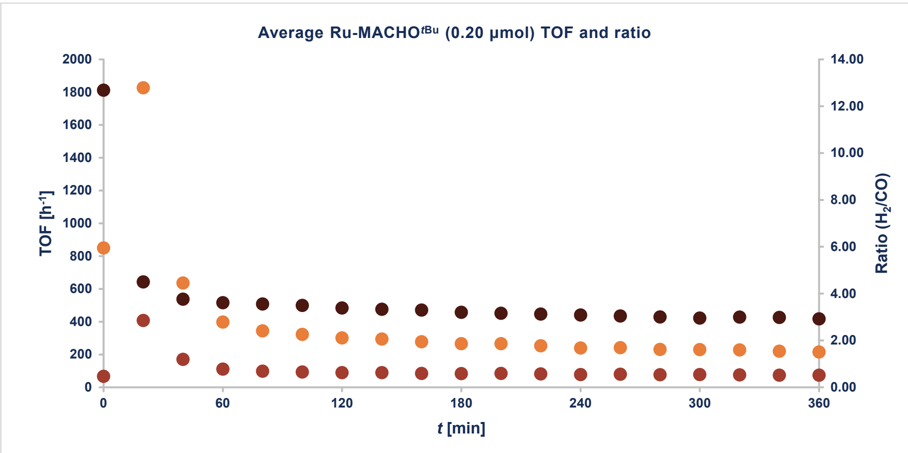

Table S9. Summary of results for Ru-MACHO^R (0.20 µmol). *Continued*.

Time [min]	Ru-MACHO^{Cy} TOF [h^{-1}] H_2	CO	Ratio (H_2/CO)	Ru-MACHO^{Ad} TOF [h^{-1}] H_2	CO	Ratio (H_2/CO)
0	2020	319	6.29	4591	1004	4.54
20	10991	2698	4.07	1648	557	2.97
40	10596	2832	3.73	779	311	2.52
60	9763	2728	3.56	486	207	2.35
80	9248	2675	3.44	332	145	2.28
100	8825	2590	3.39	271	119	2.28
120	8080	2457	3.26	239	105	2.29
140	7295	2332	3.10	212	92	2.31
160	7122	2295	3.06	185	81	2.30
180	6729	2226	3.00	175	77	2.27
200	6185	2118	2.88	157	68	2.32
220	5427	1975	2.70	150	64	2.36
240	5066	1915	2.61	138	57	2.41
260	4720	1835	2.54	136	55	2.46
280	4291	1715	2.47	130	52	2.50
300	3870	1598	2.39	131	52	2.54
320	3525	1494	2.33	127	49	2.59
340	3411	1451	2.32	125	47	2.67
360	2955	1298	2.25	124	46	2.72

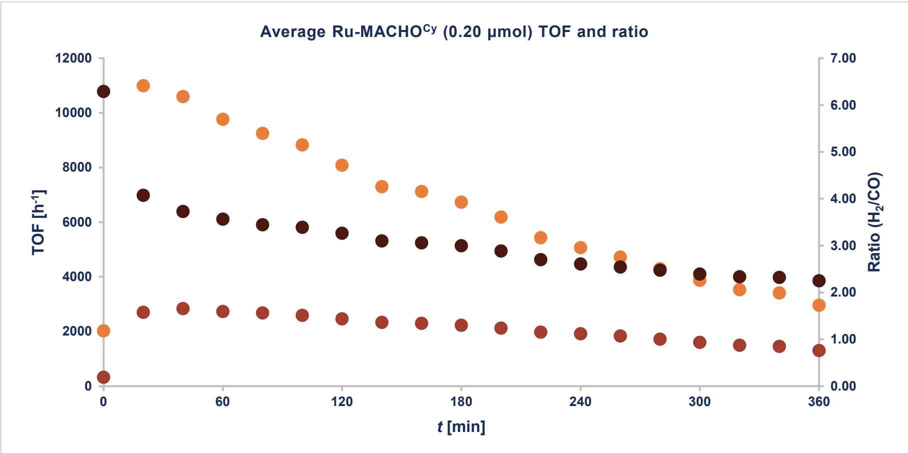

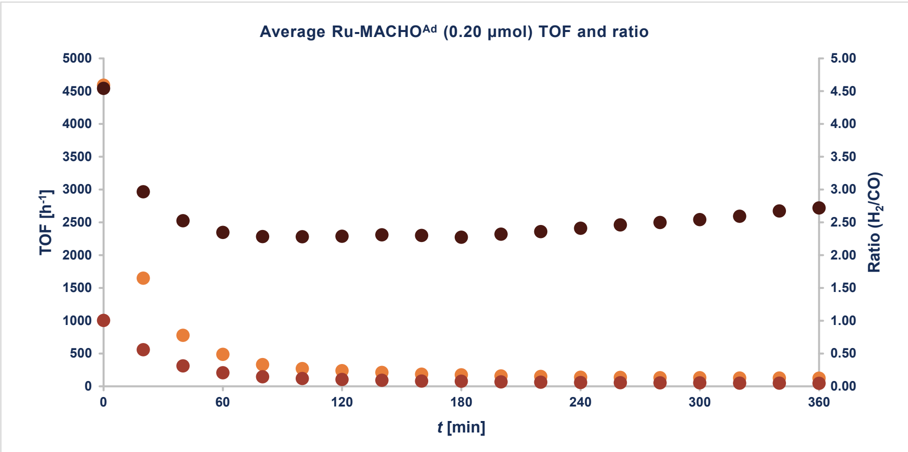

Representative Inline GC Screenshots

One representative inline-GC screenshot showing both TCD and FID chromatograms are included below for each scope entry. Equivalent data are additionally provided for the scaled-up Ru-MACHO^{Cy} experiment using the 45 mL reactor configuration.

Ru-MACHO^{Ph}

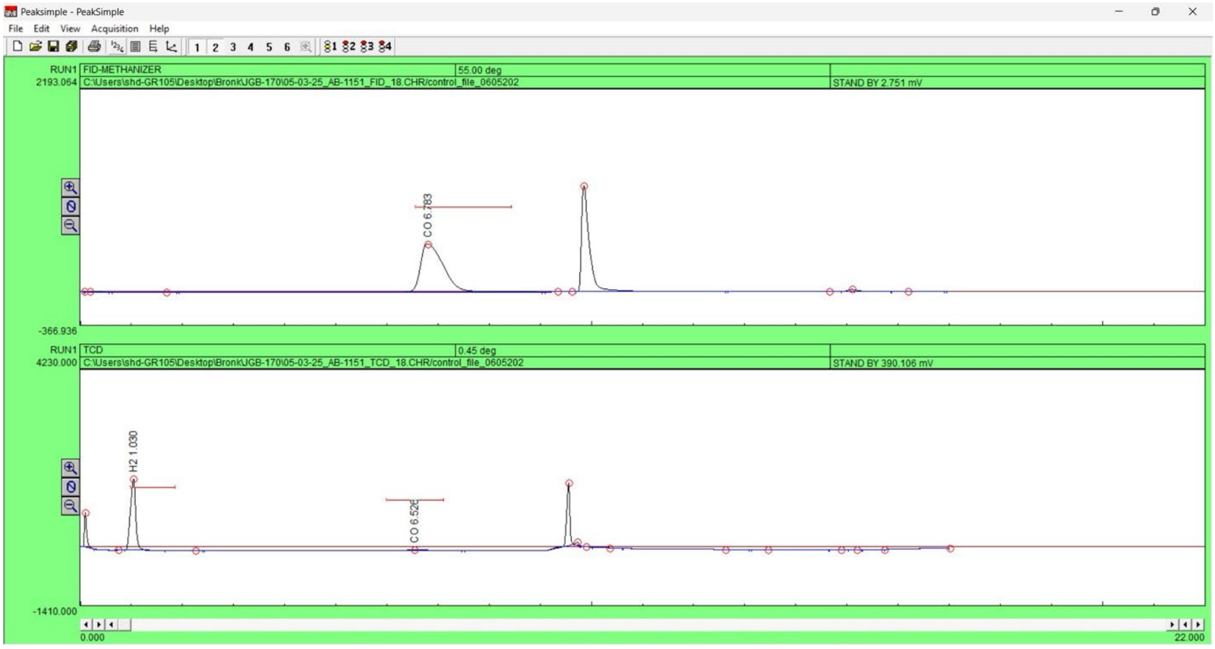

Ru-MACHO$^{p(Me)}$

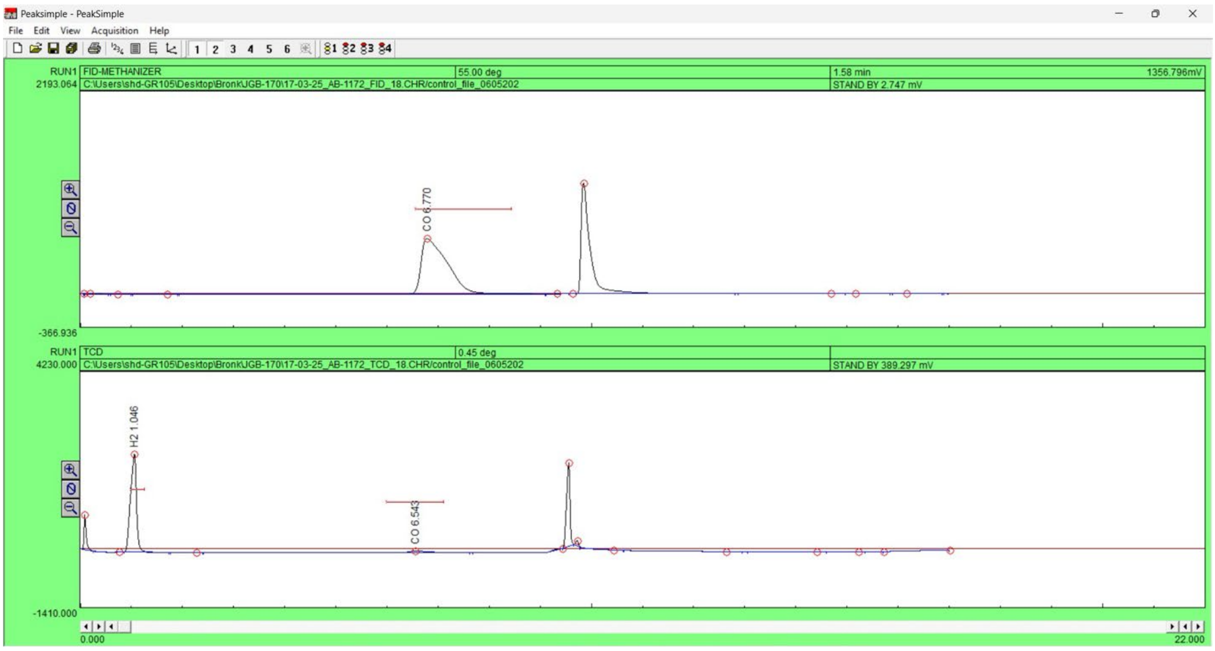

Ru-MACHO$^{m,m(\mathrm{Me})}$

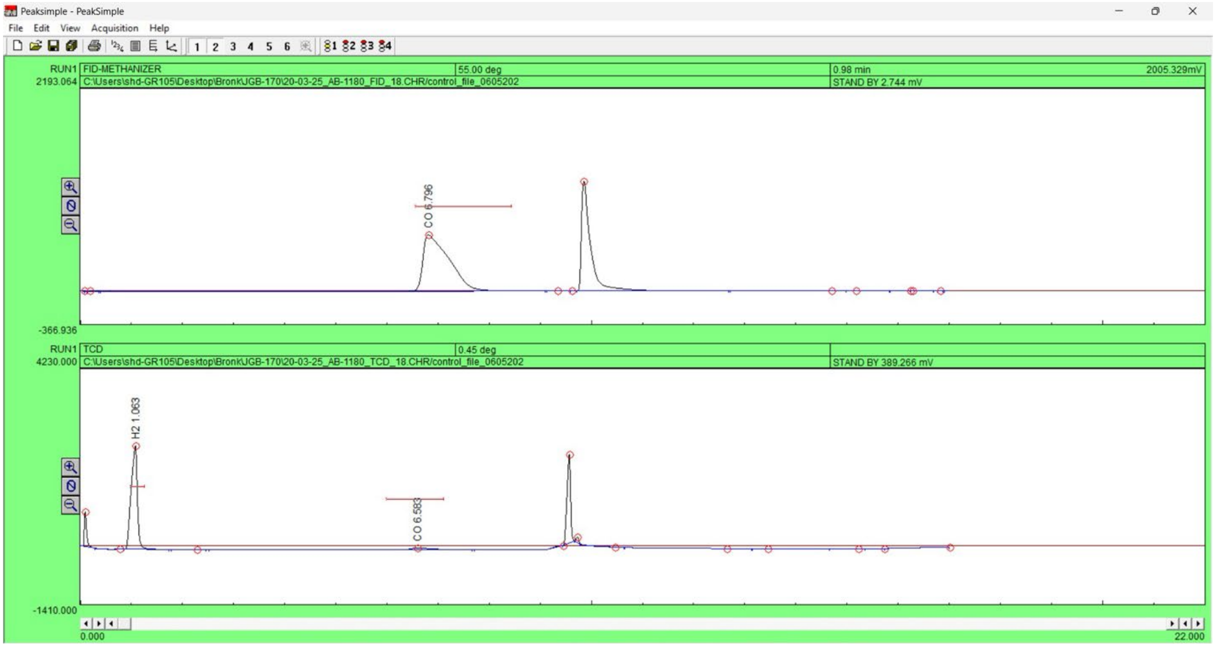

Ru-MACHO$^{p(i\mathrm{Pr})}$

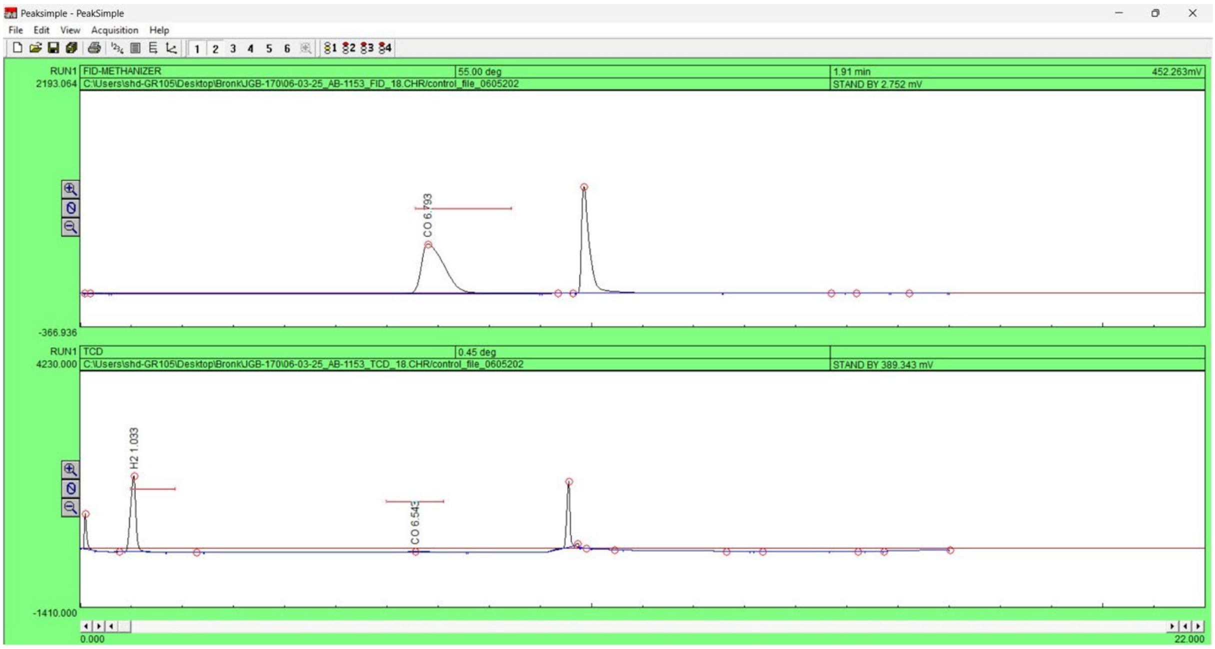

Ru-MACHO$^{p(3\text{-}Pe)}$

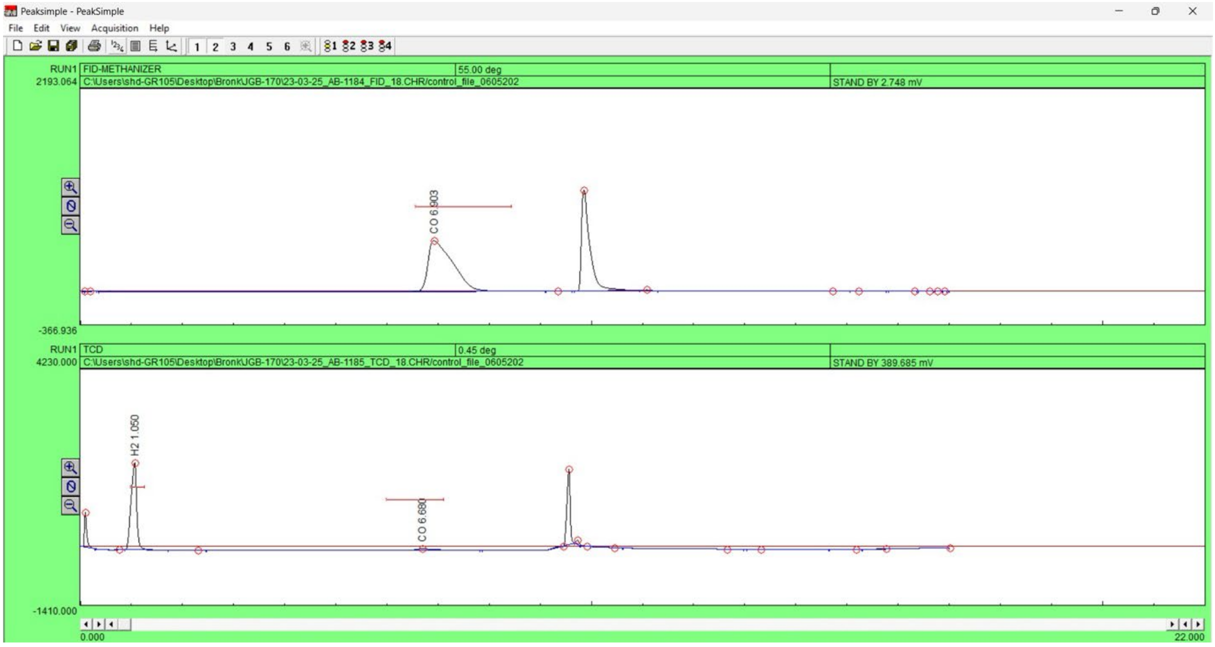

Ru-MACHO^{Naph}

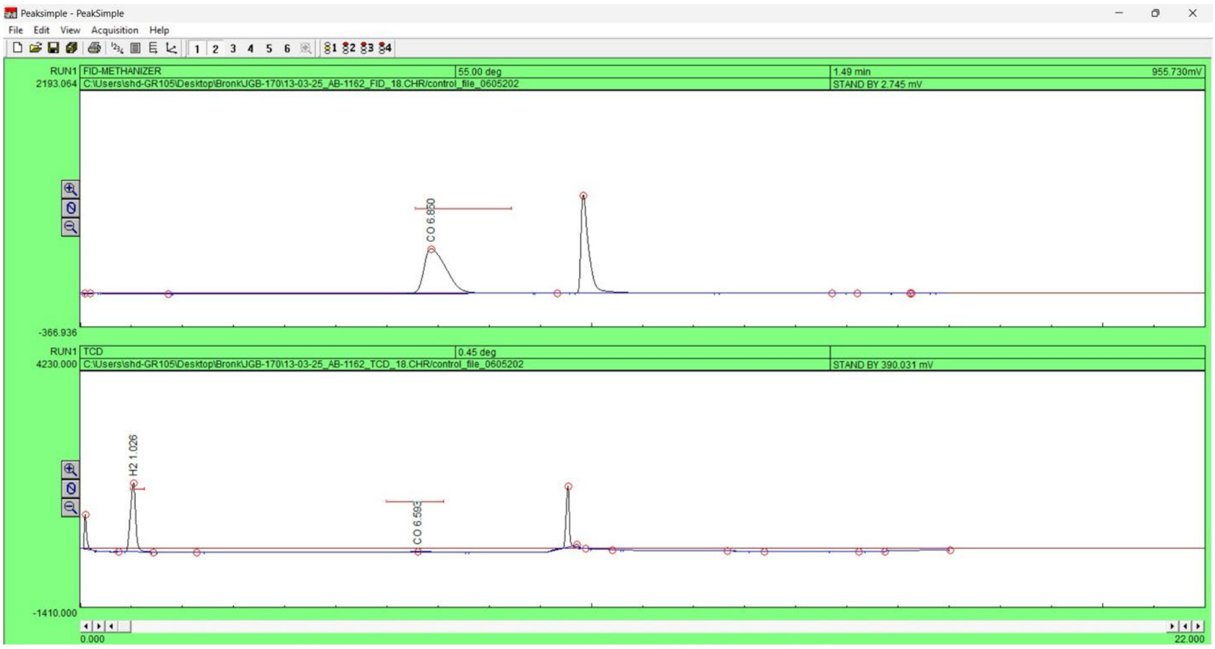

Ru-MACHO^{Biph}

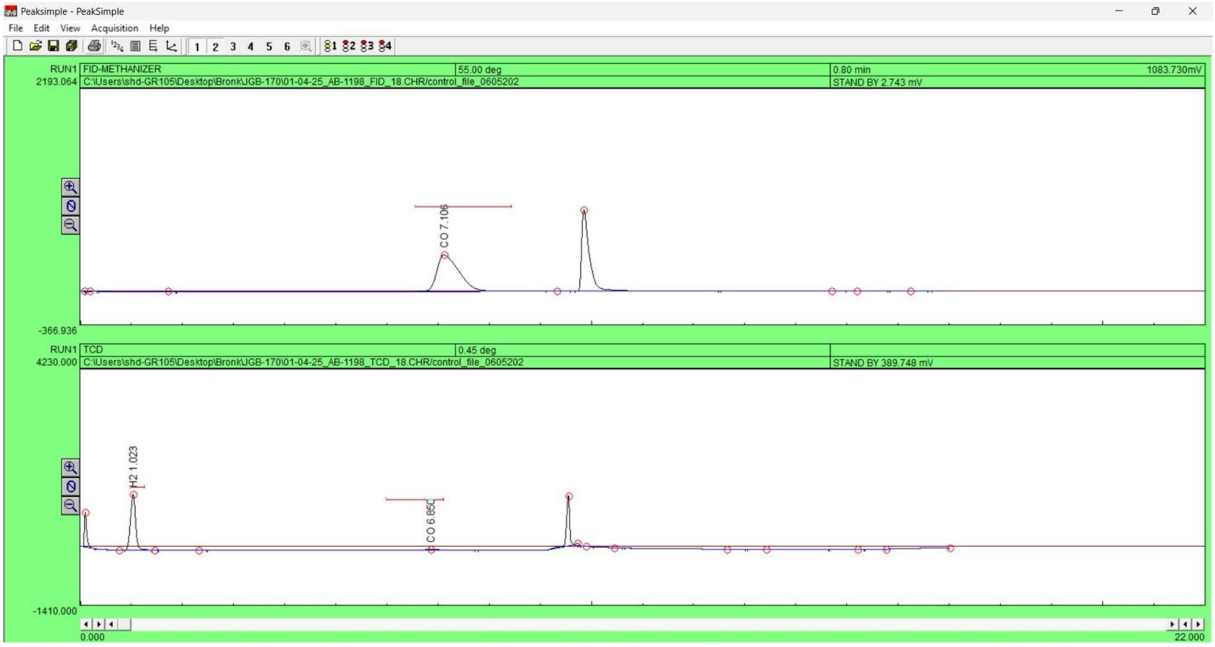

Ru-MACHO$^{p(CF3)}$

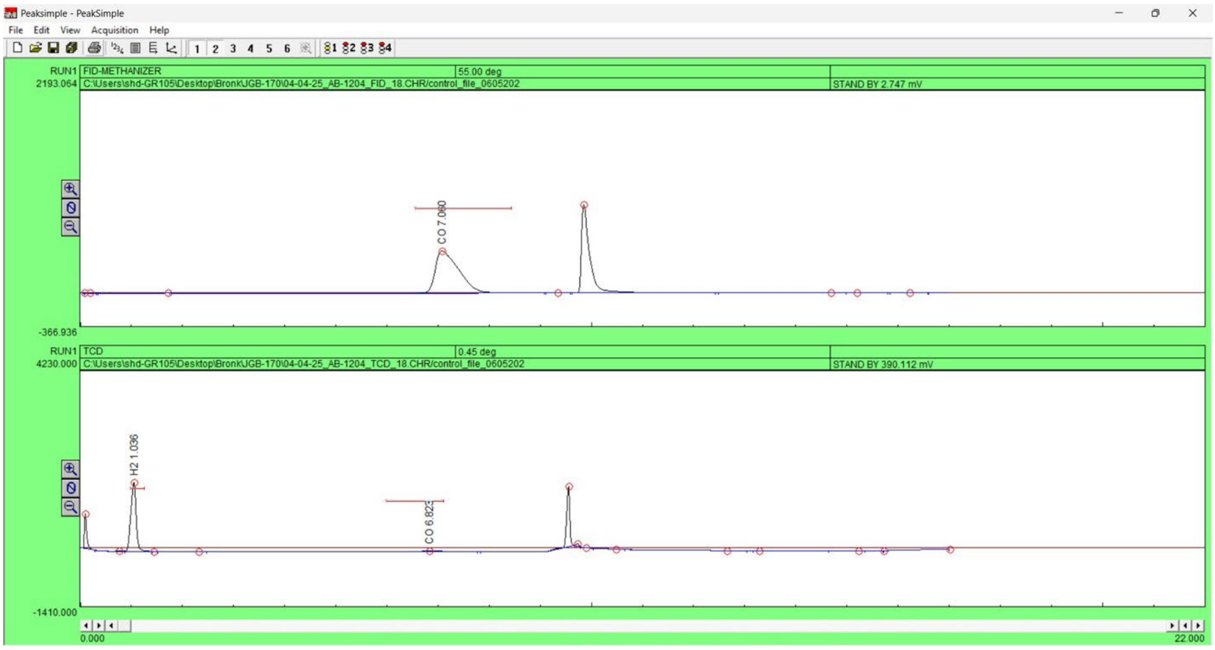

Ru-MACHO$^{p(OMe)}$

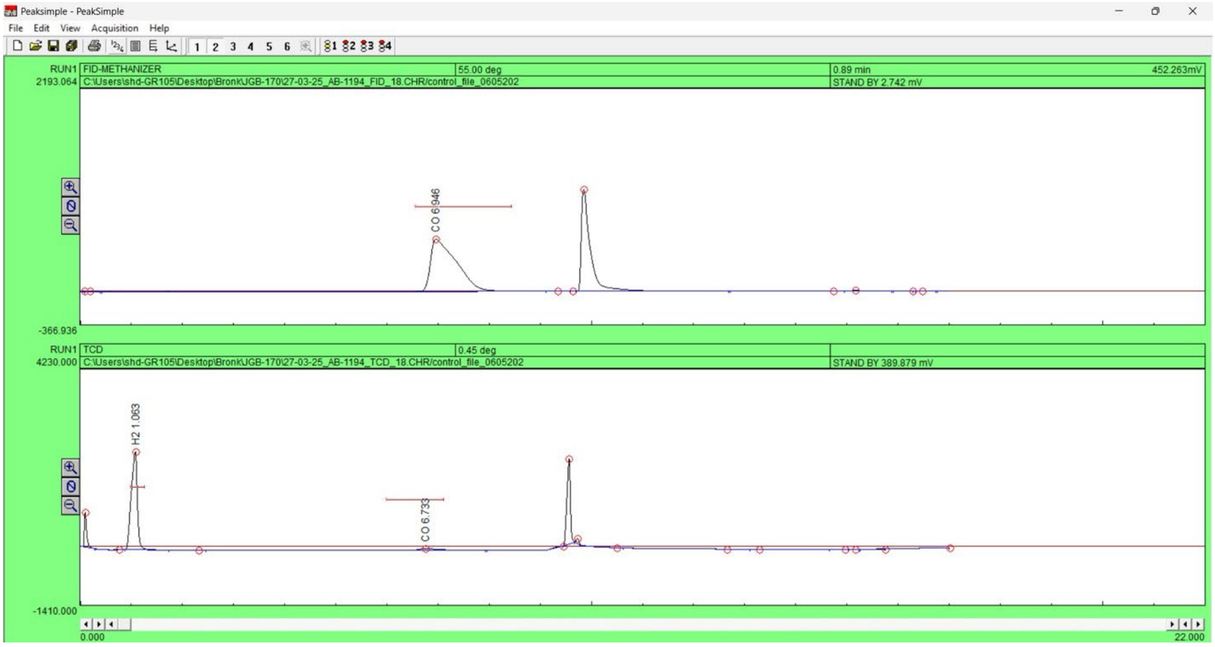

Ru-MACHO^{Et}

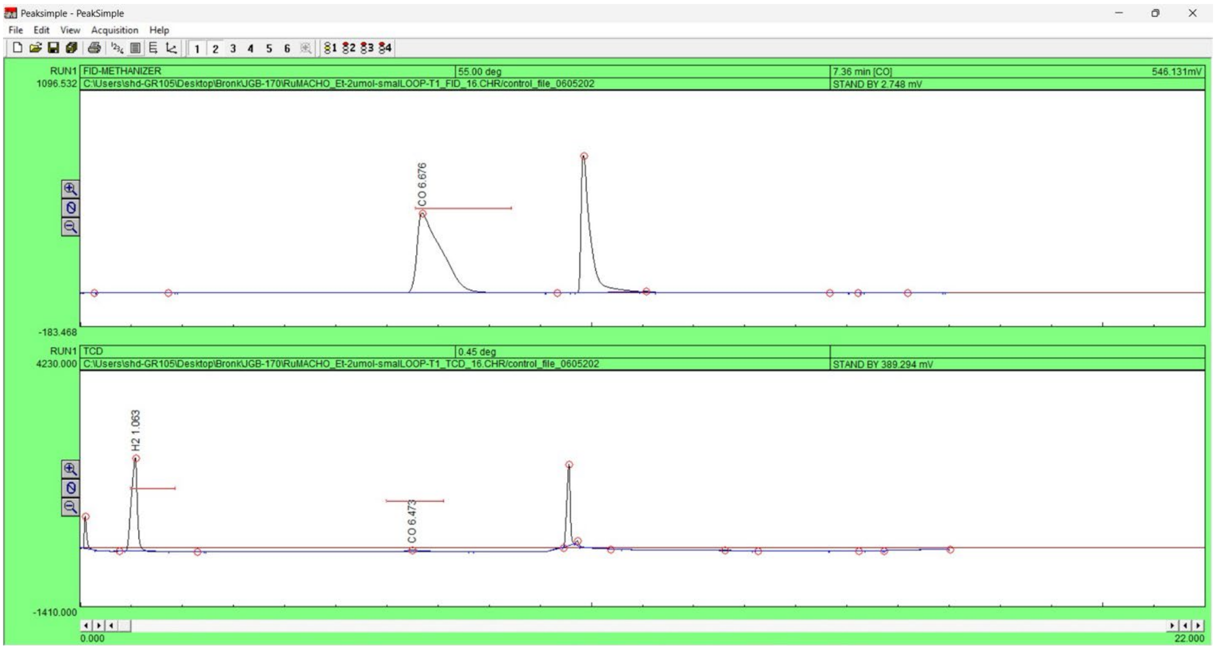

Ru-MACHO^{iPr}

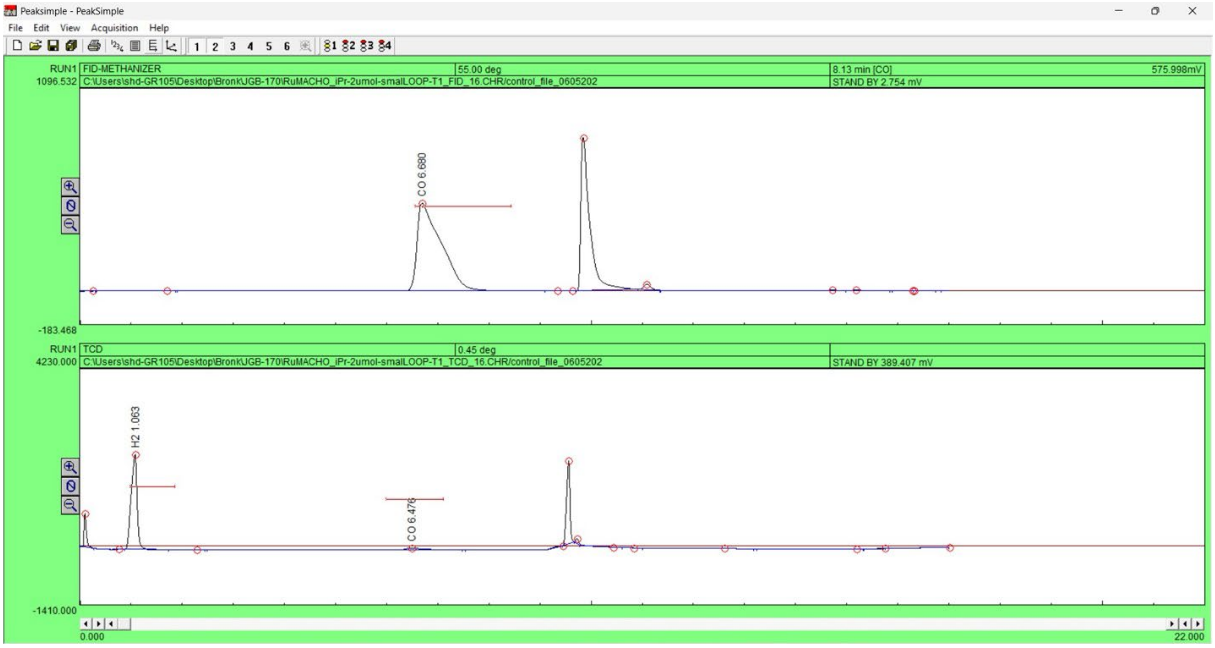

Ru-MACHO^{tBu}

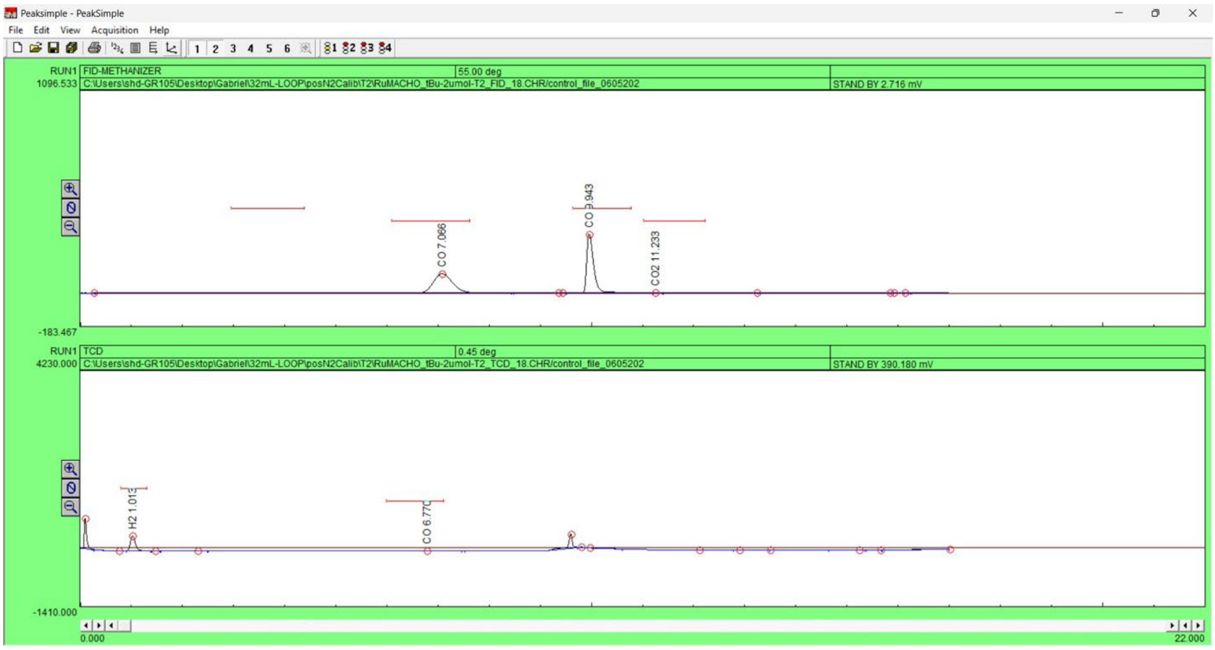

Ru-MACHO^{Cy} (2 µmol – 20 mL reactor)

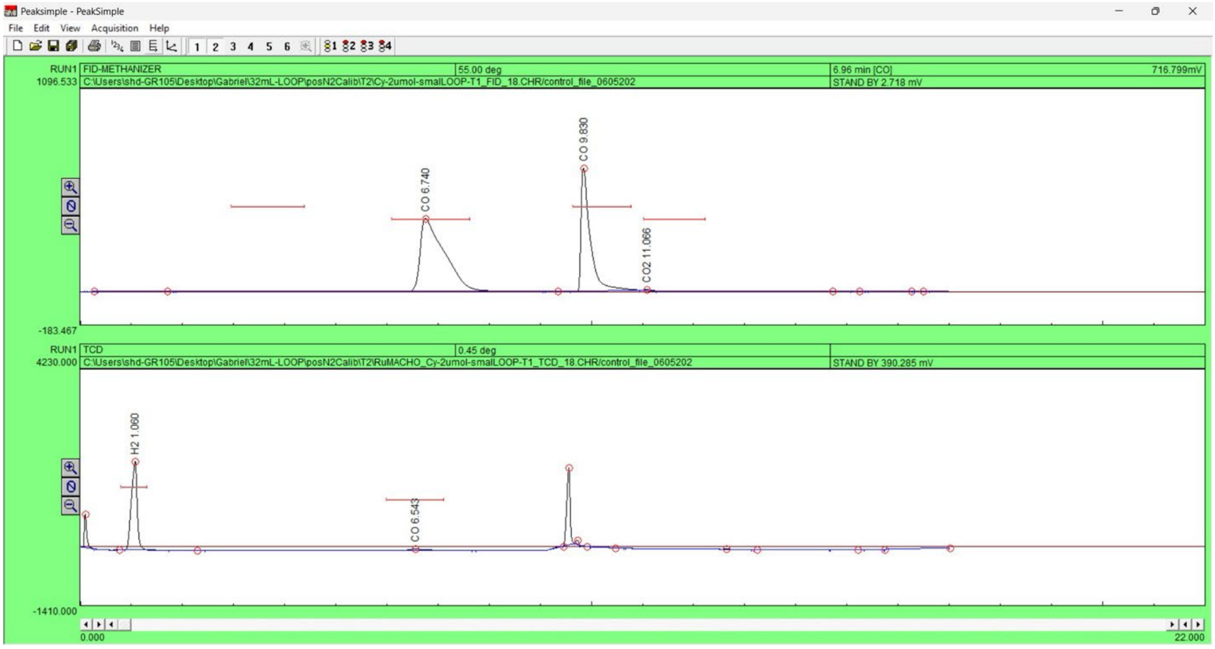

Ru-MACHO^{Cy} (4.5 µmol – 45 mL reactor)

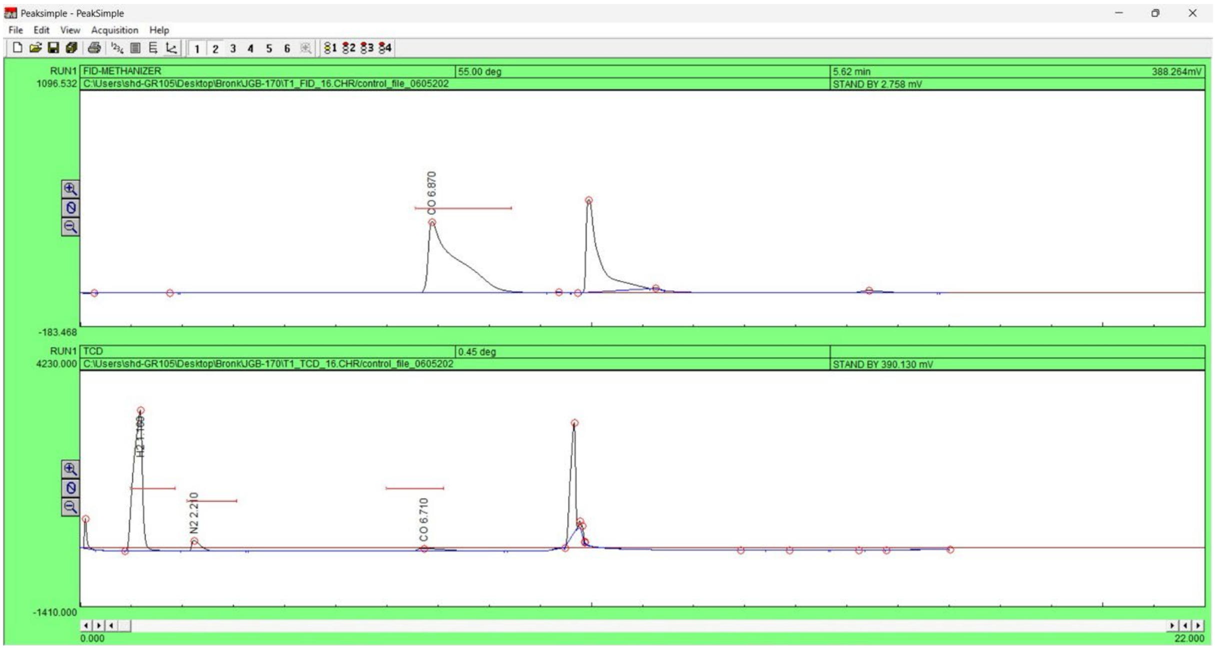

Ru-MACHO^{Ad}

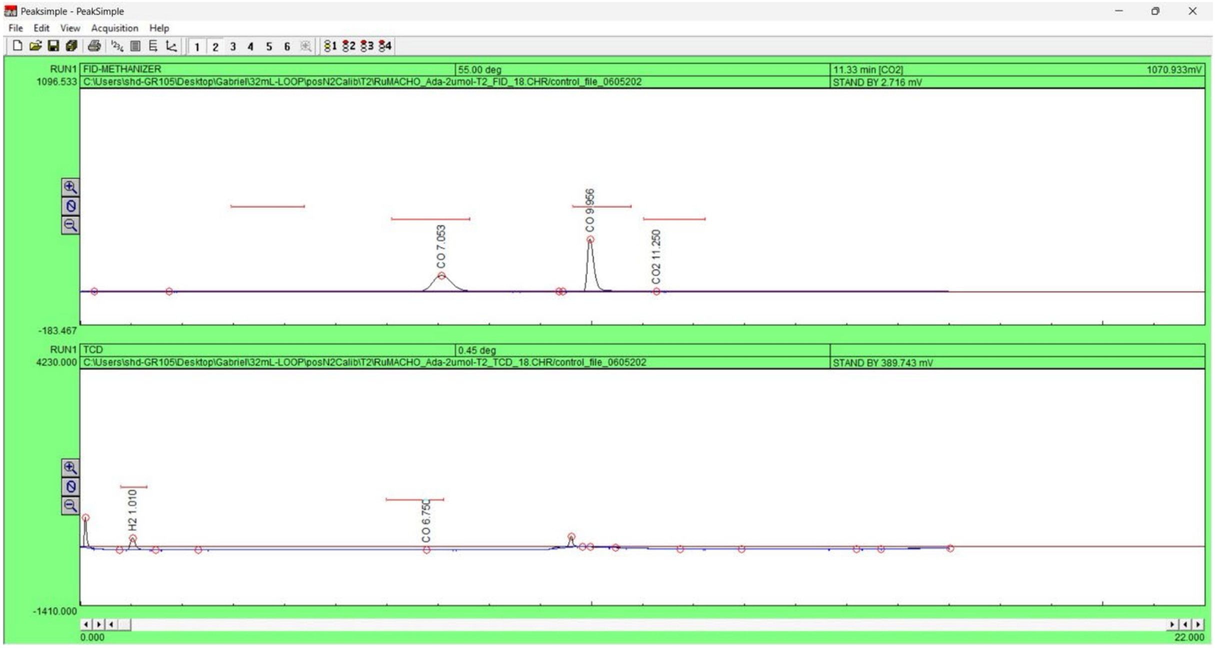

Experiment with Addition of Pd/C

To probe whether hydrogenation of the proposed Ru-enamido complex **C5** could occur under the reaction conditions, Pd/C was introduced into the flow system. The reaction was performed according to the General Procedure for Ru-MACHO Catalyst Scope, with the modification that Pd/C (8.0 mg) was added directly to the gas–liquid separator.

Table S10. Summary of results for Ru-MACHO^{Ph} (2.0 µmol) with addition of Pd/C (8.0 mg).

Time	TOF [h^{-1}]		Ratio
[min]	H_2	CO	(H_2/CO)
0	6369	1131	5.63
20	7252	3070	2.36
40	6358	3021	2.10
60	6053	2944	2.06
80	5499	2668	2.06
100	4990	2468	2.02
120	4589	2274	2.02
140	3977	1963	2.03
160	3749	1871	2.00
180	3205	1592	2.01
200	3044	1522	2.00
220	2692	1332	2.02
240	2535	1279	1.98
260	2133	1057	2.02
280	2027	1012	2.00
300	1772	867	2.04
320	1683	833	2.02
340	1548	767	2.02
360	1392	706	1.97

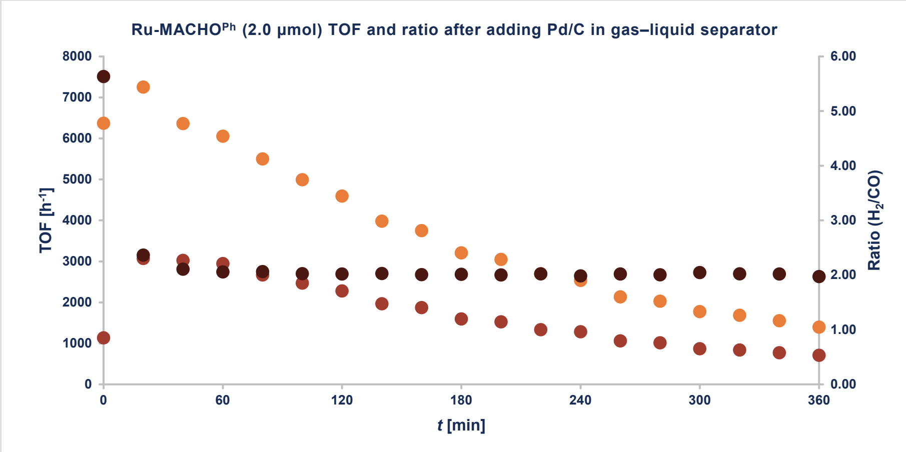

Experiment using Ru-NP$_3$

The reaction was performed according to the General Procedure for Ru-MACHO Catalyst Scope, with the modification of; inside a glovebox, Ru-NP$_3$ (2.0 µmol) was weighed into an 8 mL vial. Benzene (1 mL) and methanol (1 mL) were added, and the vial was sealed and heated to 80 °C until a clear solution was obtained (5 minutes). The resulting solution was transferred to a 20 mL GL-45 bottle (Bottle A), the vial rinsed with methanol (3 x 1 mL) and the GL-45 bottle diluted with methanol (9 mL).

Table S11. Summary of results for Ru-NP$_3$ (2.0 µmol).

Time [min]	TOF [h^{-1}] H$_2$	TOF [h^{-1}] CO	Ratio (H_2/CO)
0	1488	1	1148.28
20	2422	6	381.52
40	2931	12	239.16
60	3275	19	175.01
80	3427	24	140.95
100	3578	31	114.44
120	3514	35	99.91
140	3586	41	86.54
160	3387	43	79.25
180	3323	46	71.75
200	3147	47	66.83
220	3088	50	61.67
240	2993	52	57.86
260	2763	50	54.78
280	2678	52	51.81
300	2500	50	49.71
320	2387	50	47.31
340	2271	50	45.36
360	2139	49	44.08

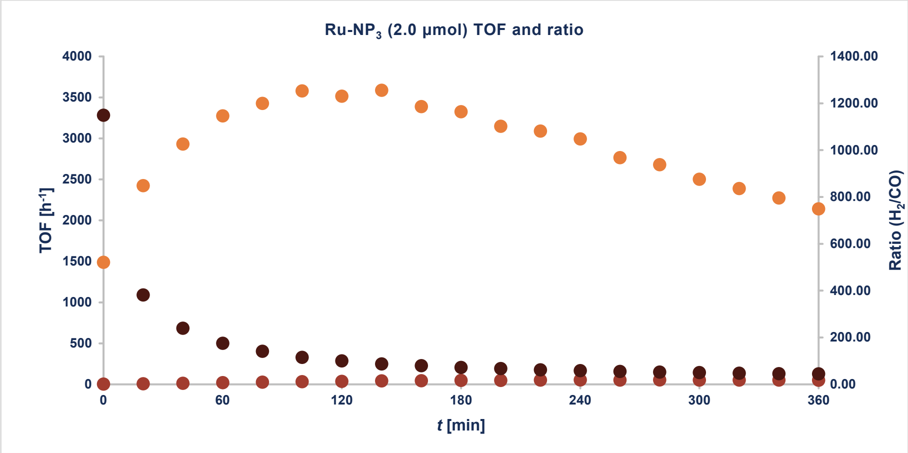

Upscaling Using Ru-MACHO^{Cy}

Software for addition of consumed methanol

During extended continuous-flow experiments, progressive methanol conversion leads to changes in catalyst concentration and, ultimately, depletion of the recirculating reservoir. Loss of liquid volume interrupts recirculation and causes cessation of syngas production. To maintain stable operating conditions, an automated feedback script was developed to continuously adjust methanol feed during operation.

The program reads GC output files generated during online analysis, extracts peak areas for H_2, CO, and the internal standard (N_2), and converts these values into gas flow rates using pre-determined calibration functions. From the measured CO production rate, methanol consumption is calculated stoichiometrically, while additional methanol loss due to evaporation is estimated using an Antoine-equation-based vapor pressure model. The required methanol replenishment rate is then calculated and transmitted to a second HPLC pump via serial communication.

The script operates continuously during reaction monitoring. After each completed GC run, the program automatically updates the methanol feed rate to compensate for both chemical conversion and evaporative losses, thereby maintaining constant reactor volume and catalyst concentration throughout long-time experiments. The fully annotated source code is available at: https://github.com/gabrielmfb/Methanol-to-syngas/

Inline-GC calibration using N_2

Upon scaling up the reactor system, additional minor peaks appeared in the GC chromatograms, necessitating recalibration using N_2 as an internal standard. Calibration of the inline GC instrument (SRI Multiple Gas Analyzer #5) was performed by mixing pure gases from high-pressure cylinders delivered through mass-flow controllers. The gas streams were thoroughly mixed under stirring prior to entering the GC. For each calibration point, an average of four measurements was collected, with a maximum deviation of 5% between the lowest and highest values. For this internal-standard calibration at higher gas concentrations, all components were analysed using the TCD detector.

Given the internal standard calibration relationship:

$$RF = \frac{A_X \cdot C_{N2}}{C_X \cdot A_{N2}}$$

Where RF is the detector response factor, A_X and A_{N2} are the chromatographic peak areas of analyte X and nitrogen (internal standard), respectively, and C_X and C_{N2} are their molar concentrations. Rearranging gives:

$$\frac{A_X}{A_{N2}} = RF \cdot \frac{C_X}{C_{N2}}$$

The molar concentration of each component in the gas mixture is defined as:

$$C_X = \frac{n_X}{n_{total}}$$

And therefore:

$$\frac{C_X}{C_{N2}} = \frac{\frac{n_X}{n_{total}}}{\frac{n_{N2}}{n_{total}}} = \frac{n_X}{n_{N2}}$$

Because all gases are introduced under identical temperature and pressure conditions, the molar amount of each component is proportional to its volumetric flow rate according to the ideal gas law:

$$n_X \propto V_X$$

therefore:

$$\frac{C_X}{C_{N2}} = \frac{V_X}{V_{N2}}$$

and the calibration expression becomes:

$$\frac{A_X}{A_{N2}} = RF \cdot \frac{V_X}{V_{N2}}$$

Accordingly, calibration curves were constructed by plotting the peak-area ratio (A_X/A_{N2}) against the volumetric flow ratio (V_X/ V_{N2}).

Table S12. TCD calibration data for hydrogen.

#	H_2 [mL/min]	Areas				Avg. area	SD	CV
1	1.79	18314	18678	18918	19045	18739	321.5	1.7
2	4.00	28622	28671	28657	28665	28654	21.93	0.1
3	7.00	34297	34052	34048	34109	34127	117.03	0.3
4	2.00	15360	15519	15531	15535	15486	84.44	0.5
5	10.00	37237	37449	37472	37526	37421	126.94	0.3
6	14.00	41984	41443	41723	41380	41632	277.73	0.7
7	18.00	43618	44340	44300	44336	44149	354.12	0.8

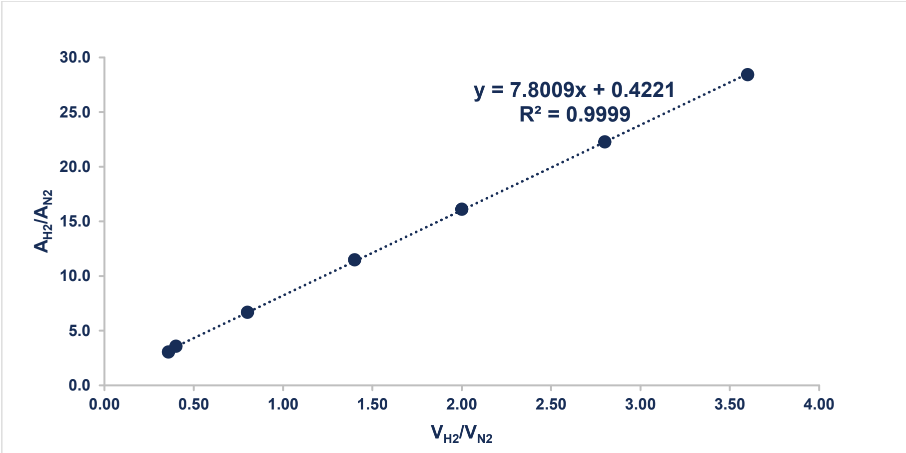

Table S13. TCD calibration data for carbon monoxide.

#	CO [mL/min]	Areas				Avg. area	SD	CV
1	0.89	1106	1102	1101	1106	1104	2.28	0.2
2	2.00	1709	1715	1711	1714	1712	2.75	0.2
3	4.00	2342	2352	2353	2358	2352	6.24	0.3
4	4.00	3476	3508	3500	3499	3496	13.77	0.4
5	5.50	2512	2530	2526	2529	2524	8.34	0.3
6	6.50	2416	2380	2384	2374	2389	18.79	0.8
7	7.50	2154	2280	2284	2284	2251	64.36	2.9

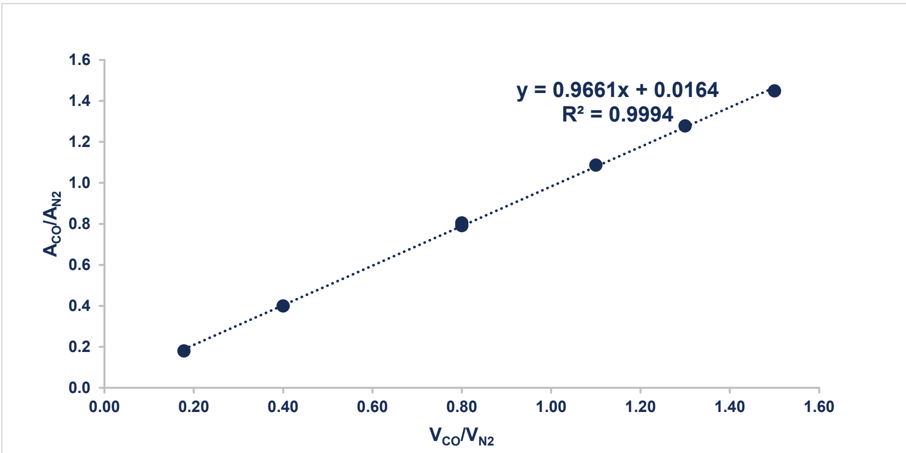

Table S14. TCD calibration data for nitrogen.

#	N_2 [mL/min]	Areas				Avg. area	SD	CV
1	5.0	6180	6146	6139	6128	6148	22.4	0.4
2	5.0	4297	4299	4282	4292	4293	7.59	0.2
3	5.0	2973	2975	2971	2972	2973	1.71	0.1
4	5.0	4318	4349	4356	4356	4345	18.14	0.4
5	5.0	2317	2324	2326	2326	2323	4.27	0.2
6	5.0	1881	1867	1866	1864	1870	7.77	0.4
7	5.0	1534	1561	1559	1561	1554	13.20	0.8

Design of Experiments optimisation of large scale setup

A small design of experiments optimisation focused on the two main parameters, flow rate and back-pressure, was performed to obtain the ideal conditions for operation with the larger reactor.

Table S15. Summary of results for the third DoE. Stability is given by percentage of CO production retainment from peak production. [a]Not determined as CO production was still increasing after 3 h.

#	Flow rate [X mL/min]	BPR [Y psi]	*n* [mmol] H_2	*n* [mmol] CO	TOF [h^{-1}] H_2	TOF [h^{-1}] CO	Ratio (H_2/CO)	Stability [%]
1	6.8	75	88.26	42.47	6537	3146	2.08	73.5
2	2.2	75	69.36	33.25	5138	2463	2.09	78.8
3	1.0	100	11.31	3.89	838	288	2.90	N/D[a]
4	8.0	100	4.27	1.90	316	141	2.25	N/D[a]
5	4.5	100	20.02	9.23	1483	683	2.17	N/D[a]
6	2.5	75	72.01	34.48	5334	2554	2.09	80.0

Ru-MACHO^{Cy} large scale experiment

Inside a glovebox, a 20 mL GL-45 flask (bottle A) was charged with Ru-MACHO^{Cy} (4.5 µmol) and diluted with methanol (3.6 mL), followed by the addition of *t*BuOK (11.2 mg, 100 µmol), followed by dilution with methanol to a total of volume of 8.6 mL. In addition, two additional 100 mL GL-45 flasks (bottle B) were charged with methanol (120 mL). All three bottles were capped and taken outside the glovebox.

Outside the glovebox, the flow system described above (Continuous Flow Setup) equipped with a back-pressure regulator (75 psi), was flushed with methanol (100 mL) into a waste container under air. The gas-tight GL-45 lid was then transferred to bottle B, and the flow system was flushed again into a waste container by disconnecting the returning line at the Y-connection, while being extensively degassed using argon. After flushing methanol (100 mL), the returning line was reconnected to the Y-connection, restoring the closed-loop flow system. Once flushing was complete and the flow system filled with methanol (36.4 mL), the gas-tight GL-45 lid was transferred to bottle A, and the flow system was operated for 6 minutes at a flow rate of 10.00 mL/min. After 6 minutes, the flow rate was adjusted to 3.30 mL/min, the mass flow controller changed to 5.00 mL/min, and the inline GC connected. Following an additional 6 minutes of operation under the desired conditions, the inline GC was started, and the composition of the produced syngas was measured at 20-minute intervals. After starting the GC, the software for addition of methanol was also started.

Table S16. Summary of results for Ru-MACHO^{Cy} (4.5 µmol) scale-up experiment.

Time [hours]	TOF [h^{-1}] H_2	TOF [h^{-1}] CO	Ratio (H_2/CO)	Time [hours]	TOF [h^{-1}] H_2	TOF [h^{-1}] CO	Ratio (H_2/CO)
0.00	8226	4060	2.03	**42.33**	3112	1487	2.09
0.33	6568	3297	1.99	**42.67**	3128	1512	2.07
0.67	5615	2926	1.92	**43.00**	3083	1494	2.06
1.00	5473	2847	1.92	**43.33**	3123	1519	2.06
1.33	5177	2660	1.95	**43.67**	3056	1475	2.07
1.67	4916	2502	1.96	**44.00**	3097	1497	2.07
2.00	4706	2365	1.99	**44.33**	3035	1472	2.06
2.33	4479	2201	2.03	**44.67**	3084	1481	2.08
2.67	4457	2204	2.02	**45.00**	3053	1487	2.05
3.00	4478	2213	2.02	**45.33**	3018	1466	2.06
3.33	4327	2134	2.03	**45.67**	3007	1460	2.06
3.67	4281	2090	2.05	**46.00**	2976	1444	2.06
4.00	4362	2157	2.02	**46.33**	3025	1450	2.09
4.33	4452	2165	2.06	**46.67**	2941	1421	2.07
4.67	4479	2176	2.06	**47.00**	2966	1435	2.07

5.00	4435	2181	2.03	**47.33**	2971	1427	2.08
5.33	4515	2218	2.04	**47.67**	2975	1438	2.07
5.67	4406	2175	2.03	**48.00**	2960	1426	2.08
6.00	4493	2201	2.04	**48.33**	2944	1427	2.06
6.33	4359	2149	2.03	**48.67**	2929	1379	2.12
6.67	4274	2087	2.05	**49.00**	2899	1405	2.06
7.00	4372	2157	2.03	**49.33**	2908	1403	2.07
7.33	4263	2088	2.04	**49.67**	2937	1419	2.07
7.67	4217	2074	2.03	**50.00**	2915	1417	2.06
8.00	4287	2115	2.03	**50.33**	2877	1392	2.07
8.33	4119	1970	2.09	**50.67**	2893	1401	2.07
8.67	4097	1986	2.06	**51.00**	2858	1389	2.06
9.00	4197	2061	2.04	**51.33**	2837	1366	2.08
9.33	4162	2024	2.06	**51.67**	2850	1375	2.07
9.67	4083	1989	2.05	**52.00**	2810	1358	2.07
10.00	4096	1995	2.05	**52.33**	2843	1370	2.08
10.33	4119	1966	2.10	**52.67**	2780	1339	2.08
10.67	4159	2027	2.05	**53.00**	2854	1375	2.07
11.00	4129	2019	2.05	**53.33**	2778	1346	2.06
11.33	4085	1993	2.05	**53.67**	2812	1353	2.08
11.67	4042	1975	2.05	**54.00**	2831	1364	2.08
12.00	4077	1994	2.05	**54.33**	2769	1340	2.07
12.33	3994	1942	2.06	**54.67**	2768	1328	2.08
12.67	3960	1923	2.06	**55.00**	2751	1326	2.08
13.00	4037	1959	2.06	**55.33**	2753	1310	2.10
13.33	4024	1948	2.07	**55.67**	2774	1339	2.07
13.67	3952	1926	2.05	**56.00**	2747	1322	2.08
14.00	4013	1963	2.04	**56.33**	2707	1314	2.06
14.33	3927	1911	2.05	**56.67**	2733	1320	2.07
14.67	3945	1931	2.04	**57.00**	2706	1302	2.08
15.00	3938	1915	2.06	**57.33**	2702	1304	2.07
15.33	3900	1897	2.06	**57.67**	2675	1302	2.05
15.67	3851	1866	2.06	**58.00**	2643	1274	2.07
16.00	3959	1931	2.05	**58.33**	2663	1282	2.08
16.33	3850	1878	2.05	**58.67**	2656	1279	2.08
16.67	3875	1896	2.04	**59.00**	2630	1263	2.08
17.00	3765	1813	2.08	**59.33**	2675	1298	2.06
17.33	3694	1802	2.05	**59.67**	2619	1266	2.07
17.67	3757	1845	2.04	**60.00**	2639	1270	2.08
18.00	3664	1780	2.06	**60.33**	2649	1279	2.07
18.33	3739	1835	2.04	**60.67**	2586	1252	2.07
18.67	3681	1796	2.05	**61.00**	2613	1259	2.08
19.00	3665	1743	2.10	**61.33**	2613	1260	2.07
19.33	3740	1824	2.05	**61.67**	2561	1236	2.07
19.67	3603	1753	2.05	**62.00**	2572	1238	2.08
20.00	3696	1800	2.05	**62.33**	2573	1236	2.08
20.33	3677	1801	2.04	**62.67**	2586	1239	2.09
20.67	3531	1726	2.05	**63.00**	2585	1249	2.07

21.00	3592	1756	2.05	**63.33**	2541	1222	2.08
21.33	3560	1734	2.05	**63.67**	2577	1243	2.07
21.67	3519	1705	2.06	**64.00**	2526	1194	2.12
22.00	3498	1701	2.06	**64.33**	2563	1238	2.07
22.33	3586	1738	2.06	**64.67**	2517	1205	2.09
22.67	3521	1714	2.05	**65.00**	2536	1221	2.08
23.00	3590	1746	2.06	**65.33**	2531	1216	2.08
23.33	3487	1696	2.06	**65.67**	2511	1204	2.09
23.67	3617	1762	2.05	**66.00**	2525	1194	2.12
24.00	3442	1689	2.04	**66.33**	2486	1197	2.08
24.33	3502	1702	2.06	**66.67**	2520	1219	2.07
24.67	3426	1668	2.05	**67.00**	2481	1188	2.09
25.00	3531	1715	2.06	**67.33**	2526	1225	2.06
25.33	3471	1677	2.07	**67.67**	2452	1179	2.08
25.67	3454	1680	2.06	**68.00**	2485	1198	2.07
26.00	3512	1706	2.06	**68.33**	2456	1176	2.09
26.33	3480	1680	2.07	**68.67**	2469	1183	2.09
26.67	3491	1696	2.06	**69.00**	2461	1187	2.07
27.00	3416	1661	2.06	**69.33**	2470	1185	2.08
27.33	3470	1701	2.04	**69.67**	2449	1183	2.07
27.67	3437	1666	2.06	**70.00**	2440	1171	2.08
28.00	3445	1664	2.07	**70.33**	2471	1184	2.09
28.33	3378	1636	2.06	**70.67**	2440	1172	2.08
28.67	3440	1675	2.05	**71.00**	2437	1175	2.07
29.00	3404	1642	2.07	**71.33**	2430	1167	2.08
29.33	3385	1652	2.05	**71.67**	2447	1179	2.08
29.67	3434	1664	2.06	**72.00**	2430	1171	2.08
30.00	3393	1653	2.05	**72.33**	2437	1153	2.11
30.33	3439	1662	2.07	**72.67**	2397	1154	2.08
30.67	3421	1681	2.03	**73.00**	2413	1160	2.08
31.00	3424	1660	2.06	**73.33**	2409	1159	2.08
31.33	3329	1617	2.06	**73.67**	2427	1167	2.08
31.67	3377	1633	2.07	**74.00**	2388	1156	2.07
32.00	3312	1601	2.07	**74.33**	2396	1144	2.09
32.33	3391	1642	2.07	**74.67**	2411	1153	2.09
32.67	3319	1620	2.05	**75.00**	2388	1146	2.08
33.00	3358	1627	2.06	**75.33**	2380	1138	2.09
33.33	3286	1616	2.03	**75.67**	2391	1152	2.08
33.67	3322	1603	2.07	**76.00**	2389	1147	2.08
34.00	3280	1592	2.06	**76.33**	2362	1133	2.09
34.33	3263	1573	2.07	**76.67**	2366	1136	2.08
34.67	3276	1595	2.05	**77.00**	2332	1118	2.09
35.00	3341	1619	2.06	**77.33**	2348	1127	2.08
35.33	3323	1608	2.07	**77.67**	2299	1102	2.09
35.67	3249	1572	2.07	**78.00**	2301	1107	2.08
36.00	3340	1623	2.06	**78.33**	2309	1086	2.13
36.33	3243	1578	2.06	**78.67**	2309	1108	2.08
36.67	3251	1570	2.07	**79.00**	2306	1109	2.08

37.00	3276	1609	2.04	**79.33**	2287	1096	2.09
37.33	3186	1543	2.06	**79.67**	2295	1101	2.08
37.67	3263	1575	2.07	**80.00**	2306	1109	2.08
38.00	3247	1581	2.05	**80.33**	2273	1089	2.09
38.33	3240	1579	2.05	**80.67**	2297	1103	2.08
38.67	3167	1536	2.06	**81.00**	2267	1088	2.08
39.00	3212	1550	2.07	**81.33**	2240	1079	2.07
39.33	3212	1553	2.07	**81.67**	2278	1094	2.08
39.67	3146	1528	2.06	**82.00**	2263	1092	2.07
40.00	3170	1530	2.07	**82.33**	2223	1063	2.09
40.33	3185	1550	2.05	**82.67**	2234	1067	2.09
40.67	3144	1514	2.08	**83.00**	2225	1068	2.08
41.00	3130	1505	2.08	**83.33**	2215	1067	2.08
41.33	3190	1543	2.07	**83.67**	2211	1037	2.13
41.67	3109	1511	2.06	**84.00**	2225	1069	2.08
42.00	3134	1512	2.07				

Ligand and Complex Synthesis

Ru-MACHO^{Ph}

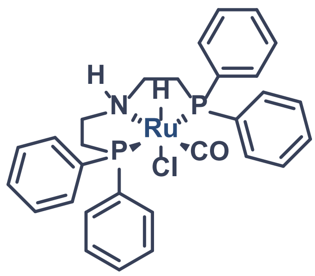

Inside a glovebox, to a COtube charged with MACHO^{Ph} (239 mg, 542 µmol) was added carbonylchlorohydridotris(triphenylphosphine)ruthenium(II) (491 mg, 516 µmol) and toluene (6.0 mL). The reaction mixture was stirred at reflux for 5 h. After reaching ambient temperature, the reaction mixture was added pentane (30 mL) to precipitate out the complex. The suspension was sonicated for 30 minutes, centrifuged, and the solvent decanted off. The remaining solids were suspended in Et_2O (20 mL) and sonicated for 30 minutes. The suspension was centrifuged, filtered, and the precipitate rinsed with Et_2O (2 x 5 mL). The solids were collected and dried in vacuo overnight, affording Ru-MACHO^{Ph} as a white solid (280 mg, 460 µmol, 89%).

^{1}H NMR (400 MHz, CD_2Cl_2) δ 7.85 – 7.76 (m, 8H), 7.43 – 7.40 (m, 12H), 3.95 – 3.90 (m, 1H), 3.49 – 3.36 (m, 2H), 3.01 – 2.96 (m, 2H), 2.57 – 2.44 (m, 4H), -14.48 (t, *J* = 20.1 Hz, 0.07H), -15.24 (t, *J* = 19.4 Hz, 0.93H). **^{13}C NMR** (101 MHz, CD_2Cl_2) δ 207.1 (t, *J* = 12.2 Hz), 138.0 (t, *J* = 22.7 Hz), 134.7 (t, *J* = 21.1 Hz), 133.6 (t, *J* = 6.5 Hz), 132.6 (t, *J* = 6.6 Hz), 130.4, 130.3, 128.9 (t, *J* = 5.0 Hz), 128.7 (t, *J* = 5.0 Hz), 52.7 (t, *J* = 5.0 Hz), 32.0 (t, *J* = 11.4 Hz). **^{31}P NMR** (162 MHz, CD_2Cl_2) δ 57.5 (0.14P), 54.9 (d, *J* = 4.4 Hz, 1.86P).

Spectroscopic data in agreement with that reported by Ogata, O. *et al.*[1]

Bis(4-methylphenyl)phosphine

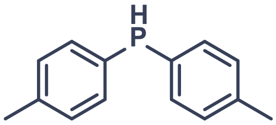

Inside a glovebox, a COtube charged with bis(4-methylphenyl)phosphine oxide (921 mg, 4.00 mmol) was added THF (12 mL) and subsequently cooled to -30 °C. DIBAL-H (1.0 M in hexanes, 14.0 mL, 14.0 mmol) was added dropwise to the cold solution over 5 minutes. Upon cessation of hydrogen evolution, the COtube was sealed and stirred at ambient temperature overnight. The reaction mixture was diluted with Et_2O (10 mL) and subsequently quenched with a saturated aqueous solution of Rochelle's salt (29 mL). The resultant biphasic mixture was stirred for 1 h, after which the organic layer was separated, and the aqueous phase was extracted with Et_2O (2 x 10 mL). The combined organic phases were dried over anhydrous $MgSO_4$, filtered, and concentrated. The resultant cloudy liquid was re-dissolved in Et_2O (5 mL) and passed through a short column of basic alumina, eluting with Et_2O (3 x 5 mL). Subsequent removal of the solvent under reduced pressure afforded bis(4-methylphenyl)phosphine as a colourless oil (735 mg, 3.43 mmol, 86%).

^{1}H NMR (400 MHz, CD_3CN) δ 7.39 – 7.35 (m, 4H), 7.17 – 7.15 (m, 4H), 5.14 (d, *J* = 218.7 Hz, 1H), 2.30 (s, 6H). **^{13}C NMR** (101 MHz, CD_3CN) δ 139.6, 134.7 (d, *J* = 17.0 Hz), 132.6 (d, *J* = 9.1 Hz), 130.3 (d, *J* = 6.5 Hz), 21.2. **^{31}P NMR** (162 MHz, CD_3CN) δ -42.7.

Spectroscopic data in agreement with that reported by Webster, R. L. *et al.*[2]

Bis(2-(bis(4-methylphenyl)phosphaneyl)ethyl)amine, MACHO$^{p(Me)}$

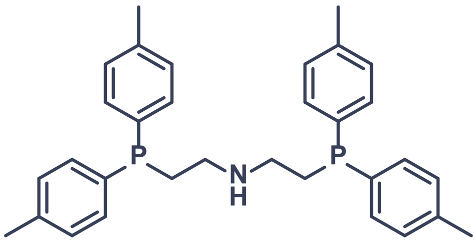

Inside a glovebox, a COtube charged with bis(4-methylphenyl)phosphine (735 mg, 3.43 mmol) was added THF (10 mL) and *t*BuOK (1.05 g, 9.36 mmol). The resultant deep red solution was stirred at ambient temperature for 15 minutes prior to the addition of bis(2-chloroethyl)amine hydrochloride (278 mg, 1.56 mmol). The COtube was sealed, and the reaction mixture was refluxed overnight. After reaching ambient temperature, the reaction mixture was diluted with Et_2O (10 mL) and subsequently quenched with water (10 mL). The organic layer was separated, and the aqueous phase was extracted with Et_2O (2 x 10 mL). The combined organic phases were dried over anhydrous Na_2SO_4, filtered, and concentrated. Outside the glovebox, purification via AFCC using degassed solvents (heptane to heptane/EtOAc 1:3) afforded MACHO$^{p(Me)}$ as a colourless oil (397 mg, 797 µmol, 51%). The compound was immediately transferred back into the glovebox after isolation.

^{1}H NMR (400 MHz, $CDCl_3$) δ 7.33 – 7.29 (m, 8H), 7.15 – 7.13 (m, 8H), 2.74 – 2.68 (m, 4H), 2.34 (s, 12H), 2.21 – 2.17 (m, 4H). **^{13}C NMR** (101 MHz, $CDCl_3$) δ 138.6, 135.1 (d, *J* = 11.3 Hz), 132.7 (d, *J* = 19.0 Hz), 129.4 (d, *J* = 7.0 Hz), 46.5 (d, *J* = 20.9 Hz), 29.2 (d, *J* = 11.6 Hz), 21.4. **^{31}P NMR** (162 MHz, $CDCl_3$) δ -22.7.

Spectroscopic data in agreement with that reported by Liu, W. *et al.*[3]

Ru-MACHO$^{p(Me)}$

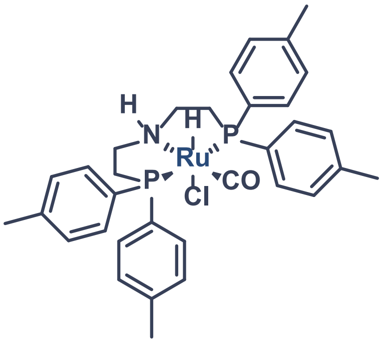

Inside a glovebox, to a COtube charged with MACHO$^{p(Me)}$ (396 mg, 796 µmol) was added carbonylchlorohydridotris(triphenylphosphine)ruthenium(II) (721 mg, 758 µmol) and toluene (10 mL). The reaction mixture was stirred at reflux for 5 h. After reaching ambient temperature, the reaction mixture was concentrated under reduced pressure followed by the addition of Et_2O (10 mL) to precipitate out the complex. The suspension was sonicated for 30 minutes, centrifuged, and the solvent decanted off. The remaining solids were suspended in Et_2O (10 mL) and sonicated for 30 minutes. The suspension was centrifuged, filtered, and the precipitate rinsed with Et_2O (2 x 5 mL). The solids were collected and dried in vacuo overnight, affording Ru-MACHO$^{p(Me)}$ as a white solid (425 mg, 642 µmol, 85%).

^{1}H NMR (400 MHz, C_6D_6) δ 8.12 – 8.08 (m, 4H), 7.78 – 7.74 (m, 4H), 7.02 (d, *J* = 7.7 Hz, 4H), 6.85 (d, *J* = 7.7 Hz, 4H), 4.63 – 4.58 (m, 1H), 2.87 – 2.75 (m, 2H), 2.48 – 2.46 (m, 2H), 2.41 – 2.32 (m, 2H), 2.06 – 1.95 (m, 14H), -14.82 (t, *J* = 19.7 Hz, 1H). **^{13}C NMR** (101 MHz, C_6D_6) δ 207.8 (t, *J* = 12.1 Hz), 139.8, 139.5, 136.1 (t, *J* = 23.3 Hz), 134.3 (t, *J* = 6.6 Hz), 132.6 (t, *J* = 6.6 Hz), 132.3 (t, *J* = 21.7 Hz), 129.4 (t, *J* = 5.0 Hz), 129.2 (t, *J* = 5.1 Hz), 52.4 (t, *J* = 4.5 Hz), 32.3 (t, *J* = 11.3 Hz), 21.3, 21.1. **^{31}P NMR** (162 MHz, C_6D_6) δ 50.8 (d, *J* = 2.9 Hz). **HRMS** (ESI^+) m/z: Calcd for $C_{33}H_{38}NOP_2Ru$ $[M - Cl]^+$ 628.1467; Found 628.1490.

Spectroscopic data in agreement with that reported by Ogata, O. *et al.*[1]

Bis(3,5-dimethylphenyl)phosphine

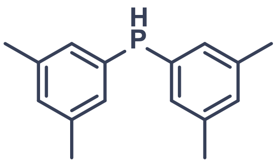

Inside a glovebox, a COtube charged with bis(3,5-dimethylphenyl)phosphine oxide (1.03 g, 4.00 mmol) was added THF (12 mL) and subsequently cooled to -30 °C. DIBAL-H (1.0 M in hexanes, 14.0 mL, 14.0 mmol) was added dropwise to the cold solution over 5 minutes. Upon cessation of hydrogen evolution, the COtube was sealed and stirred at ambient temperature overnight. The reaction mixture was diluted with Et_2O (10 mL) and subsequently quenched with a saturated aqueous solution of Rochelle's salt (29 mL). The resultant biphasic mixture was stirred for 1 h, after which the organic layer was separated, and the aqueous phase was extracted with Et_2O (2 x 10 mL). The combined organic phases were dried over anhydrous $MgSO_4$, filtered, and concentrated. The resultant cloudy liquid was re-dissolved in Et_2O (5 mL) and passed through a short column of basic alumina, eluting with Et_2O (3 x 5 mL). Subsequent removal of the solvent under reduced pressure afforded bis(3,5-dimethylphenyl)phosphine as a colourless oil (922 mg, 3.81 mmol, 95%).

^{1}**H NMR** (400 MHz, C_6D_6) δ 7.22 (d, *J* = 7.8 Hz, 4H), 6.70 (s, 2H), 5.32 (d, *J* = 215.0 Hz, 1H), 2.02 (s, 12H). ^{13}**C NMR** (101 MHz, C_6D_6) δ 138.2 (d, *J* = 6.6 Hz), 135.4 (d, *J* = 10.3 Hz), 132.3 (d, *J* = 16.9 Hz), 130.5, 21.2. ^{31}**P NMR** (162 MHz, C_6D_6) δ -39.9.

Spectroscopic data in agreement with that reported by Selke, R. *et al.*[4]

Bis(2-(bis(3,5-dimethylphenyl)phosphaneyl)ethyl)amine, MACHO$^{m,m(Me)}$

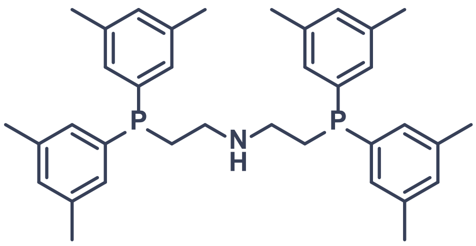

Inside a glovebox, a COtube charged with bis(3,5-dimethylphenyl)phosphine (922 mg, 3.81 mmol) was added THF (10 mL) and *t*BuOK (1.17 g, 10.4 mmol). The resultant deep red solution was stirred at ambient temperature for 15 minutes prior to the addition of bis(2-chloroethyl)amine hydrochloride (309 mg, 1.73 mmol). The COtube was sealed, and the reaction mixture was refluxed overnight. After reaching ambient temperature, the reaction mixture was diluted with Et_2O (10 mL) and subsequently quenched with water (10 mL). The organic layer was separated, and the aqueous phase was extracted with Et_2O (2 x 10 mL). The combined organic phases were dried over anhydrous Na_2SO_4, filtered, and concentrated. Outside the glovebox, purification via AFCC using degassed solvents (heptane to heptane/EtOAc 1:3) afforded MACHO$^{m,m(Me)}$ as a colourless oil (374 mg, 675 μmol, 39%). The compound was immediately transferred back into the glovebox after isolation.

^{1}**H NMR** (400 MHz, C_7D_8) δ 7.20 (d, *J* = 7.6 Hz, 8H), 6.71 (s, 4H), 2.77 – 2.71 (m, 4H), 2.23 – 2.19 (m, 4H), 2.08 (s, 24H). ^{13}**C NMR** (101 MHz, C_7D_8) δ 139.7 (d, *J* = 13.9 Hz), 137.8 (d, *J* = 6.9 Hz), 130.9 (d, *J* = 19.0 Hz), 130.5, 47.0 (d, *J* = 21.3 Hz), 29.7 (d, *J* = 13.1 Hz), 21.2. ^{31}**P NMR** (162 MHz, C_7D_8) δ -21.0.

Spectroscopic data in agreement with that reported by Ogata, O. *et al.*[1]

Ru-MACHO$^{m,m(Me)}$

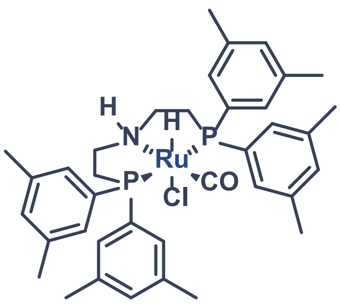

Inside a glovebox, to a COtube charged with MACHO$^{m,m(Me)}$ (373 mg, 674 μmol) was added carbonylchlorohydridotris(triphenylphosphine)ruthenium(II) (611 mg, 642 μmol) and toluene (10 mL). The reaction mixture was stirred at reflux for 5 h. After reaching ambient temperature, the reaction mixture was concentrated under reduced pressure followed by the addition of Et_2O (10 mL) to precipitate out the complex. The suspension was sonicated for 30 minutes, centrifuged, and the solvent decanted off. The remaining solids were suspended in Et_2O (10 mL) and sonicated for 30 minutes. The suspension was centrifuged, filtered, and the precipitate rinsed with Et_2O (2 x 5 mL). The solids were collected and dried in vacuo overnight, affording Ru-MACHO$^{m,m(Me)}$ as a white solid (371 mg, 517 μmol, 81%).

^{1}H NMR (400 MHz, C_6D_6) δ 7.94 – 7.91 (m, 4H), 7.66 – 7.64 (m, 4H), 6.73 (s, 2H), 6.63 (s, 2H), 5.03 – 4.98 (m, 1H), 3.05 – 2.93 (m, 2H), 2.61 – 2.58 (m, 2H), 2.53 – 2.45 (m, 2H), 2.20 – 2.08 (m, 14H), 1.97 (s, 12H), -14.72 (t, *J* = 19.6 Hz, 1H). **^{13}C NMR** (101 MHz, C_6D_6) δ 208.2, 139.3 (t, *J* = 22.2 Hz), 138.0 (t, *J* = 5.1 Hz), 137.8 (t, *J* = 5.2 Hz), 135.6 (t, *J* = 20.5 Hz), 131.9, 131.8 (t, *J* = 6.5 Hz), 131.6, 130.3 (t, *J* = 6.4 Hz), 52.5 (t, *J* = 4.7 Hz), 32.1 (t, *J* = 11.1 Hz), 21.5, 21.3. **^{31}P NMR** (162 MHz, C_6D_6) δ 52.1 (d, *J* = 3.9 Hz). **HRMS** (ESI^{+}) m/z Calcd for $C_{37}H_{46}NOP_2Ru$ [M - Cl]$^{+}$ 684.2093; Found 684.2109.

Spectroscopic data in agreement with that reported by Ogata, O. *et al.*[1]

Bis(4-isopropylphenyl)phosphine oxide

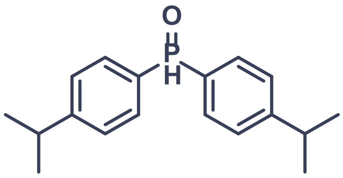

A round-bottomed flask charged with 1-bromo-4-isopropylbenzene (1.74 g, 8.75 mmol) was added THF (10 mL) and subsequently cooled to -78 °C, after which *t*BuLi (1.7 M in hexanes, 8.8 mL, 15 mmol) was added dropwise. The resultant mixture was stirred for 30 min prior to the addition of diethyl phosphate (345 mg, 2.50 mmol). The reaction mixture was stirred at -78 °C for 1 h before slowly warming to ambient temperature to be stirred overnight. The reaction mixture was diluted with DCM (30 mL) and subsequently quenched with a 1 M HCl (30 mL). The organic layer was separated, and the aqueous phase was extracted with DCM (2 x 30 mL). The combined organic phases were dried over anhydrous $MgSO_4$, filtered, and concentrated. Purification via AFCC (heptane to heptane/EtOAc 1:1) afforded bis(4-isopropylphenyl)phosphine oxide as a white solid (605 mg, 2.11 mmol, 84%).

^{1}H NMR (400 MHz, C_6D_6) δ 7.95 (d, *J* = 471.2 Hz, 1H), 7.61 – 7.56 (m, 4H), 6.96 – 6.94 (m, 4H), 2.55 (sept, *J* = 6.9 Hz, 2H), 1.0 (d, *J* = 7.0 Hz, 12H). **^{13}C NMR** (101 MHz, $CDCl_3$) δ 153.9 (d, *J* = 2.9 Hz), 131.0 (d, *J* = 11.8 Hz), 128.8 (d, *J* = 103.7 Hz), 127.2 (d, *J* = 13.0 Hz), 34.4, 23.8. **^{31}P NMR** (162 MHz, C_6D_6) δ 17.2.

Bis(4-isopropylphenyl)phosphine

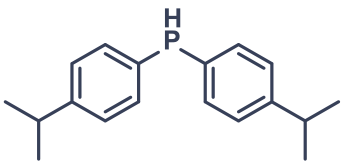

Inside a glovebox, a COtube charged with bis(4-isopropylphenyl)phosphine (604 mg, 2.11 mmol) was added THF (10 mL) and subsequently cooled to -30 °C. DIBAL-H (1.0 M in hexanes, 7.4 mL, 7.4 mmol) was added dropwise to the cold solution over 5 minutes. Upon cessation of hydrogen evolution, the COtube was sealed and stirred at ambient temperature overnight. The reaction mixture was diluted with Et_2O (10 mL) and subsequently quenched with a saturated aqueous solution of Rochelle's salt (16 mL). The resultant biphasic mixture was stirred for 1 h, after which the organic layer was separated, and the aqueous phase was extracted with Et_2O (2 x 10 mL). The combined organic phases were dried over anhydrous $MgSO_4$, filtered, and concentrated. The resultant cloudy liquid was re-dissolved in Et_2O (5 mL) and passed through a short column of basic alumina, eluting with Et_2O (3 x 5 mL). Subsequent removal of the solvent under reduced pressure afforded bis(4-isopropylphenyl)phosphine as a colourless oil (440 mg, 1.63 mmol, 77%).

^{1}H NMR (400 MHz, C_6D_6) δ 7.47 – 7.42 (m, 4H), 6.99 – 6.96 (m, 4H), 5.32 (d, *J* = 214.4 Hz, 1H), 2.62 (sept, *J* = 6.9 Hz, 2H), 1.07 (d, *J* = 7.0 Hz, 12H). **^{13}C NMR** (101 MHz, C_6D_6) δ 149.3, 134.6 (d, *J* = 17.2 Hz), 132.6 (d, *J* = 9.6 Hz), 127.1 (d, *J* = 6.4 Hz), 34.2, 24.0. **^{31}P NMR** (162 MHz, C_6D_6) δ -43.0.

Bis(2-(bis(4-isopropylphenyl)phosphaneyl)ethyl)amine, Ru-MACHO$^{p(i\mathrm{Pr})}$

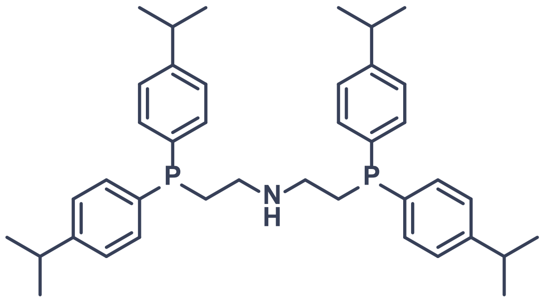

Inside a glovebox, a COtube charged with bis(4-isopropylphenyl)phosphine (440 mg, 1.63 mmol) was added THF (10 mL) and *t*BuOK (498 mg, 4.43 mmol). The resultant deep red solution was stirred at ambient temperature for 15 minutes prior to the addition of bis(2-chloroethyl)amine hydrochloride (132 mg, 0.739 mmol). The COtube was sealed, and the reaction mixture was refluxed overnight. After reaching ambient temperature, the reaction mixture was diluted with Et_2O (10 mL) and subsequently quenched with water (10 mL). The organic layer was separated, and the aqueous phase was extracted with Et_2O (2 x 10 mL). The combined organic phases were dried over anhydrous Na_2SO_4, filtered, and concentrated. Outside the glovebox, purification via AFCC using degassed solvents (heptane to heptane/EtOAc 1:3) afforded MACHO$^{p(i\mathrm{Pr})}$ as a colourless oil (278 mg, 455 µmol, 62%). The compound was immediately transferred back into the glovebox after isolation.

^{1}H NMR (400 MHz, CD_2Cl_2) δ 7.36 – 7.32 (m, 8H), 7.20 – 7.19 (m, 8H), 2.88 (sept, *J* = 6.9 Hz, 4H), 2.71 – 2.65 (m, 4H), 2.19 – 2.15 (m, 4H), 1.44 (bs, 1H), 1.23 (d, *J* = 6.9 Hz, 24H). **^{13}C NMR** (101 MHz, CD_2Cl_2) δ 149.9, 136.1 (d, *J* = 12.0 Hz), 133.0 (d, *J* = 19.1 Hz), 127.0 (d, *J* = 7.0 Hz), 46.7 (d, *J* = 20.9 Hz), 34.3, 29.2 (d, *J* = 11.7 Hz), 24.0. **^{31}P NMR** (162 MHz, CD_2Cl_2) δ -23.3. **HRMS** (ESI^{+}) m/z Calcd for $C_{40}H_{54}NP_2$ $[M + H]^{+}$ 610.3726; Found 610.3766.

Ru-MACHO$^{p(i\mathrm{Pr})}$

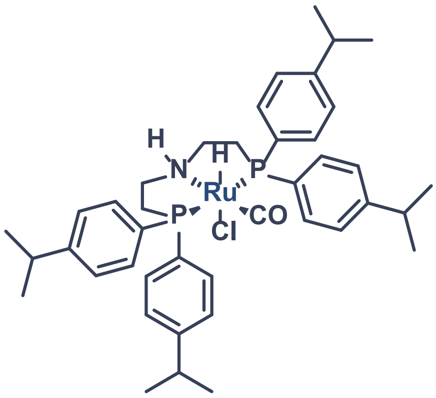

Inside a glovebox, to a COtube charged with MACHO$^{p(i\mathrm{Pr})}$ (240 mg, 394 µmol) was added carbonylchlorohydridotris(triphenylphosphine)ruthenium(II) (357 mg, 375 µmol) and toluene (10 mL). The COtube was sealed, and the reaction mixture was stirred at reflux for 5 h. After reaching ambient temperature, the solvent was evaporated under reduced pressure and the remaining sticky oil redissolved in Et_2O (3 mL). The solution was left at -30 °C overnight after which a white solid had precipitated. The solvent was decantated off and the solids rinsed with Et_2O (2 mL) which was decanted off. The solids were added Et_2O (2 mL), sonicated for 30 minutes, centrifuged, solvent decantated, and at last the solids were dried in vacuo to afford Ru-MACHO$^{p(i\text{Pr})}$ as a white solid (158 mg, 204 µmol, 85%).

^{1}H NMR (400 MHz, CD_2Cl_2) δ 7.78 – 7.68 (m, 8H), 7.30 – 7.27 (m, 8H), 3.93 – 3.88 (m, 1H), 3.46 – 3.34 (m, 2H), 3.00 – 2.88 (m, 6H), 2.54 – 2.38 (m, 4H), 1.25 (t, *J* = 7.1 Hz, 24H), -15.41 (t, *J* = 19.5 Hz, 1H). **^{13}C NMR** (101 MHz, CD_2Cl_2) δ 207.5 (t, *J* = 11.8 Hz), 151.3, 151.3, 135.3 (t, *J* = 23.5 Hz), 133.6 (t, *J* = 6.6 Hz), 132.5 (t, *J* = 6.7 Hz), 132.0 (t, *J* = 21.7 Hz), 127.0 (t, *J* = 5.0 Hz), 126.8 (t, *J* = 5.2 Hz), 52.7 (t, *J* = 5.1 Hz), 34.4, 34.3, 31.9 (t, *J* = 11.5 Hz), 23.9, 23.9. **^{31}P NMR** (162 MHz, CD_2Cl_2) δ 50.3 (d, *J* = 6.6 Hz). **HRMS** (ESI^+) m/z Calcd for $C_{41}H_{54}NOP_2Ru$ $[M - Cl]^+$ 740.2719; Found 740.2750.

3-(4-Bromophenyl)pentan-3-ol

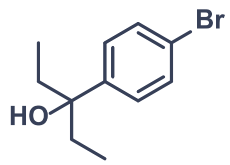

A round-bottomed flask charged with 1,4-dibromobenzene (14.2 g, 60.0 mmol) was added THF (100 mL) and subsequently cooled to -78 °C, after which *n*BuLi (1.5 M in hexanes, 33.3 mL, 50.0 mmol) was added dropwise. The resultant mixture was stirred for 1 h prior to the addition of 3-pentanone (8.61 g, 100 mmol). The reaction mixture was stirred at -78 °C for 1 h before slowly warming to ambient temperature to be stirred overnight. The reaction mixture was diluted with EtOAc (100 mL) and subsequently quenched with a saturated aqueous solution of NH_4Cl (100 mL). The organic layer was separated, and the aqueous phase was extracted with EtOAc (2 x 100 mL). The combined organic phases were dried over anhydrous $MgSO_4$, filtered, and concentrated. Purification via AFCC (heptane to heptane/EtOAc 9:1) afforded 3-(4-bromophenyl)pentan-3-ol as a colourless oil (10.7 g, 43.9 mmol, 88%).

^{1}H NMR (400 MHz, $CDCl_3$) δ 7.47 – 7.43 (m, 2H), 7.26 – 7.24 (m, 2H), 1.88 – 1.73 (m, 4H), 1.59 – 1.57 (m, 1H), 0.75 (t, *J* = 7.4 Hz, 6H). **^{13}C NMR** (101 MHz, $CDCl_3$) δ 144.9, 131.2, 127.6, 120.4, 77.4, 35.2, 7.9.

Spectroscopic data in agreement with that reported by Aubrey, M. *et al.*[5]

1-Bromo-4-(1-ethylpropyl)benzene

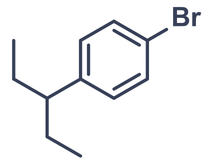

A round-bottomed flask charged with 3-(4-bromophenyl)pentan-3-ol (10.7 g, 43.9 mmol) was added DCM (150 mL) and subsequently cooled to 0 °C, after which Et_3SiH (17.7 mL, 110 mmol) and TFA (16.9 mL, 219 mmol) were added dropwise in that order. The reaction mixture was stirred for at 0 °C for 1 h before slowly warming to ambient temperature to be stirred overnight. The reaction mixture was quenched with a saturated aqueous solution of $NaHCO_3$ (150 mL). The organic layer was separated, and the aqueous phase was extracted with DCM (2 x 100 mL). The combined organic phases were dried over anhydrous $MgSO_4$, filtered, and concentrated. Purification via AFCC (heptane) afforded 1-bromo-4-(1-ethylpropyl)benzene as a colourless oil (9.79 g, 43.1 mmol, 98%).

^{1}H NMR (400 MHz, $CDCl_3$) δ 7.42 – 7.38 (m, 2H), 7.03 – 6.99 (m, 2H), 2.32 – 2.24 (m, 1H), 1.73 – 1.62 (m, 2H), 1.56 – 1.44 (m, 2H), 0.75 (t, *J* = 7.4 Hz, 6H). **^{13}C NMR** (101 MHz, $CDCl_3$) δ 144.9, 131.3, 129.7, 119.5, 49.4, 29.3, 12.2.

Spectroscopic data in agreement with that reported by Aubrey, M. *et al.*[5]

Bis(4-(pentan-3-yl)phenyl)phosphine oxide

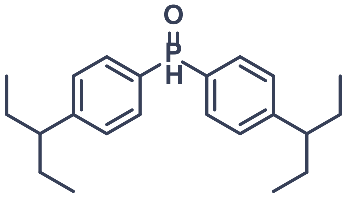

A round-bottomed flask charged with 1-bromo-4-(1-ethylpropyl)benzene (1.99 g, 8.75 mmol) was added THF (10 mL) and subsequently cooled to -78 °C, after which *t*BuLi (1.7 M in hexanes, 8.8 mL, 15 mmol) was added dropwise. The resultant mixture was stirred for 30 min prior to the addition of diethyl phosphate (345 mg, 2.50 mmol). The reaction mixture was stirred at -78 °C for 1 h before slowly warming to ambient temperature to be stirred overnight. The reaction mixture was diluted with DCM (30 mL) and subsequently quenched with 1 M HCl (30 mL). The organic layer was separated, and the aqueous phase was extracted with DCM (2 x 30 mL). The combined organic phases were dried over anhydrous $MgSO_4$, filtered, and concentrated. Purification via AFCC (heptane to heptane/EtOAc 1:1) afforded bis(4-(pentan-3-yl)phenyl)phosphine oxide as a colourless oil (769 mg, 2.25 mmol, 90%).

^{1}H NMR (400 MHz, $CDCl_3$) δ 8.05 (d, J = 477.9 Hz, 1H), 7.65 – 7.59 (m, 4H), 7.28 – 7.26 (m, 4H), 2.42 – 2.34 (m, 2H), 1.76 – 1.64 (m, 4H), 1.61 – 1.49 (m, 4H), 0.76 (t, J = 7.4 Hz, 12H). **^{13}C NMR** (101 MHz, $CDCl_3$) δ 151.2, 131.0 (d, J = 11.8 Hz), 128.8 (d, J = 103.7 Hz), 128.6 (d, J = 13.1 Hz), 50.0, 29.2, 12.3. **^{31}P NMR** (162 MHz, $CDCl_3$) δ 21.9.

Bis(4-(pentan-3-yl)phenyl)phosphine

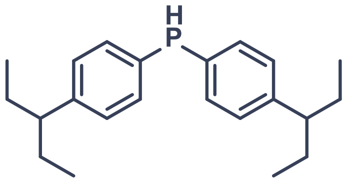

Inside a glovebox, a COtube charged with bis(4-(pentan-3-yl)phenyl)phosphine oxide (769 mg, 2.25 mmol) was added THF (10 mL) and subsequently cooled to -30 °C. DIBAL-H (1.0 M in hexanes, 7.9 mL, 7.9 mmol) was added dropwise to the cold solution over 5 minutes. Upon cessation of hydrogen evolution, the COtube was sealed and stirred at ambient temperature overnight. The reaction mixture was diluted with Et_2O (10 mL) and subsequently quenched with a saturated aqueous solution of Rochelle's salt (17 mL). The resultant biphasic mixture was stirred for 1 h, after which the organic layer was separated, and the aqueous phase was extracted with Et_2O (2 x 10 mL). The combined organic phases were dried over anhydrous $MgSO_4$, filtered, and concentrated. The resultant cloudy liquid was re-dissolved in Et_2O (5 mL) and passed through a short column of basic alumina, eluting with Et_2O (3 x 5 mL). Subsequent removal of the solvent under reduced pressure afforded bis(4-(pentan-3-yl)phenyl)phosphine as a colourless oil (597 mg, 1.83 mmol, 81%).

^{1}H NMR (400 MHz, C_6D_6) δ 7.47 – 7.42 (m, 4H), 6.93 – 6.90 (m, 4H), 5.34 (d, J = 214.2, 1H), 2.14 – 2.06 (m, 2H), 1.54 – 1.36 (m, 8H), 0.71 (t, J = 7.4 Hz, 12H). **^{13}C NMR** (101 MHz, $CDCl_3$) δ -43.5. **^{31}P NMR** (162 MHz, $CDCl_3$) δ 146.3, 134.5 (d, J = 17.2 Hz), 132.4 (d, J = 9.5 Hz), 128.5 (d, J = 6.3 Hz), 49.7, 29.5, 12.4.

Bis(2-(bis(4-(pentan-3-yl)phenyl)phosphaneyl)ethyl)amine, MACHO$^{p(3\text{-}Pe)}$

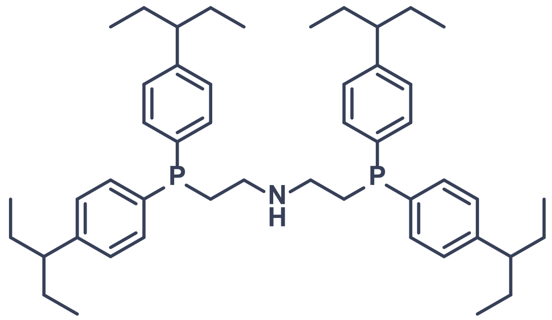

Inside a glovebox, a COtube charged with bis(4-(pentan-3-yl)phenyl)phosphine (597 mg, 1.83 mmol) was added THF (10 mL) and *t*BuOK (559 mg, 4.99 mmol). The resultant deep red solution was stirred at ambient temperature for 15 minutes prior to the addition of bis(2-chloroethyl)amine hydrochloride (148 mg, 0.831 mmol). The COtube was sealed, and the reaction mixture was refluxed overnight. After reaching ambient temperature, the reaction mixture was diluted with Et_2O (10 mL) and subsequently quenched with water (10 mL). The organic layer was separated, and the aqueous phase was extracted with Et_2O (2 x 10 mL). The combined organic phases were dried over anhydrous Na_2SO_4, filtered, and concentrated. Outside the glovebox, purification via AFCC using degassed solvents (heptane to heptane/EtOAc 1:4) afforded MACHO$^{p(3\text{-}Pe)}$ as a colourless oil (324 mg, 449 µmol, 54%). The compound was immediately transferred back into the glovebox after isolation.

^{1}**H NMR** (400 MHz, CD_2Cl_2) δ 7.35 – 7.31 (m, 8H), 7.12 – 7.10 (m, 8H), 2.71 – 2.65 (m, 4H), 2.34 – 2.27 (m, 4H), 2.18 – 2.15 (m, 4H), 1.73 – 1.63 (m, 8H), 1.58 – 1.47 (m, 8H), 0.75 (t, J = 7.4 Hz, 24H). ^{13}**C NMR** (101 MHz, CD_2Cl_2) δ 146.9, 136.1 (d, J = 12.0 Hz), 132.9 (d, J = 19.1 Hz), 128.4 (d, J = 7.0 Hz), 49.8, 46.8 (d, J = 20.8 Hz), 29.5, 29.4, 12.4. ^{31}**P NMR** (162 MHz, CD_2Cl_2) δ -22.7. **HRMS** (ESI$^+$) m/z Calcd for $C_{48}H_{70}NP_2$ [M + H]$^+$ 722.4978; Found 722.5017.

Ru-MACHO$^{p(3\text{-}Pe)}$

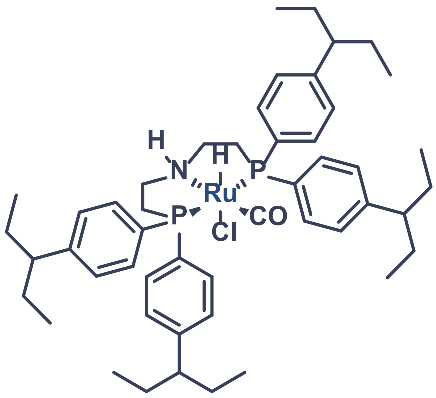

Inside a glovebox, to a COtube charged with MACHO$^{p(3\text{-}Pe)}$ (324 mg, 0.449 mmol) was added carbonylchlorohydridotris(triphenylphosphine)ruthenium(II) (407 mg, 0.428 mmol) and toluene (10 mL). The COtube was sealed, and the reaction mixture was stirred at reflux for 5 h. After reaching ambient temperature, the solvent was evaporated under reduced pressure and the remaining sticky oil redissolved in Et_2O (3 mL). The solution was left at -30 °C overnight after which a white solid had precipitated. The solvent was decantated off and the solids rinsed with Et_2O (2 mL) which was decanted off. The solids were re-dissolved in Et_2O (3 mL), and the solution was left at -30 °C overnight after which a white solid had precipitated. The solvent was decantated off and the solids rinsed with Et_2O (2 mL) which was decanted off, and at last the solids were dried in vacuo to afford Ru-MACHO$^{p(3\text{-}Pe)}$ as a white solid (91.2 mg, 103 µmol, 24%).

^{1}H NMR (400 MHz, CD_2Cl_2) δ 7.76 – 7.70 (m, 8H), 7.72 – 7.19 (m, 8H), 4.09 – 4.03 (m, 1H), 3.40 – 3.29 (m, 2H), 2.92 – 2.87 (m, 2H), 2.51 – 2.32 (m, 8H), 1.62 – 1.50 (m, 8H), 0.81 – 0.75 (m, 24H), -15.30 (t, J = 19.3 Hz, 1H). **^{13}C NMR** (101 MHz, CD_2Cl_2) δ 207.4 (t, J = 12.4 Hz), 148.5, 148.4, 135.0 (t, J = 23.4 Hz), 133.5 (t, J = 6.5 Hz), 132.7 (t, J = 6.7 Hz), 132.2 (t, J = 21.6 Hz), 128.3 (t, J = 5.0 Hz), 128.1 (t, J = 5.1 Hz), 52.6 (t, J = 4.9 Hz), 49.8, 49.8 32.4 (t, J = 11.4 Hz), 29.4, 29.3, 29.3, 29.3, 12.4, 12.4, 12.4, 12.3. **^{31}P NMR** (162 MHz, CD_2Cl_2) δ 50.6 (d, J = 4.1 Hz). **HRMS** (ESI^+) m/z Calcd for $C_{49}H_{70}NOP_2Ru$ $[M - Cl]^+$ 852.3971; Found 852.4029.

Bis(2-naphthyl)phosphine

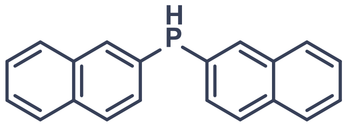

Inside a glovebox, a COtube charged with bis(2-naphthyl)phosphine oxide (1.36 g, 4.50 mmol) was added THF (12 mL) and subsequently cooled to -30 °C. DIBAL-H (1.0 M in hexanes, 15.8 mL, 15.8 mmol) was added dropwise to the cold solution over 5 minutes. Upon cessation of hydrogen evolution, the COtube was sealed and stirred at ambient temperature overnight. The reaction mixture was diluted with Et_2O (20 mL) and subsequently quenched with a saturated aqueous solution of Rochelle's salt (33 mL). The resultant biphasic mixture was stirred for 1 h, after which the organic layer was separated, and the aqueous phase was extracted with Et_2O (3 x 20 mL). The combined organic phases were dried over anhydrous $MgSO_4$, filtered, and concentrated. The resultant cloudy liquid was re-dissolved in Et_2O (10 mL) and passed through a short column of basic alumina, eluting with Et_2O (3 x 10 mL). Subsequent removal of the solvent under reduced pressure afforded bis(2-naphthyl)phosphine as a white solid (1.20 g, 4.20 mmol, 93%).

^{1}H NMR (400 MHz, C_6D_6) δ 7.95 (d, J = 8.6 Hz, 2H), 7.73 – 7.66 (m, 6H), 7.44 – 7.37 (m, 6H), 5.44 (d, J = 218.9 Hz, 1H). **^{13}C NMR** (101 MHz, C_6D_6) δ 134.6 (d, J = 22.1 Hz), 134.0 (d, J = 7.9 Hz), 133.7, 132.8 (d, J = 11.2 Hz), 131.0 (d, J = 12.7 Hz), 128.5 (d, J = 5.4 Hz), 128.2, 126.7 (d, J = 19.4 Hz). **^{31}P NMR** (162 MHz, C_6D_6) δ -39.7.

Spectroscopic data in agreement with that reported by Bibal, B. *et al.*[6]

Bis(2-(bis(2-naphthyl)phosphaneyl)ethyl)amine, MACHO^{Naph}

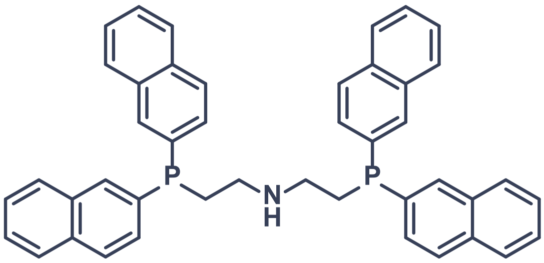

Inside a glovebox, a COtube charged with bis(2-naphthyl)phosphine (441 mg, 1.54 mmol) was added THF (10 mL) and *t*BuOK (471 mg, 4.20 mmol). The resultant deep red solution was stirred at ambient temperature for 15 minutes prior to the addition of bis(2-chloroethyl)amine hydrochloride (125 mg, 0.700 mmol). The COtube was sealed, and the reaction mixture was refluxed overnight. After reaching ambient temperature, the reaction mixture was diluted with Et_2O (10 mL) and subsequently quenched with water (10 mL). The organic layer was separated, and the aqueous phase was extracted with Et_2O (3 x 10 mL). The combined organic phases were dried over anhydrous Na_2SO_4, filtered, and concentrated. Outside the glovebox, purification via AFCC using degassed solvents (heptane to heptane/EtOAc

1:2) afforded MACHO^{Naph} as a white solid (272 mg, 424 μmol, 61%). The compound was immediately transferred back into the glovebox after isolation.

^{1}H NMR (400 MHz, $CDCl_3$) δ 7.99 – 7.97 (m, 4H), 7.80 – 7.76 (m, 8H), 7.74 – 7.72 (m, 4H), 7.51 – 7.44 (m, 8H), 7.41 – 7.37 (m, 4H), 2.82 – 2.76 (m, 4H), 2.42 – 2.38 (m, 4H), 1.26 (bs, 1H). **^{13}C NMR** (101 MHz, $CDCl_3$) δ 135.8 (d, J = 12.6 Hz), 133.5 (d, J = 3.6 Hz), 133.3 (d, J = 8.4 Hz), 133.2, 129.1 (d, J = 14.4 Hz), 128.2 (d, J = 6.0 Hz), 128.1, 127.9, 126.8, 126.5, 46.5 (d, J = 20.5 Hz), 29.0 (d, J = 12.3 Hz). **^{31}P NMR** (162 MHz, $CDCl_3$) δ -19.6.

Spectroscopic data in agreement with that reported by Liu, W. *et al.*[3]

Ru-MACHO^{Naph}

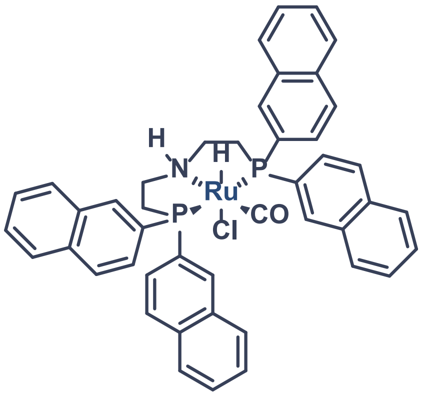

Inside a glovebox, to a COtube charged with MACHO^{Naph} (33.7 mg, 52.5 μmol) was added carbonylchlorohydridotris(triphenylphosphine)ruthenium(II) (47.6 mg, 50.0 μmol) and toluene (0.45 mL). The COtube was sealed, and the reaction mixture was stirred at 120 °C for 5 h. After reaching ambient temperature, a white precipitate could be observed in the reaction, and the COtube was taken inside the glovebox where Et_2O (3 mL) was added. The solids were filtrated, followed by rinsing with Et_2O (10 mL) and pentane (10 mL), the solids were then dried in vacuo to afford Ru-MACHO^{Naph} as a white solid (24.6 mg, 30.5 μmol, 61%).

^{1}H NMR (400 MHz, CD_2Cl_2) δ 8.51 (t, J = 6.0 Hz, 2H), 8.41 (t, J = 6.1 Hz, 2H), 7.96 – 7.78 (m, 16H), 7.57 – 7.51 (m, 8H), 4.10 – 4.03 (m, 1H), 3.60 – 3.48 (m, 2H), 3.21 – 3.16 (m, 2H), 2.77 – 2.62 (m, 4H), -14.91 (t, J = 19.4 Hz, 1H). Poor solubility prevented **^{13}C NMR** measurements. **^{31}P NMR** (162 MHz, CD_2Cl_2) δ 53.8. **HRMS** (ESI$^+$) m/z Calcd for $C_{45}H_{38}NOP_2Ru$ [M - Cl]$^+$ 772.1467; Found 772.1517.

Bis([1,1'-biphenyl]-4-yl)phosphine oxide

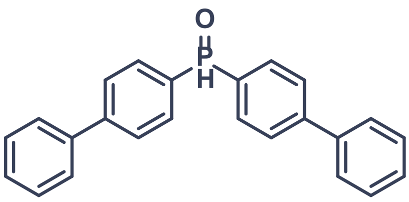

Inside a glovebox, a COtube was charged with magnesium turnings (729 mg, 30.0 mmol) followed by sealing. The flask was stirred overnight at 110 °C without solvent. To the flask was added THF (20 mL) and a crystal of iodine. The slight orange solution was stirred for 30 min, at which point a grey suspension could be observed. The flask was slowly added *p*-bromobiphenyl (6.99 g, 30.0 mmol), after which the mixture was heated to 65 °C and stirred for 2 h. The mixture was cooled to ambient temperature prior to the dropwise addition of diethyl phosphate (1.38 g, 10.0 mmol). The reaction mixture was stirred at ambient temperature overnight. The reaction mixture was quenched with 1 M HCl (50 mL) and the aqueous phase extracted with DCM (3 x 50 mL). The combined organic phases were washed twice with water (2 x 30 mL), dried over Na_2SO_4, and evaporated onto celite®. Purification via AFCC (Heptane/EtOAc 3:1 EtOAc) afforded bis([1,1'-biphenyl]-4-yl)phosphine oxide as a white solid (3170 mg, 8.9 mmol, 89%).

^{1}H NMR (400 MHz, $CDCl_3$) δ 8.18 (d, *J* = 481.1 Hz, 1H), 7.86 – 7.78 (m, 4H), 7.77 – 7.71 (m, 4H), 7.65 – 7.59 (m, 4H), 7.51 – 7.44 (m, 4H), 7.44 – 7.38 (m, 2H). **^{13}C NMR** (101 MHz, $CDCl_3$) δ 145.6 (d, *J* = 2.9 Hz), 139.9, 131.4 (d, *J* = 11.7 Hz), 130.1 (d, *J* = 102.8 Hz), 129.1, 128.4, 127.8 (d, *J* = 13.2 Hz), 127.4. **^{31}P NMR** (162 MHz, $CDCl_3$) δ 21.0.

Spectroscopic data in agreement with that reported by Qiu, R. *et al.*[7]

Bis([1,1'-biphenyl]-4-yl)phosphine

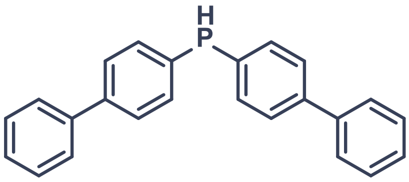

Inside a glovebox, a COtube charged with bis([1,1'-biphenyl]-4-yl)phosphine oxide (1.60 g, 4.50 mmol) was added THF (14 mL) and subsequently cooled to -30 °C. DIBAL-H (1.0 M in hexanes, 15.8 mL, 15.8 mmol) was added dropwise to the cold solution over 5 minutes. Upon cessation of hydrogen evolution, the COtube was sealed and stirred at ambient temperature overnight. The reaction mixture was diluted with Et_2O (10 mL) and subsequently quenched with a saturated aqueous solution of Rochelle's salt (33 mL). The resultant biphasic mixture was stirred for 1 h, after which the organic layer was separated, and the aqueous phase was extracted with Et_2O (3 x 10 mL). The combined organic phases were dried over anhydrous $MgSO_4$, filtered, and concentrated. The resultant cloudy liquid was re-dissolved in Et_2O (5.0 mL) and passed through a short column of basic alumina, eluting with Et_2O (3 x 5.0 mL). Subsequent removal of the solvent under reduced pressure afforded bis([1,1'-biphenyl]-4-yl)phosphine as a white solid (1.36 g, 4.03 mmol, 90%).

^{1}H NMR (400 MHz, $CDCl_3$) δ 7.61 – 7.56 (m, 6H), 7.46 – 7.42 (m, 2H), 7.38 – 7.33 (m, 1H), 5.33 (d, *J* = 219.6 Hz, 1H). **^{13}C NMR** (101 MHz, $CDCl_3$) δ 141.6, 140.7, 134.6 (d, *J* = 16.9 Hz), 133.6 (d, *J* = 9.9 Hz), 129.0, 127.7, 127.5 (d, *J* = 6.5 Hz), 127.2. **^{31}P NMR** (162 MHz, $CDCl_3$) δ -42.6.

Bis(2-(di([1,1'-biphenyl]-4-yl)phosphaneyl)ethyl)amine, MACHO^{Biph}

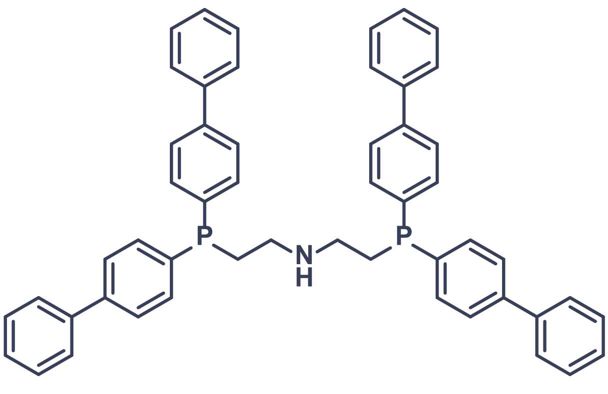

Inside a glovebox, a COtube charged with bis([1,1'-biphenyl]-4-yl)phosphine (521 mg, 1.54 mmol) was added 2-MeTHF (10 mL) and *t*BuOK (471 mg, 4.20 mmol). The resultant deep red solution was stirred at ambient temperature for 15 minutes prior to the addition of bis(2-chloroethyl)amine hydrochloride (125 mg, 0.700 mmol). The COtube was sealed, and the reaction mixture was refluxed overnight. After reaching ambient temperature, the reaction mixture was diluted with Et_2O (10 mL) and subsequently quenched with water (10 mL). The organic layer was separated, and the aqueous phase was extracted with EtOAc (3 x 10 mL). The combined organic phases were dried over anhydrous Na_2SO_4, filtered, and concentrated. Outside the glovebox, purification via AFCC using degassed solvents (heptane to EtOAc) afforded MACHO^{Biph} as an off-white solid (120 mg, 161 µmol, 23%). The compound was immediately transferred back into the glovebox after isolation.

^{1}H NMR (400 MHz, $CDCl_3$) δ 7.59 – 7.55 (m, 16H), 7.53 – 7.49 (m, 8H), 7.44 – 7.41 (m, 8H), 7.36 – 7.33 (m, 4H), 2.85 – 2.79 (m, 4H), 2.33 – 2.30 (m, 4H). **^{13}C NMR** (101 MHz, $CDCl_3$) δ 141.7, 140.6, 137.3 – 137.1 (m), 133.3 (d, J = 18.8 Hz), 129.0, 127.7, 127.4 (d, J = 7.0 Hz), 127.2, 46.5 – 46.3 (m), 29.1 – 28.9 (m). **^{31}P NMR** (162 MHz, $CDCl_3$) δ -22.2. **HRMS** (ESI$^+$) m/z Calcd for $C_{52}H_{46}NP_2$ [M + H]$^+$ 746.3100; Found 746.3109.

Ru-MACHO^{Biph}

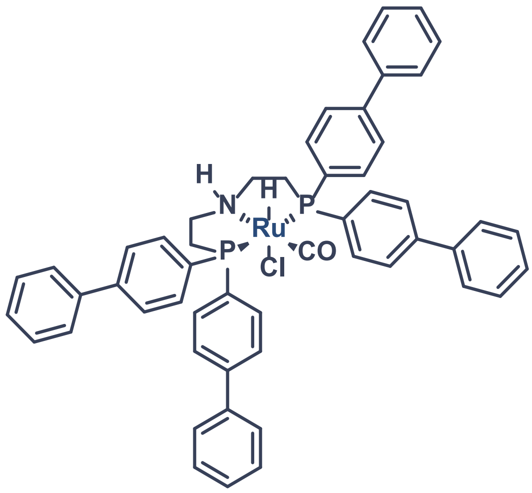

Inside a glovebox, to a COtube charged with MACHO^{Biph} (38.7 mg, 50.0 µmol) was added carbonylchlorohydridotris(triphenylphosphine)ruthenium(II) (47.6 mg, 50.0 µmol) and toluene (0.45 mL). The COtube was sealed, and the reaction mixture was stirred at reflux for 5 h. After reaching ambient temperature, white precipitate could be observed in the reaction, and the COtube was taken inside the glovebox where Et_2O (5 mL) was added. The solids were filtered, followed by rinsing the solids with Et_2O (10 mL) and pentane (10 mL), the solids were then dried in vacuo to afford Ru-MACHO^{Biph} as a white solid (37.4 mg, 41.1 µmol, 82%).

^{1}H NMR (400 MHz, $CDCl_3$) δ 7.99 – 7.89 (m, 8H), 7.65 – 7.58 (m, 16H), 7.46 – 7.35 (m, 12H), 4.23 – 4.18 (m, 1H), 3.52 – 3.42 (m, 2H), 3.04 – 2.98 (m, 2H), 2.65 – 2.52 (m, 4H), -15.29 (t, J = 19.5 Hz, 1H). **^{13}C NMR** (101 MHz, $CDCl_3$) δ 142.9, 142.9, 140.7, 140.3, 136.2 (t, J = 23.4 Hz), 133.9 (t, J = 6.7 Hz), 133.2 – 132.9 (m), 129.0, 129.0, 128.0, 127.8, 127.4, 127.3, 127.3, 127.3, 52.5 – 52.4 (m), 32.3 – 32.1 (m). **^{31}P NMR** (162 MHz, $CDCl_3$) δ 51.1 (d, J = 3.8 Hz). **HRMS** (ESI$^+$) m/z Calcd for $C_{53}H_{46}NOP_2Ru$ [M - Cl]$^+$ 876.2093; Found 876.2129.

Bis(4-(trifluoromethyl)phenyl)phosphine oxide

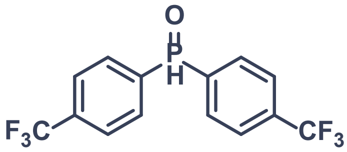

Under argon, a flame-dried round-bottomed flask charged with 4-bromobenzotrifluoride (4.05 g, 18.0 mmol) was added anhydrous THF (10 mL) and subsequently cooled to -78 °C, after which *t*BuLi (1.7 M in hexanes, 8.8 mL, 15 mmol) was added dropwise. The resultant mixture was stirred for 30 min prior to the addition of diethyl phosphate (345 mg, 2.50 mmol). The reaction mixture was stirred at -78 °C for 1 h before slowly warming to ambient temperature to be stirred overnight. The reaction mixture was diluted with DCM (30 mL) and subsequently quenched with a solution of HCl (1 M in water, 30 mL). The organic layer was separated, and the aqueous phase was extracted with DCM (2 x 30 mL). The combined organic phases were dried over anhydrous $MgSO_4$, filtered, and concentrated. Purification via AFCC (heptane to heptane/EtOAc 1:1) afforded bis(3,5-di(pentan-3-yl)phenyl)phosphine oxide as a white solid (971 mg, 2.01 mmol, 80%).

^{1}H NMR (400 MHz, $CDCl_3$) δ 8.24 (d, *J* = 504.8 Hz, 1H), 7.89 – 7.78 (m, 8H). **^{13}C NMR** (101 MHz, $CDCl_3$) δ 134.9 (d, *J* = 99.7 Hz), 134.8 (dd, *J* = 33.0, 2.9 Hz), 131.3 (d, *J* = 12.0 Hz), 126.1 (dq, *J* = 13.2, 3.7 Hz), 123.4 (q, *J* = 272.4 Hz). **^{19}F NMR** (176 MHz, $CDCl_3$) δ -63.0. **^{31}P NMR** (162 MHz, $CDCl_3$) δ 14.4.

Spectroscopic data in agreement with that reported by Xie, X. *et al.*[8]

Bis(4-(trifluoromethyl)phenyl)phosphine

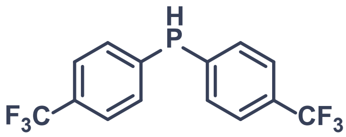

Inside a glovebox, a COtube charged with bis(4-(trifluoromethyl)phenyl)phosphine oxide (947 mg, 2.80 mmol) was added THF (10 mL) and subsequently cooled to -30 °C. DIBAL-H (1.0 M in hexanes, 9.8 mL, 9.8 mmol) was added dropwise to the cold solution over 5 minutes. Upon cessation of hydrogen evolution, the COtube was sealed and stirred at ambient temperature overnight. The reaction mixture was diluted with Et_2O (10 mL) and subsequently quenched with a saturated aqueous solution of Rochelle's salt (21 mL). The resultant biphasic mixture was stirred for 1 h, after which the organic layer was separated, and the aqueous phase was extracted with Et_2O (3 x 10 mL). The combined organic phases were dried over anhydrous $MgSO_4$, filtered, and concentrated. The resultant cloudy liquid was re-dissolved in Et_2O (5.0 mL) and passed through a short column of basic alumina, eluting with Et_2O (3 x 5.0 mL). Subsequent removal of the solvent under reduced pressure afforded bis(4-(trifluoromethyl)phenyl)phosphine as a colourless oil (883 mg, 2.74 mmol, 98%).

^{1}H NMR (400 MHz, C_6D_6) δ 7.18 (d, *J* = 7.8 Hz, 4H), 6.99 (t, *J* = 7.4 Hz, 4H), 4.85 (d, *J* = 219.6 Hz, 1H). **^{13}C NMR** (101 MHz, $CDCl_3$) δ 138.9 (d, *J* = 12.6 Hz), 134.3 (d, *J* = 17.0 Hz), 131.2 (q, *J* = 32.6 Hz), 125.7 – 125.4 (m), 124.1 (q, *J* = 272.2 Hz). **^{19}F NMR** (176 MHz, $CDCl_3$) δ -62.9. **^{31}P NMR** (162 MHz, $CDCl_3$) δ -41.2.

Spectroscopic data in agreement with that reported by Qi, G.-H. *et al.*[9]

Bis(2-(bis(4-(trifluoromethyl)phenyl)phosphaneyl)ethyl)amine, MACHO$^{p(CF3)}$

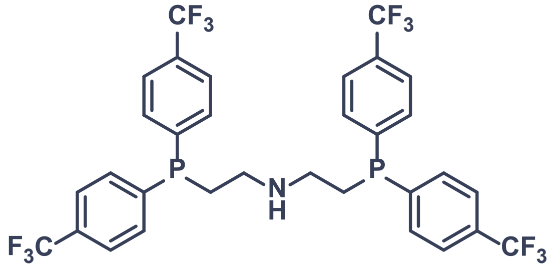

Inside a glovebox, a COtube charged with bis(4-(trifluoromethyl)phenyl)phosphine (672 mg, 2.09 mmol) was added THF (15 mL) and *t*BuOK (638 mg, 5.69 mmol). The resultant deep red solution was stirred at ambient temperature for 15 minutes prior to the addition of bis(2-chloroethyl)amine hydrochloride (169 mg, 0.948 mmol). The COtube was sealed, and the reaction mixture was refluxed for 3 days. After reaching ambient temperature, the reaction mixture was diluted with Et_2O (10 mL) and subsequently quenched with water (10 mL). The organic layer was separated, and the aqueous phase was extracted with Et_2O (3 x 10 mL). The combined organic phases were dried over anhydrous Na_2SO_4, filtered, and concentrated. Outside the glovebox, purification via AFCC using degassed solvents (heptane to heptane/EtOAc 3:7) afforded MACHO$^{p(CF3)}$ as a yellow oil (567 mg, 794 µmol, 84%). The compound was immediately transferred back into the glovebox after isolation.

^{1}H NMR (400 MHz, $CDCl_3$) δ 7.59 – 7.58 (m, 8H), 7.51 – 7.47 (m, 8H), 2.75 – 2.69 (m, 4H), 2.27 – 2.24 (m, 4H), 1.43 (bs, 1H). **^{13}C NMR** (101 MHz, $CDCl_3$) δ 142.7 (d, *J* = 16.0 Hz), 133.1 (d, *J* = 19.1 Hz), 131.5 – 130.6 (m), 131.2 (q, *J* = 32.6 Hz), 125.6 – 125.4 (m), 124.0 (q, *J* = 272.3 Hz), 46.1 (d, *J* = 19.9 Hz), 28.8 (d, *J* = 12.8 Hz). **^{19}F NMR** (176 MHz, $CDCl_3$) δ -62.9. **^{31}P NMR** (162 MHz, $CDCl_3$) δ -20.0. **HRMS** (ESI^+) m/z Calcd for $C_{32}H_{26}F_{12}NP_2$ $[M + H]^+$ 714.1343; Found 714.1352.

Ru-MACHO$^{p(CF3)}$

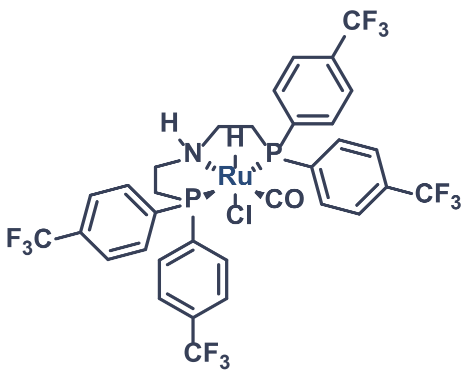

Inside a glovebox, to a COtube charged with MACHO$^{p(CF3)}$ (38.9 mg, 50.0 µmol) was added carbonylchlorohydridotris(triphenylphosphine)ruthenium(II) (47.6 mg, 50.0 µmol) and toluene (0.45 mL). The COtube was sealed, and the reaction mixture was stirred reflux for 5 h. After reaching ambient temperature, the reaction mixture was diluted with pentane (4 mL), and the solution was left at -30 °C overnight after which a white solid had precipitated. The solids were filtered off and rinsed with pentane (10 mL), after which a white solid was obtained. The solids were dried in vacuo to afford Ru-MACHO$^{p(CF3)}$ as a white solid (27.5 mg, 31.3 µmol, 63%).

^{1}H NMR (400 MHz, C_6D_6) δ 7.91 – 7.87 (m, 4H), 7.50 – 7.46 (m, 4H), 7.36 (d, *J* = 7.9 Hz, 4H), 7.19 (d, *J* = 8.1 Hz, 4H), 4.74 – 4.68 (m, 1H), 2.88 – 2.74 (m, 2H), 2.25 – 2.22 (m, 2H), 2.09 – 2.01 (m, 2H), 1.86 – 1.79 (m, 2H), -15.07 (t, *J* = 20.1 Hz, 1H). **^{13}C NMR** (101 MHz, C_6D_6) δ 206.1 (t, *J* = 12.7 Hz), 141.9 (t, *J* = 21.7 Hz), 138.2 (t, *J* = 19.4 Hz), 134.6 (t, *J* = 6.8 Hz), 132.9 – 132.3 (m), 133.3 (t, *J* = 6.9

Hz), 132.3 – 131.8 (m), 128.7 – 120.4 (m), 128.2 – 120.2 (m), 125.9 – 125.7 (m), 125.5 – 125.3 (m), 52.4 (t, *J* = 4.4 Hz), 31.8 (t, *J* = 11.1 Hz). **^{19}F NMR** (176 MHz, C_6D_6) δ -62.7 (s), -62.9 (s). **^{31}P NMR** (162 MHz, C_6D_6) δ 53.8 (bs). **HRMS** (ESI$^+$) m/z Calcd for $C_{33}H_{26}F_{12}NOP_2Ru$ [M - Cl]$^+$ 844.0341; Found 844.0370.

Bis(4-methoxyphenyl)phosphine

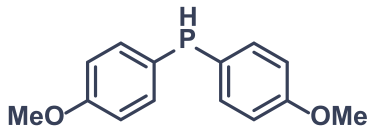

Inside a glovebox, a COtube charged with bis(4-methoxyphenyl)phosphine oxide (1.18 g, 4.50 mmol) was added THF (14 mL) and subsequently cooled to -30 °C. DIBAL-H (1.0 M in hexanes, 15.8 mL, 15.8 mmol) was added dropwise to the cold solution over 5 minutes. Upon cessation of hydrogen evolution, the COtube was sealed and stirred at ambient temperature overnight. The reaction mixture was diluted with Et_2O (10 mL) and subsequently quenched with a saturated aqueous solution of Rochelle's salt (33 mL). The resultant biphasic mixture was stirred for 1 h, after which the organic layer was separated, and the aqueous phase was extracted with Et_2O (3 x 10 mL). The combined organic phases were dried over anhydrous $MgSO_4$, filtered, and concentrated. The resultant cloudy liquid was re-dissolved in Et_2O (5 mL) and passed through a short column of basic alumina, eluting with Et_2O (3 x 5 mL). Subsequent removal of the solvent under reduced pressure afforded bis(4-methoxyphenyl)phosphine as a colourless oil (1.10 g, 4.47 mmol, 99%).

^{1}H NMR (400 MHz, C_6D_6) δ 7.42 – 7.37 (m, 4H), 6.72 – 6.68 (m, 4H), 5.30 (d, *J* = 214.3 Hz, 1H), 3.22 (s, 6H). **^{13}C NMR** (101 MHz, C_6D_6) δ 160.7, 135.9 (d, *J* = 18.5 Hz), 126.5 (d, *J* = 8.4 Hz), 114.7 (d, *J* = 7.1 Hz), 54.7. **^{31}P NMR** (162 MHz, C_6D_6) δ -44.9.

Spectroscopic data in agreement with that reported by Senanayake, C. H. *et al.*[10]

Bis(2-(bis(4-methoxyphenyl)phosphaneyl)ethyl)amine, MACHO$^{p(OMe)}$

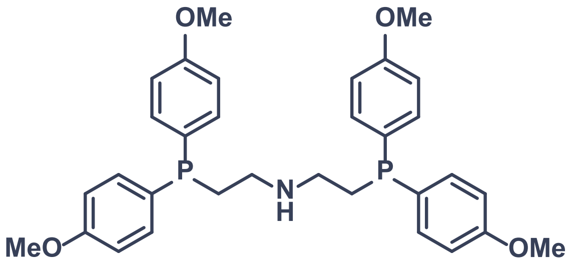

Inside a glovebox, a COtube charged with bis(4-methoxyphenyl)phosphine (542 mg, 2.20 mmol) was added THF (15 mL) and *t*BuOK (673 mg, 6.00 mmol). The resultant deep red solution was stirred at ambient temperature for 15 minutes prior to the addition of bis(2-chloroethyl)amine hydrochloride (178 mg, 1.00 mmol). The COtube was sealed, and the reaction mixture was refluxed overnight. After reaching ambient temperature, the reaction mixture was diluted with Et_2O (10 mL) and subsequently quenched with water (10 mL). The organic layer was separated, and the aqueous phase was extracted with Et_2O (3 x 10 mL). The combined organic phases were dried over anhydrous Na_2SO_4, filtered, and concentrated. Outside the glovebox, purification via AFCC using degassed solvents (heptane to EtOAc) afforded MACHO$^{p(OMe)}$ as a yellow oil (258 mg, 460 µmol, 46%). The compound was immediately transferred back into the glovebox after isolation.

^{1}H NMR (400 MHz, $CDCl_3$) δ 7.35 – 7.30 (m, 8H), 6.88 – 6.84 (m, 8H), 3.79 (s, 12H), 3.12 (bs, 1H), 2.72 – 2.66 (m, 4H), 2.17 – 2.13 (m, 4H). **^{13}C NMR** (101 MHz, $CDCl_3$) δ 160.3, 134.2 (d, *J* = 20.2 Hz), 129.4 (d, J = 9.7 Hz), 114.3 (d, J = 7.7 Hz), 55.3, 46.3 (d, J = 21.2 Hz), 29.3 (d, J = 11.3 Hz). ^{31}**P NMR** (162 MHz, $CDCl_3$) δ -24.6.

Spectroscopic data in agreement with that reported by Liu, W. *et al.*[3]

Ru-MACHO$^{p(OMe)}$

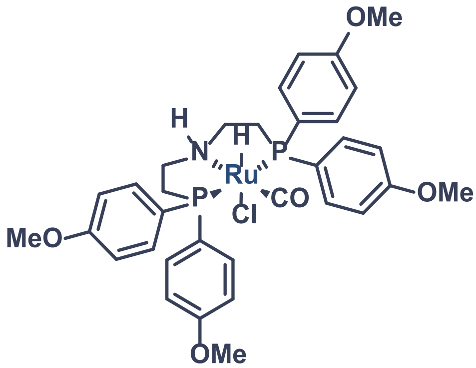

Inside a glovebox, to a COtube charged with MACHO$^{p(OMe)}$ (29.5 mg, 52.5 μmol) was added carbonylchlorohydridotris(triphenylphosphine)ruthenium(II) (47.6 mg, 50.0 μmol) and toluene (0.45 mL). The COtube was sealed, and the reaction mixture was stirred at reflux for 5 h. After reaching ambient temperature, white precipitate could be observed, and the reaction mixture was diluted with Et_2O (5 mL). The solvent was decantated off and the solids rinsed with Et_2O (5 mL) and pentane which were decanted off, after which the solids were dried in vacuo to afford Ru-MACHO$^{p(OMe)}$ as a white solid (30.4 mg, 41.8 μmol, 84%).

^{1}**H NMR** (400 MHz, $CDCl_3$) δ 7.79 – 7.70 (m, 8H), 6.93 – 6.90 (m, 8H), 3.96 (bs, 1H), 3.81 (s, 6H), 3.79 (s, 6H), 3.40 – 3.29 (m, 2H), 2.86 – 2.84 (m, 2H), 2.50 – 2.43 (m, 4H), -15.55 (t, J = 19.5 Hz, 1H). ^{13}**C NMR** (101 MHz, $CDCl_3$) δ 161.0, 161.0, 135.0 (t, J = 7.2 Hz), 134.2 (t, J = 7.3 Hz), 128.9 (t, J = 25.1 Hz), 125.7 (t, J = 23.1 Hz), 114.1 (t, J = 5.5 Hz), 114.0 (t, J = 5.5 Hz), 55.4, 55.3, 52.4 (t, J = 5.2 Hz), 32.5 (t, J = 11.2 Hz). ^{31}**P NMR** (162 MHz, $CDCl_3$) δ 48.9 (d, J = 8.1 Hz). **HRMS** (ESI^+) m/z Calcd for $C_{33}H_{38}NO_5P_2Ru$ $[M - Cl]^+$ 692.1269; Found 692.1283.

Ru-MACHO^{Et}

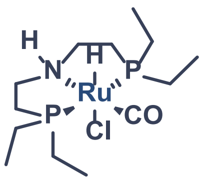

Inside a glovebox, to a COtube charged with MACHO^{Et} (52.4 mg, 210 μmol) was added carbonylchlorohydridotris(triphenylphosphine)ruthenium(II) (190.0 mg, 200 μmol) and toluene (2.0 mL). The reaction mixture was stirred at reflux for 5 h. After reaching ambient temperature, the reaction mixture was added pentane (4 mL). The suspension was sonicated for 30 minutes, centrifuged, and the solvent decanted off. The remaining solids were suspended in Et_2O (5 mL) and sonicated for 30 minutes. The suspension was centrifuged, filtered, and the precipitate rinsed with Et_2O (2 x 5 mL). The solids were collected and dried in vacuo to afford Ru-MACHO^{Et} as a white solid (63.1 mg, 152 μmol, 76%).

^{1}**H NMR** (400 MHz, CD_3Cl) δ 3.35 – 3.19 (m, 3H), 2.19 – 1.99 (m, 6H), 1.92 – 1.78 (m, 4H), 1.75 – 1.66 (m, 2H), 1.26 – 1.14 (m, 12H), -16.73 (t, J = 19.1 Hz, 1H). ^{13}**C NMR** (101 MHz, CD_3Cl) δ 206.7 (t, J = 12.0 Hz), 53.0 (t, J = 5.1 Hz), 29.2 (t, J = 10.2 Hz), 22.5 (t, J = 13.9 Hz), 17.4 (t, J = 12.2 Hz), 8.7 (d, J = 6.0 Hz). ^{31}**P NMR** (162 MHz, CD_3Cl) δ 53.8 (bs). **HRMS** (ESI^+) m/z Calcd for $C_{13}H_{30}NOP_2Ru$ $[M - Cl]^+$ 380.0846; Found 380.0844.

Ru-MACHO^{iPr}

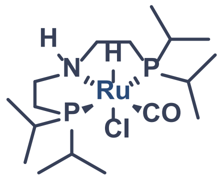

Inside a glovebox, to a COtube charged with MACHO^{iPr} (197 mg, 646 µmol) was added carbonylchlorohydridotris(triphenylphosphine)ruthenium(II) (585 mg, 615 µmol) and toluene (10 mL). The reaction mixture was stirred at reflux for 5 h. After reaching ambient temperature, the reaction mixture was added pentane (30 mL) to precipitate out the complex. The suspension was sonicated for 30 minutes followed by filtering off the precipitate and rinsed with pentane (2 x 5.0 mL). The solids were collected and dried in vacuo overnight, affording Ru-MACHO^{iPr} as a white solid (223 mg, 474 µmol, 77%).

^{1}H NMR (400 MHz, CD_2Cl_2) δ 3.42 – 3.36 (m, 1H), 3.29 – 3.15 (m, 2H), 2.72 – 2.60 (m, 2H), 2.33 – 2.11 (m, 6H), 1.81 – 1.71 (m, 2H), 1.45 – 1.39 (m, 6H), 1.27 – 1.22 (m, 6H), 1.20 – 1.15 (m, 6H), 1.13 – 1.07 (m, 6H), -16.10 (t, J = 19.2 Hz, 0.08H), -16.31 (t, J = 17.9 Hz, 0.92H). **^{13}C NMR** (101 MHz, CD_2Cl_2) δ 208.3 (t, J = 11.7 Hz), 54.3 (t, J = 4.8 Hz), 30.2 (t, J = 9.0 Hz), 27.1 (t, J = 11.2 Hz), 24.1 (t, J = 12.5 Hz), 20.9 (m), 19.0 (t, J = 1.1 Hz), 17.5 (d, J = 1.8 Hz). **^{31}P NMR** (162 MHz, CD_2Cl_2) δ 76.8 (0.16P), 76.7 (1.84P). **HRMS** (ESI^+) m/z Calcd for $C_{17}H_{38}NOP_2Ru$ $[M - Cl]^+$ 436.1472; Found 436.1481.

Spectroscopic data in agreement with that reported by Oestreich, M. *et al.*[11]

Ru-MACHO^{tBu}

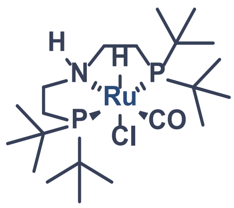

Inside a glovebox, to a COtube charged with MACHO^{tBu} (75.9 mg, 210 µmol) was added carbonylchlorohydridotris(triphenylphosphine)ruthenium(II) (190.0 mg, 200 µmol) and diglyme (2.0 mL). The reaction mixture was stirred at 165 °C for 19 h. After reaching ambient temperature, the reaction mixture was added pentane (4 mL). The suspension was sonicated for 30 minutes, centrifuged, and the solvent decanted off. The remaining solids were suspended in Et_2O (5 mL) and sonicated for 30 minutes. The suspension was centrifuged, filtered, and the precipitate rinsed with Et_2O (2 x 5 mL). The solids were collected and dried in vacuo to afford Ru-MACHO^{tBu} as a light grey solid (88.6 mg, 168 µmol, 84%).

^{1}H NMR (400 MHz, CD_2Cl_2) δ 5.25 (bs, 1H), 3.36 – 3.23 (m, 2H), 2.46 – 2.35 (m, 2H), 2.20 – 2.04 (m, 4H), 1.42 – 1.39 (m, 18H), 1.34 – 1.31 (m, 18H), -15.82 (t, J = 20.0 Hz, 0.19H), -18.63 (t, J = 20.0, 0.72H). **^{13}C NMR** (101 MHz, CD_2Cl_2) δ 207.9 (t, J = 11.6 Hz), 53.5 (t, J = 4.1 Hz), 38.7 (t, J = 6.4 Hz), 36.7 (t, J = 10.8 Hz), 31.2 (t, J = 2.9 Hz), 31.0 (t, J = 2.7 Hz), 30.1 (t, J = 2.3 Hz), 25.8 (t, J = 5.8 Hz). **^{31}P NMR** (162 MHz, CD_2Cl_2) δ 87.0 (d, J = 8.0 Hz, 0.35P), 86.7 (d, J = 5.9 Hz, 1.65P). **HRMS** (ESI^+) m/z Calcd for $C_{21}H_{46}NOP_2Ru$ $[M - Cl]^+$ 492.2098; Found 492.2115.

Spectroscopic data in agreement with that reported by Ogata, O. *et al.*[12]

Ru-MACHO^{Cy}

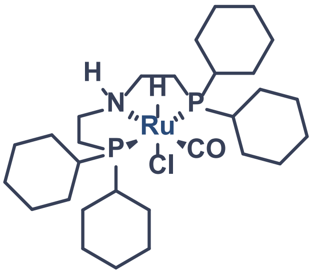

Inside a glovebox, to a COtube charged with MACHO^{Cy} (195.6 mg, 420 µmol) was added carbonylchlorohydridotris(triphenylphosphine)ruthenium(II) (380.6 mg, 400 µmol) and diglyme (4.0 mL). The reaction mixture was stirred at 165 °C for 19 h. After reaching ambient temperature, the reaction mixture was added pentane (10 mL) to precipitate out the complex. The suspension was sonicated for 30 minutes, centrifuged, and the solvent decanted off. The remaining solids were suspended in Et_2O (10 mL) and sonicated for 30 minutes. The suspension was centrifuged, filtered, and the precipitate rinsed with Et_2O (2 x 10 mL). The solids were collected and dried in vacuo to afford Ru-MACHO^{Cy} as a pale yellow solid (207.8 mg, 329 µmol, 82%).

^{1}H NMR (400 MHz, $CDCl_3$) δ 3.55 – 3.51 (m, 0.34H), 3.26 – 3.12 (m, 2H), 2.91 – 2.77 (m, 0.68H), 2.52 – 2.11 (m, 8H), 1.97 – 1.22 (m, 42H), -16.39 (t, J = 19.6 Hz, 0.20H), -16.59 (t, J = 18.3 Hz, 0.71H). **^{13}C NMR** (101 MHz, CD_2Cl_2) δ 208.4 (t, J = 11.8 Hz), 54.3 (t, J = 4.9 Hz), 37.6 (t, J = 10.7 Hz), 35.3 (t, J = 12.4 Hz), 31.3 (t, J = 2.5 Hz), 30.9 (t, J = 3.1 Hz), 29.1 (t, J = 9.2 Hz), 28.5 (t, J = 6.7 Hz), 28.5, 28.2, 27.7 (t, J = 4.1 Hz), 27.3 (t, J = 5.2 Hz), 27.0 (t, J = 6.5 Hz), 26.9, 26.5. **^{31}P NMR** (162 MHz, $CDCl_3$) δ 65.3 (d, J = 5.9 Hz, 0.78P), 64.6 (d, J = 5.9 Hz, 0.22P). **HRMS** (ESI$^+$) m/z Calcd for $C_{29}H_{54}NOP_2Ru$ [M - Cl]$^+$ 596.2724; Found 596.2733.

Spectroscopic data in agreement with that reported by Beller, M. *et al.*[13]

Ru-MACHO^{Ad}

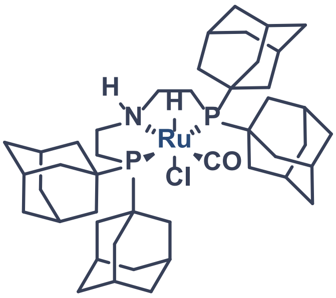

Inside a glovebox, to a COtube charged with MACHO^{Ad} (79.0 mg, 116 µmol) was added carbonylchlorohydridotris(triphenylphosphine)ruthenium(II) (100.0 mg, 105 µmol) and diglyme (1.0 mL). The reaction mixture was stirred at 165 °C for 19 h. After reaching ambient temperature, the reaction mixture was added pentane (4 mL) to precipitate out the complex. The suspension was sonicated for 30 minutes, centrifuged, and the solvent decanted off. The remaining solids were suspended in Et_2O (5 mL) and sonicated for 30 minutes. The suspension was centrifuged, filtered, and the precipitate rinsed with Et_2O (2 x 5 mL). The solids were collected and dried in vacuo to afford Ru-MACHO^{Ad} as a white solid (34.6 mg, 41 µmol, 39%).

^{1}H NMR (400 MHz, CD_3Cl) δ 7.53 (bs, 1H), 3.67 – 3.54 (m, 2H), 2.50 – 1.57 (m, 66H), -26.05 (t, J = 15.4 Hz, 1H). **^{13}C NMR** (101 MHz, CD_3Cl) δ 55.1 (t, J = 3.8 Hz), 42.9 (t, J = 8.1 Hz), 40.1, 39.5, 39.2 (t, J = 8.6 Hz), 36.8, 36.7, 28.5 (t, J = 4.4 Hz), 28.3 (t, J = 4.3 Hz), 21.1 (t, J = 7.9 Hz). **^{31}P NMR** (162

MHz, CD_3Cl) δ 84.5 (d, J = 11.8 Hz). **HRMS** (ESI^+) m/z Calcd for $C_{45}H_{70}NOP_2Ru$ $[M - Cl]^+$ 804.3976; Found 804.3987.

Spectroscopic data in agreement with that reported by Kuiling, D. *et al.*[14]

Tris(2-(diphenylphosphino)ethyl)amine, NP_3

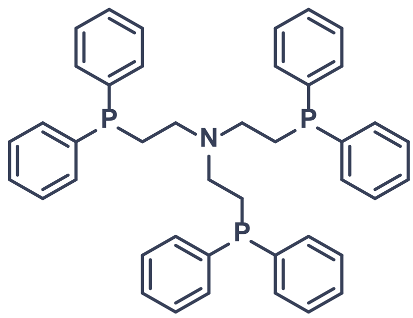

Inside a glovebox, to a COtube charged with *t*BuOK (1.81 g, 16.1 mmol) and THF (30 mL) was added diphenylphosphine (1.1 mL, 6.3 mmol) and the mixture was stirred for 10 minutes at room temperature. The mixture was added tris(2-chloroethyl)ammonium hydrochloride (501 mg, 2.08 mmol), the COtube sealed, and the reaction mixture heated to reflux for 20 h. The mixture was then cooled to ambient temperature and poured into degassed water in a round-bottomed flask. The flask was cooled to °C, leading to a precipitate. The precipitate was then filtered and rapidly washed with ethanol (2 x 10 mL). The white precipitate was dried in vacuo to yield NP_3 as a white solid (362.8 mg, 555 µmol, 27%).

^{1}H NMR (400 MHz, $CDCl_3$) δ 7.34 – 7.23 (m, 30H), 2.53 – 2.47 (m, 6H), 1.98 – 1.94 (m, 6H). **^{13}C NMR** (101 MHz, $CDCl_3$) δ 138.6 (d, J = 12.9 Hz), 132.9 (d, J = 18.7 Hz), 128.7, 128.5 (d, J = 6.6 Hz), 49.5 (d, J = 22.8 Hz), 25.5 (d, J = 12.3 Hz). **^{31}P NMR** (162 MHz, $CDCl_3$) δ -19.9.

Ru-NP_3

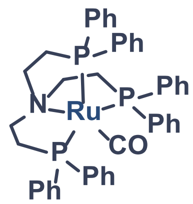

Inside a glovebox, a COtube was charged with $Ru_3(CO)_{12}$ (32.4 mg, 50.7 µmol), tris(2-(diphenylphosphanyl)ethyl)amine (100 mg, 153 µmol), and toluene (3 mL). The COtube was sealed and the reaction mixture stirred at 135 °C for 16 h. After cooling to ambient temperature, an orange precipitate had formed. The reaction mixture was centrifuged, and the supernatant was removed inside the glovebox. The resulting solid was washed with benzene (2 x 3 mL). Benzene (2 mL) and methanol (0.25 mL) were then added, the COtube resealed, and the mixture heated to 80 °C for 3 h, affording a clear yellow solution. After cooling to ambient temperature, the solution was filtered through a 0.2 µm PTFE syringe filter and the solvent removed in vacuo to afford Ru-NP_3 as an orange solid (79.6 mg, 102 µmol, 67%).

Due to very poor solubility, the following data is only partially assigned, hence impurities appear more asserted and **^{13}C NMR** data was not possible to obtain. **^{1}H NMR** (400 MHz, C_6D_6) δ 7.57 – 7.51 (m, 8H), 7.37 – 7.35 (m, 2H), 7.09 – 6.96 (m, 12H), 6.81 – 6.54 (m, 6H), 2.15 – 1.98 (m, 8H), 1.65 – 1.61 (m, 4H). **^{31}P NMR** (162 MHz, C_6D_6) δ 55.3.

Spectroscopic data in agreement with that reported by Schaub, T. *et al.*[15]

References

1 Kuriyama, W., Matsumoto, T., Ino, Y. & Ogata, O. Noval ruthenium carbonyl complex having tridentate ligand, its production method and use. US2011237814A1 (2011).

2 Barrett, A. N. *et al.* Hydrogen/Halogen Exchange of Phosphines for the Rapid Formation of Cyclopolyphosphines. *Inorg. Chem.* **60**, 16826–16833 (2021).

3 Guo, J., Tang, J., Xi, H., Zhao, S.-Y. & Liu, W. Manganese catalyzed urea and polyurea synthesis using methanol as C1 source. *Chin. Chem. Lett.* **34**, 107731 (2023).

4 Fehring, V. *et al.* Synthesis of achiral, but unsymmetric, seven-membered rhodium(I)-chelates for hydrogenation in the chiral environment of alkyl polyglucoside micelles. *J. Organomet. Chem.* **621**, 120–129 (2001).

5 Zhang, Y.-K., Zhou, Y., Liu, C., Liu, C. Y. & Aubrey, M. Chemical Compounds. WO2021061823A1 (2021).

6 Cao, Z. *et al.* Silica-Supported Phosphine–Gold Complexes as an Efficient Catalytic System for a Dearomative Spirocyclization. *Chem. Eur. J.* **27**, 427–433 (2021).

7 Yang, X. *et al.* Synthesis of (Deoxy)difluoromethylated Phosphines by Reaction of $R_2P(O)H$ with $TMSCF_3$ and Their Application in Cu(I) Clusters in Sonogashira Coupling. *J. Org. Chem.* **87**, 7720–7733 (2022).

8 Wang, Y. *et al.* Sequential KOtBu/$FeCl_3$-catalyzed reductive phosphonylation of tertiary amides for the synthesis of α-amino phosphonates and phosphines. *Org. Biomol. Chem.* **21**, 2955–2959 (2023).

9 Li, C.-J. *et al.* Copper-catalyzed C–P cross-coupling of secondary phosphines with (hetero)aromatic bromide. *Res. Chem. Intermed.* **44**, 4547–4562 (2018).

10 Busacca, C. A. *et al.* A Superior Method for the Reduction of Secondary Phosphine Oxides. *Org. Lett.* **7**, 4277–4280 (2005).

11 Seliger, J. & Oestreich, M. Dynamic Kinetic Resolution of Alcohols by Enantioselective Silylation Enabled by Two Orthogonal Transition-Metal Catalysts. *Angew. Chem. Int. Ed.* **60**, 247–251 (2021).

12 Hideki, N. & Ogata, O. Method for alkylation of amines. US2016009632A1 (2016).

13 Nielsen, M. *et al.* Low-temperature aqueous-phase methanol dehydrogenation to hydrogen and carbon dioxide. *Nature* **495**, 85–89 (2013).

14 Han, Z. *et al.* Catalytic Hydrogenation of Cyclic Carbonates: A Practical Approach from CO_2 and Epoxides to Methanol and Diols. *Angew. Chem. Int. Ed.* **51**, 13041–13045 (2012).

15 Anaby, A. *et al.* Study of Precatalyst Degradation Leading to the Discovery of a New Ru^0 Precatalyst for Hydrogenation and Dehydrogenation. *Organometallics* **37**, 2193–2201 (2018).

NMR Spectra

^{1}H NMR (400 MHz, CD_2Cl_2) spectrum of **Ru-MACHO^{Ph}**.

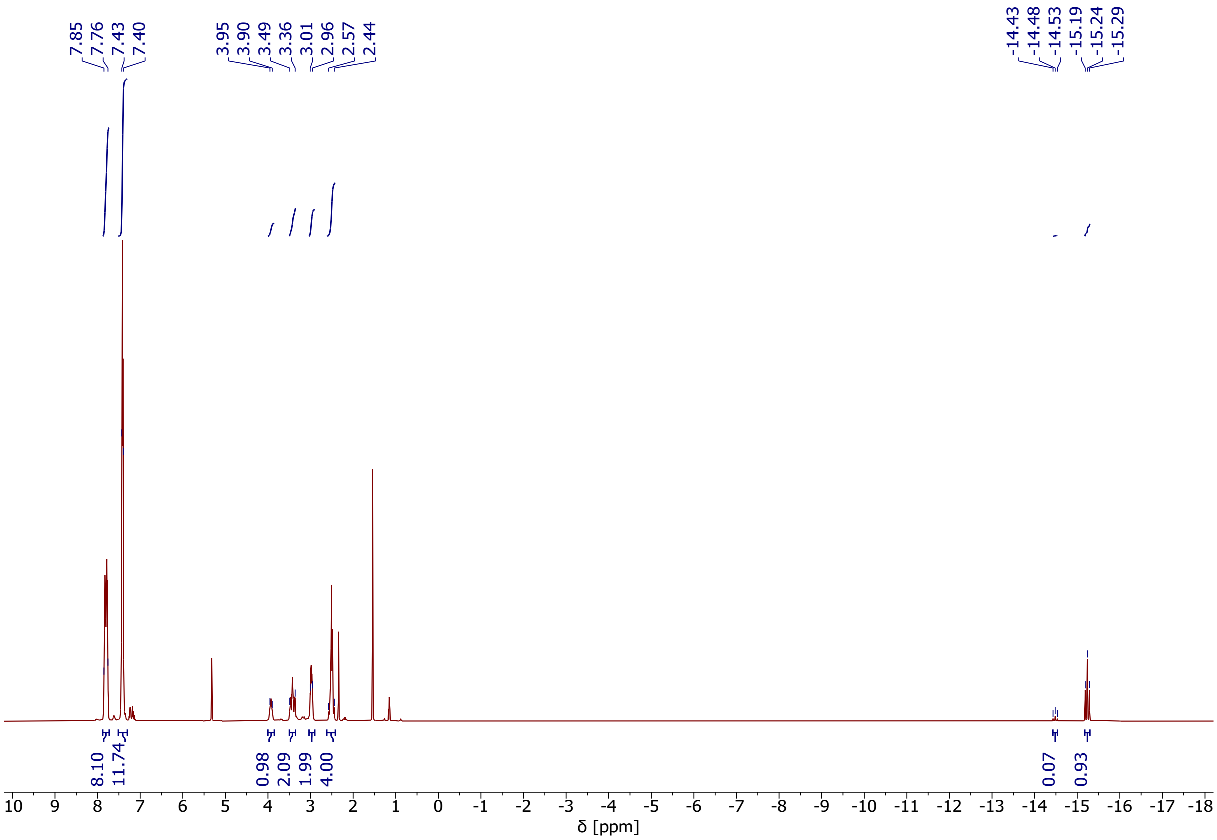

^{13}C NMR (101 MHz, CD_2Cl_2) spectrum of **Ru-MACHO^{Ph}**.

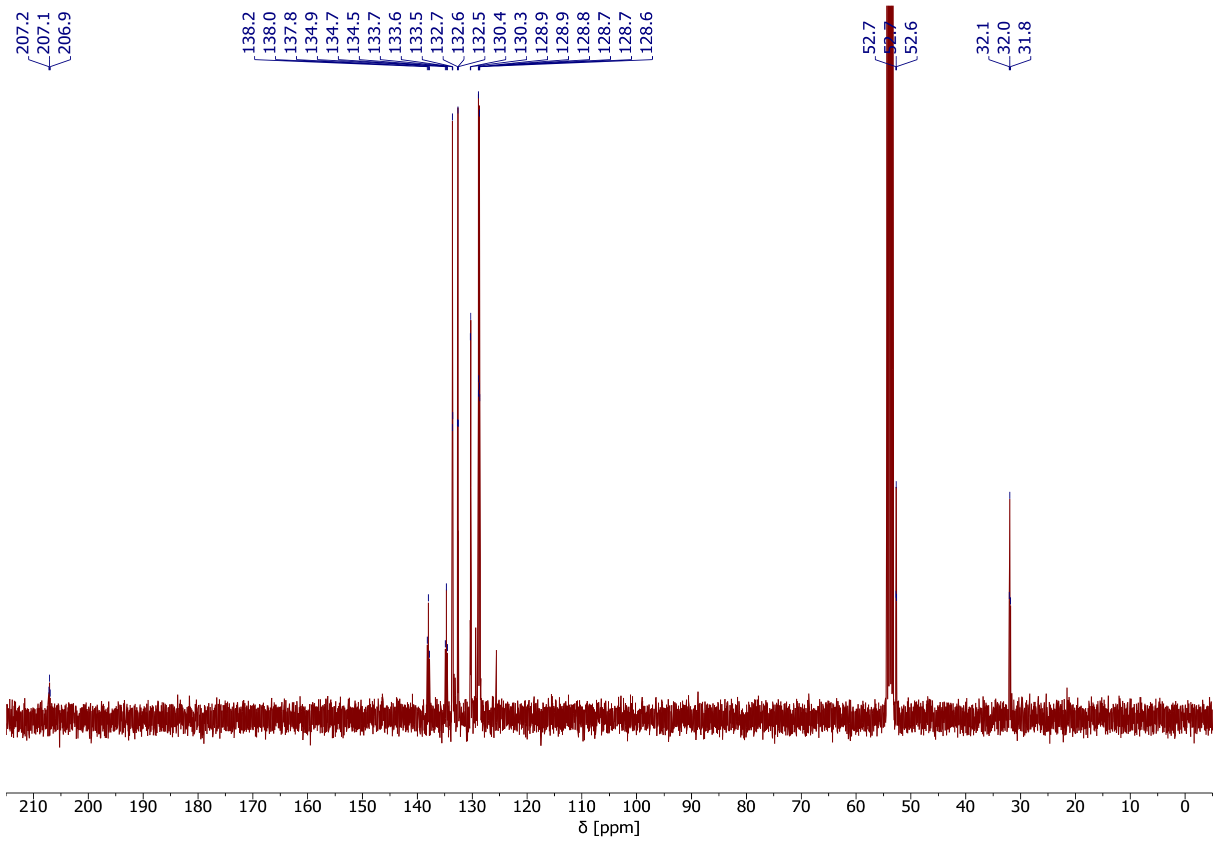

^{31}P NMR (162 MHz, CD_2Cl_2) spectrum of **Ru-MACHO^{Ph}**.

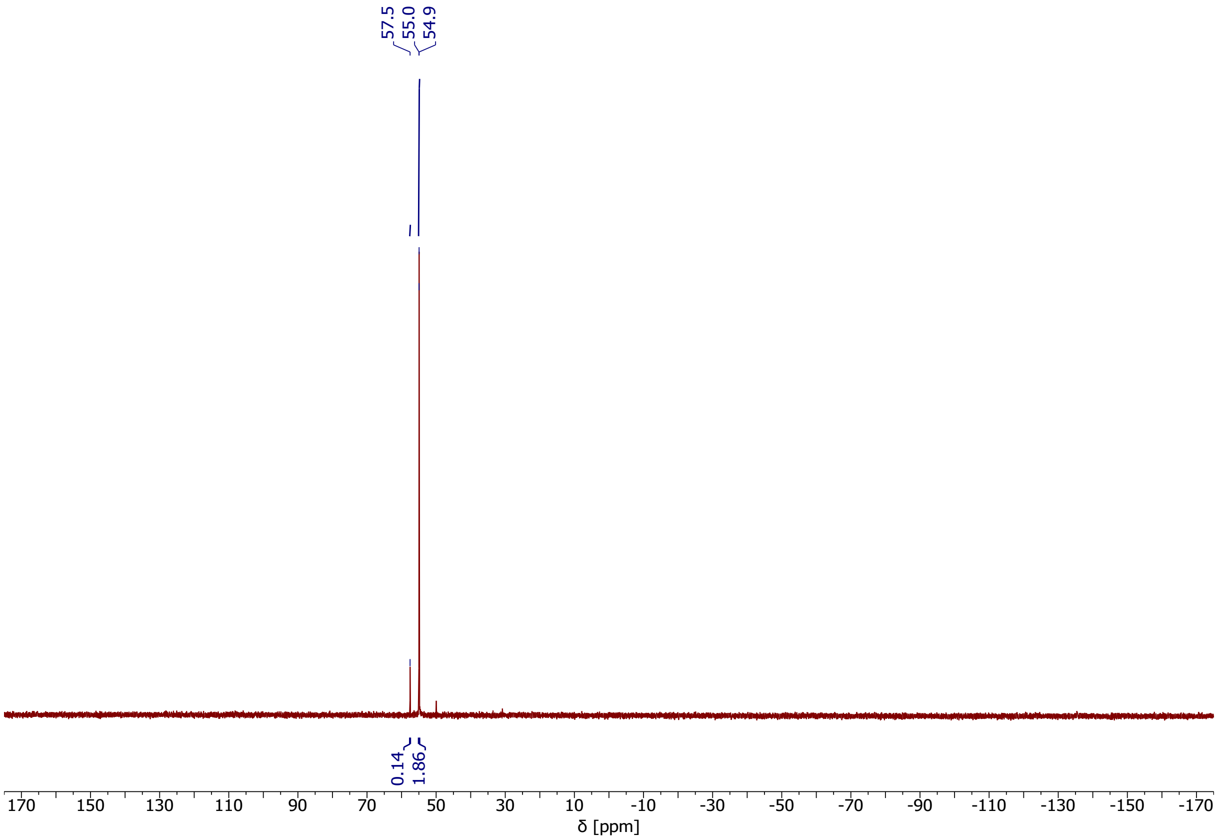

^{1}H NMR (400 MHz, $CDCl_3$) spectrum of **MACHO$^{p(Me)}$**.

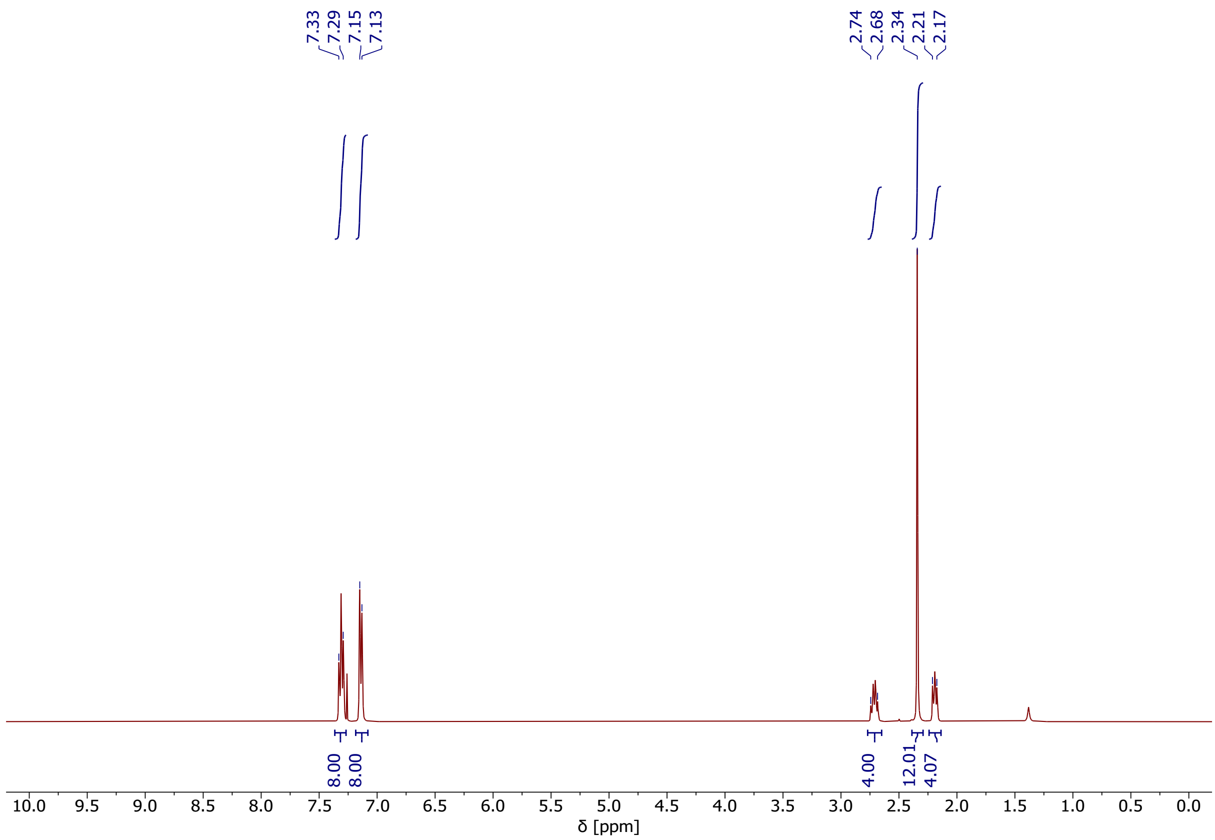

^{13}C NMR (101 MHz, $CDCl_3$) spectrum of **MACHO$^{p(Me)}$**.

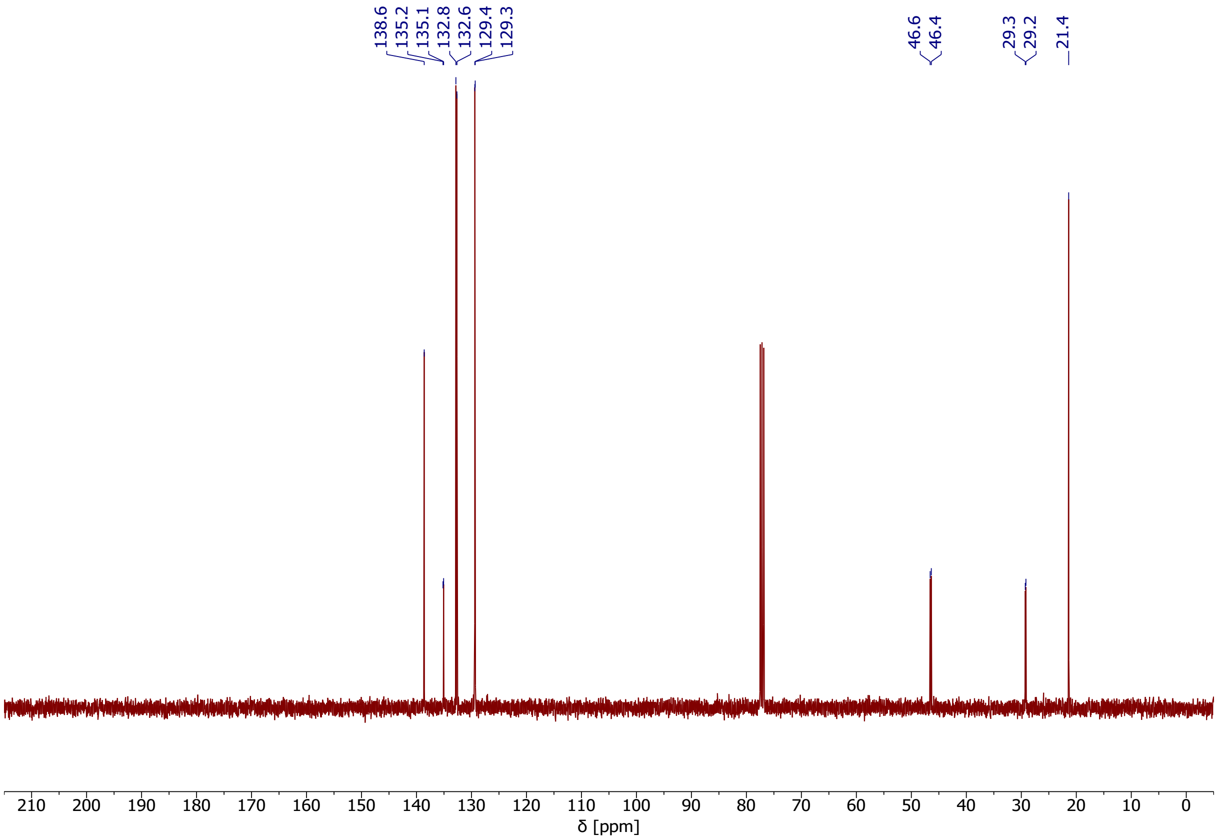

^{31}P NMR (162 MHz, $CDCl_3$) spectrum of **MACHO$^{p(Me)}$**.

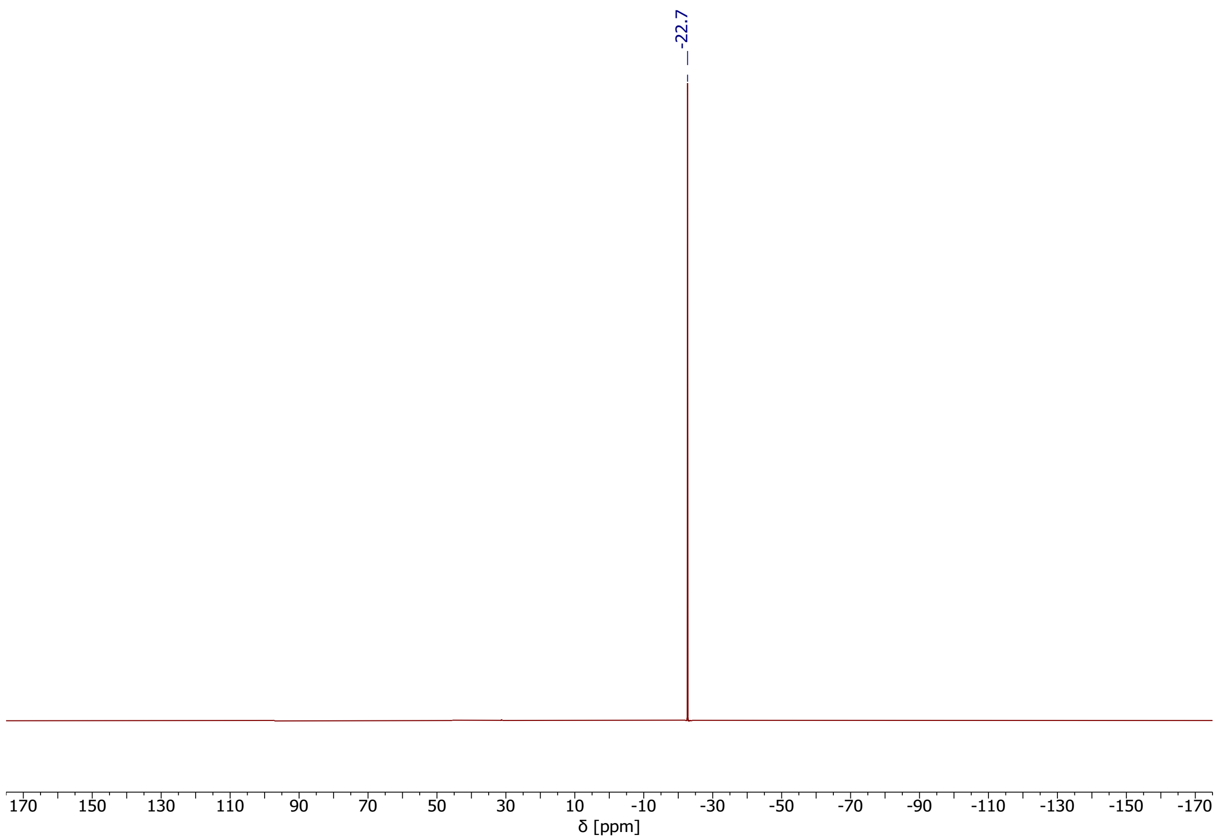

^{1}H NMR (400 MHz, C_6D_6) spectrum of **Ru-MACHO$^{p(Me)}$**.

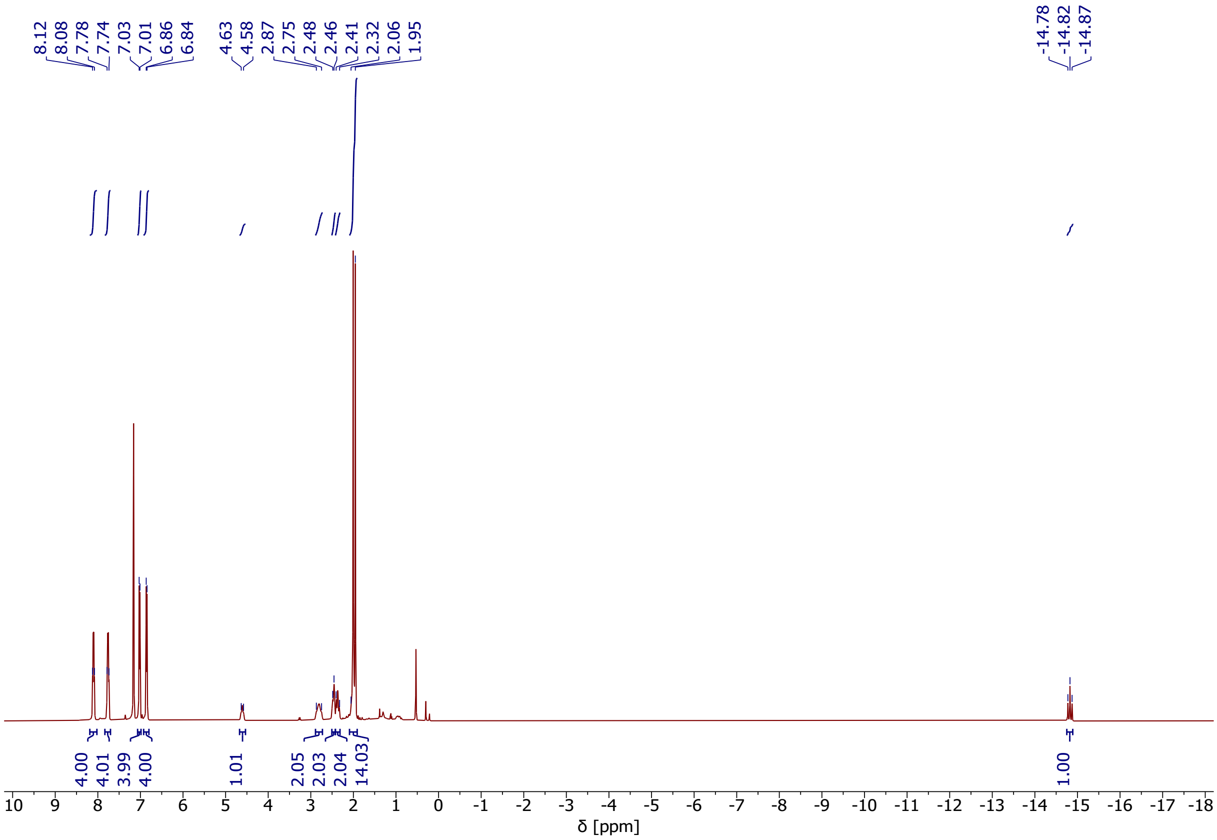

^{13}C NMR (101 MHz, C_6D_6) spectrum of **Ru-MACHO**$^{p(Me)}$.

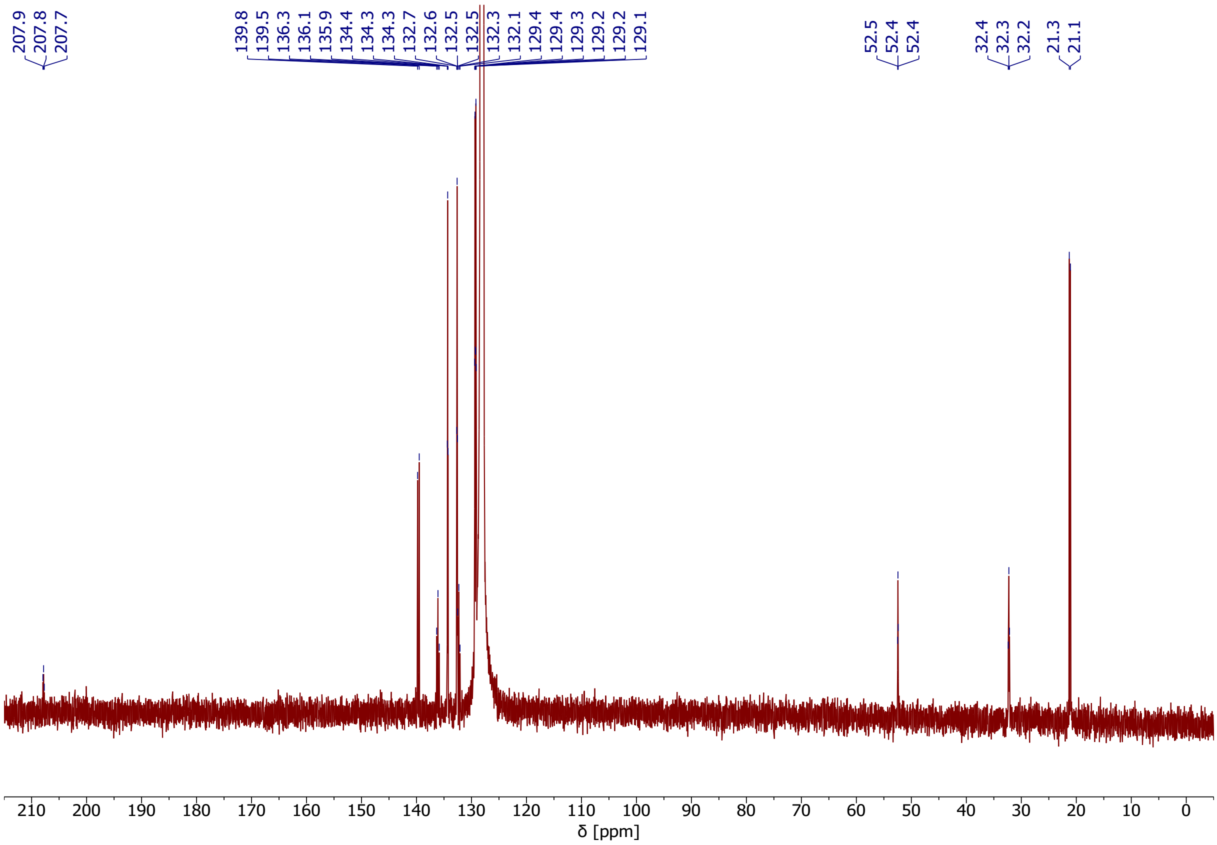

^{31}P NMR (162 MHz, C_6D_6) spectrum of **Ru-MACHO**$^{p(Me)}$.

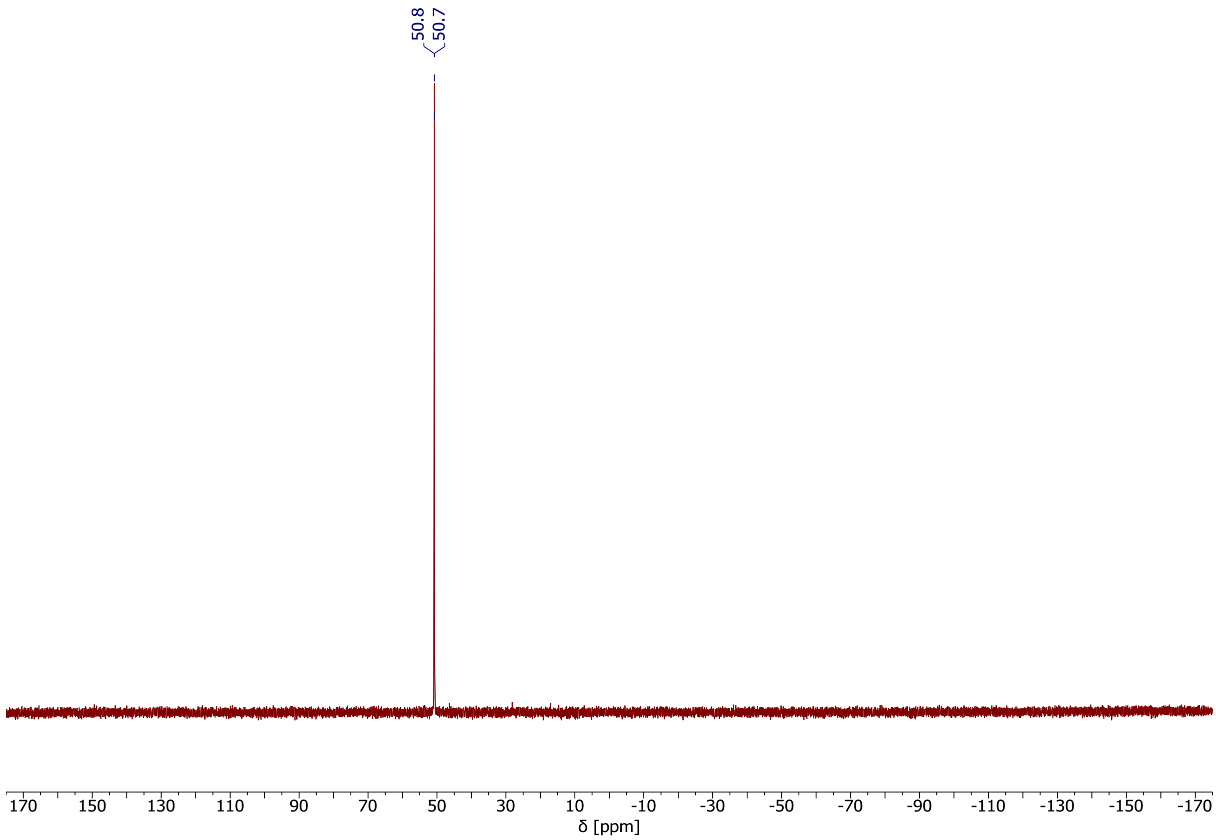

^{1}H NMR (400 MHz, C_7D_8) spectrum of **MACHO$^{m,m(Me)}$**.

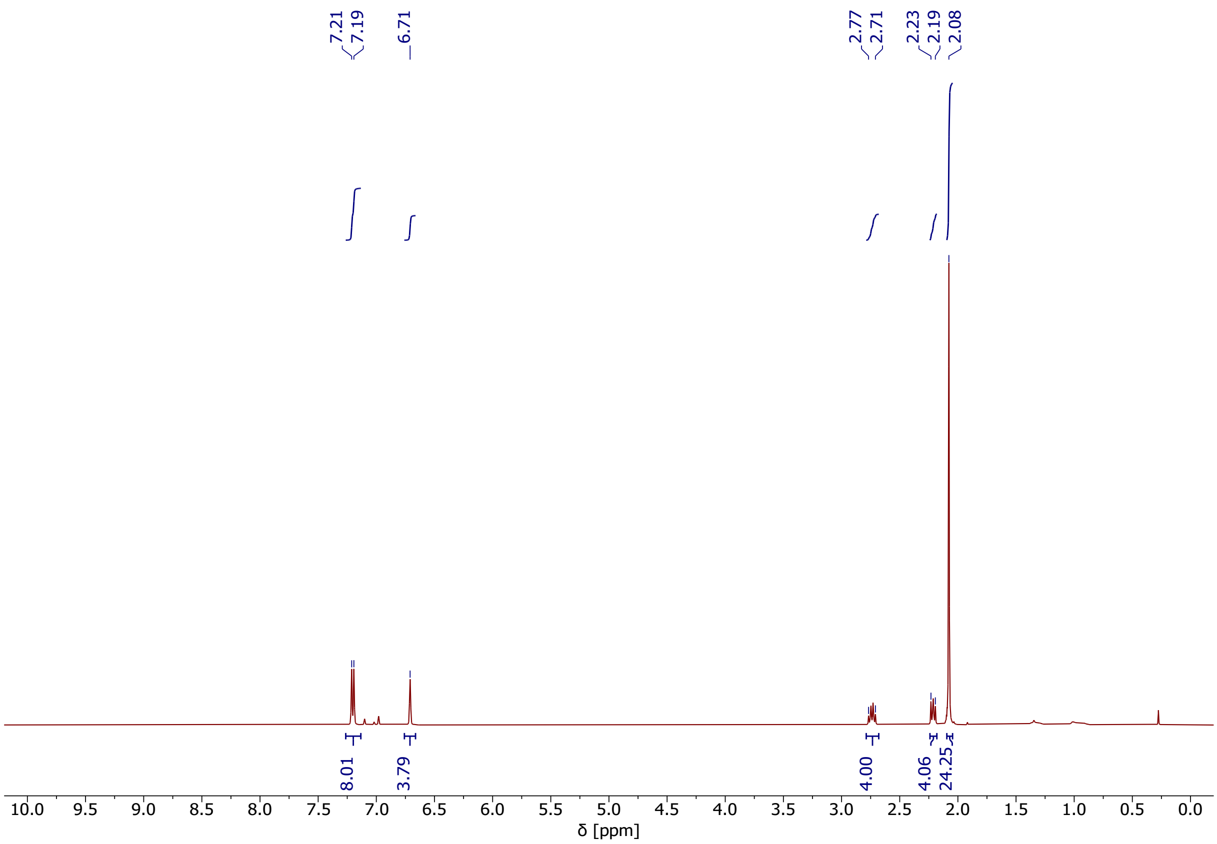

^{13}C NMR (101 MHz, C_7D_8) spectrum of **MACHO$^{m,m(Me)}$**.

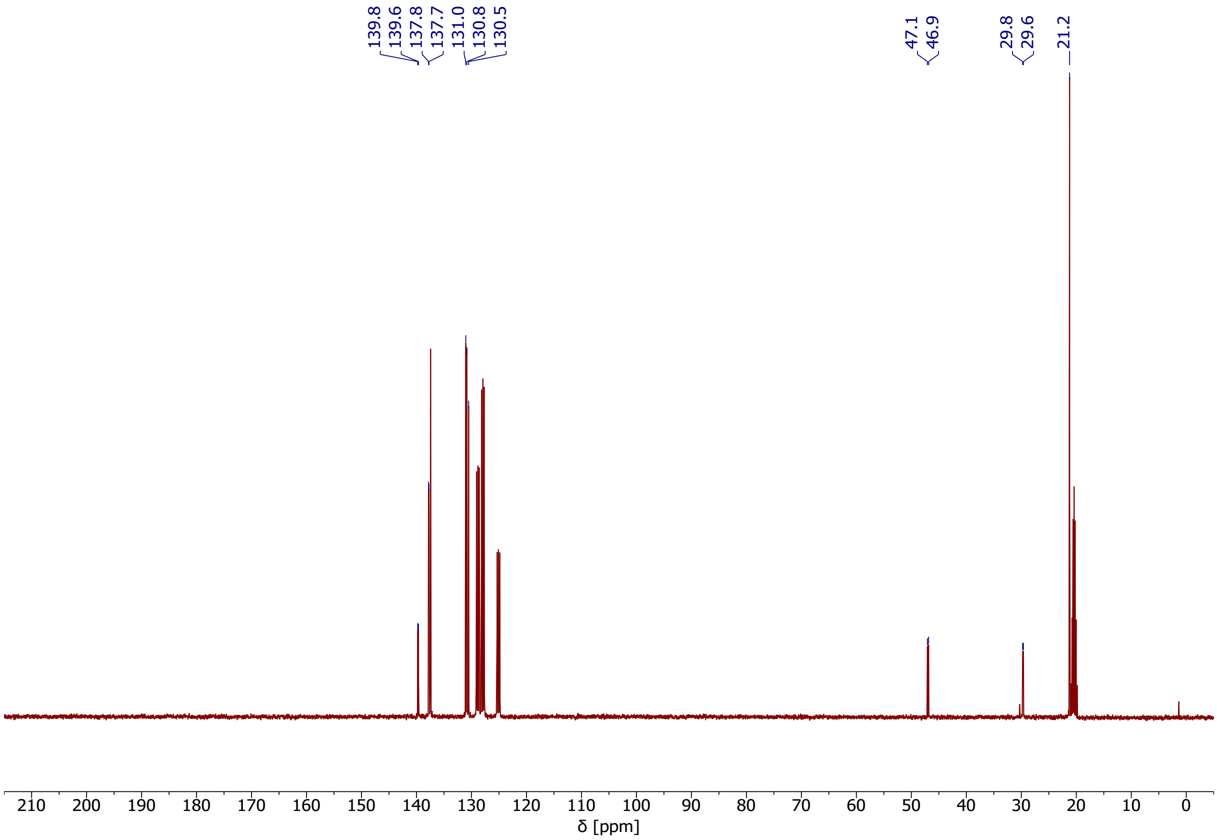

^{31}P NMR (162 MHz, C_7D_8) spectrum of **MACHO$^{m,m(Me)}$**.

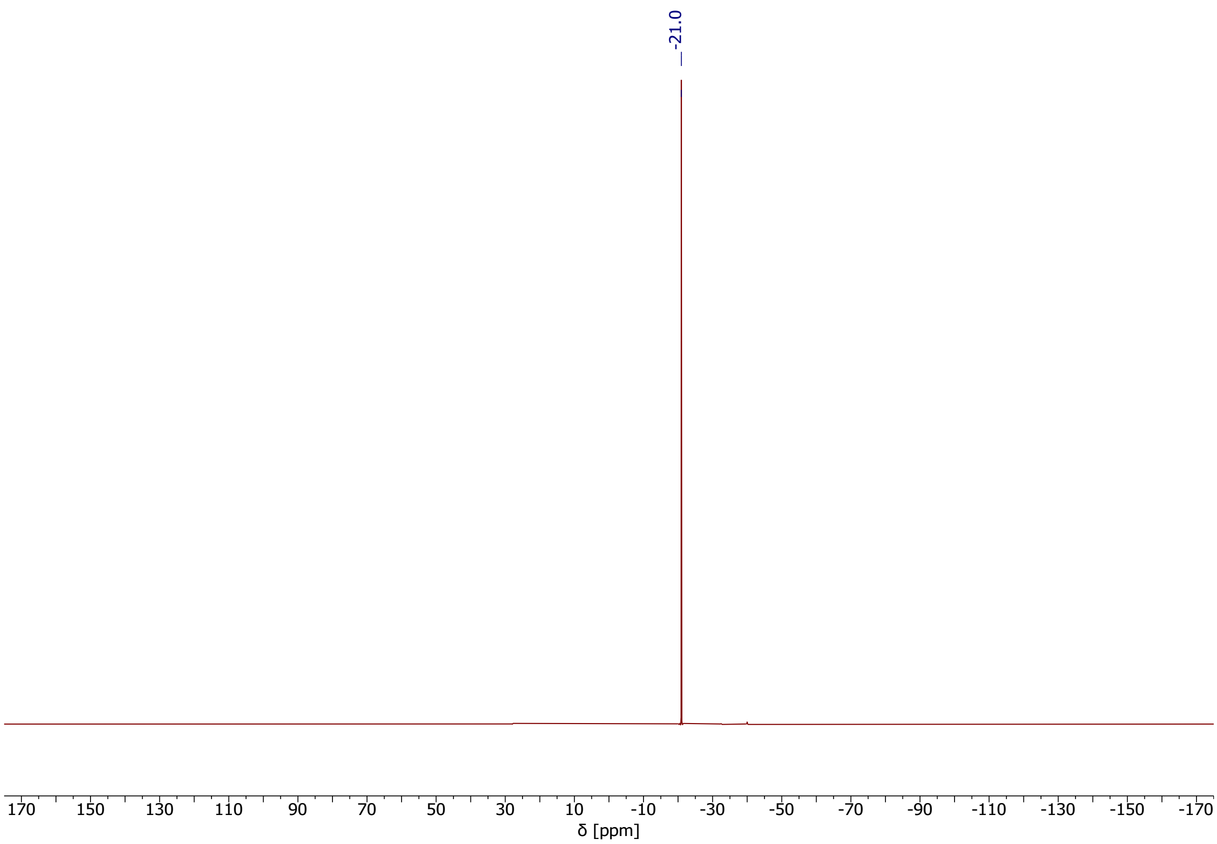

^{1}H NMR (400 MHz, C_6D_6) spectrum of **Ru-MACHO$^{m,m(Me)}$**.

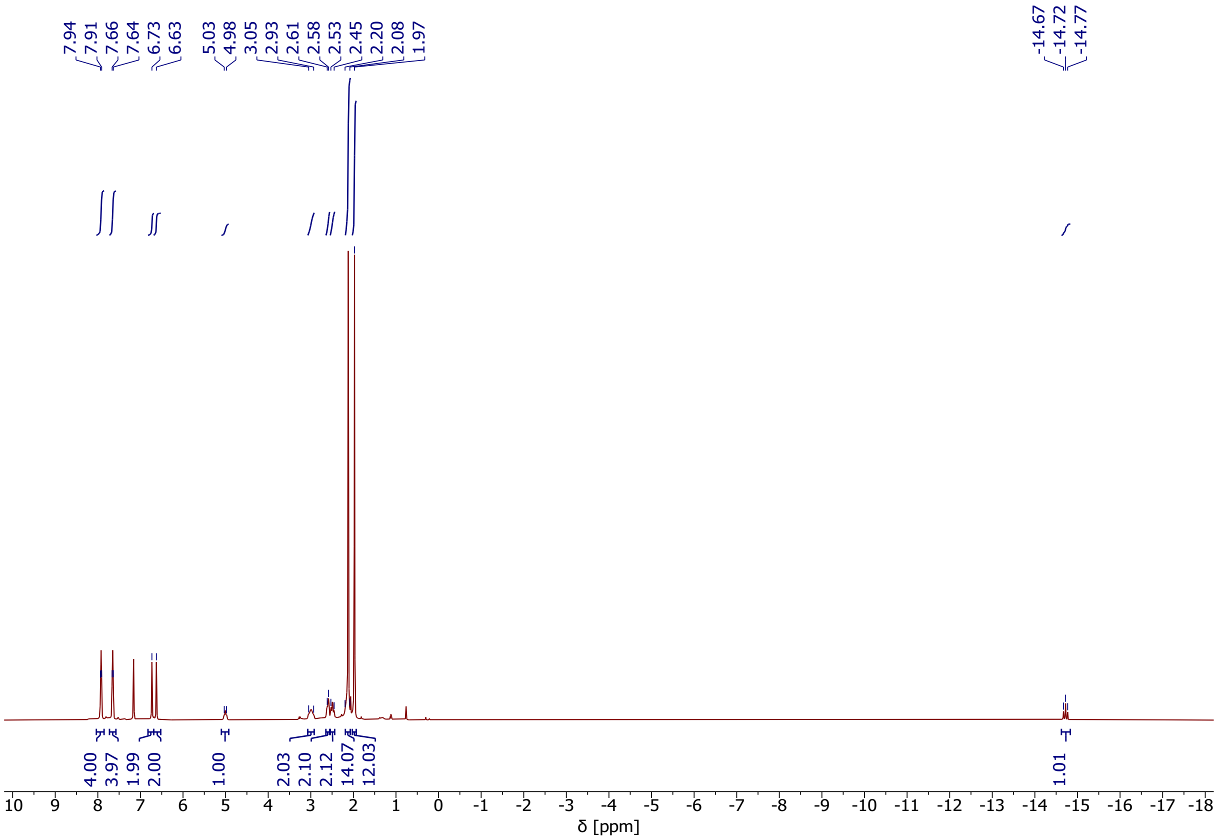

^{13}**C NMR** (101 MHz, C_6D_6) spectrum of **Ru-MACHO$^{m,m(Me)}$**.

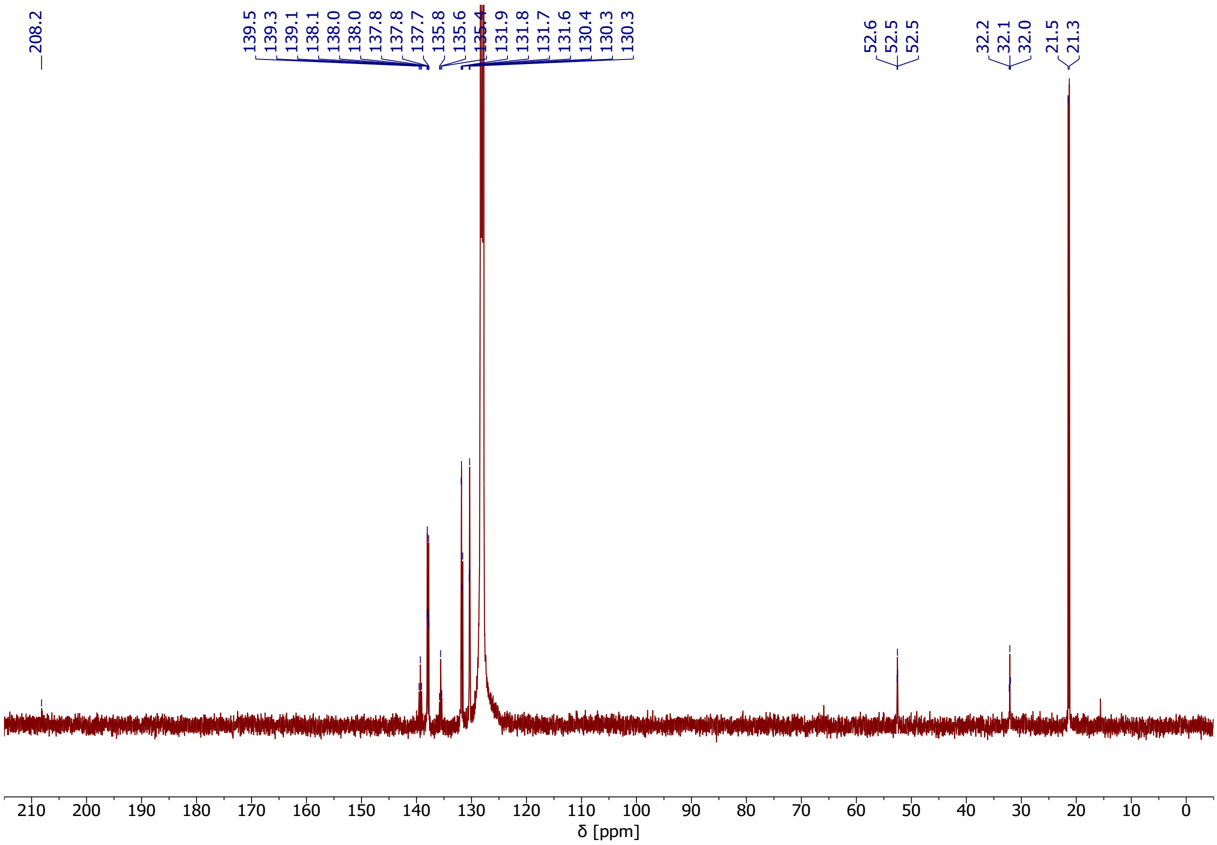

^{31}**P NMR** (162 MHz, C_6D_6) spectrum of **Ru-MACHO$^{m,m(Me)}$**.

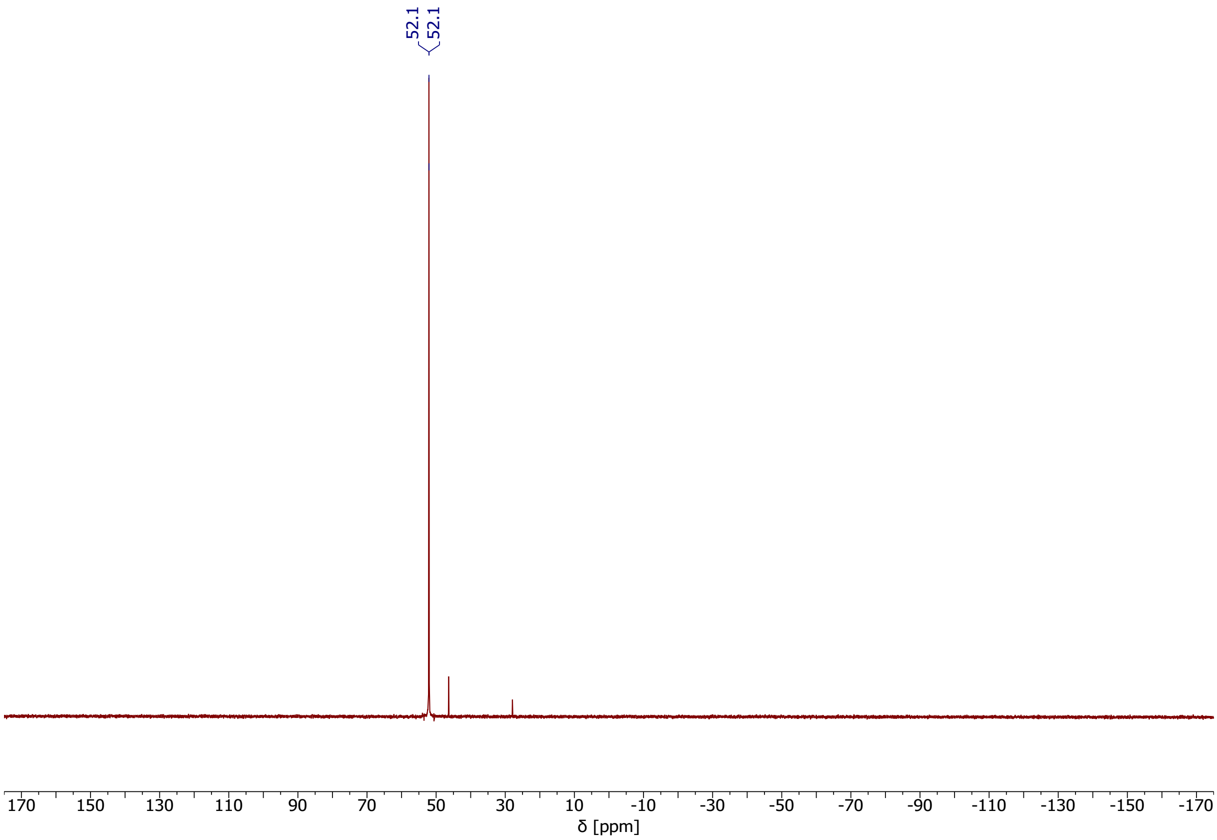

^{1}H NMR (400 MHz, CD_2Cl_2) spectrum of **MACHO$^{p(i\mathrm{Pr})}$**.

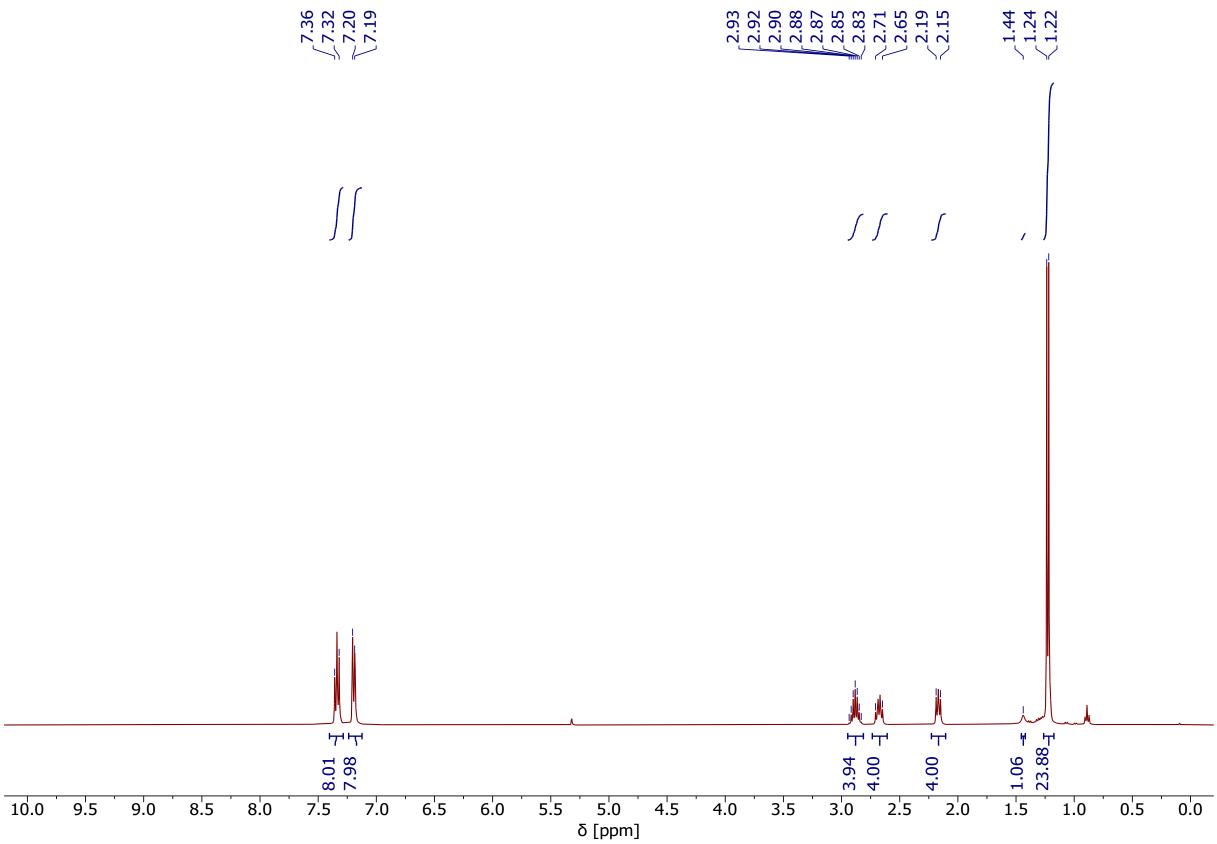

^{13}C NMR (101 MHz, CD_2Cl_2) spectrum of **MACHO$^{p(i\mathrm{Pr})}$**.

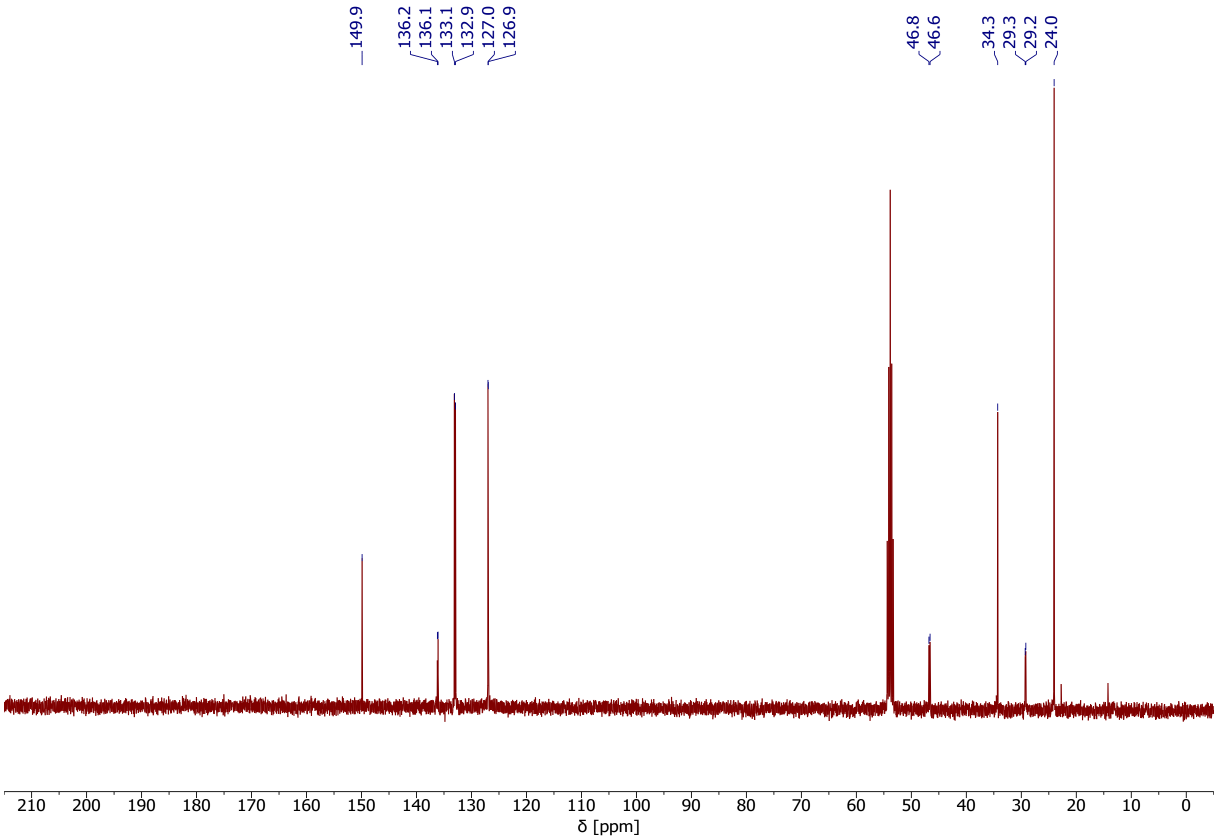

^{31}P NMR (162 MHz CD_2Cl_2) spectrum of **MACHO$^{p(i\text{Pr})}$**.

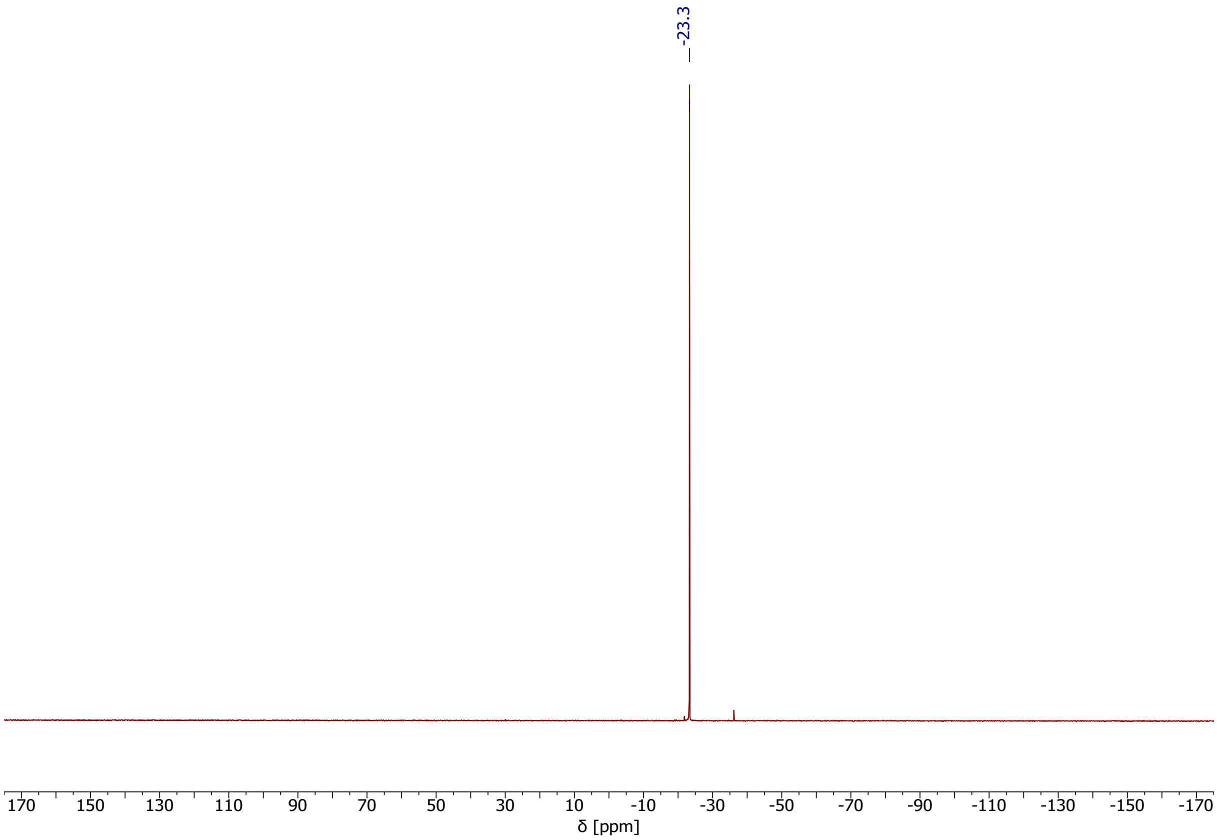

^{1}H NMR (400 MHz, CD_2Cl_2) spectrum of **Ru-MACHO$^{p(i\text{Pr})}$**.

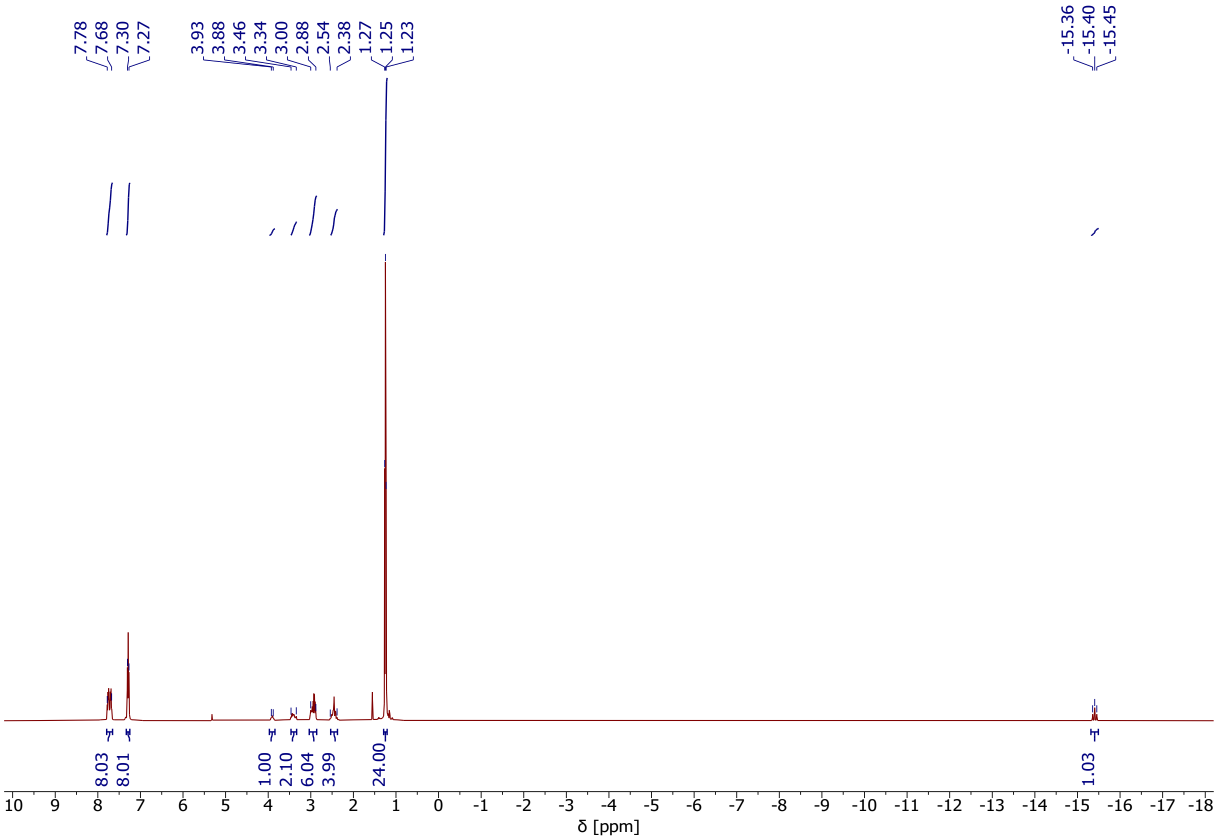

^{13}C NMR (101 MHz, CD_2Cl_2) spectrum of **Ru-MACHO$^{p(i\mathrm{Pr})}$**.

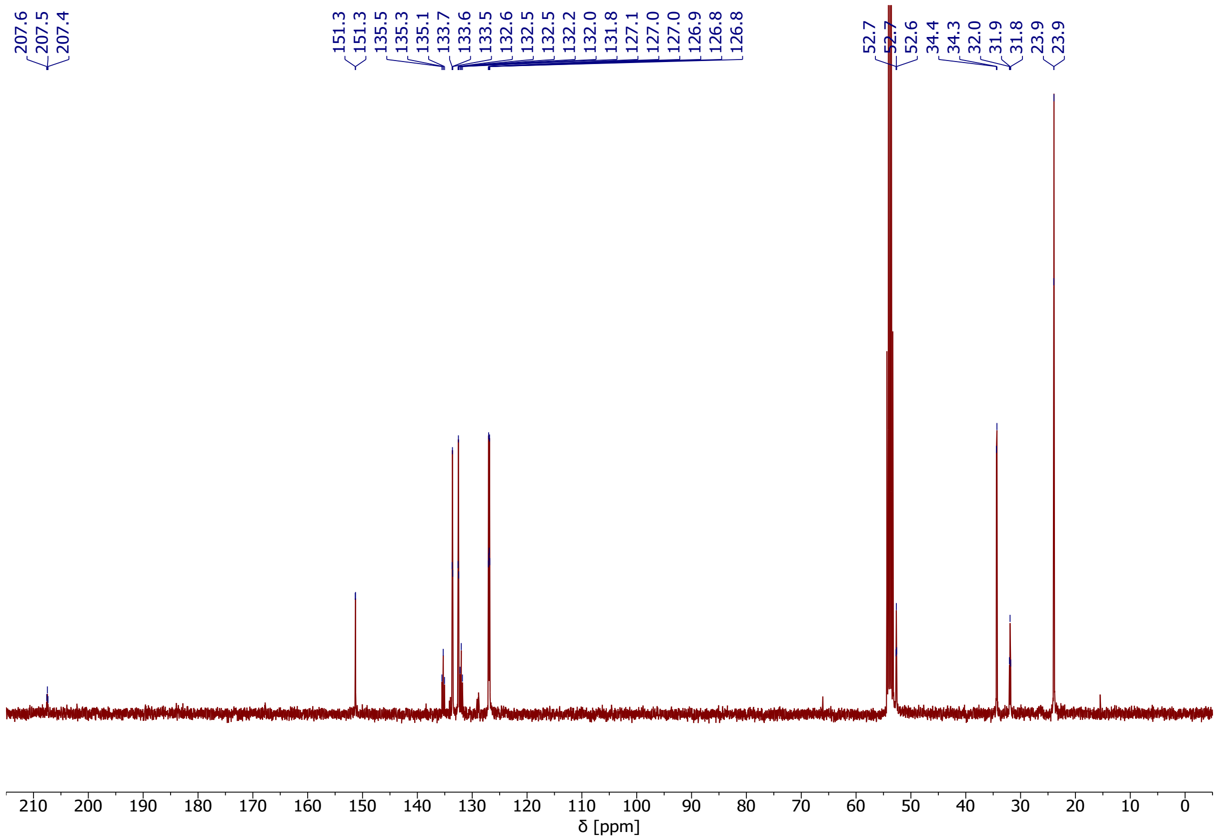

^{31}P NMR (162 MHz, CD_2Cl_2) spectrum of **Ru-MACHO$^{p(i\mathrm{Pr})}$**.

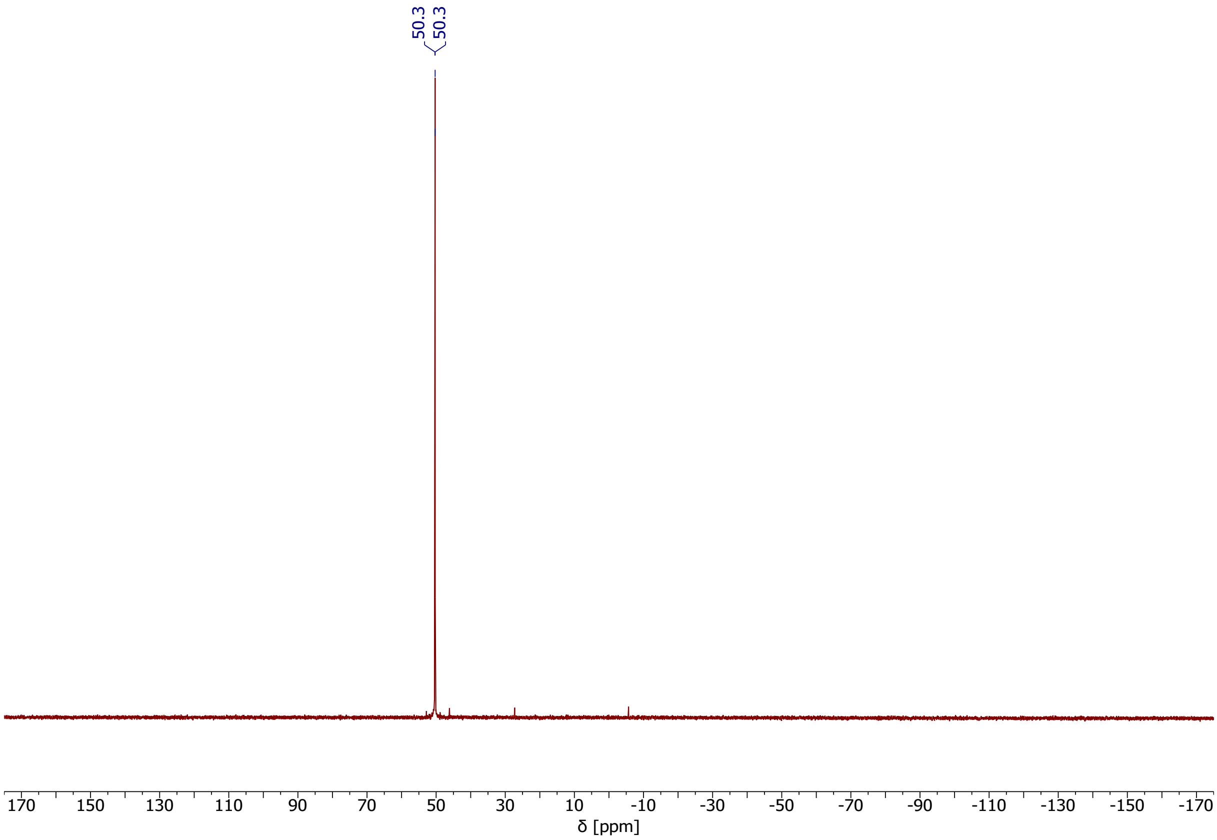

^{1}H NMR (400 MHz, CD_2Cl_2) spectrum of **MACHO$^{p(3\text{-}Pe)}$**.

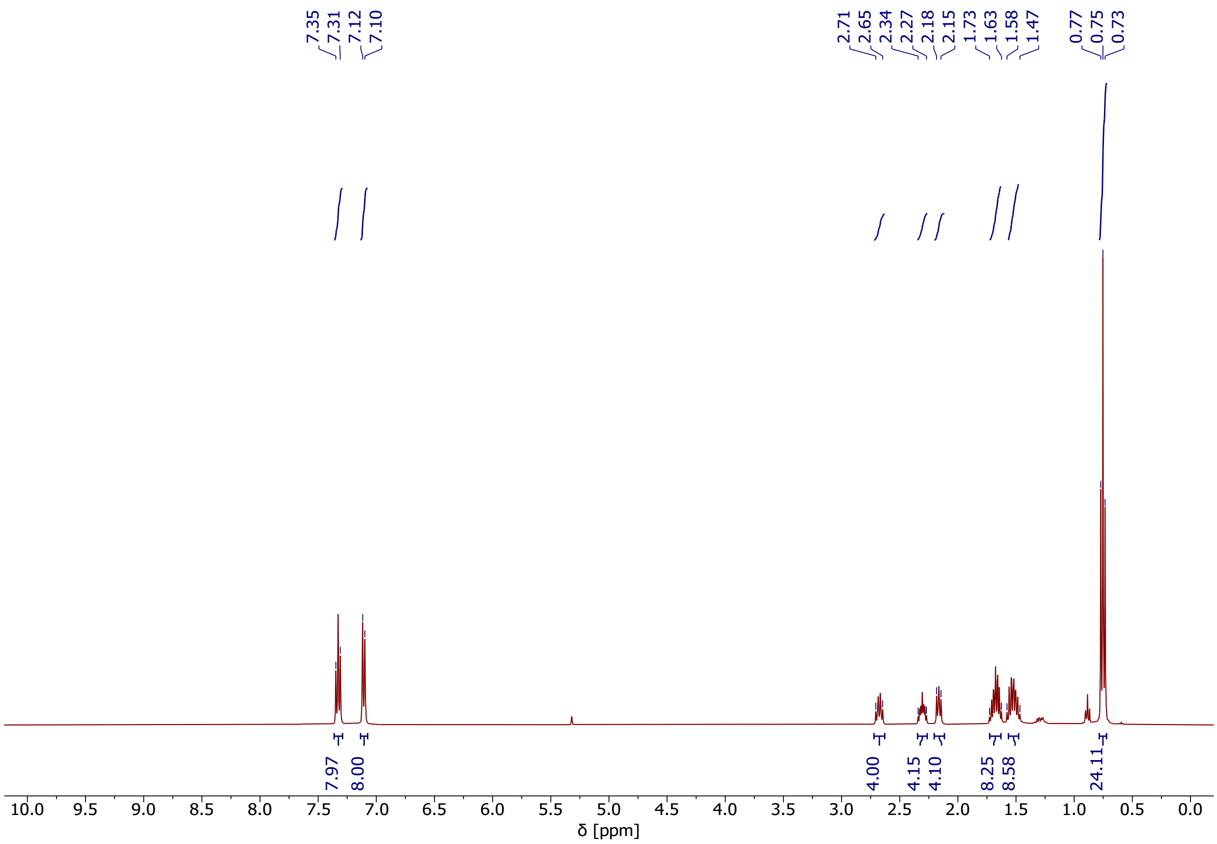

^{13}C NMR (101 MHz, CD_2Cl_2) spectrum of **MACHO$^{p(3\text{-}Pe)}$**.

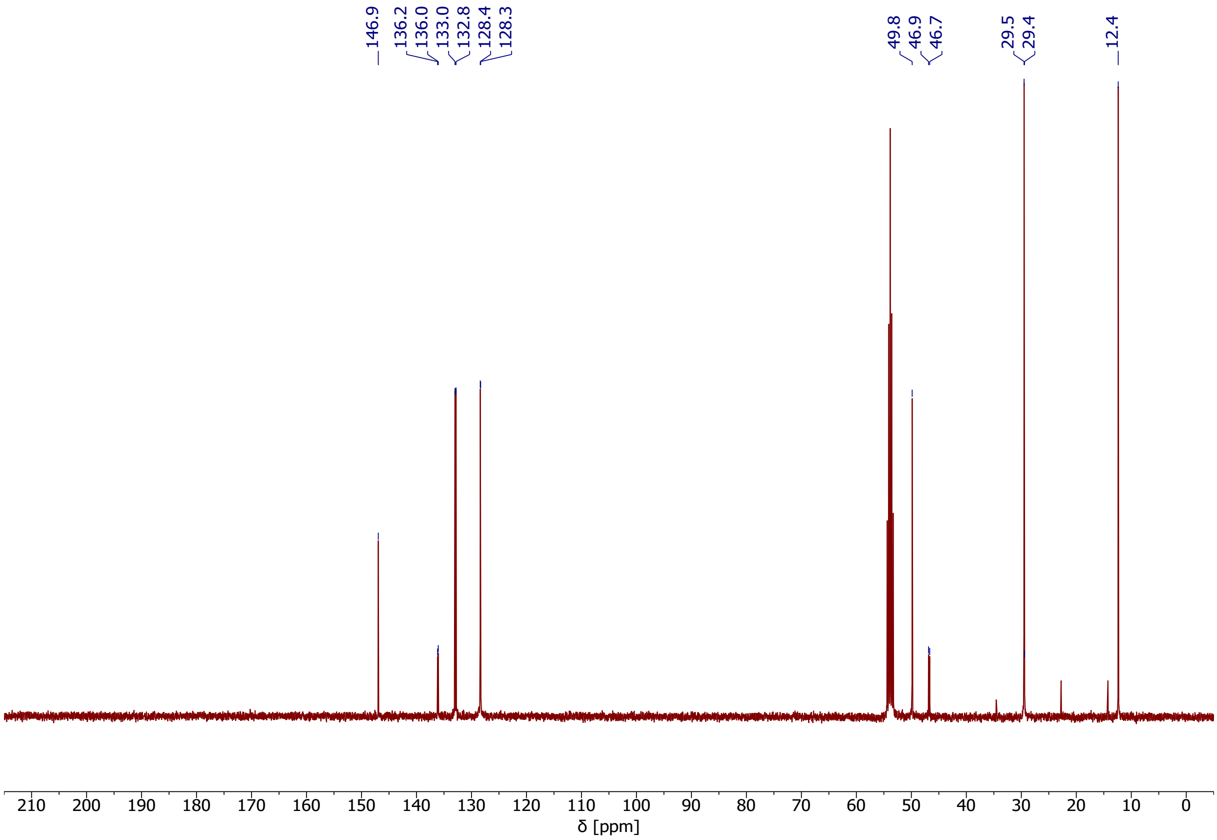

^{31}P NMR (162 MHz, CD_2Cl_2) spectrum of **MACHO$^{p(3\text{-}Pe)}$**.

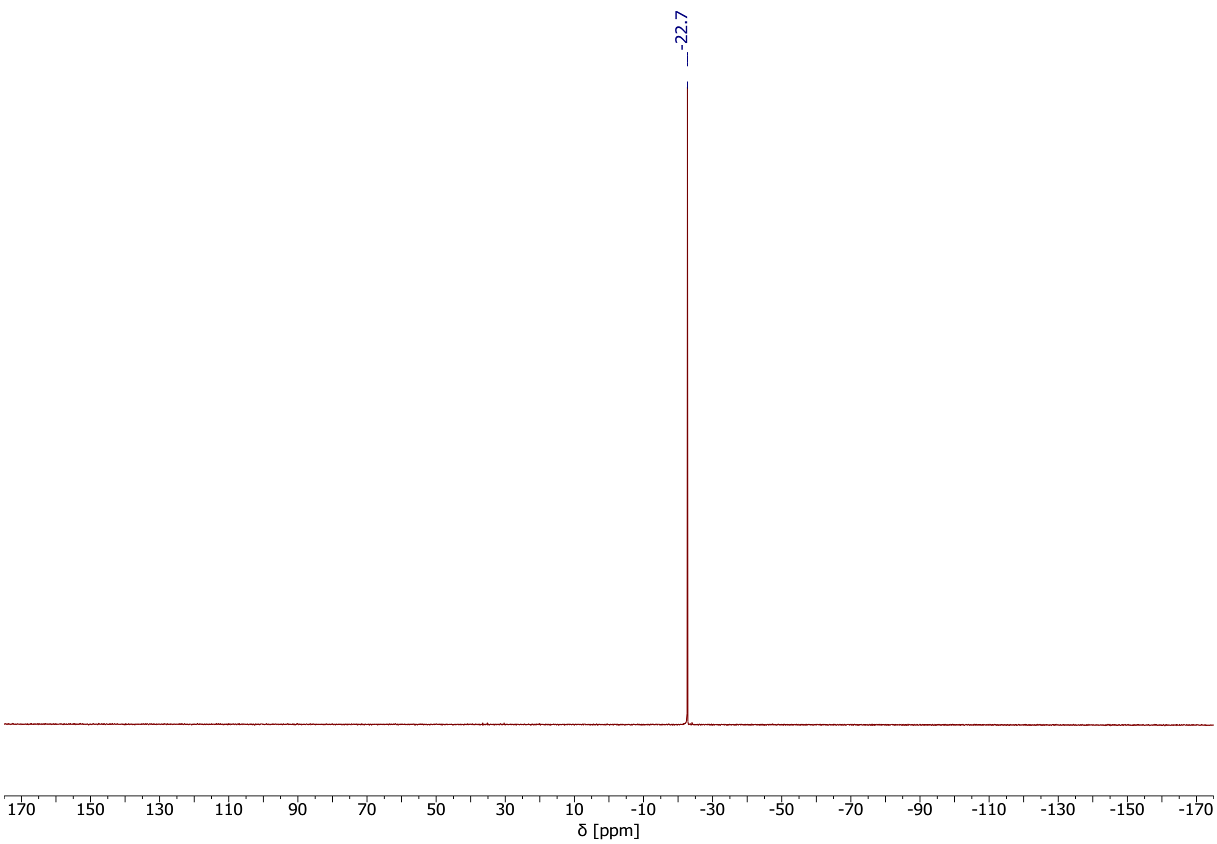

^{1}H NMR (400 MHz, CD_2Cl_2) spectrum of **Ru-MACHO$^{p(3\text{-}Pe)}$**.

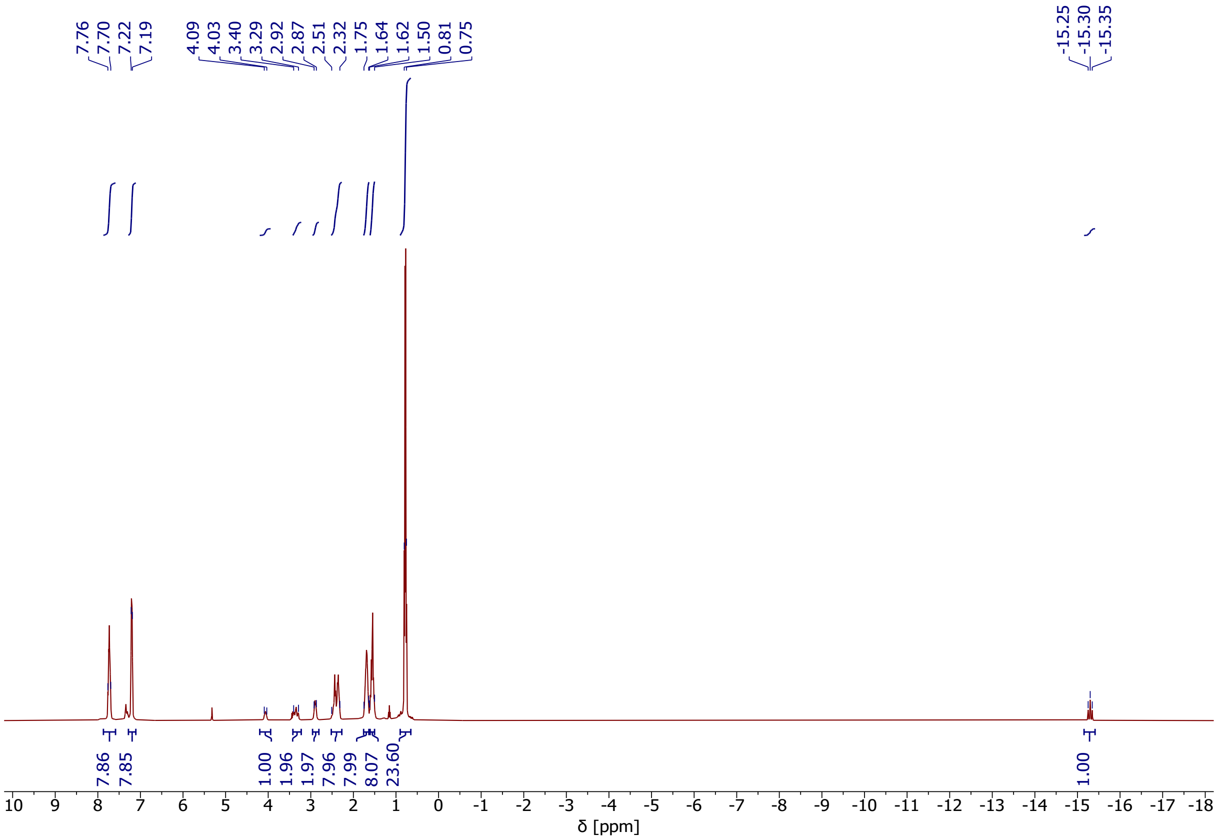

^{13}C NMR (101 MHz, CD_2Cl_2) spectrum of **Ru-MACHO$^{p(3\text{-}Pe)}$**.

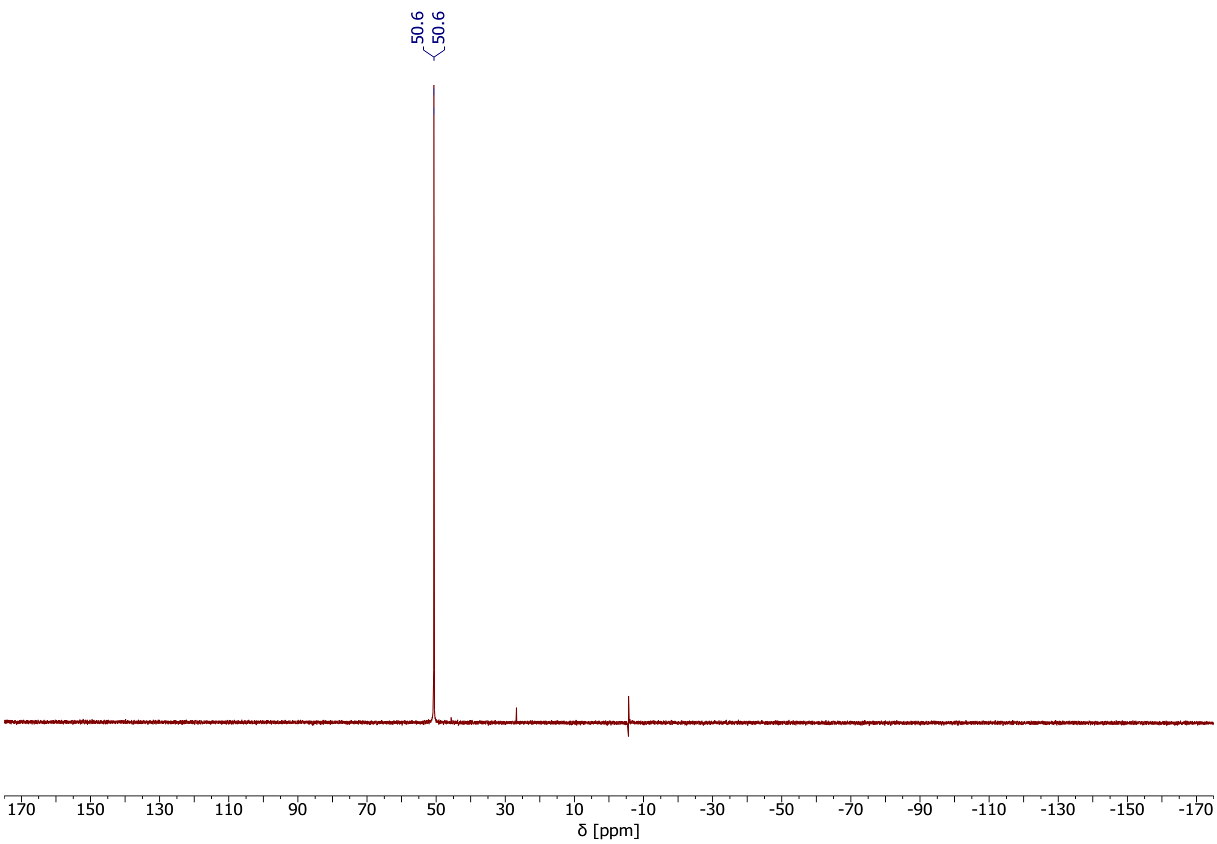

^{31}P NMR (162 MHz, CD_2Cl_2) spectrum of **Ru-MACHO$^{p(3\text{-}Pe)}$**.

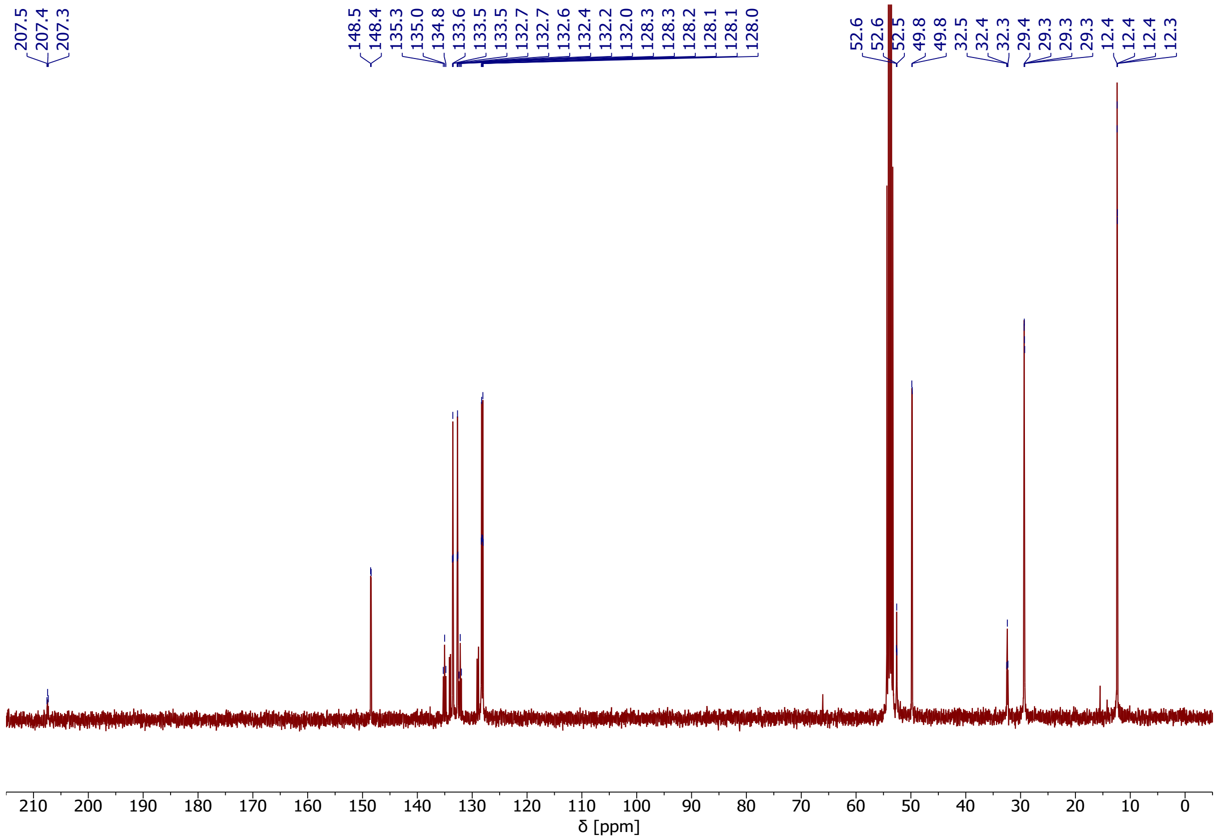

^{1}H NMR (400 MHz, $CDCl_3$) spectrum of **MACHO^{Naph}**.

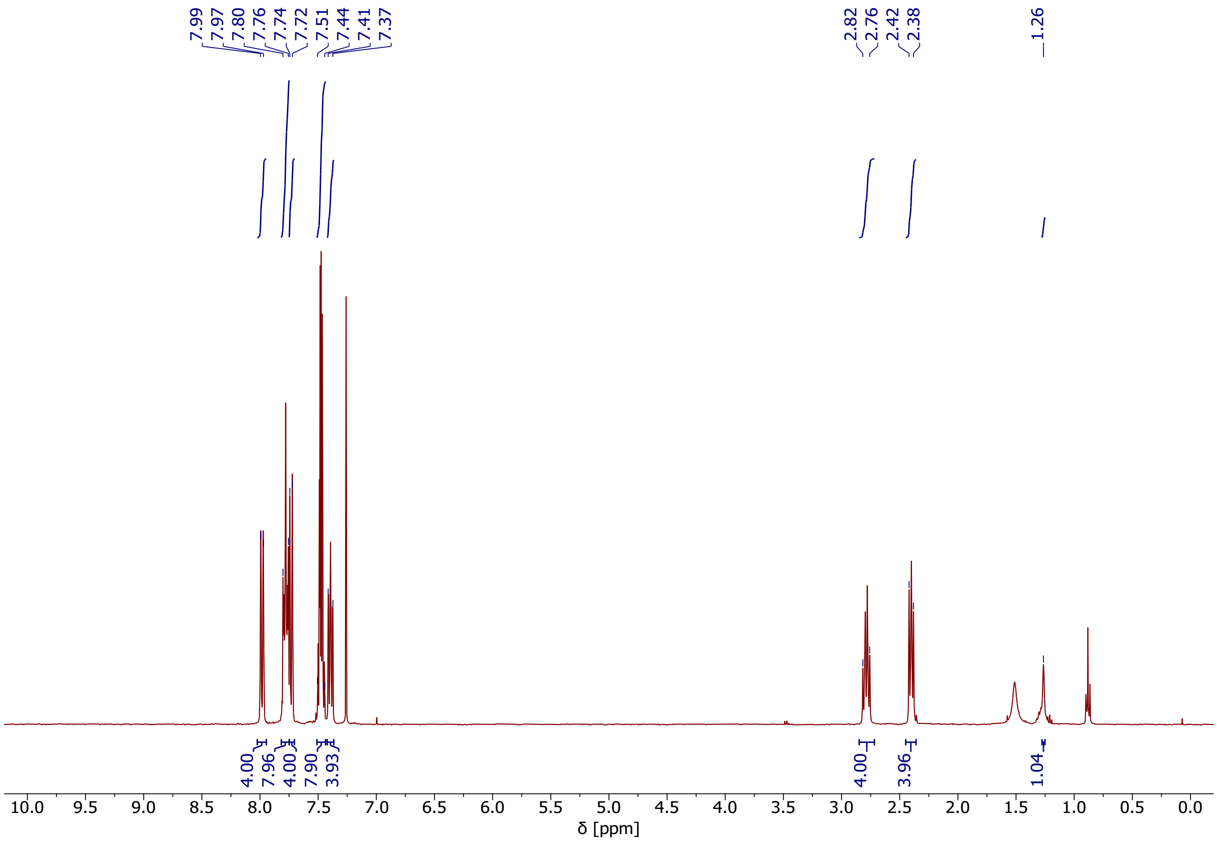

^{13}C NMR (101 MHz, $CDCl_3$) spectrum of **MACHO^{Naph}**.

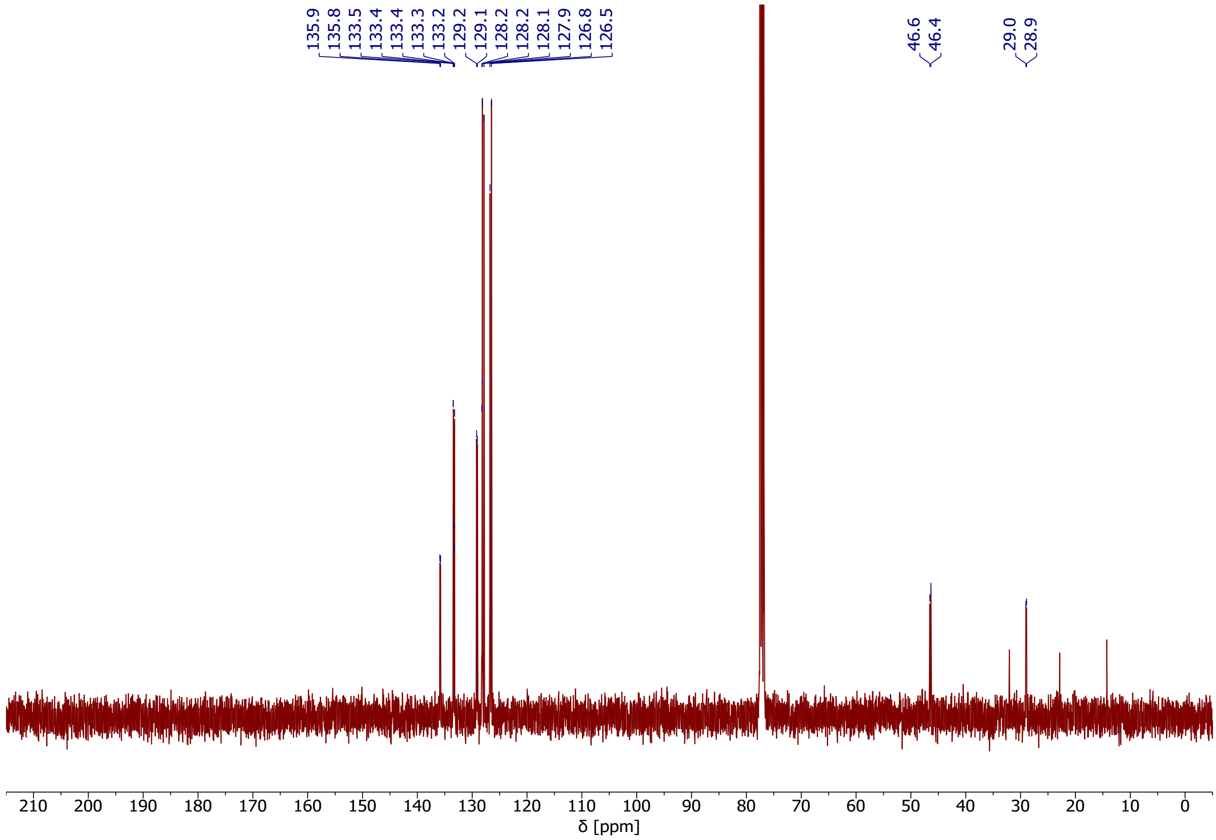

^{31}**P NMR** (162 MHz, $CDCl_3$) spectrum of **MACHO^{Naph}**.

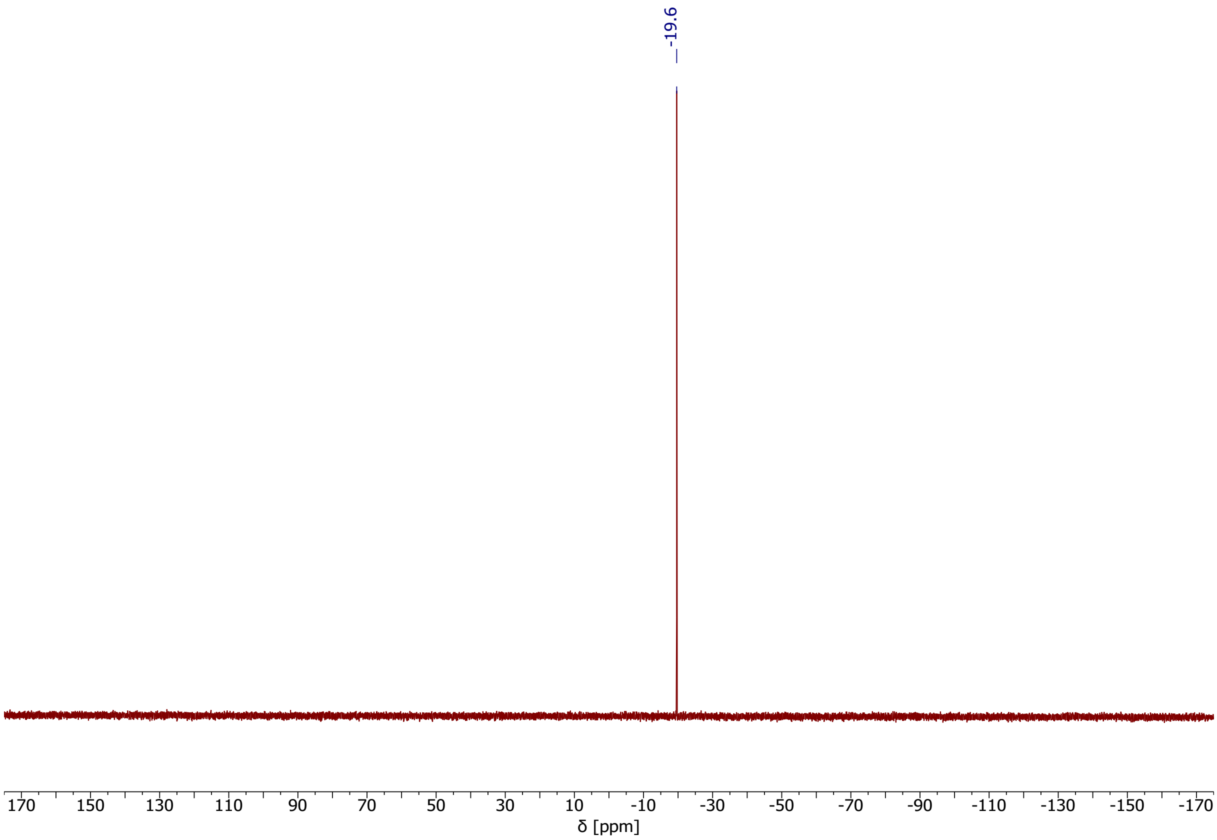

^{1}**H NMR** (400 MHz, CD_2Cl_2) spectrum of **Ru-MACHO^{Naph}**.

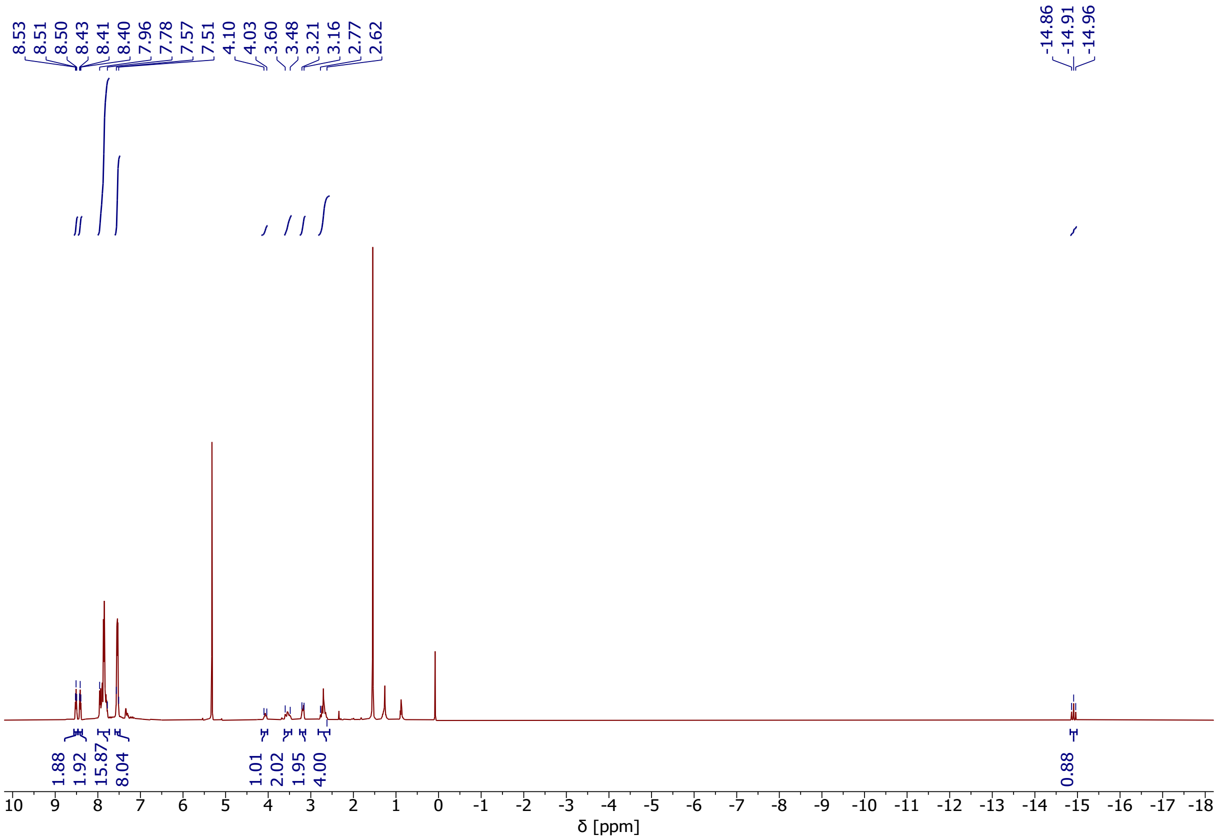

^{31}P NMR (162 MHz, CD_2Cl_2) spectrum of **Ru-MACHO^{Naph}**.

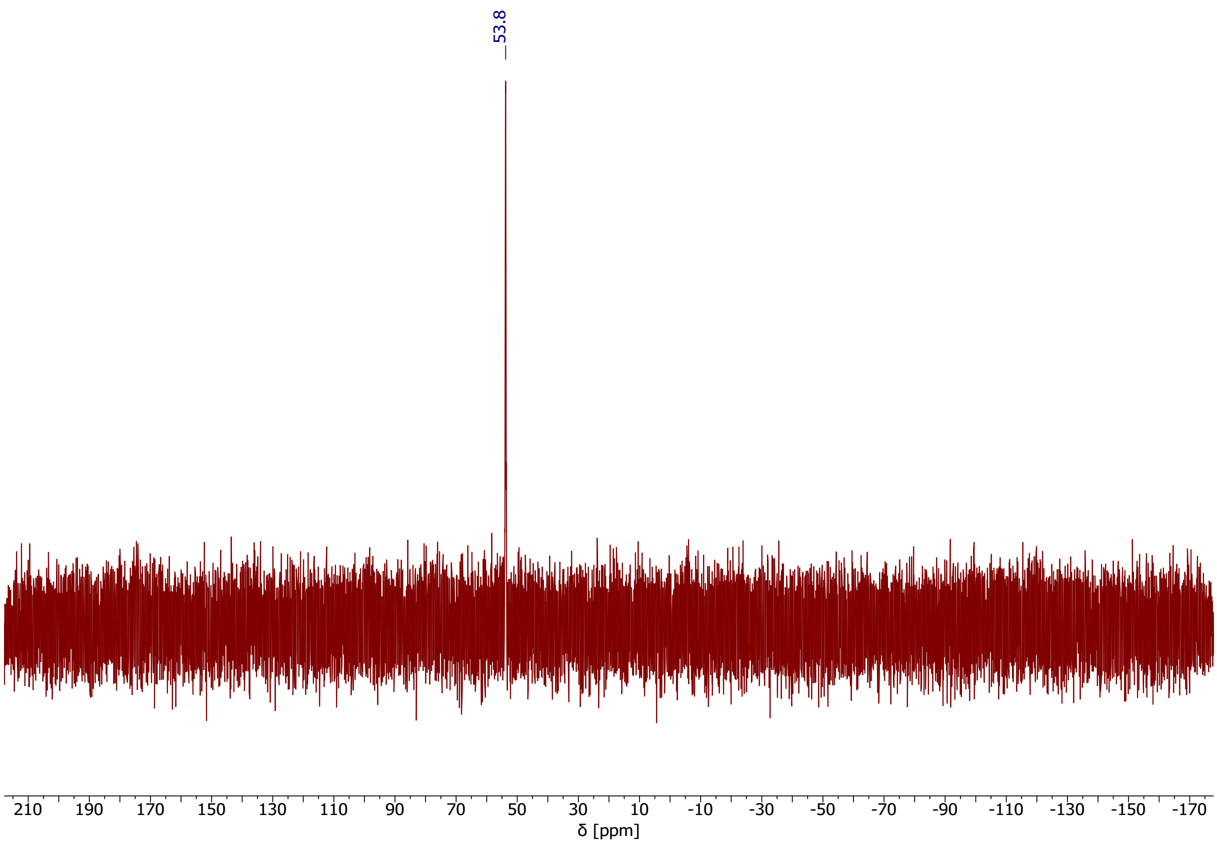

^{1}H NMR (400 MHz, $CDCl_3$) spectrum of **MACHO^{Biph}**.

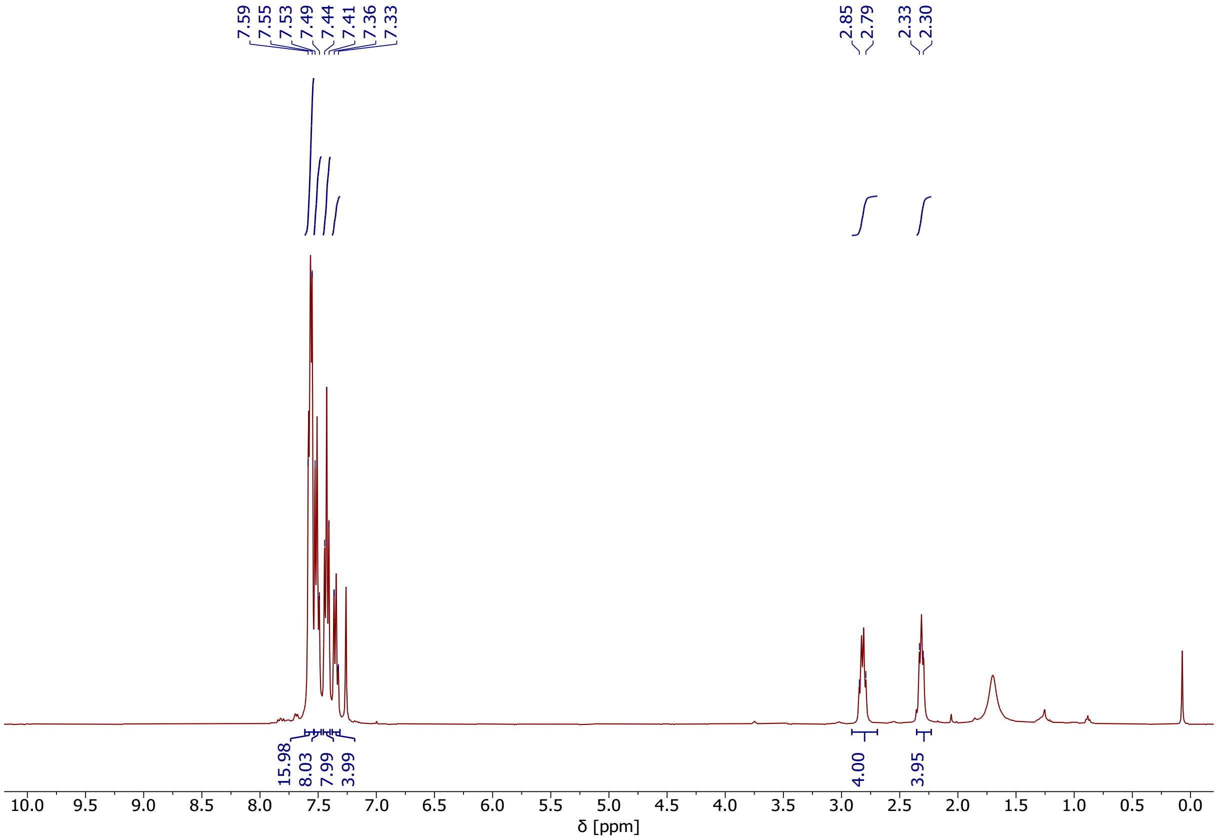

^{13}C NMR (101 MHz, $CDCl_3$) spectrum of **MACHO^{Biph}**.

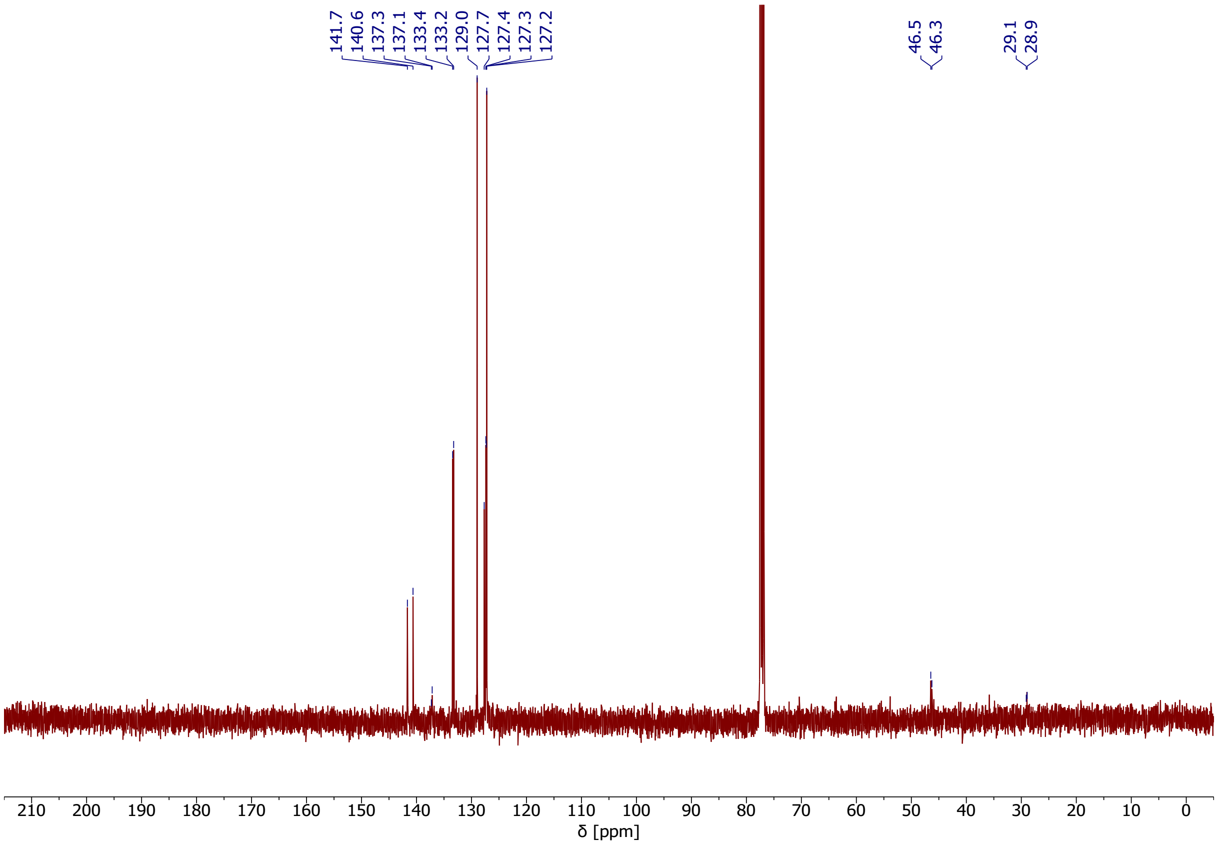

^{31}P NMR (162 MHz, $CDCl_3$) spectrum of **MACHO^{Biph}**.

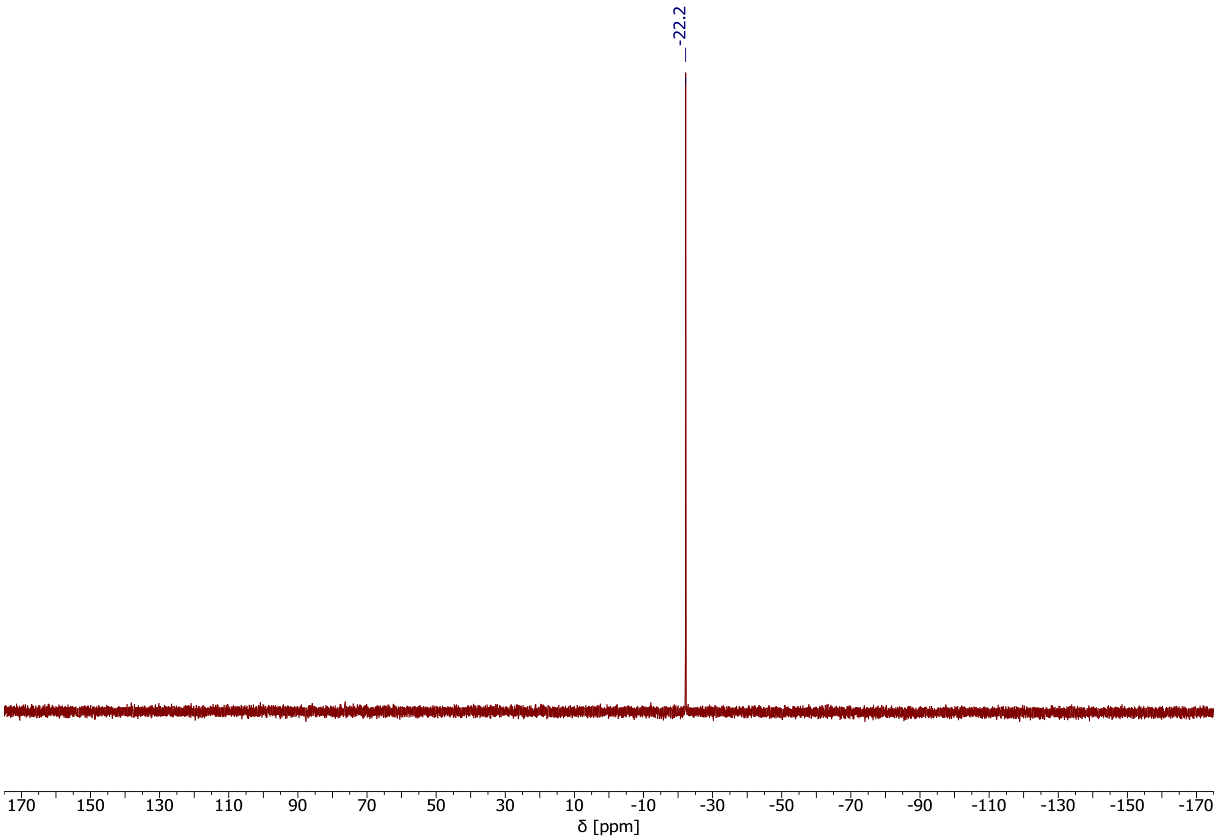

^{1}H NMR (400 MHz, $CDCl_3$) spectrum of **Ru-MACHO$^{\mathbf{Biph}}$**.

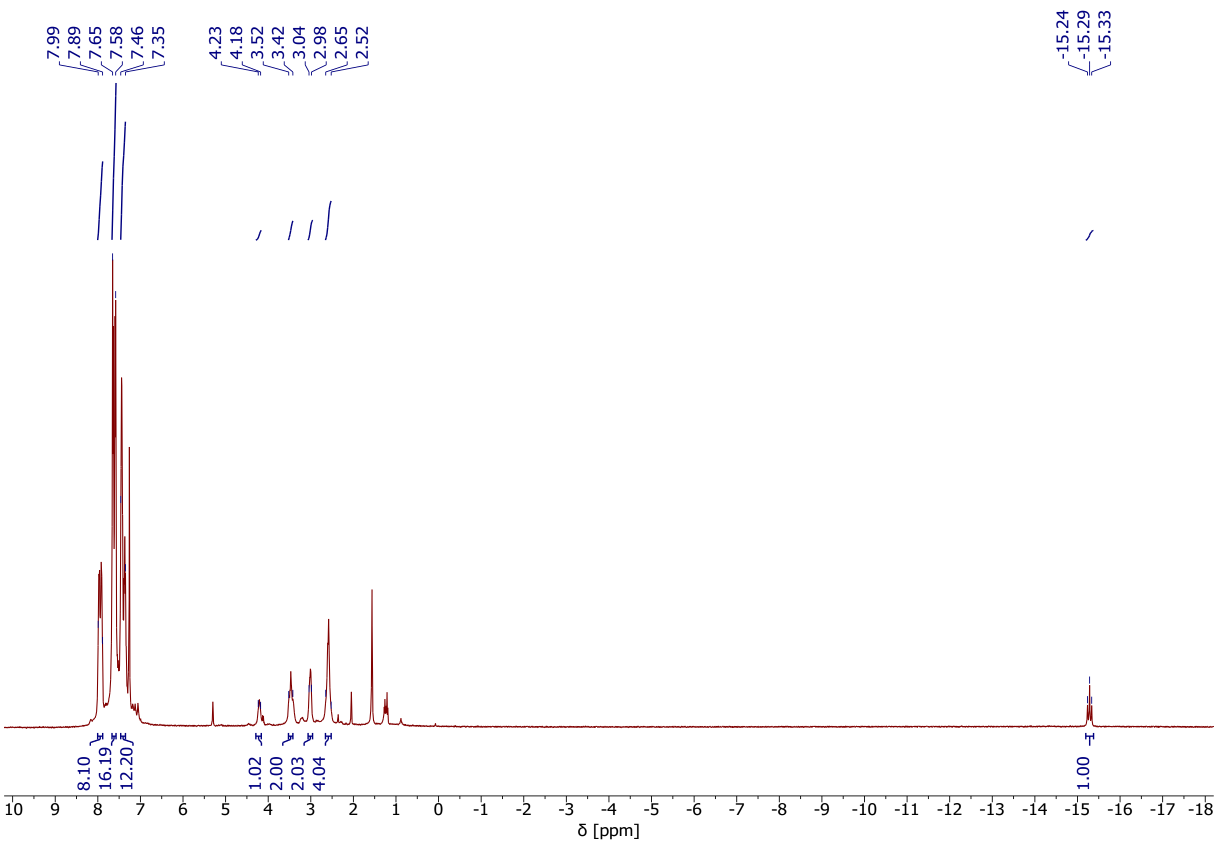

^{13}C NMR (101 MHz, $CDCl_3$) spectrum of **Ru-MACHO$^{\mathbf{Biph}}$**.

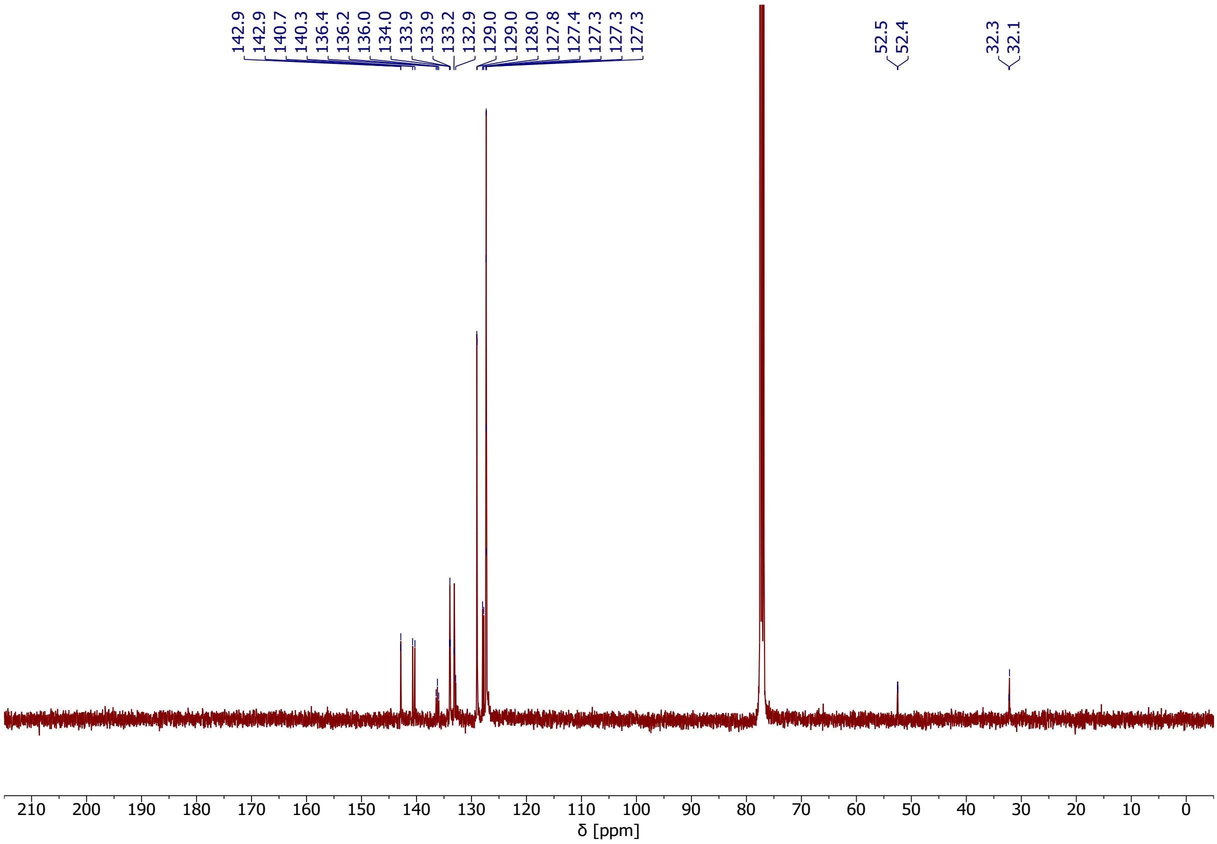

^{31}P NMR (162 MHz, $CDCl_3$) spectrum of **Ru-MACHO^{Biph}**.

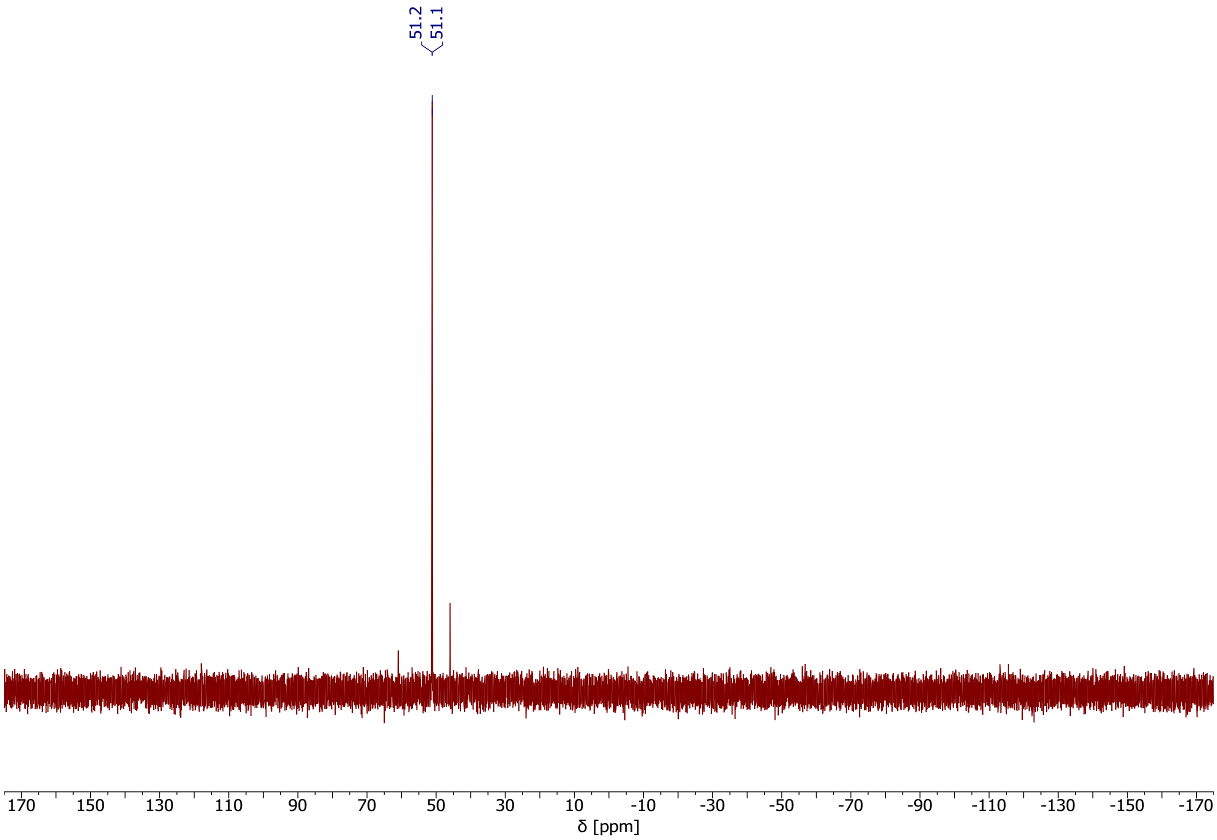

^{1}H NMR (400 MHz, $CDCl_3$) spectrum of **MACHO$^{p(CF3)}$**.

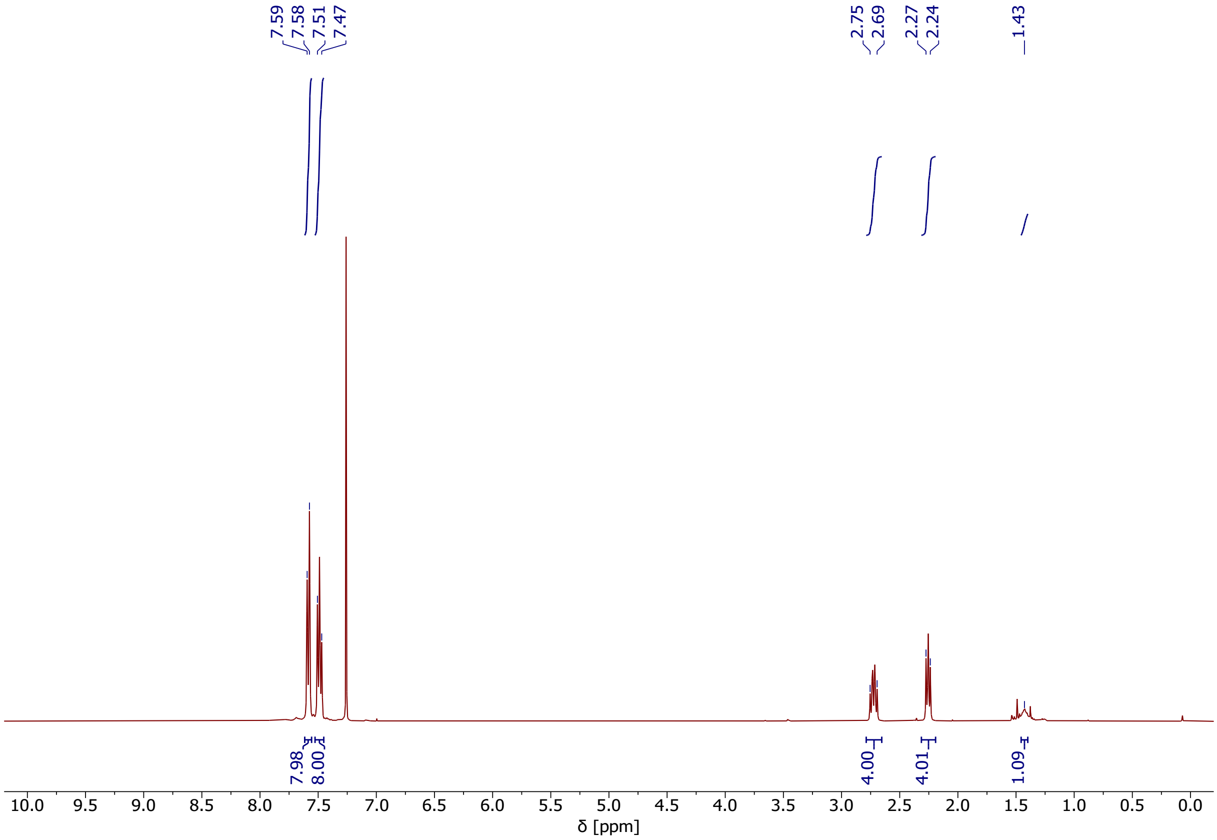

^{13}**C NMR** (101 MHz, $CDCl_3$) spectrum of **MACHO$^{p(CF3)}$**.

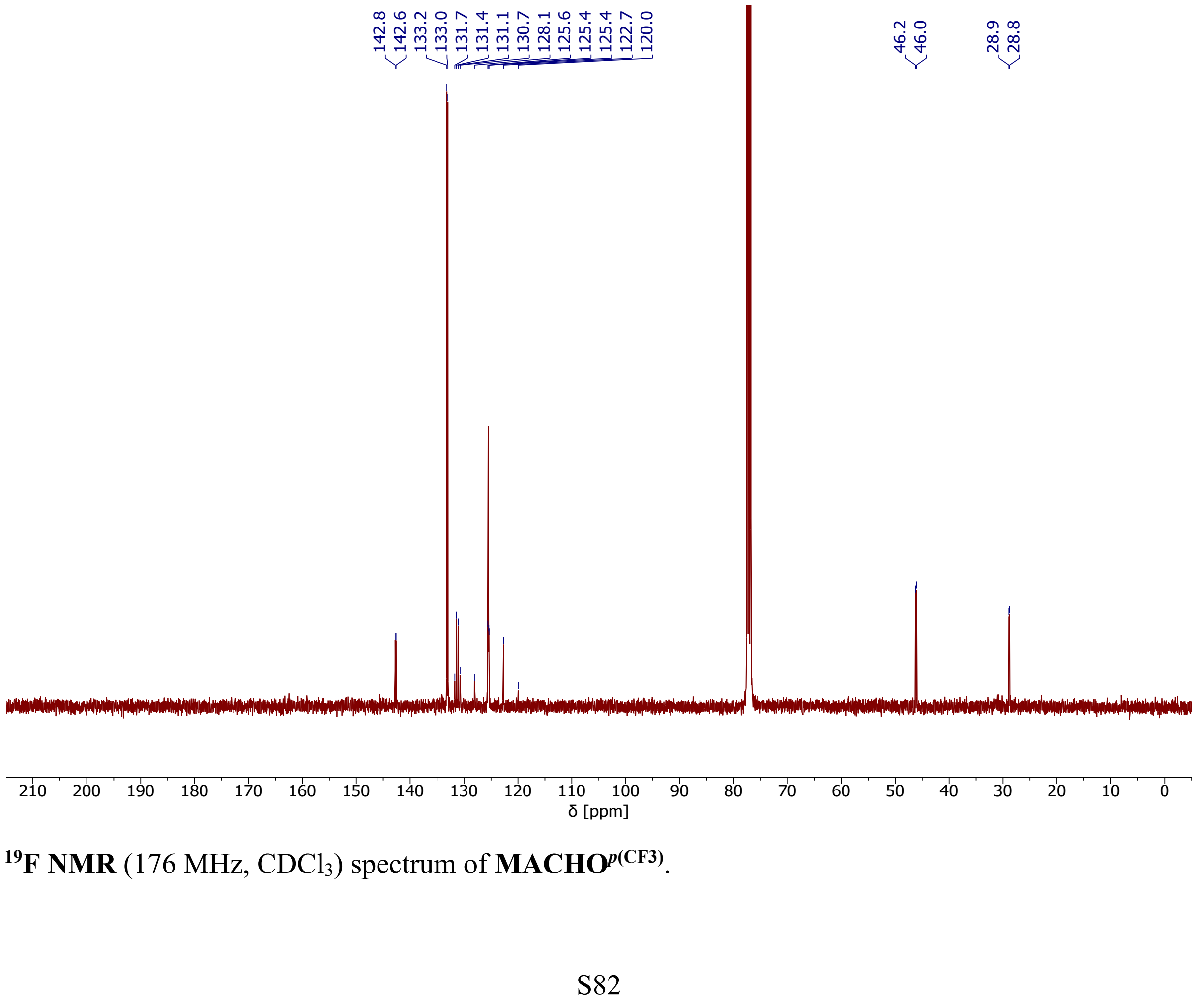

^{19}**F NMR** (176 MHz, $CDCl_3$) spectrum of **MACHO$^{p(CF3)}$**.

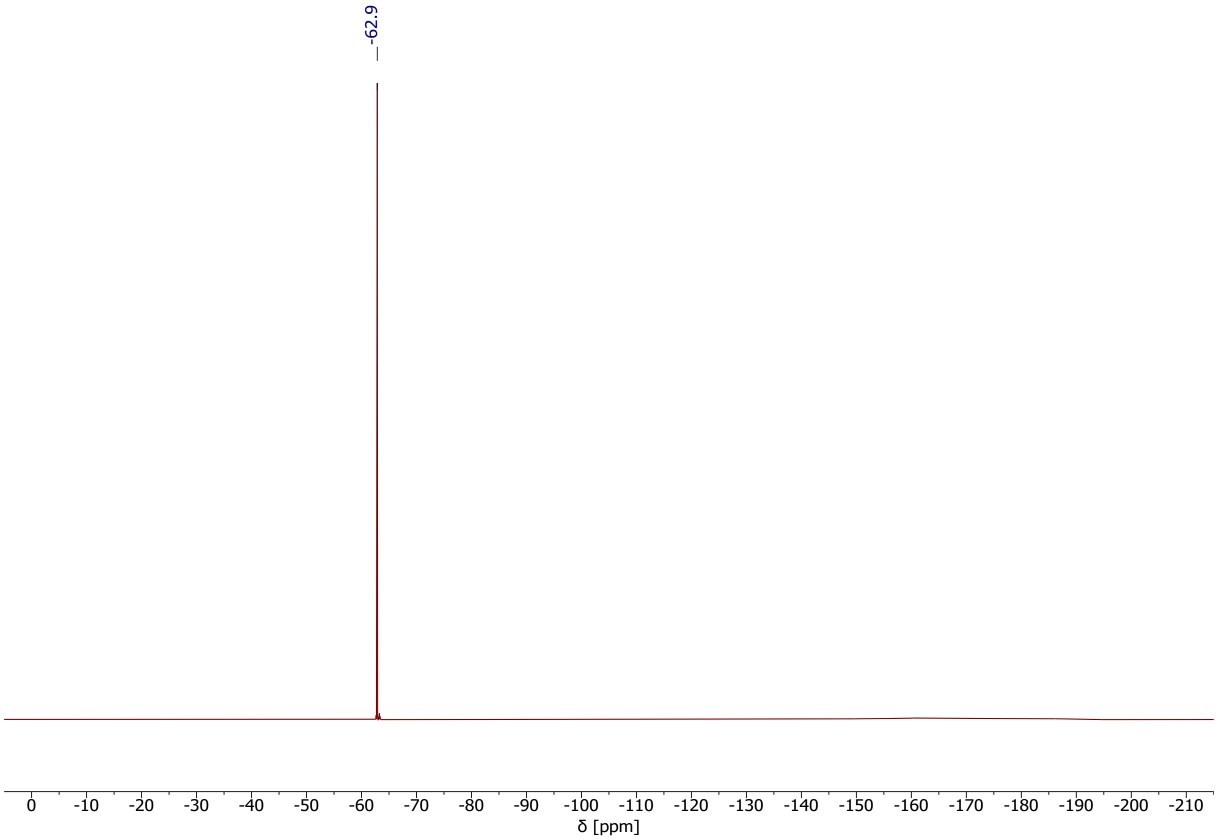

^{31}P NMR (162 MHz, $CDCl_3$) spectrum of **MACHO$^{p(CF3)}$**.

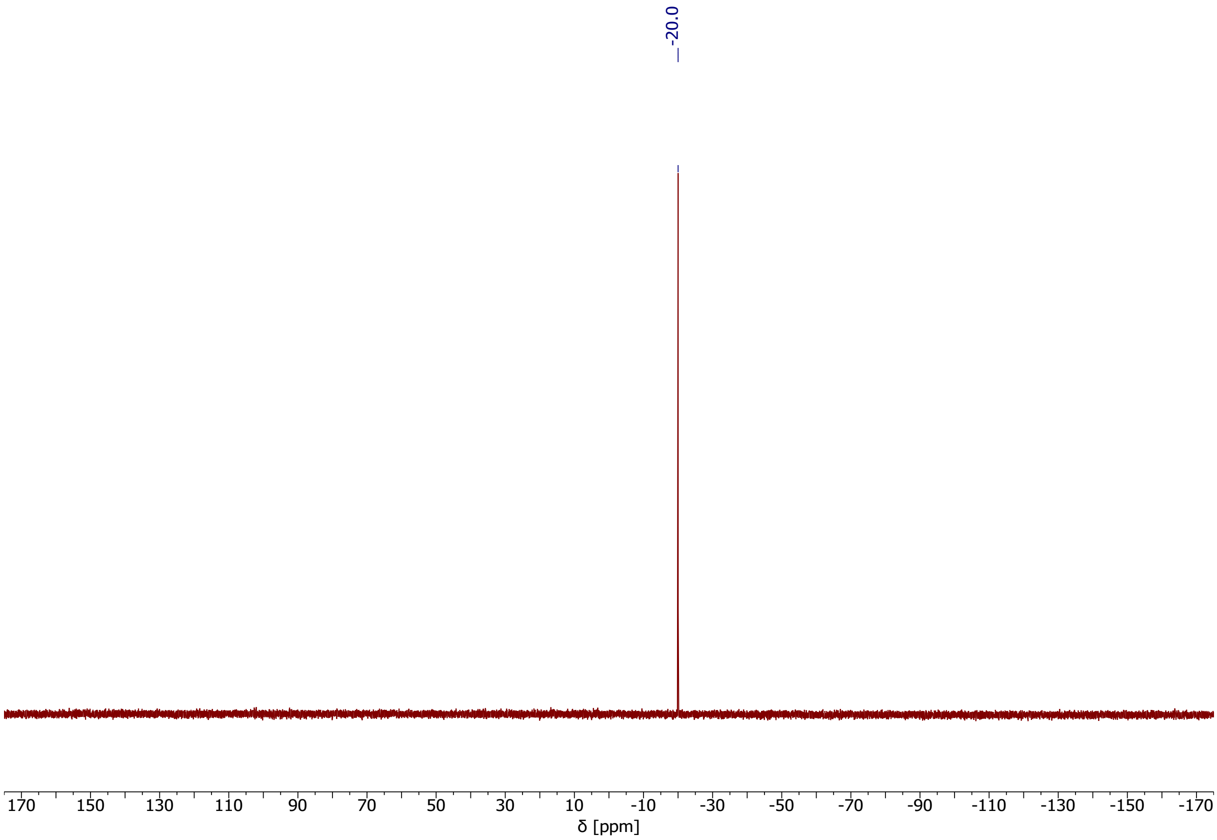

^{1}H NMR (400 MHz, C_6D_6) spectrum of **Ru-MACHO$^{p(CF3)}$**.

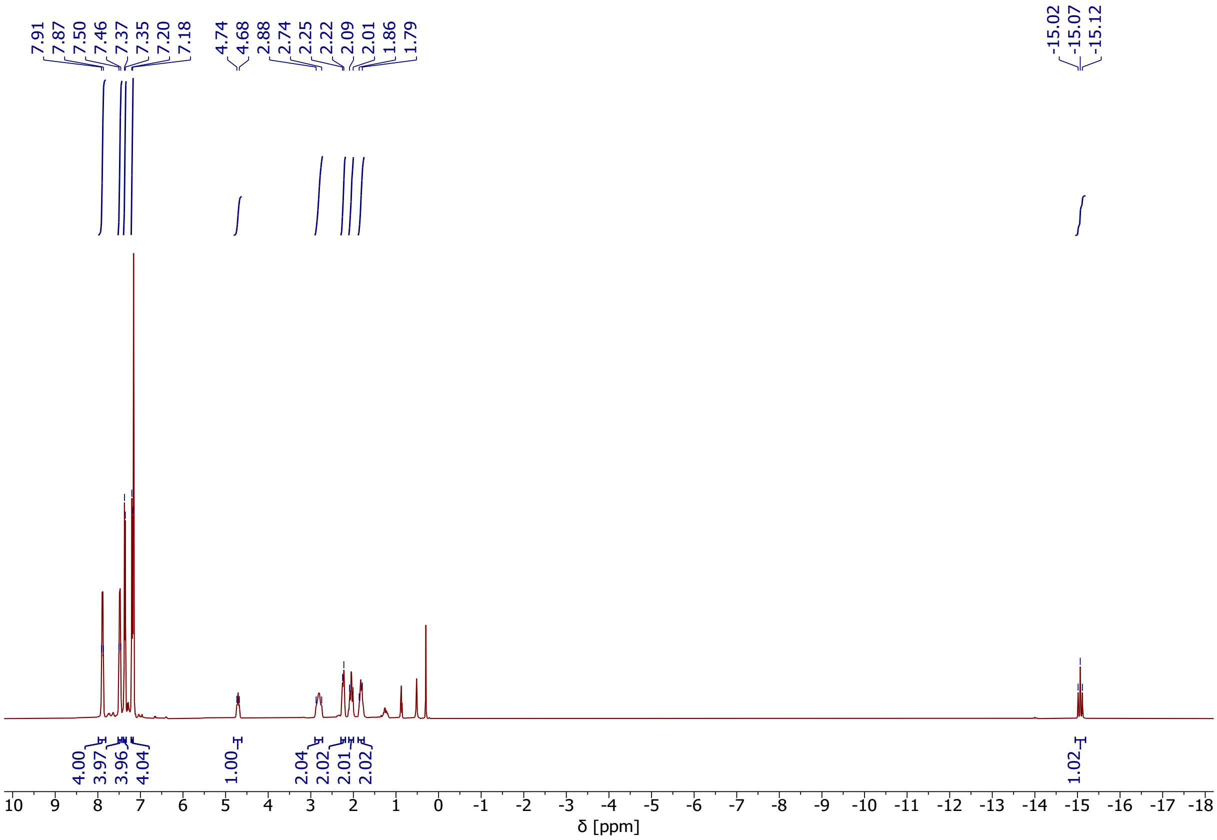

^{13}C NMR (101 MHz, C_6D_6) spectrum of **Ru-MACHO$^{p(CF3)}$**.

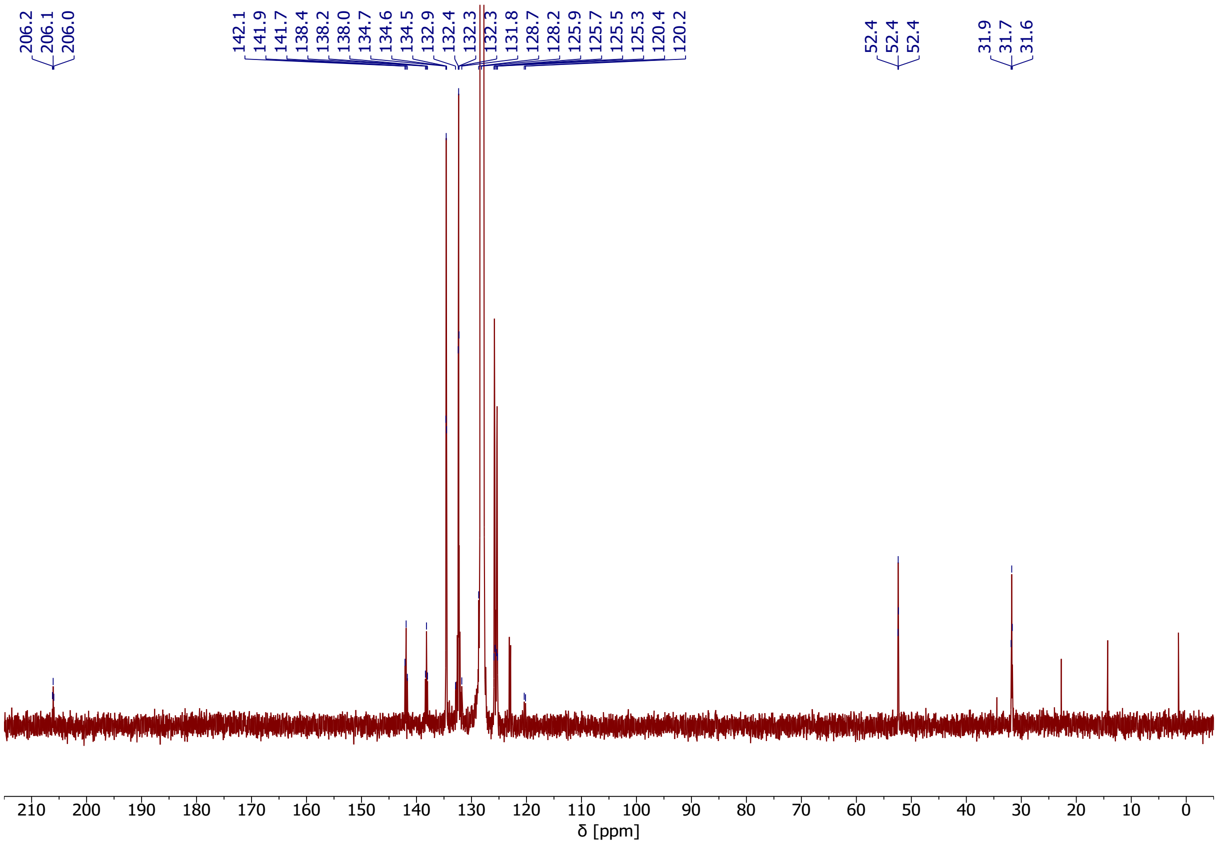

^{19}F NMR (176 MHz, C_6D_6) spectrum of **Ru-MACHO$^{p(CF3)}$**.

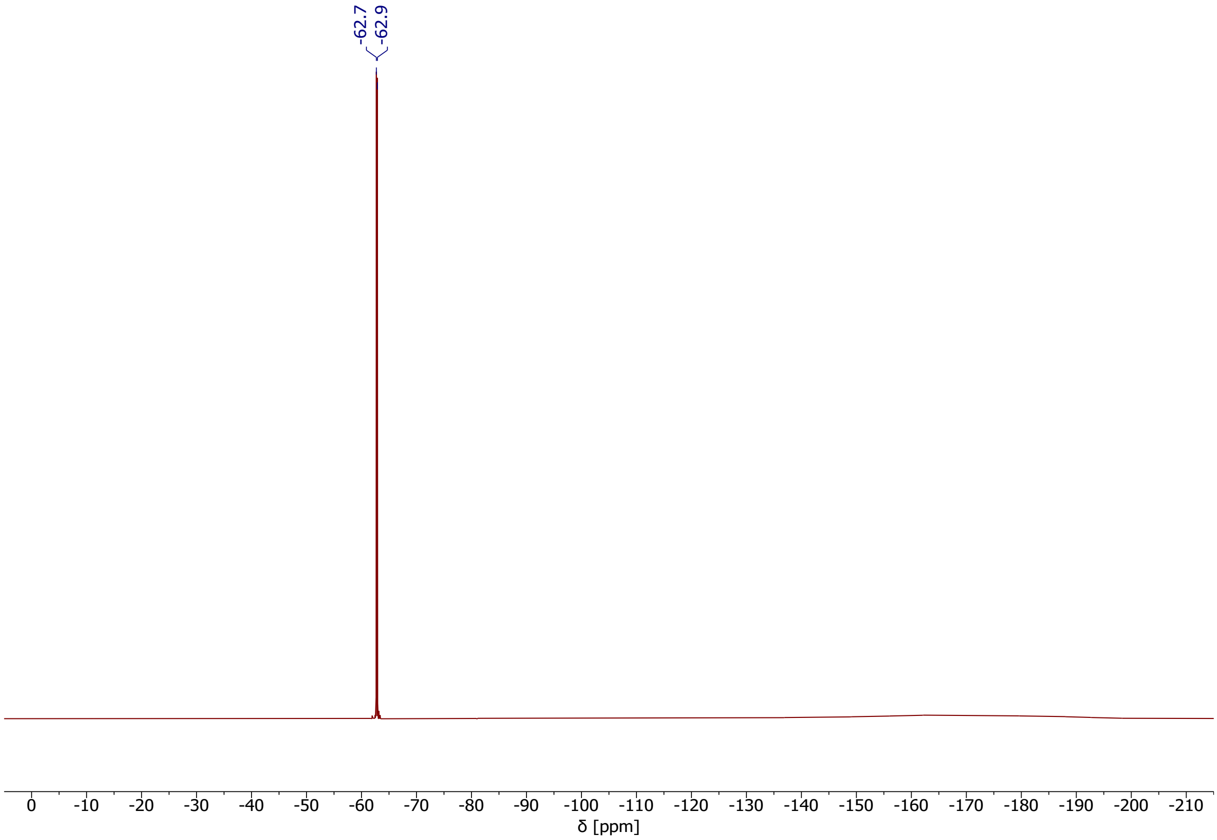

^{31}P NMR (162 MHz, C_6D_6) spectrum of **Ru-MACHO$^{p(CF3)}$**.

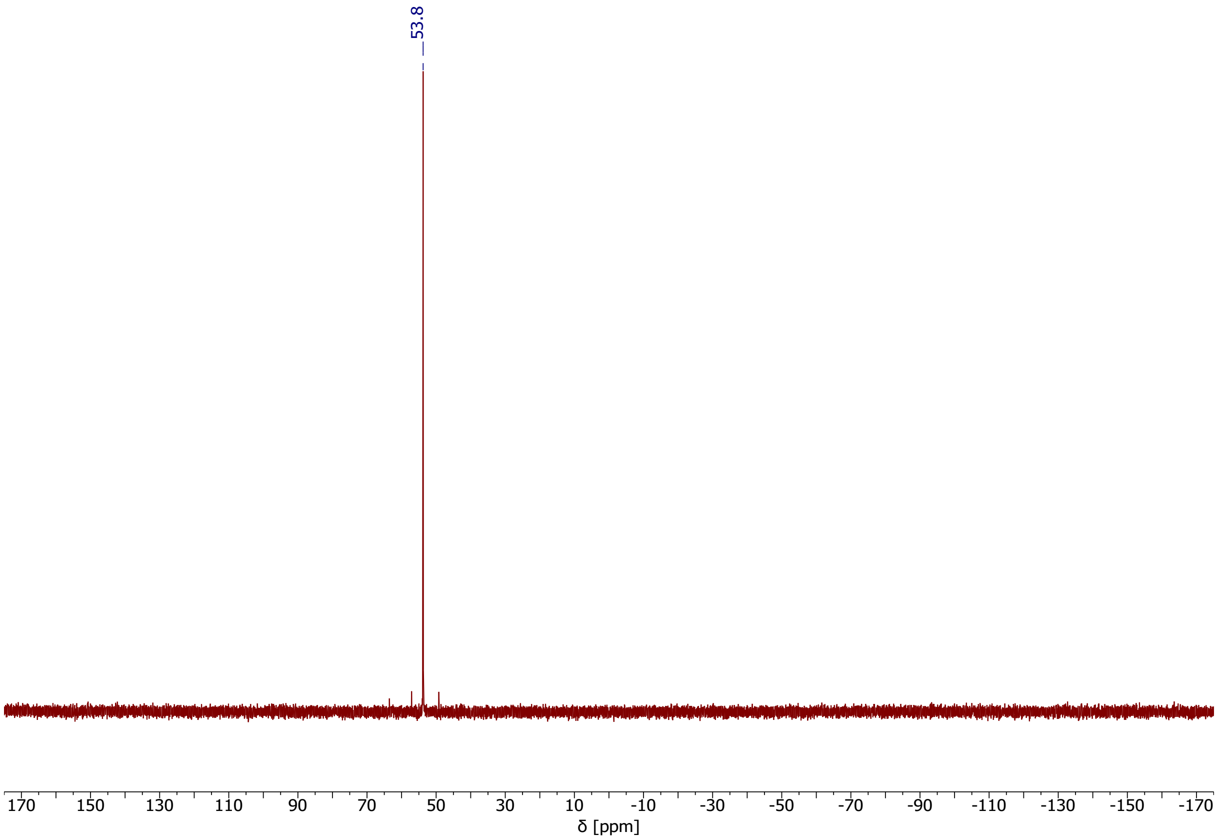

^{1}H NMR (400 MHz, $CDCl_3$) spectrum of **MACHO$^{p(OMe)}$**.

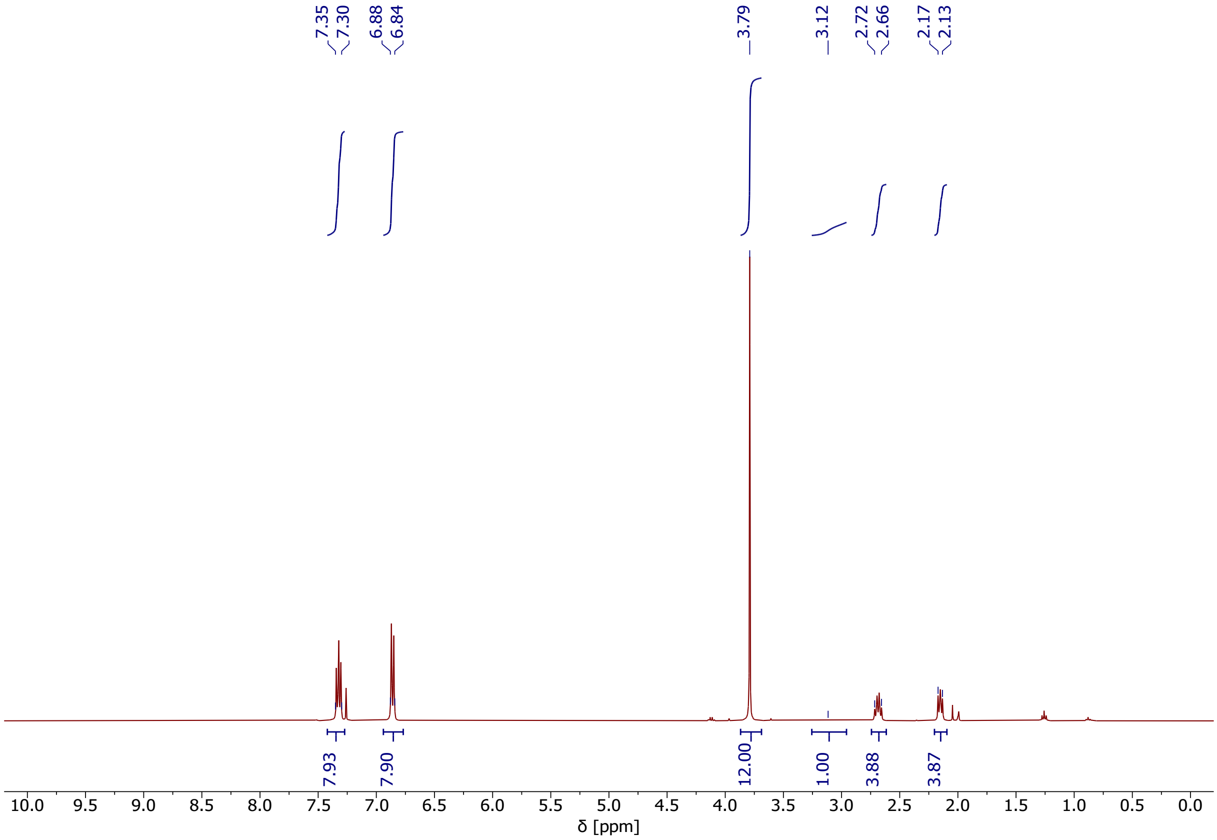

^{13}C NMR (101 MHz, $CDCl_3$) spectrum of **MACHO$^{p(OMe)}$**.

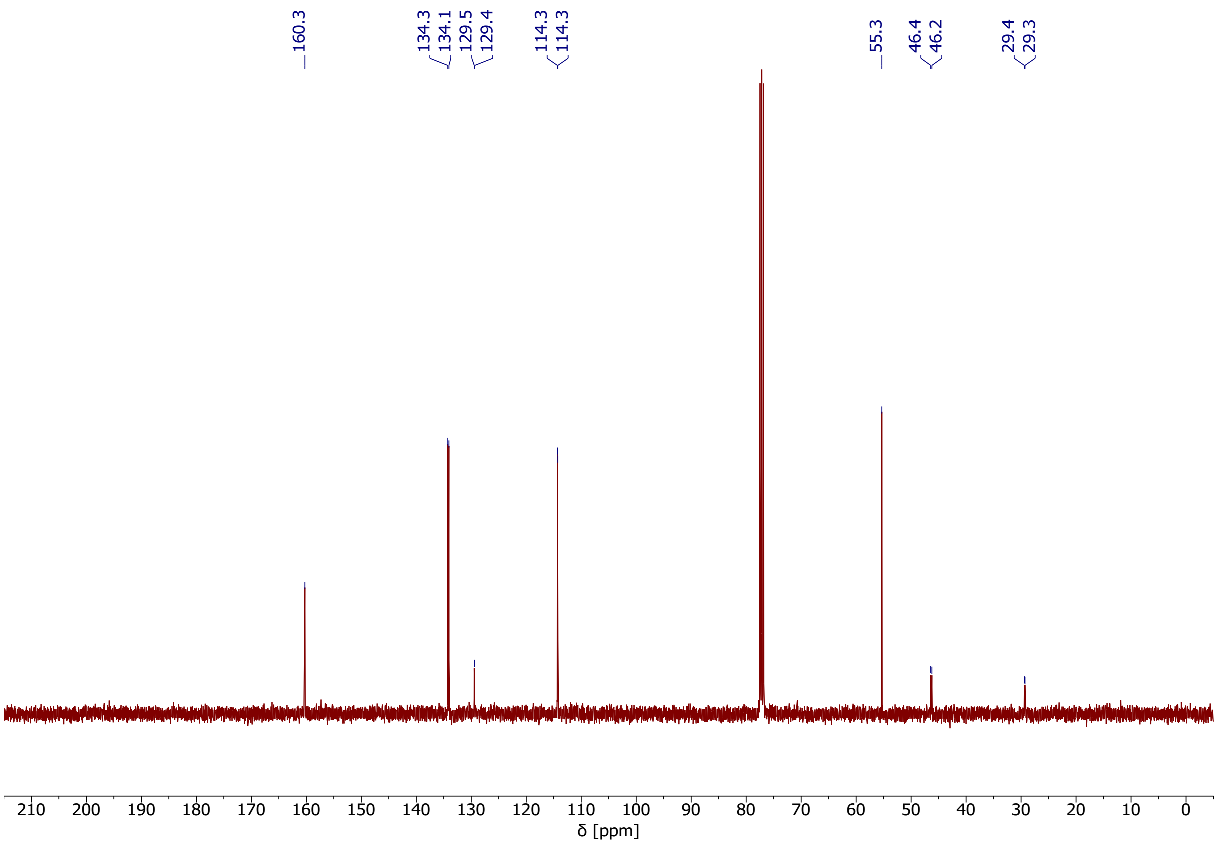

^{31}P NMR (162 MHz, $CDCl_3$) spectrum of **MACHO$^{p(OMe)}$**.

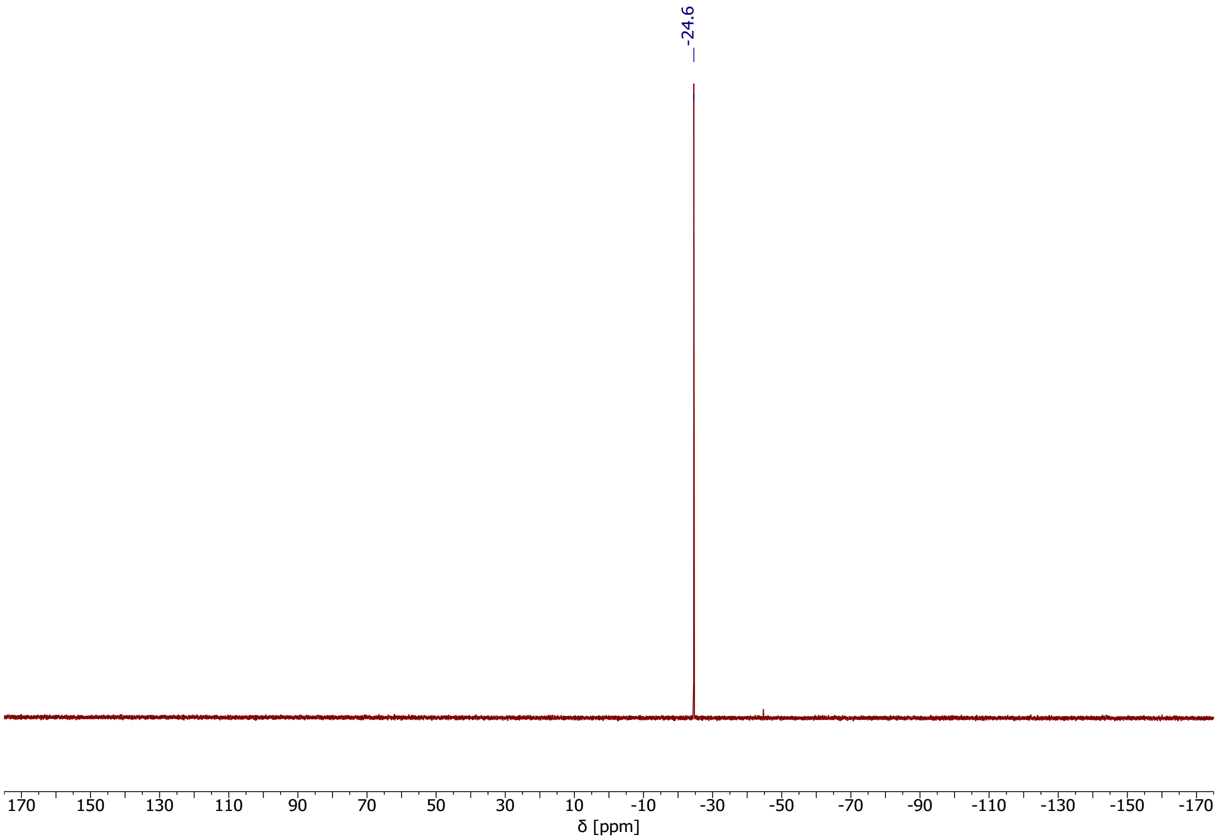

^{1}H NMR (400 MHz, $CDCl_3$) spectrum of **Ru-MACHO$^{p(OMe)}$**.

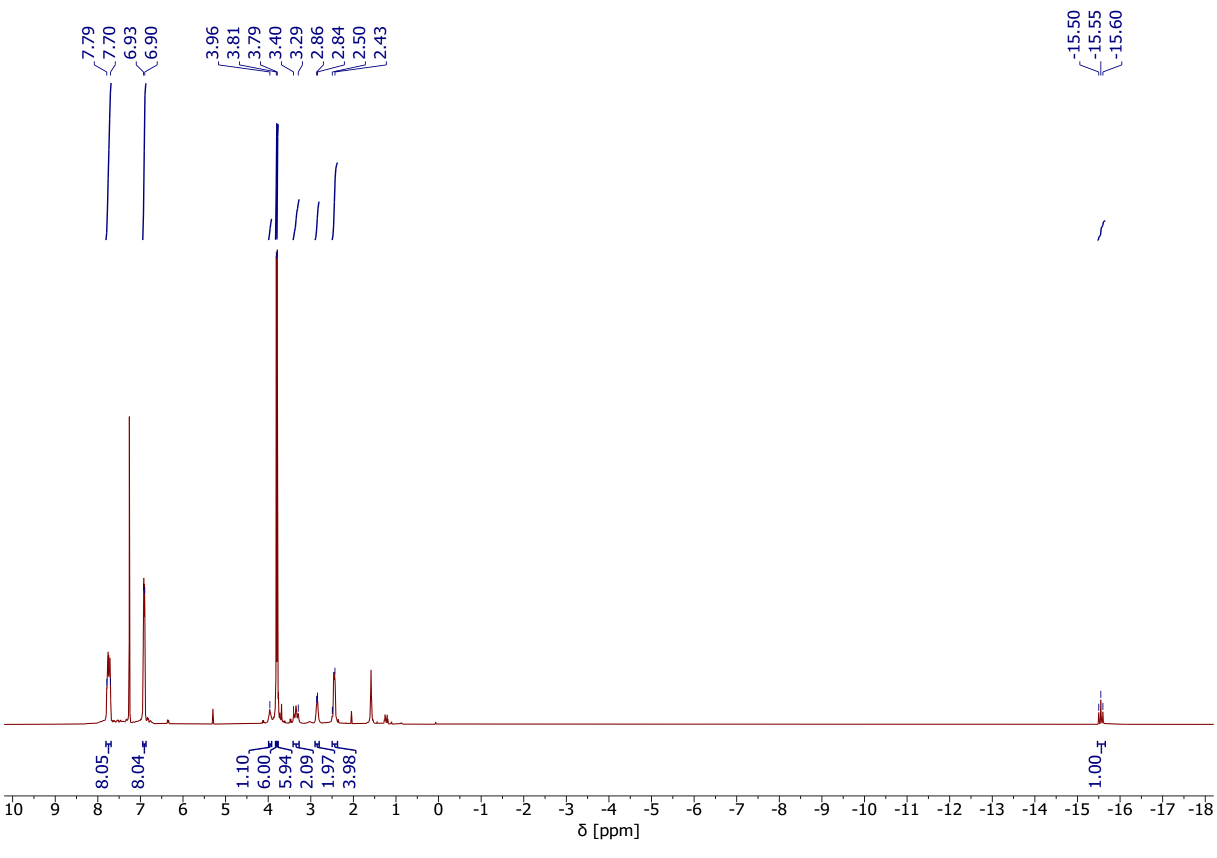

^{13}C NMR (101 MHz, $CDCl_3$) spectrum of **Ru-MACHO$^{p(OMe)}$**.

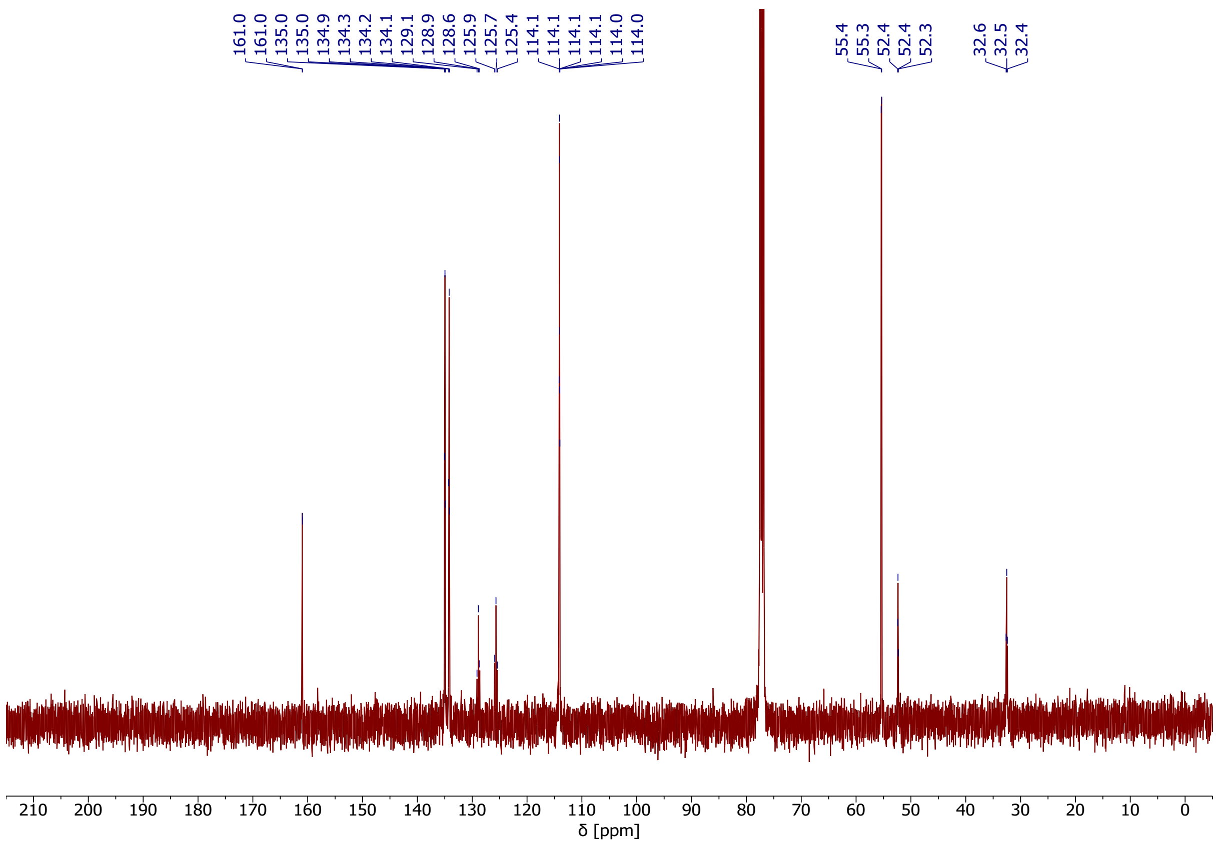

^{31}P NMR (162 MHz, $CDCl_3$) spectrum of **Ru-MACHO$^{p(OMe)}$**.

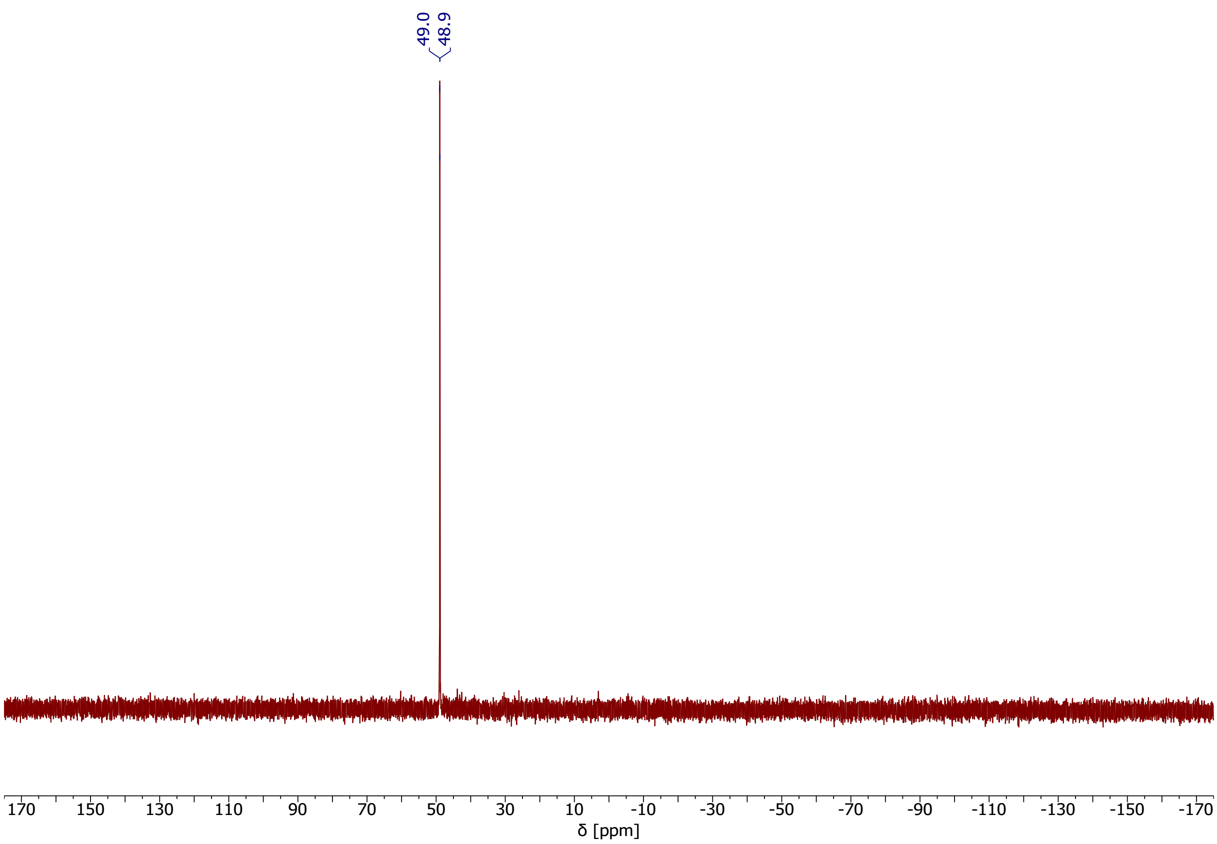

^{1}H NMR (400 MHz, CD_3Cl) spectrum of **Ru-MACHO^{Et}**.

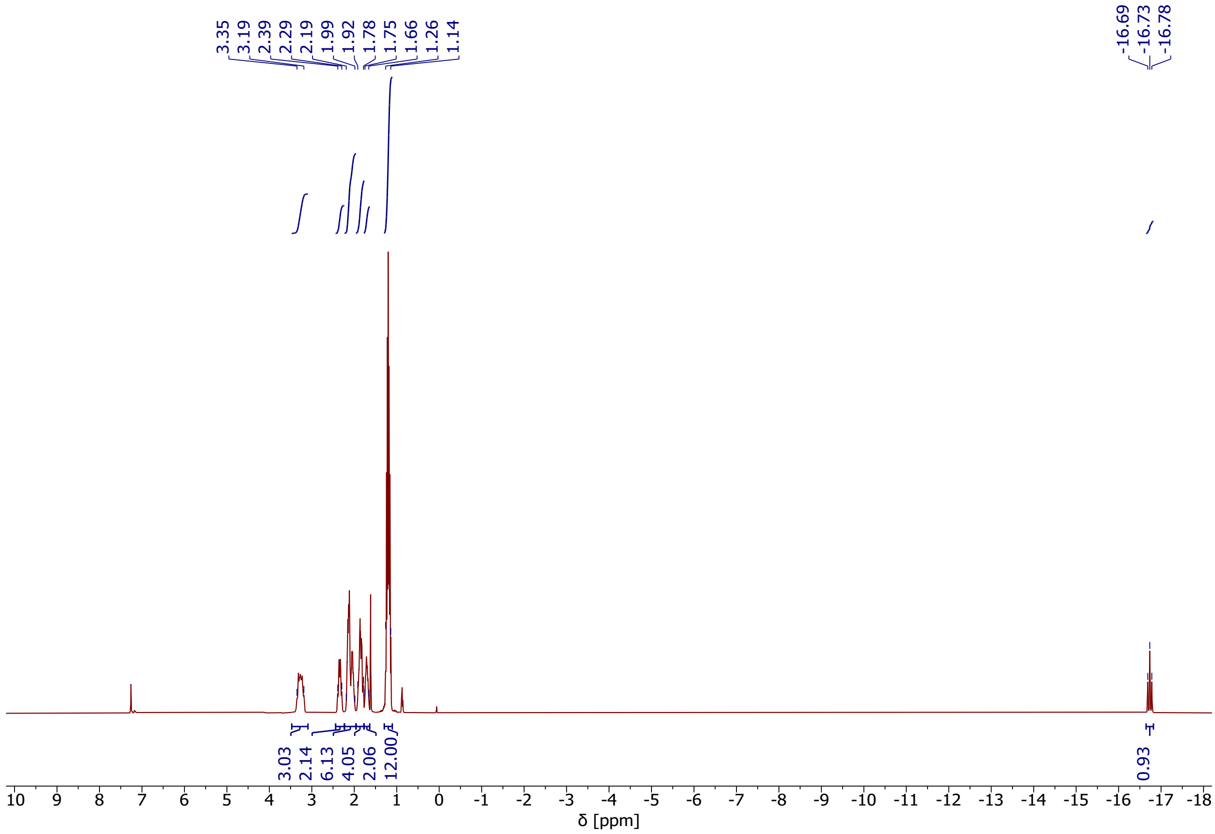

^{13}C NMR (101 MHz, CD_3Cl) spectrum of **Ru-MACHO^{Et}**.

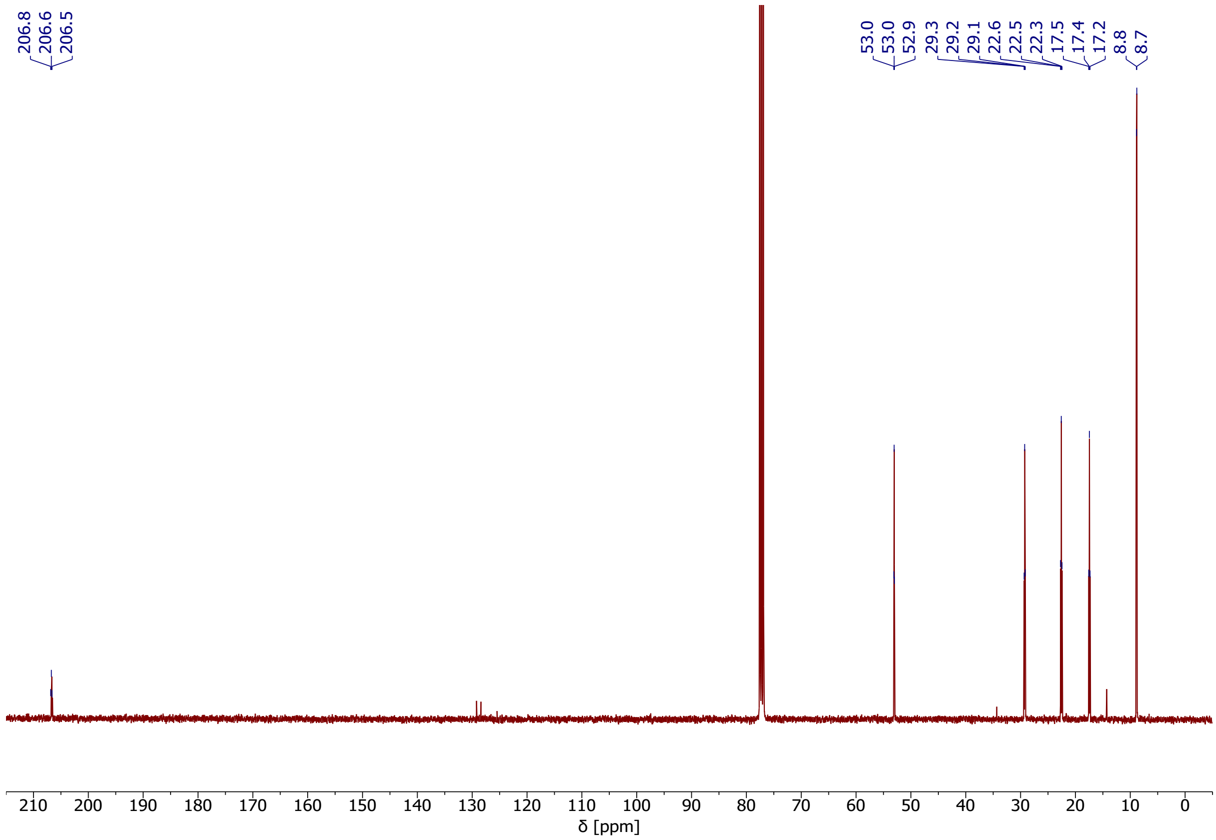

^{31}P NMR (162 MHz, CD_3Cl) spectrum of **Ru-MACHO^{Et}**.

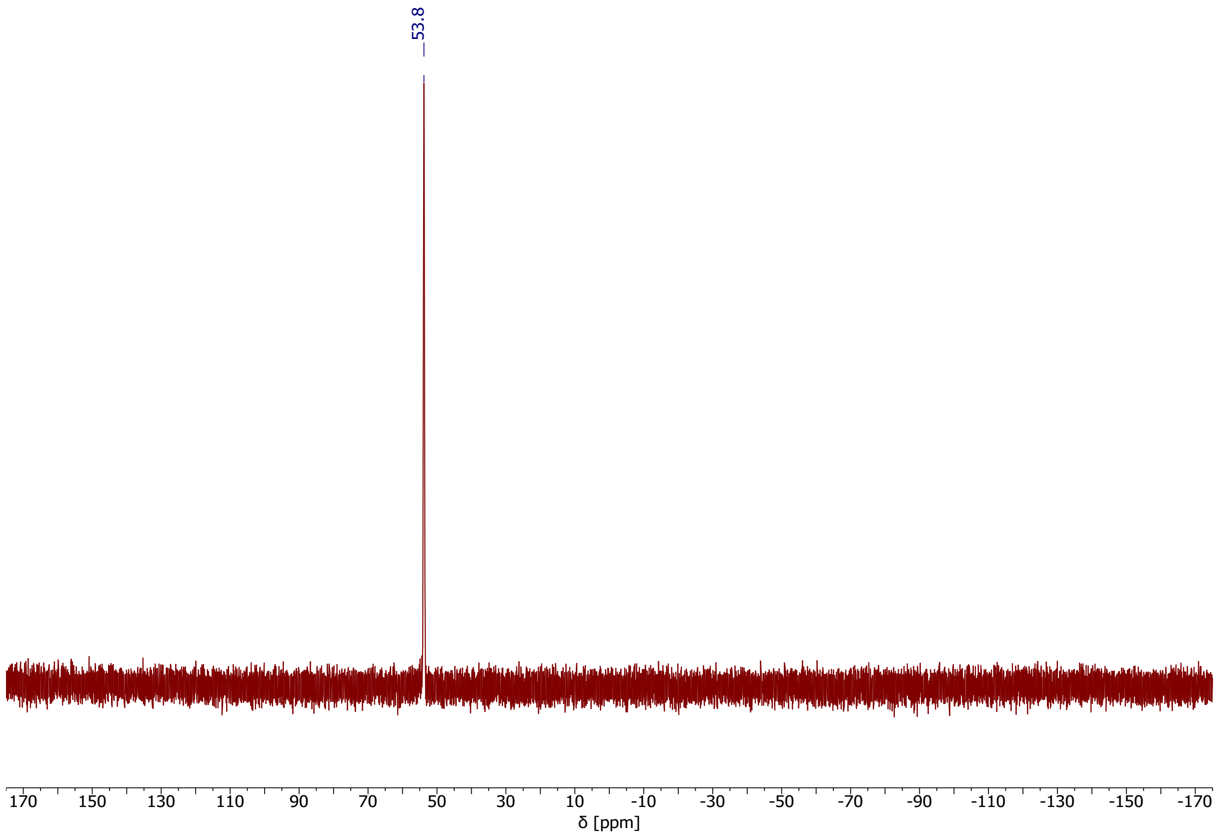

^{1}H NMR (400 MHz, CD_2Cl_2) spectrum of **Ru-MACHO^{iPr}**.

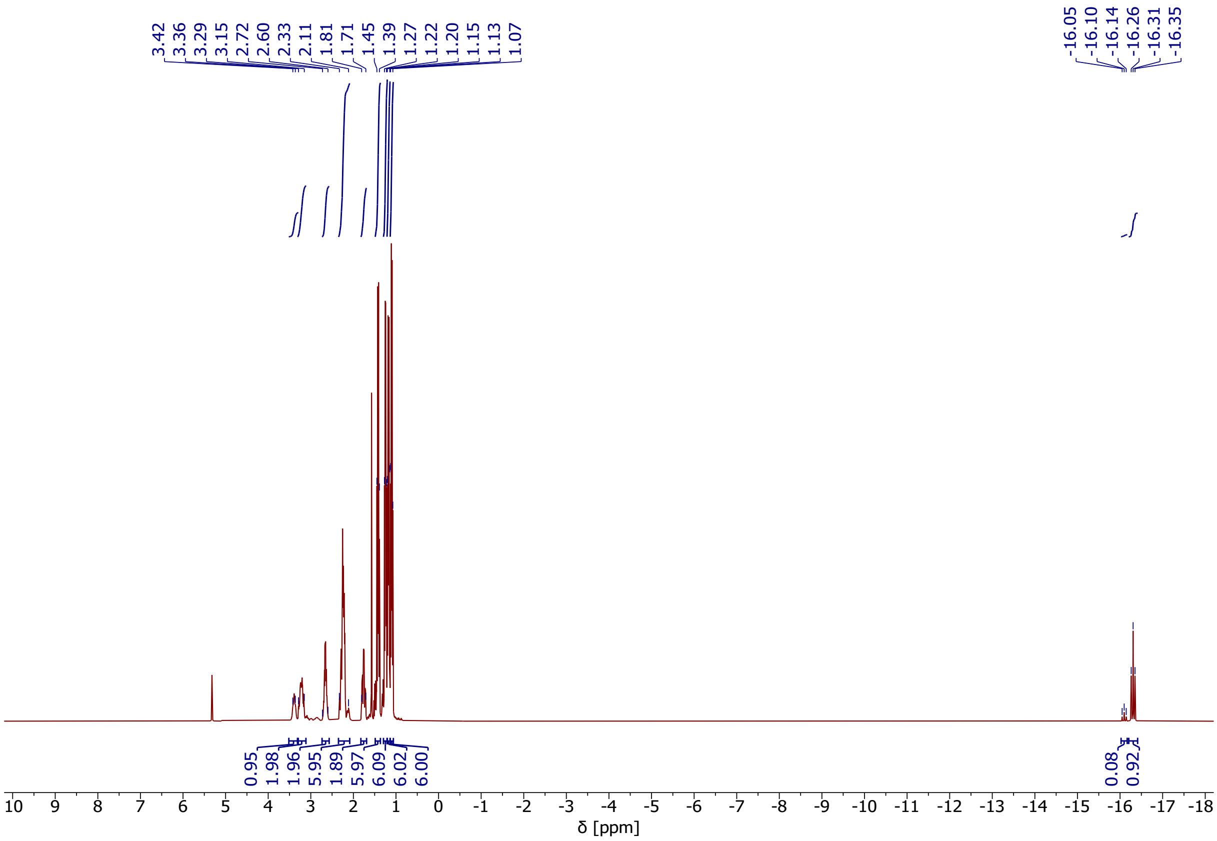

^{13}C NMR (101 MHz, CD_2Cl_2) spectrum of **Ru-MACHO^{iPr}**.

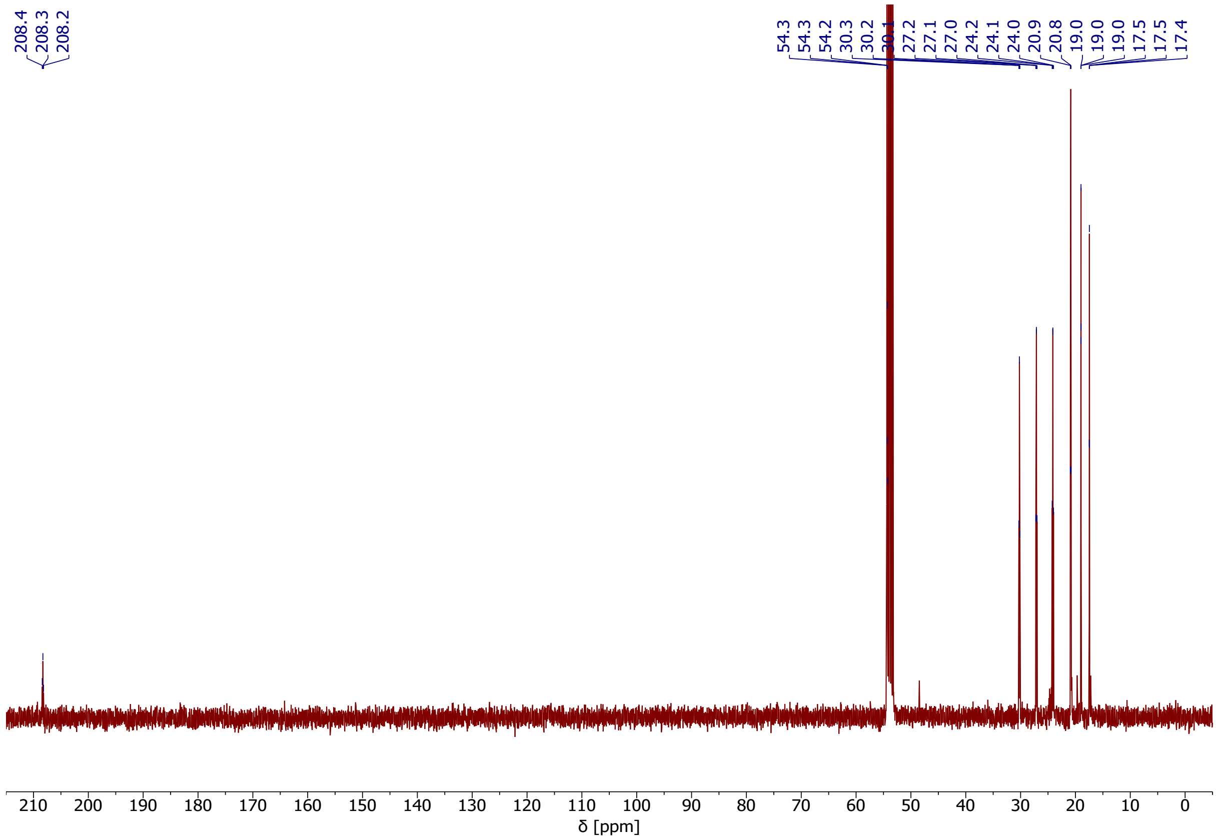

^{31}P NMR (162 MHz, CD_2Cl_2) spectrum of **Ru-MACHO^{iPr}**.

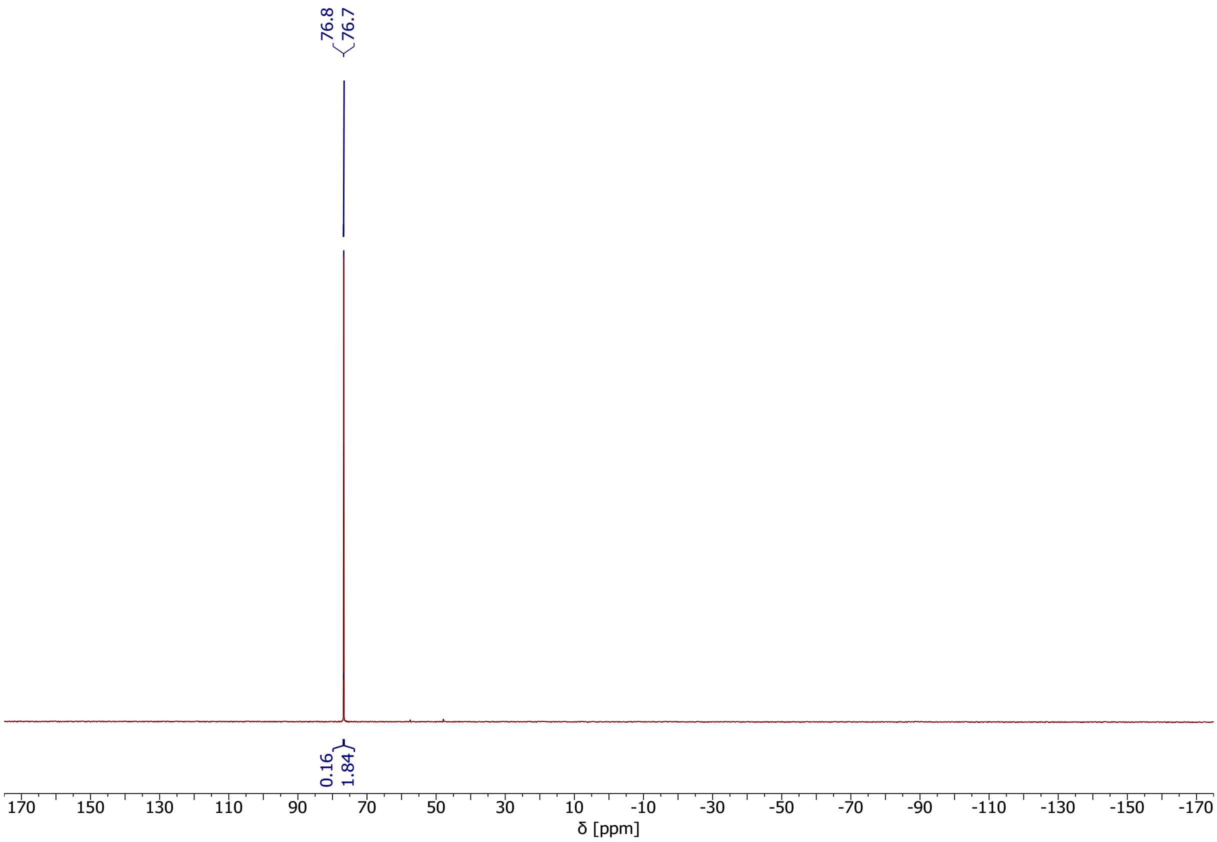

^{1}H NMR (400 MHz, CD_2Cl_2) spectrum of **Ru-MACHO^{tBu}**.

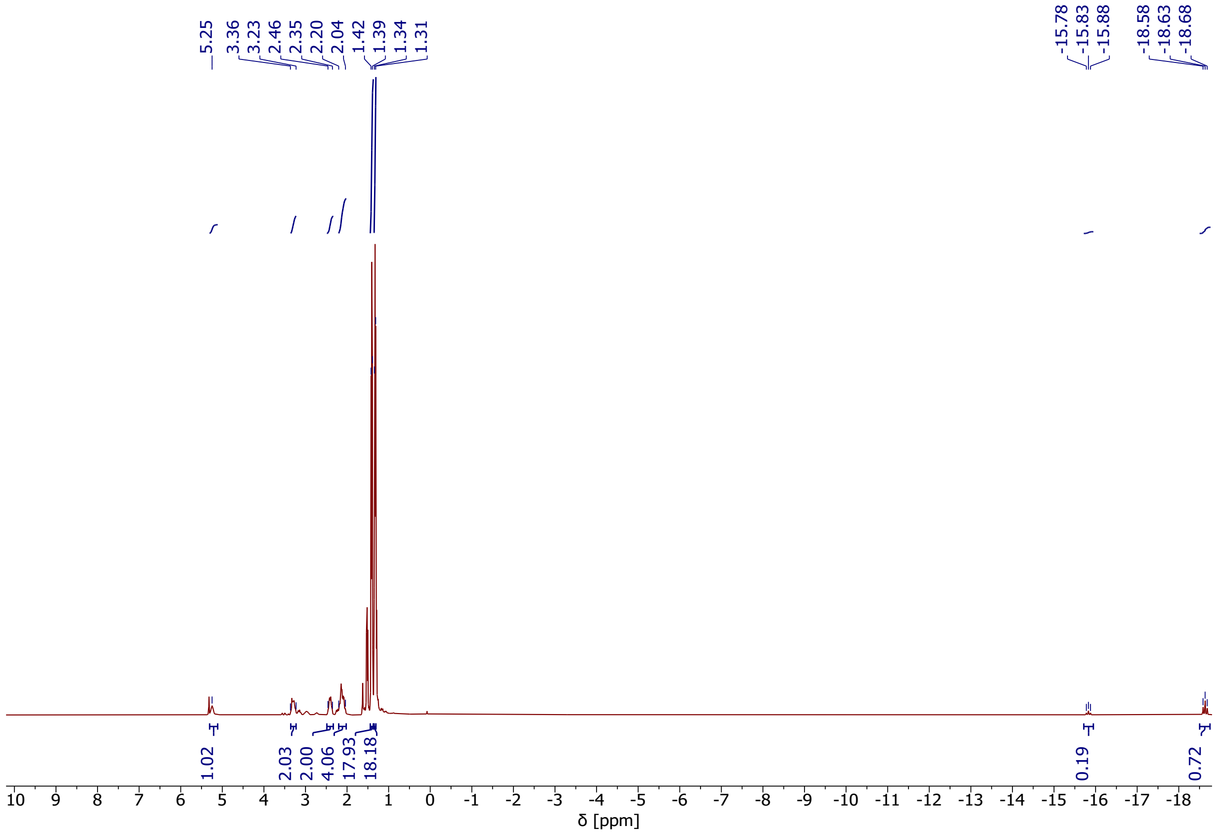

^{13}C NMR (101 MHz, CD_2Cl_2) spectrum of **Ru-MACHO^{tBu}**.

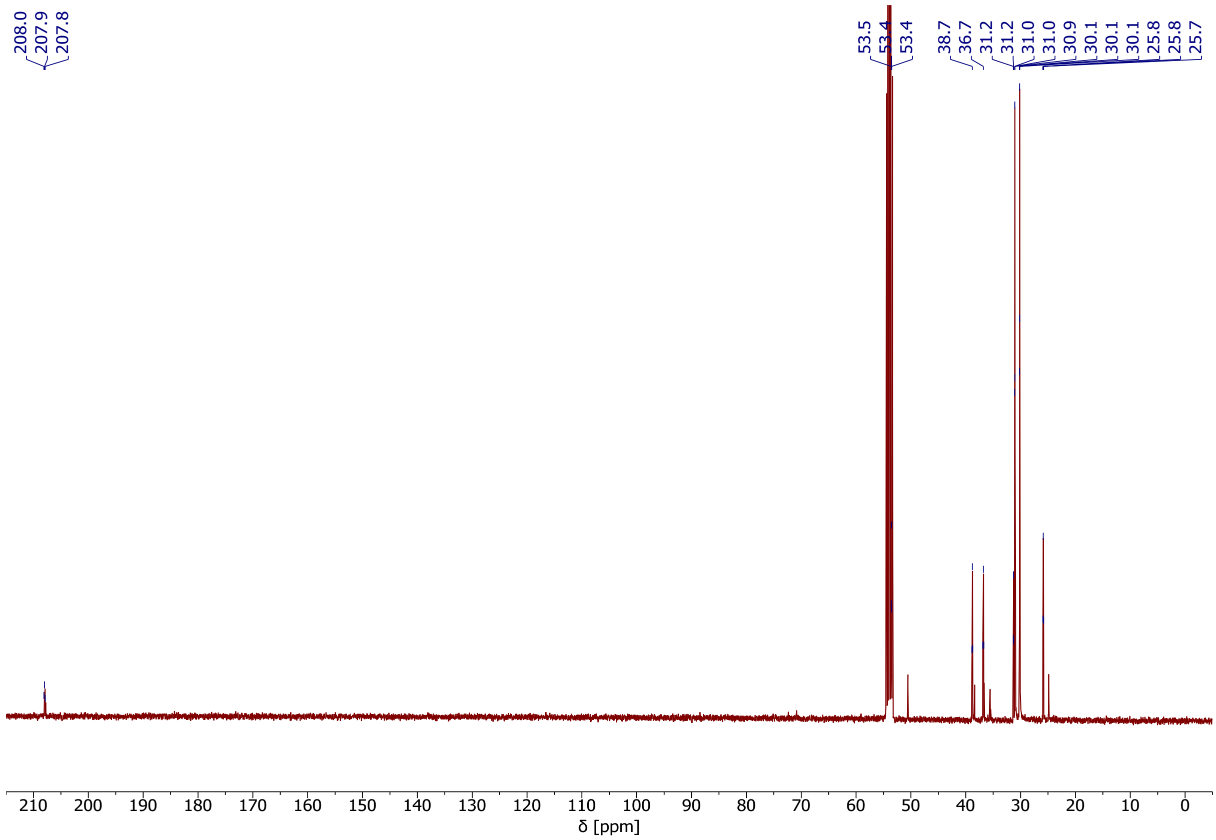

^{31}**P NMR** (162 MHz, CD_2Cl_2) spectrum of **Ru-MACHO^{tBu}**.

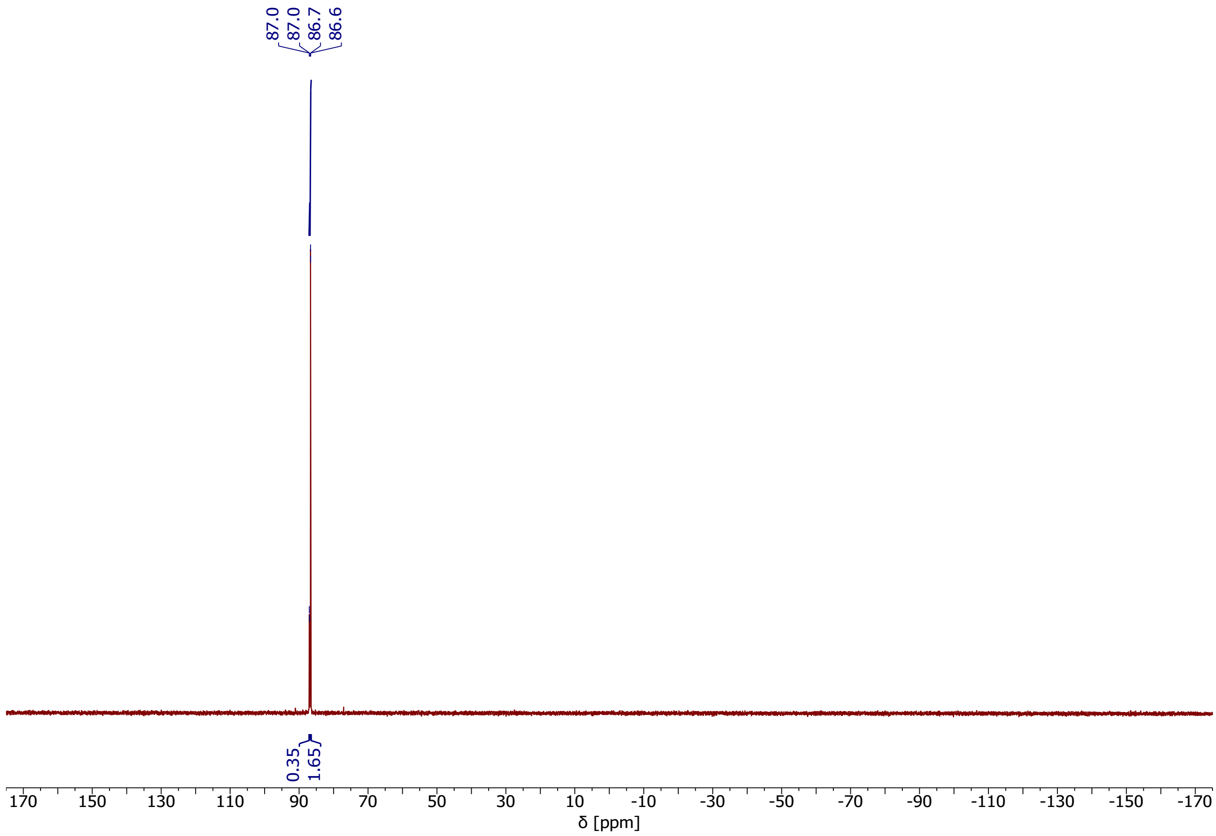

^{1}**H NMR** (400 MHz, $CDCl_3$) spectrum of **Ru-MACHO^{Cy}**.

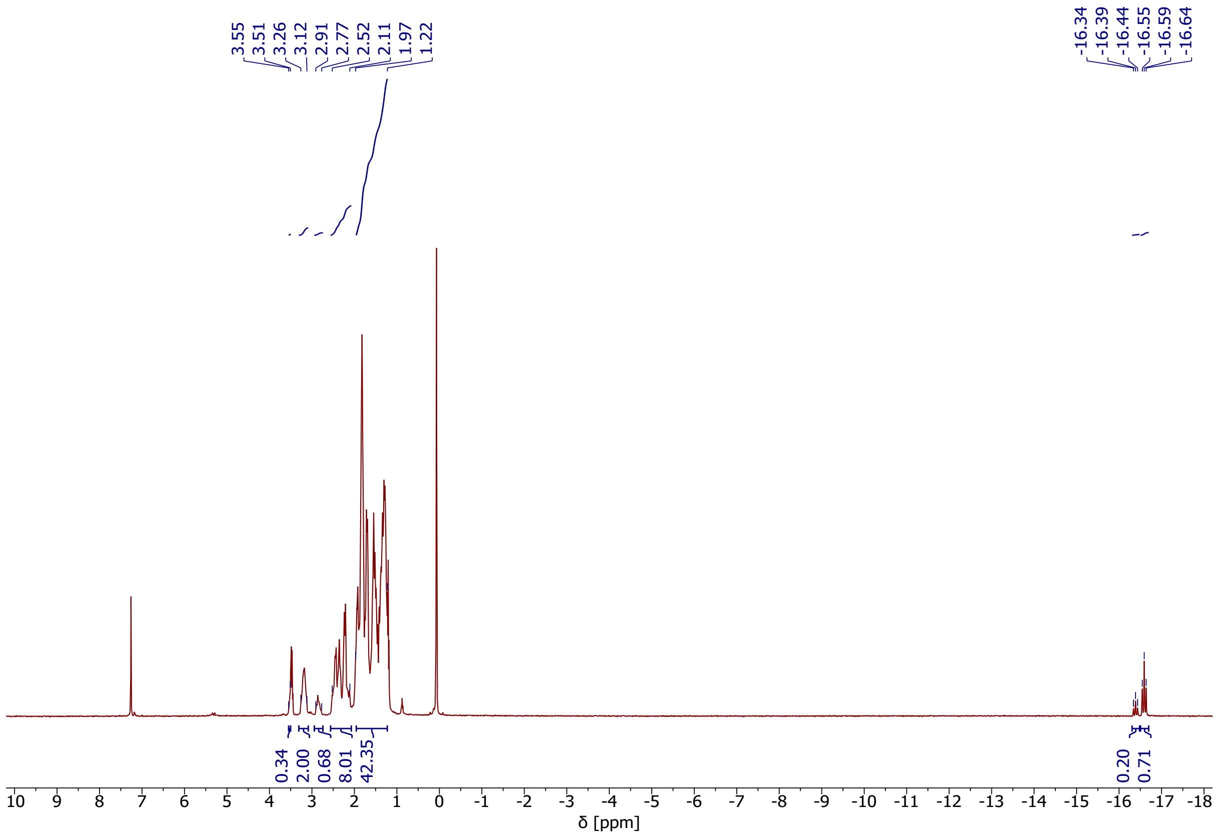

^{13}C NMR (101 MHz, CD_2Cl_2) spectrum of **Ru-MACHO^{Cy}**.

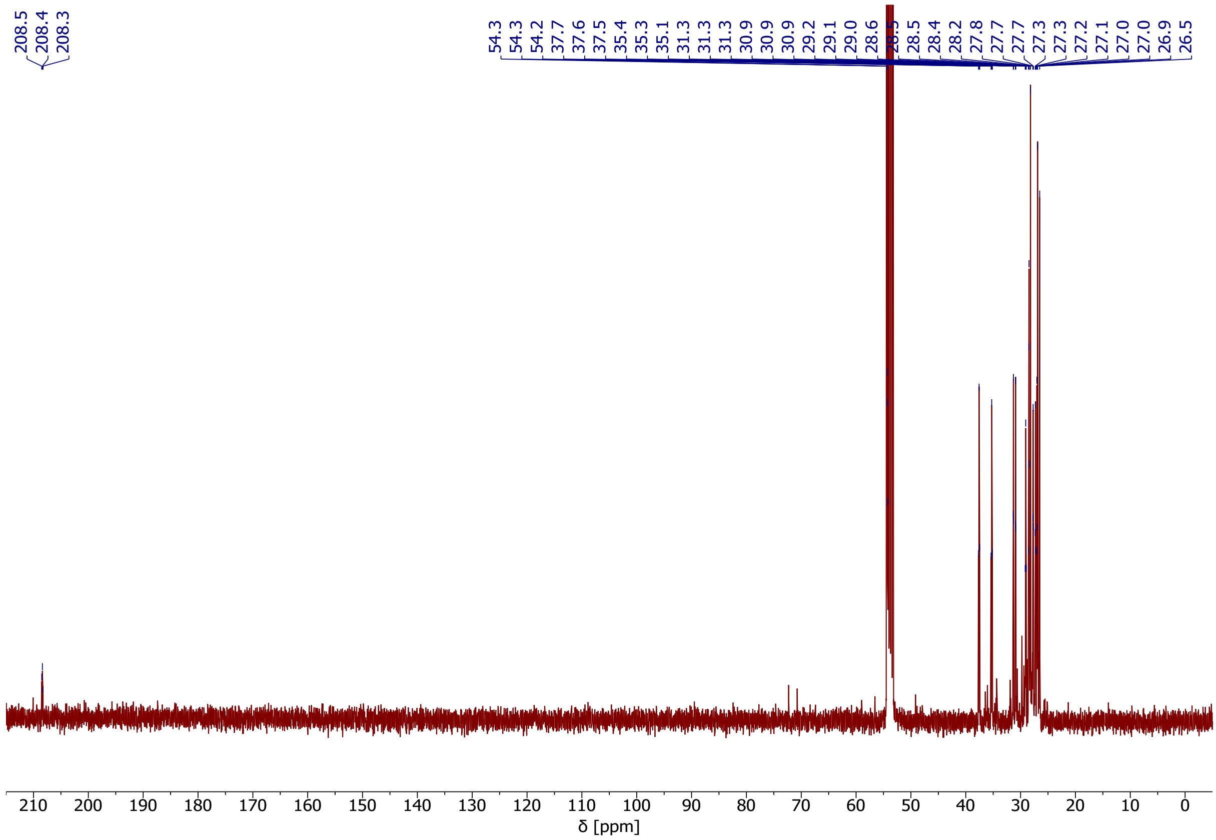

^{31}P NMR (162 MHz, $CDCl_3$) spectrum of **Ru-MACHO^{Cy}**.

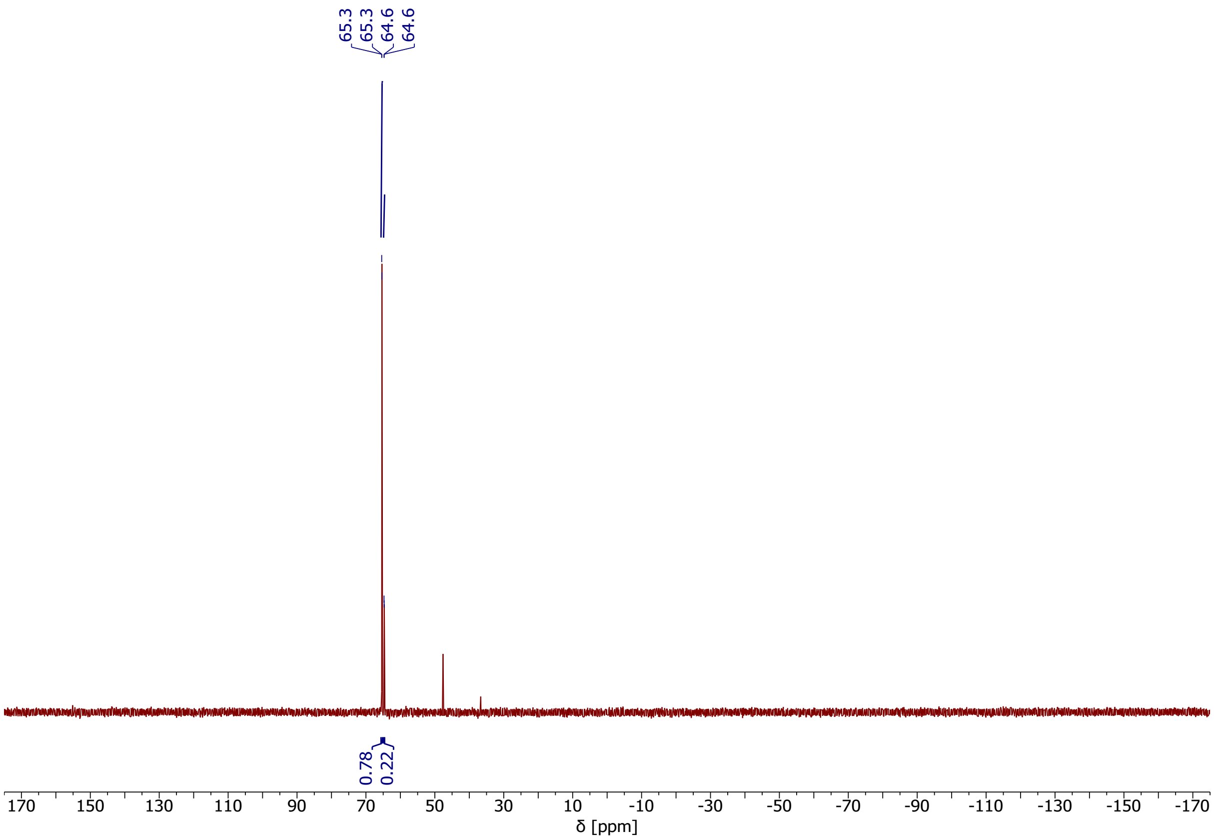

[1]H NMR (400 MHz, CD_3Cl) spectrum of **Ru-MACHO[Ad]**.

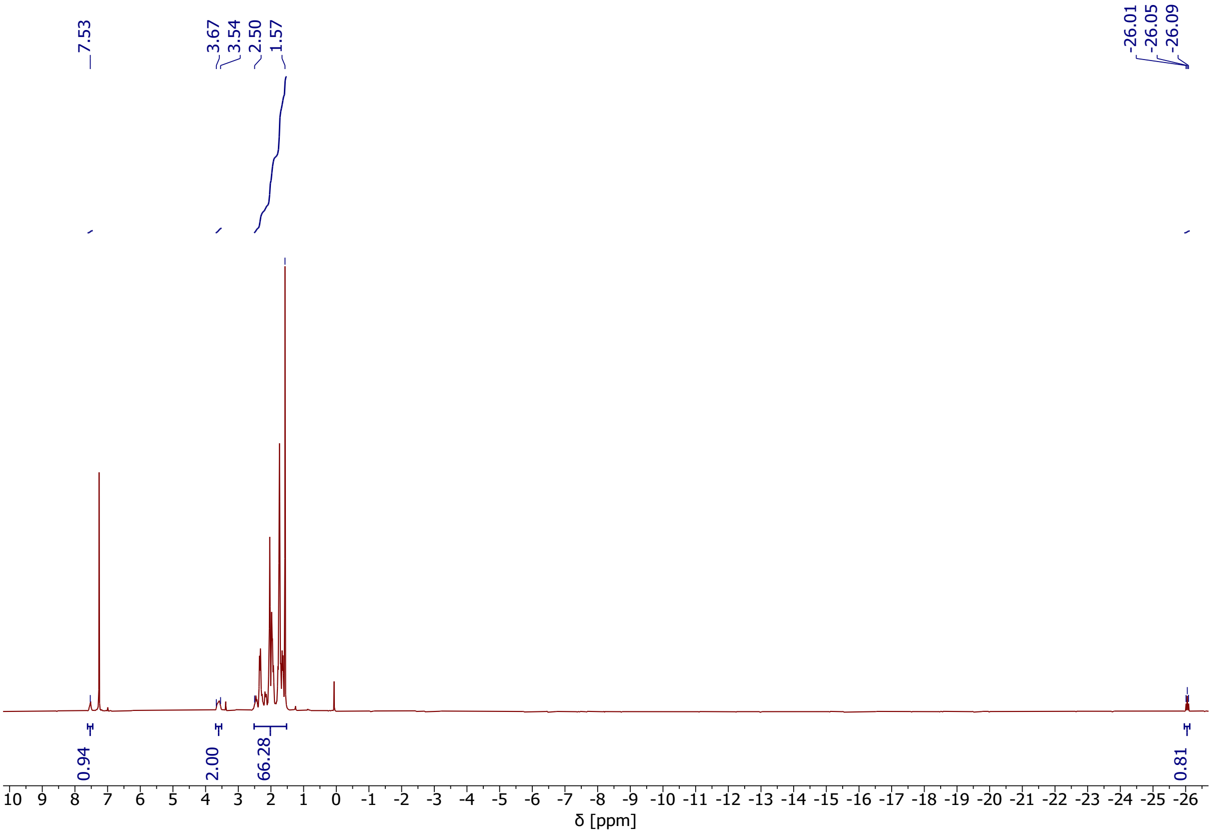

[13]C NMR (101 MHz, CD_3Cl) spectrum of **Ru-MACHO[Ad]**.

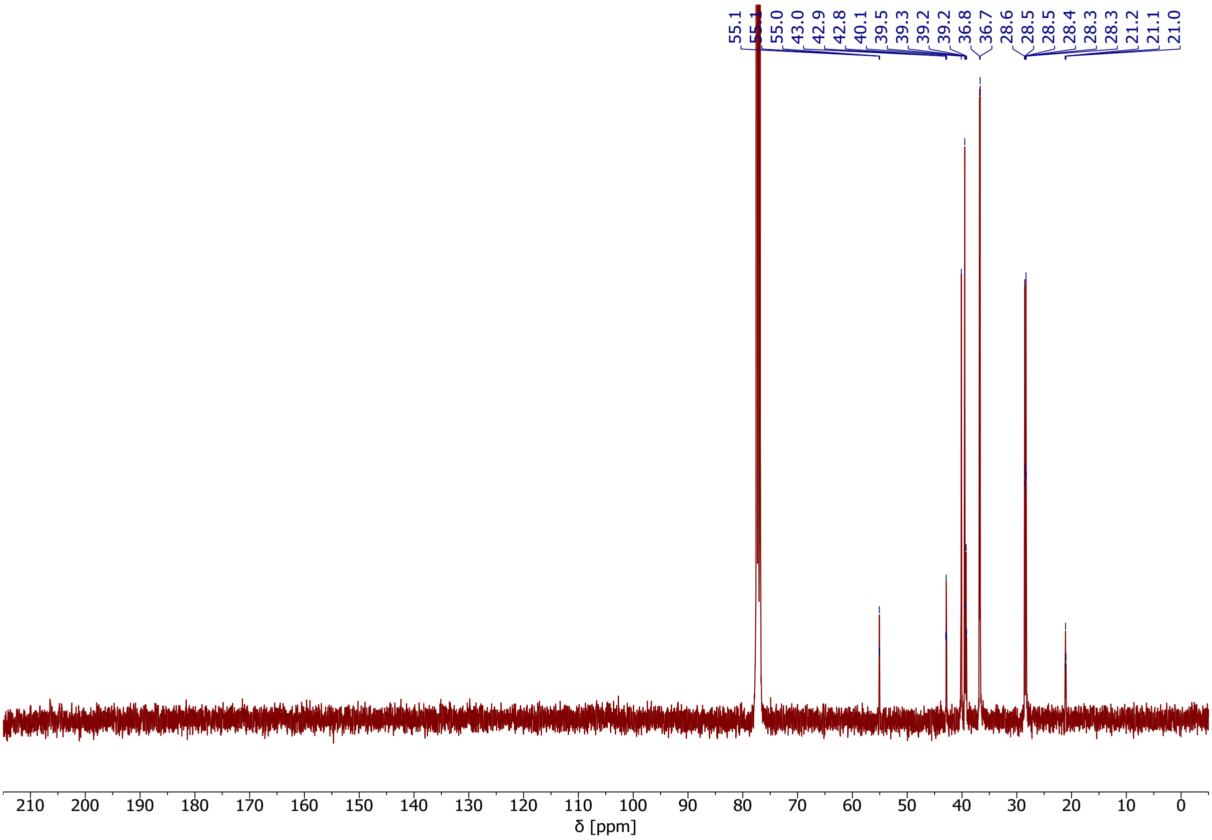

^{31}**P NMR** (162 MHz, CD_3Cl) spectrum of **Ru-MACHO^{Ad}**.

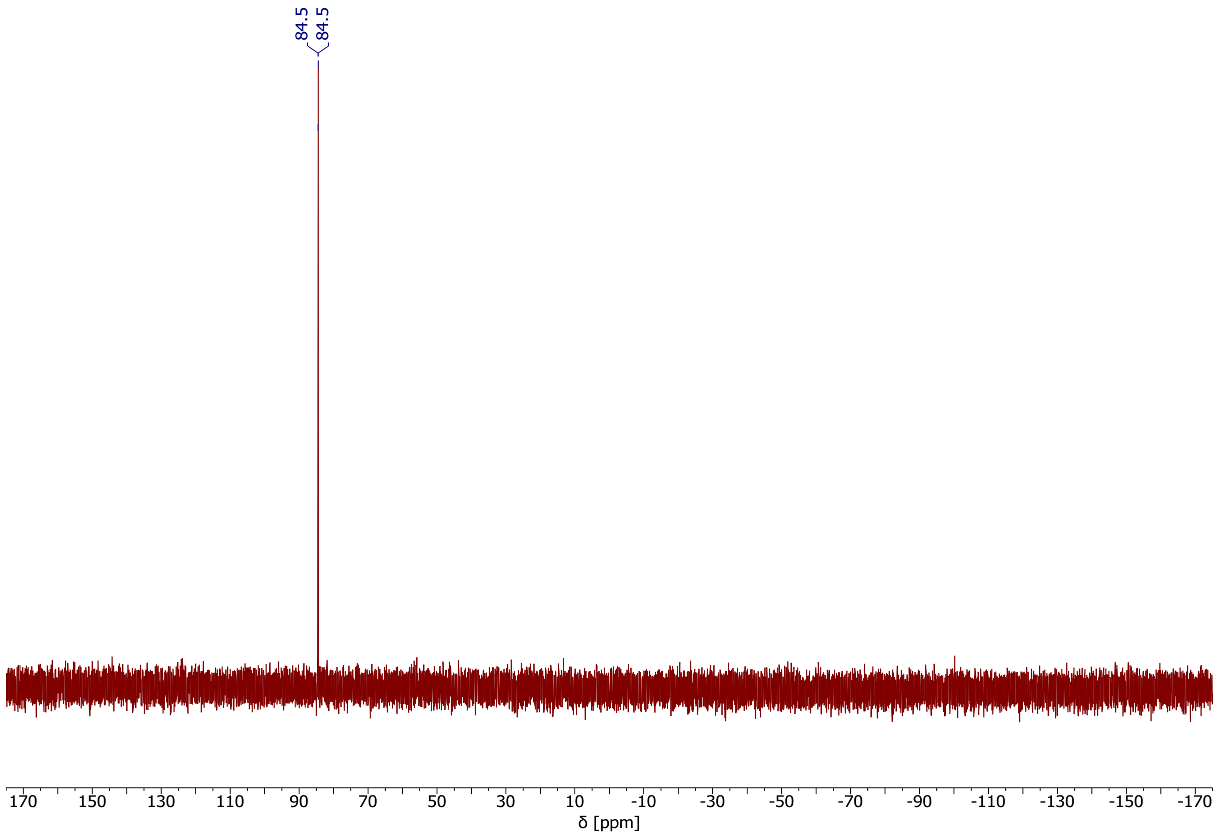

^{1}**H NMR** (400 MHz, CD_3Cl) spectrum of **NP$_3$**.

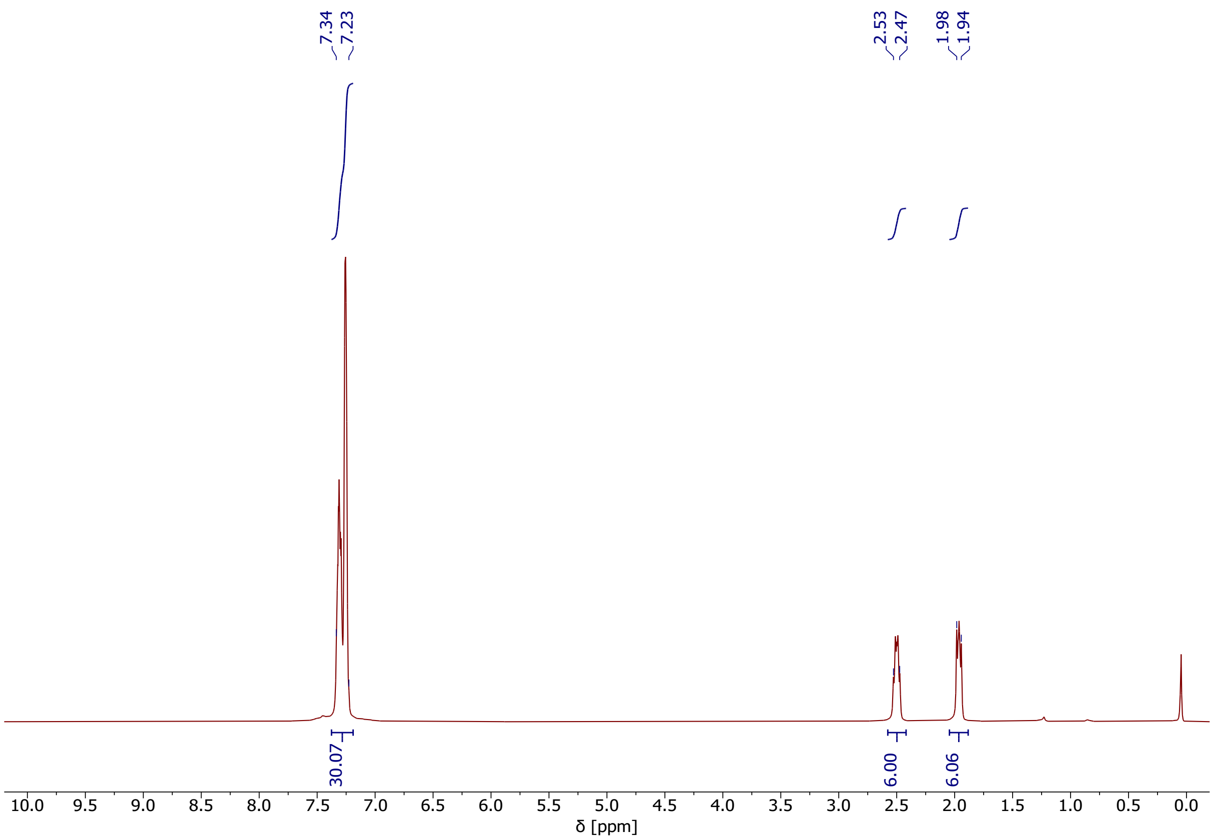

[13]C NMR (101 MHz, CD_3Cl) spectrum of **NP_3**.

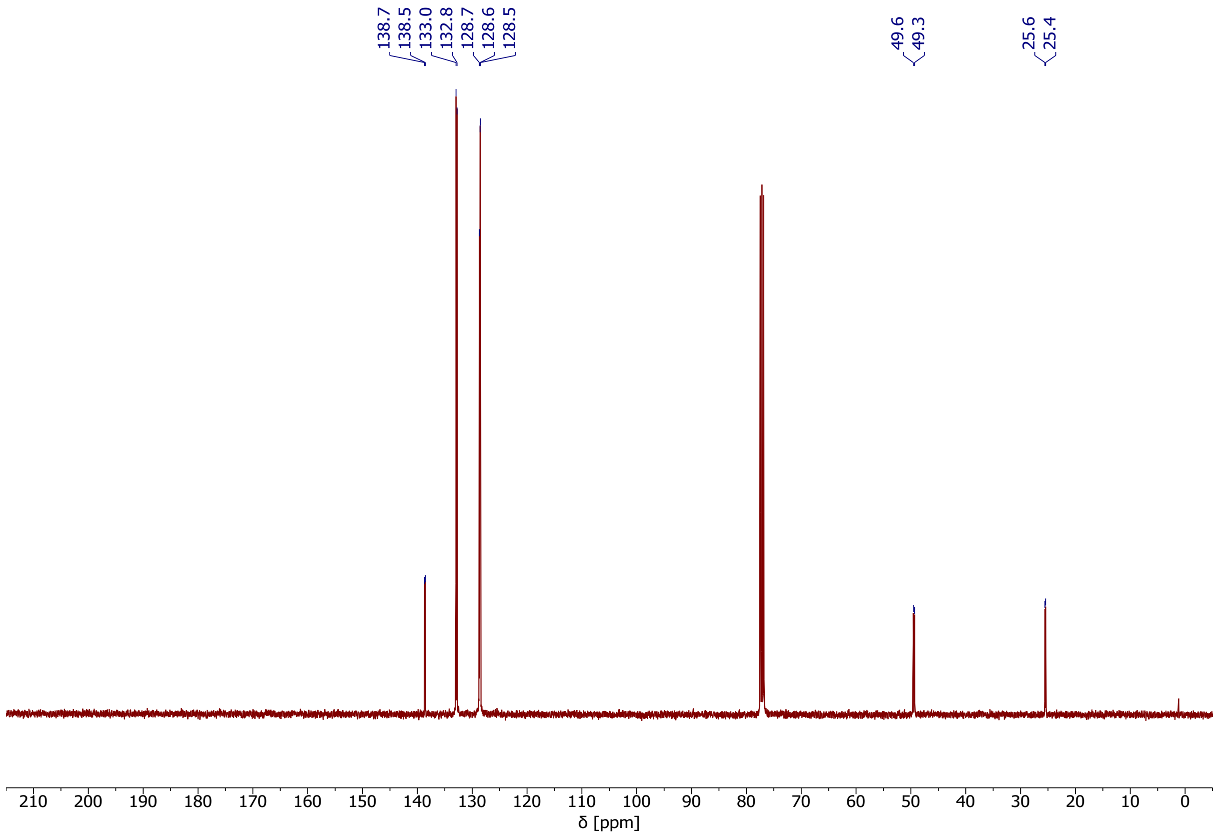

[31]P NMR (162 MHz, CD_3Cl) spectrum of **NP_3**.

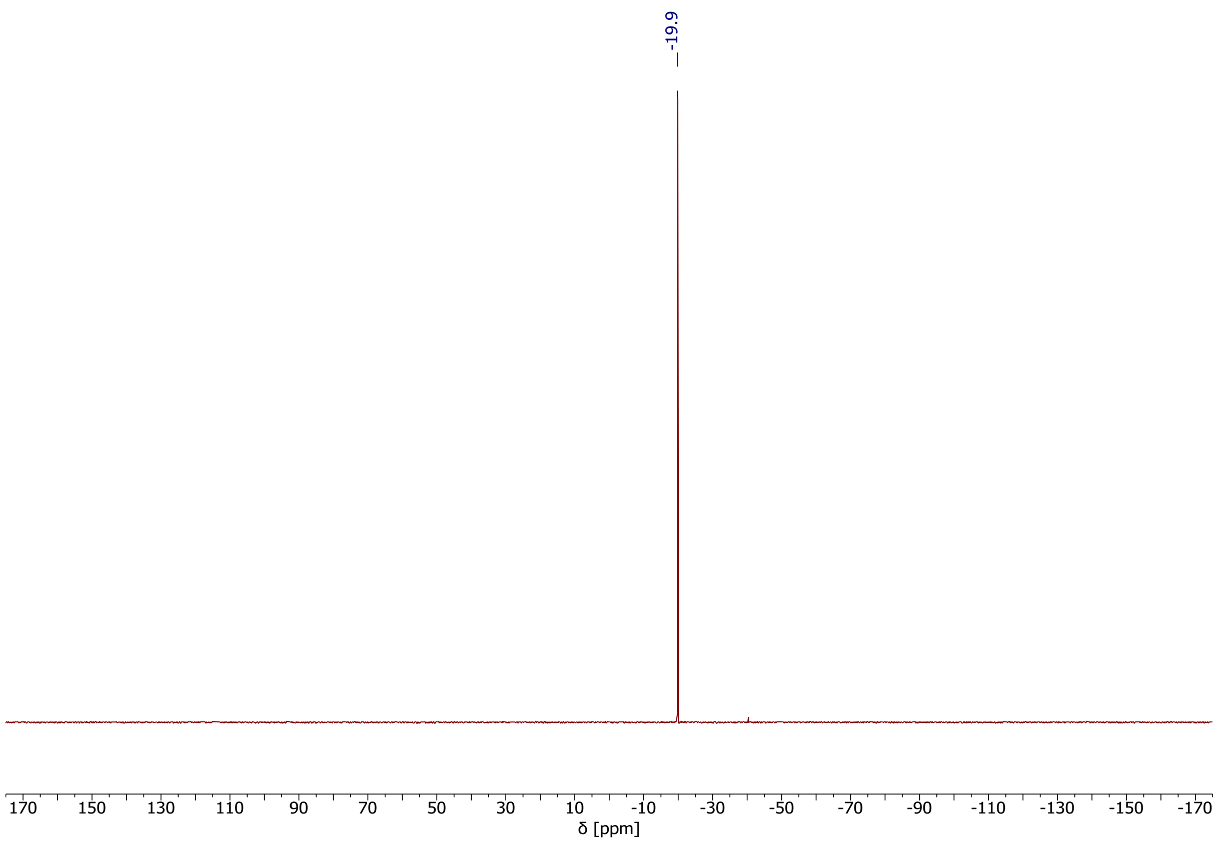

^{1}H NMR (400 MHz, C_6D_6) spectrum of **Ru-NP$_3$**.

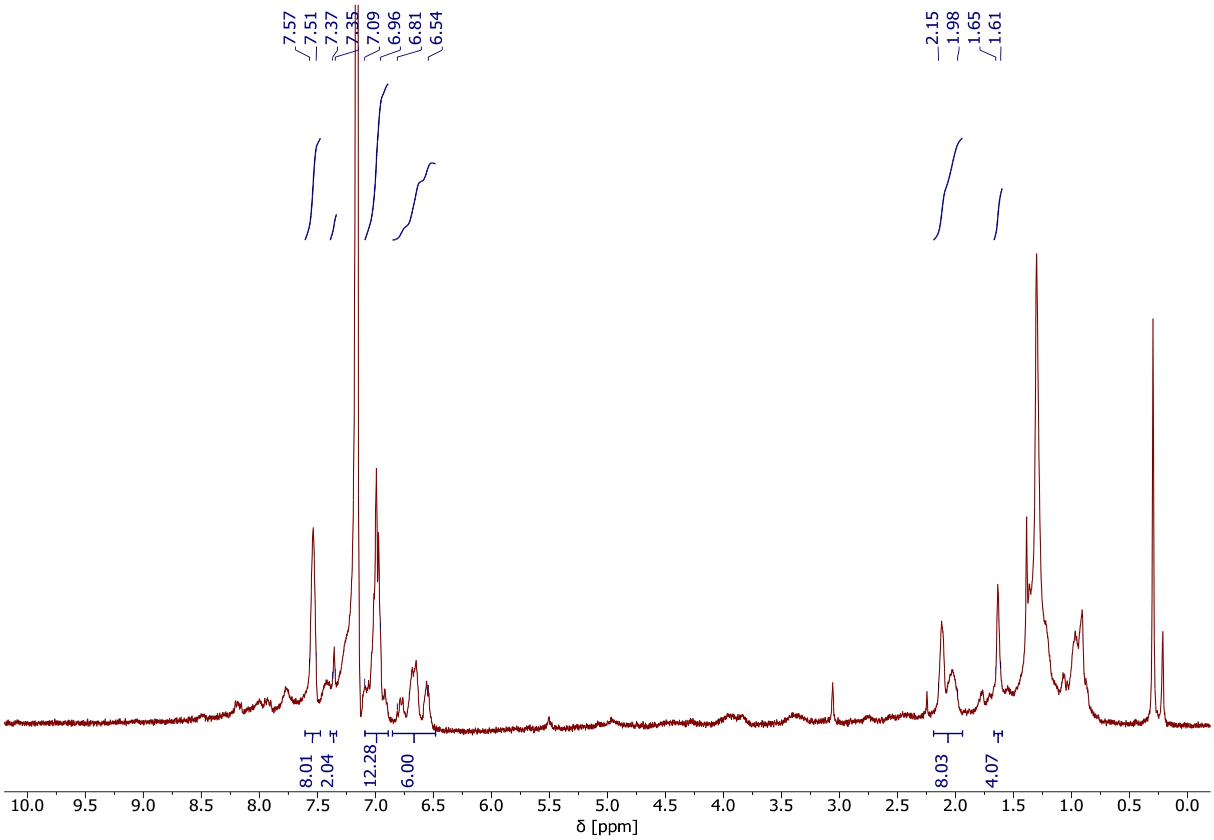

^{31}P NMR (162 MHz, C_6D_6) spectrum of **Ru-NP$_3$**.